

TSINGHUA-PRINCETON-COMBUSTION INSTITUTE
2022 SUMMER SCHOOL ON COMBUSTION

**COMBUSTION CHEMISTRY AND
KINETIC MECHANISM DEVELOPMENT**

Tiziano Faravelli
Politecnico di Milano
July 11-15, 2022



TSINGHUA-PRINCETON-COMBUSTION INSTITUTE

2022 SUMMER SCHOOL ON COMBUSTION

Schedule					
Beijing Time	July 11 (Mon.)	July 12 (Tue.)	July 13 (Wed.)	July 14 (Thu.)	July 15 (Fri.)
08:00 ~ 11:00			Mechanism Reduction and Stiff Chemistry Solvers Tianfeng Lu VMN: 52667557219		Mechanism Reduction and Stiff Chemistry Solvers Tianfeng Lu VMN: 52667557219
*10:00 ~ 12:00		Virtual Poster Session 10:00~12:00 VMN: 388239275		Virtual Lab Tour 10:00~12:00 VMN: 231842246	
14:00 ~ 17:00 Session I	Fundamental of Flames Suk Ho Chung VMN: 42399313194		Combustion in Microgravity and Microscale Kaoru Maruta VMN: 71656262918		
14:00 ~ 17:00 Session II	Soot Markus Kraft VMN: 39404905340		Current Status of Ammonia Combustion William Roberts VMN: 80506726244		
19:00 ~ 22:00 Session I	Combustion Chemistry and Kinetic Mechanism Development Tiziano Faravelli VMN: 35989357660				
19:00 ~ 22:00 Session II	Combustion Fundamentals of Fire Safety José Torero VMN: 57002781862				

Note:

¹Session I and Session II are simultaneous courses.

²VMN: Voov Meeting Number

Guidelines for Virtual Participation

1. General Guidelines

- Tencent Meeting software (腾讯会议) is recommended for participants whose IP addresses locate within Mainland China; Voov Meeting (International version of Tencent Meeting) is recommended for other IP addresses. The installation package can be found in the following links:
 - a) 腾讯会议
<https://meeting.tencent.com/download/>
 - b) Voov Meeting
<https://voovmeeting.com/download-center.html?from=1001>
- All the activities listed in the schedule are “registrant ONLY” due to content copyright.
- To facilitate virtual communications, each participant shall connect using stable internet and the computer or portable device shall be equipped with video camera, speaker (or earphone) and microphone.

2. Lectures

- The lectures are also “registrant ONLY”. Only the students who registered for the course can be granted access to the virtual lecture room.
- To enter the course, each registered participant shall open the software and join the conference using the corresponding Voov Meeting Number (VMN) provided in the schedule; only participants who show unique identification codes and real names as “xxxxxx-Last Name, First Name” will be granted access to the lecture room; the identification code will be provided through email.
- During the course, each student shall follow the recommendation from the lecturer regarding the timing and protocol to ask questions or to further communicate with the lecturer.
- For technical or communication issues, the students can contact the TA in the virtual lecture or through emails.
- During the course, the students in general will not be allowed to use following functions in the software: 1) share screen; 2) annotation; 3) record.

3. Lab Tour

- The event will be hosted by graduate students from Center for Combustion Energy, Tsinghua University and live streamed using provided Voov Meeting Number.
- During the activity, the participants will not be allowed to use following functions in the software: 1) share screen; 2) annotation; 3) record.
- Questions from the virtual participants can be raised using the chat room.

4. Poster Session

- The event will be hosted by the poster authors (one Voov Meeting room per poster) and live streamed using provided Voov Meeting Number.
- During the activity, the participants will not be allowed to use following functions in the software: 1) share screen; 2) annotation; 3) record.
- Questions from the virtual participants can be raised using the chat room or request access to audio and video communication.

Teaching Assistants

- **Fundamentals of Flame (Prof. Suk Ho Chung)**

TA1: Hengyi Zhou (周恒毅); zhouhy19@mails.tsinghua.edu.cn

TA2: Xinyu Hu (胡馨予); hxy21@mails.tsinghua.edu.cn

- **Combustion Chemistry and Kinetic Mechanism Development (Prof. Tiziano Faravelli)**

TA1: Shuqing Chen (陈舒晴); chen-sq19@mails.tsinghua.edu.cn

TA2: Jingzan Shi (史京瓚); sjz21@mails.tsinghua.edu.cn

- **Current Status of Ammonia Combustion (Prof. William Roberts)**

TA1: Yuzhe Wen (温禹哲); wyz20@mails.tsinghua.edu.cn

TA2: Haodong Chen (陈皓东); chd20@mails.tsinghua.edu.cn

- **Soot (Prof. Markus Kraft)**

TA1: Yuzhe Wen (温禹哲); wyz20@mails.tsinghua.edu.cn

TA2: Haodong Chen (陈皓东); chd20@mails.tsinghua.edu.cn

- **Combustion Fundamentals of Fire Safety (Prof. José Torero)**

TA1: Xuechun Gong (巩雪纯); gxc19@mails.tsinghua.edu.cn

TA2: Weitian Wang (王巍添); wwt20@mails.tsinghua.edu.cn

- **Combustion in Microgravity and Microscale (Prof. Kaoru Maruta)**

TA1: Hengyi Zhou (周恒毅); zhouhy19@mails.tsinghua.edu.cn

TA2: Xinyu Hu (胡馨予); hxy21@mails.tsinghua.edu.cn

- **Mechanism Reduction and Stiff Chemistry Solvers (Prof. Tianfeng Lu)**

TA1: Shuqing Chen (陈舒晴); chen-sq19@mails.tsinghua.edu.cn

TA2: Jingzan Shi (史京瓚); sjz21@mails.tsinghua.edu.cn



**POLITECNICO
MILANO 1863**

2022 Tsinghua Summer School

Combustion chemistry and kinetic mechanism development

Tiziano Faravelli

Who I am



Tiziano Faravelli professor at Politecnico di Milano.

My researches are mainly devoted to the chemical reaction engineering of complex systems.

The CRECK modeling group, where I am an active (and the oldest) research member, develops detailed models for the pyrolysis, partial oxidation and combustion of both traditional and renewable fuels, i.e. bio-gas, bio-oil and biomass.

I have been working for more than 30 years on detailed kinetic mechanisms of gas, liquid and solid fuels. Particularly, this activity focuses on pollutant formation, like NO_x, SO_x, PAHs and soot, from all thermal processes.

Recently I also started studying circular economy applied to the chemical recycle of waste and especially of plastics. Detailed models of the biomass and polymer pyrolysis and gasification have been proposed and are continuously developed and updated.

Together with the chemical modeling at the molecular scale, I work on understanding the physical phenomena at the mesoscale. This activity refers to the investigation of solid-gas interactions in particles, or the multiphase gas-liquid flow of isolated droplets.

The lesson aim

The course aims at showing the main steps of the development of detailed chemical kinetic mechanisms to describe the oxidation of both fossil and bio fuels.

To this goal, thermodynamics and kinetics fundamentals will be presented. Molecular and radical stability, classes of reactions, kinetic constant estimation, analogy and rate rules and lumping techniques will be discussed in details.

The course will cover hydrogen and simple fuels, expanding to large hydrocarbons, possibly oxygenated, to analyze their behavior, like ignition and laminar flame speed.

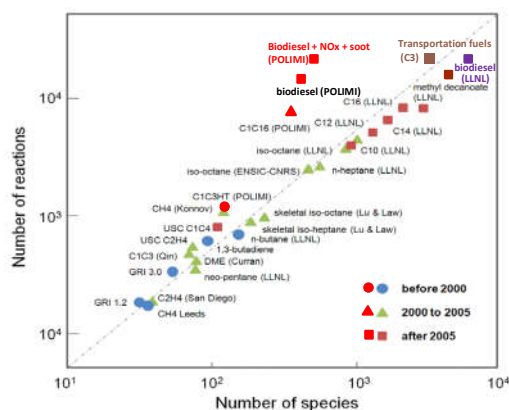
Surrogate definition will allow to discuss the oxidation characteristics of real fuels. Mechanisms of the formation of main pollutants, like nitrogen oxides, polycyclic aromatic hydrocarbons and soot, will also be illustrated. Tools to support this mechanism development activity will be part of the course.

Let's start from ... the end

A mechanism example

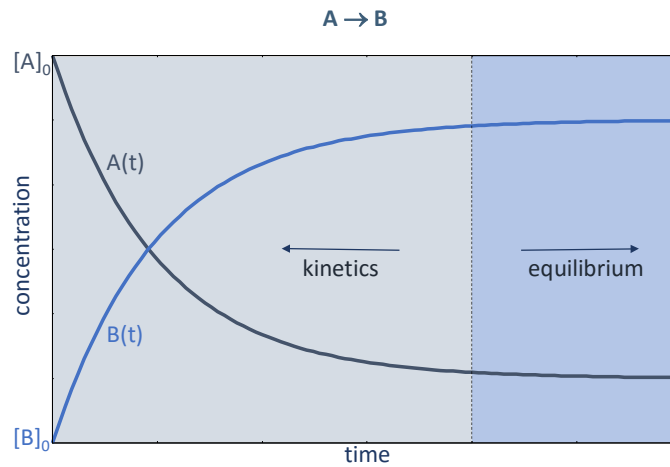
H2+M=2H+M	4.577e+19	-1.400	104400.00
H2/ 2.50/ H2O/ 12.00/ CO/ 1.90/ CO2/ 3.80/ HE/ 0.83/			
H2+O=H+OH	5.080e+04	2.670	6292.00
H2+OH=H+H2O	4.380e+13	0.000	6990.00
2O+M=O2+M	6.165e+15	-0.500	0.00
H2/ 2.50/ H2O/ 12.00/ AR/ 0.83/ CO/ 1.90/ CO2/ 3.80/ HE/ 0.83/			
H+O2=O+OH	1.140e+14	0.000	15286.00
H+OH+M=H2O+M	3.500e+22	-2.000	0.00
H2/ 0.73/ H2O/ 3.65/ AR/ 0.38/			
O+H2O=2OH	6.700e+07	1.704	14986.80
H+O+M=OH+M	4.714e+18	-1.000	0.00
H2/ 2.50/ H2O/ 12.00/ AR/ 0.75/ CO/ 1.50/ CO2/ 2.00/ HE/ 0.75/			
H2O2(+M)=2OH(+M)	2.000e+12	0.900	48749.00
LOW/ 2.49e+24 -2.300 48749.0/			
TROE/ 0.4300 1.000e-30 1.000e+30/			
H2O/ 7.65/ CO2/ 1.60/ N2/ 1.50/ O2/ 1.20/ HE/ 0.65/ H2O2/ 7.70/ H2/ 3.70/ CO/ 2.80/			
H+H2O2=H2O+OH	2.410e+13	0.000	3970.00
H+H2O2=H2+HO2	2.150e+10	1.000	6000.00

...



Adapted from: T.F. Lu, C.K. Law, *Prog. Energy Comb. Sci.*, 35 (2009)

Back to the beginning



Thermodynamics allows to predict the equilibrium state, when time approaches infinite.
Chemical kinetics describes the system evolution and the required times.

After H. Curran Combustion Summer School, 2016

Thermochemistry and Thermodynamics

Classical laws of **Thermodynamics** define and govern the final state of a homogeneous system (after very long time: infinite).

Thermochemistry is the branch of **Thermodynamics** which focuses on the study of heat released or absorbed in chemical reactions.

Heat release from combustion reactions induces temperature increase, therefore combustion reactions are **self accelerating**.

It is first necessary to define thermodynamic variables:

- **Standard Enthalpy of Formation** (molar enthalpy)
- **Standard Entropy of Formation** (molar entropy)
- **Molar heat capacities**

Standard Enthalpy of Formation

Standard Conditions: 298.15 K and 1 bar

The standard enthalpy of formation $\Delta h_{f,i}^0$ of a compound is the reaction enthalpy (experimentally measured with a calorimeter) of its formation from pure elements in their most stable state at standard conditions :

Here and in the following, capital letters are used for a property and the small ones for the unit mass basis of the property :
H [J]; h [J/kg]



Standard Enthalpy of Formation of H_2 , O_2 , N_2 and solid carbon C_s are chosen as **zero**, because they represent the chemical elements

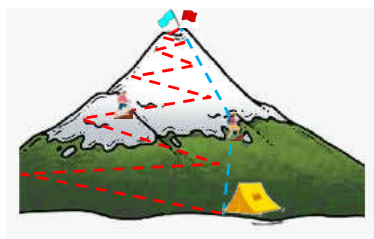
A more negative (or less positive) enthalpy of formation indicates a more stable species: CO_2 is more stable than CH_4

State function

A state function is a property that describes the system and is dependent on the state variables. When a change of state occurs, the change in value of a state function depends only on the initial and final locations of the system, not on the path taken.

In other words:

The value of a state function does not depend on the particular history of the sample, only its present condition.

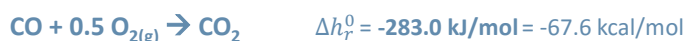


Climbers gain the same gravitational potential energy (mgh) whether they take the red or blue path.

Enthalpy is a state function

Enthalpy is a state function

Often, direct formation of a compound from the elements is not feasible or easy. Formation enthalpy can be determined by combining different reactions.



Subtracting these two reactions, one obtains:



Enthalpy of Formation ΔH^0 @ 1 bar and 298.15 K

Chemical	Name	State	Δh_f [kJ/mol]	Δh_f [kJ/g]	Δh_f [kcal/mol]
O2	Oxygen	Gas	0	0	0.0
N2	Nitrogen	Gas	0	0	0.0
H2	Hydrogen	Gas	0	0	0.0
C	Carbon	Solid	0	0	0.0
H2O	Water	Gas	-241.83	-13.44	-57.8
H2O	Water	Liquid	-285.1	-15.84	-68.1
CO	Carbon monoxide	Gas	-110.53	-3.95	-26.4
CO2	Carbon dioxide	Gas	-393.52	-8.94	-94.0
CH4	Methane	Gas	-74.87	-4.68	-17.9
C2H2	Acetylene	Gas	227.06	8.79	54.2
C2H4	Ethylene	Gas	52.38	1.87	12.5
C2H6	Ethane	Gas	-84.81	-2.83	-20.3
C4H10	Butane	Gas	-124.9	-2.15	-29.8
C6H6	Benzene	Gas	82.96	1.06	19.8
C6H6	Benzene	Liquid	49.06	0.63	11.7
C8H18	Octane	Liquid	-250.31	-2.19	-59.8
C12H26	Dodecane	Liquid	-347.77	-2.17	-83.1
C	Carbon	Vapor	716.67	59.72	171.2
N	Nitrogen atom	Gas	472.68	33.76	112.9
O	Oxygen atom	Gas	249.17	15.57	59.5
H	Hydrogen	Gas	218	218	52.1
OH	Hydroxyl radical	Gas	38.99	2.29	9.3
NO	Nitric oxide	Gas	90.29	3.01	21.6
NH3	Ammonia	Gas	-45.9	-2.7	-11.0
N2H4	Hydrazine	Liquid	50.63	1.58	12.1
SO2	Sulfur dioxide	Gas	-296.84	-4.64	-70.9
SO3	Sulfur trioxide	Gas	-395.77	-4.95	-94.5

Species with positive heat of formation decompose to their elements and release heat

Enthalpy of reaction ΔH_r

Reaction enthalpy is the change in the enthalpy of a chemical reaction that occurs at a constant pressure. It is the enthalpy of the final state minus the initial state of the system.

$$\Delta h_r^0 = \sum_{i=1}^{NS} \nu_i \Delta h_{fi}^0 \quad \nu_i \text{ stoichiometric coefficient of } i\text{-th species}$$

Heat of reaction is the opposite of the reaction enthalpy $Q_r = -\Delta h_r^0$



If energy is given off during a reaction, such as in the burning of a fuel, the products have less heat content than the reactants and Δh will have a negative value; the reaction is said to be exothermic. If energy is consumed during a reaction, Δh will have a positive value; the reaction is said to be endothermic.

Heat of combustion

The **heat of combustion** is the energy released as heat when a compound undergoes complete combustion reaction with O_2 under standard conditions

$$Q_{comb}^0 = -\Delta h_{comb}^0 = -\sum_{i=1}^{NS} \nu_i \Delta h_{fi}^0$$



$$Q_{comb,CH_4}^0 = -(74.85 - 393.5 - 2 \times 241.8) = 802.2 \text{ kJ/mol} = 191.7 \text{ kcal/mol} = 11960 \text{ kcal/kg}_{CH_4}$$



$$Q_{comb,C_2H_6}^0 = -(84.81 - 2 \times 393.5 - 3 \times 241.8) = 1427.6 \text{ kJ/mol} = 341.0 \text{ kcal/mol} = 11400 \text{ kcal/kg}_{C_2H_6}$$



$$Q_{comb,C_3H_8}^0 = -(103.8 - 3 \times 393.5 - 4 \times 241.8) = 2043.0 \text{ kJ/mol} = 488.0 \text{ kcal/mol} = 11100 \text{ kcal/kg}_{C_3H_8}$$



$$Q_{comb,C_4H_{10}}^0 = -(127.1 - 4 \times 393.5 - 5 \times 241.8) = 2656.0 \text{ kJ/mol} = 634.5 \text{ kcal/mol} = 10940 \text{ kcal/kg}_{C_4H_{10}}$$

Heat of combustion @298 K and 1 bar

Table 1.4. Heats of combustion at 25°C and constant pressure

Formula (gas)	Name	\bar{q}_p (kcal/mol)	Lower heating value [H ₂ O(g)] (cal/g)
Hydrogen	H ₂	57.80	28672.3
Methane	CH ₄	191.85	11958.7
Methanol	CH ₃ O	152.55	4760.9
Carbon Monoxide	CO	67.65	2415.2
Acetylene	C ₂ H ₂	300.40	11553.8
Ethylene	C ₂ H ₄	316.20	11271.2
Ethane	C ₂ H ₆	341.30	11350.3
Allene	C ₃ H ₄	443.25	11063.3
Propyne	C ₃ H ₄	441.95	11030.9
Cyclopropane	C ₃ H ₆	468.25	11127.4
Propane	C ₃ H ₈	488.35	11074.6
1,3-Butadiene	C ₄ H ₆	575.90	10646.7
<i>n</i> -Butane	C ₄ H ₁₀	635.20	10928.5
<i>n</i> -Pentane	C ₅ H ₁₂	781.95	10837.8
Benzene	C ₆ H ₆	757.50	9697.4
Cyclohexane	C ₆ H ₁₂	881.60	10475.1
<i>n</i> -Hexane	C ₆ H ₁₄	929.00	10780.1
Toluene	C ₇ H ₈	901.55	9784.5
<i>n</i> -Heptane	C ₇ H ₁₆	1075.85	10736.6
<i>o</i> -Xylene	C ₈ H ₁₀	1046.00	9852.4
<i>n</i> -Octane	C ₈ H ₁₈	1222.70	10703.8
iso-Octane	C ₈ H ₁₈	1219.10	10672.2
<i>n</i> -Hexadecane	C ₁₆ H ₃₄	2397.80	10588.8

Oxygen presence inside the fuel reduces the heating value

Aromatics
~9700 kcal/kg

Heat of combustion are similar for homologous Fuels.

E.g.

Alkanes
LHV = 10500-11000 kcal/kg

Law, C. K. (2006). *Combustion Physics*. Cambridge University Press.

Heating value

Heating value is the heat release per unit mass when the fuel (at 25°C and 1 atm) reacts completely with O₂ and the products are returned at 25 °C. It corresponds to the heat of combustion in the same conditions.

The **higher heating value (HHV)** refers to liquid water, while the **Lower Heating Value (LHV)** refers to non condensed water:

$$LHV = HHV - \frac{m_{H_2O}}{m_{fuel}} h_{fg}$$

where h_{fg} is the latent heat of vaporization of water at 25°C (2440 kJ/kg ~583 kcal/kg)



$$Q_{comb}^0 = LHV = 11960 \text{ (kcal/kg)}$$

$$HHV = LHV + \frac{m_{H_2O}}{m_{fuel}} h_{fg} = 11960 + \frac{2 \times 18}{16} 583 = 13300$$

Several databases containing LHV and HHV of most of the fuels are available

Specific Enthalpy of a compound

Specific enthalpy of a compound at a state other than the standard state can be evaluated by adding the specific enthalpy change ΔH between the standard state and the state of interest to the enthalpy of formation

$$h(T, p) = \Delta h_f^0 + [h(T, p) - h(T_{ref}, p_{ref})] = \Delta h_f^0 + \Delta h$$

Defining the specific heat at constant pressure $c_p = \frac{dh}{dT}$

$$\Delta h = \int_{T_{ref}}^T c_p dT$$

Specific heat is needed to evaluate enthalpy of reaction at temperatures different from the standard ones

Standard Entropy

Entropy (S) measures the number of possible microscopic arrangements or states of individual atoms and molecules of a system that comply with the macroscopic condition of the system.

Thus, entropy affects in some way the reaction rate. We will see how.

The entropy of a pure crystalline substance is zero at the absolute zero of temperature, 0 K (*third law of thermodynamics*).

Standard entropy (S^0) refers to a temperature of 298 K and 1 atm pressure (i.e. the entropy of a pure substance at 298 K and 1 atm pressure).

When comparing standard molar entropies for a substance that is either a solid, liquid or gas at 298 K and 1 atm pressure, the gas has more entropy than the liquid, and the liquid has more entropy than the solid.

Unlike *enthalpies of formation*, standard molar entropies of elements are not 0.

The entropy change in a chemical reaction is given by the sum of the entropies of the products minus the sum of the entropies of the reactants.

Entropy change for ideal gas

From thermodynamics: $ds = \frac{dh}{T} - \frac{v}{T} dp$ Being v the molar volume

Ideal gas: $pv = RT$ $dh = c_p dT$

$ds = c_p \frac{dT}{T} - R \frac{dp}{p}$ In case of isobaric process: $ds = c_p \frac{dT}{T}$

$$\Delta s = s(T_2, p_2) - s(T_1, p_1) = \int_{T_1}^{T_2} c_p \frac{dT}{T} - R \ln \frac{p_2}{p_1}$$

Standard entropy @ 1 atm and temperature T
(generally tabulated at 298 K for many gases) $s^0 = \int_0^T c_p \frac{dT}{T}$

$$\begin{aligned} \Delta s = s(T_2, p_2) - s(T_1, p_1) &= \int_{T_1}^{T_2} c_p \frac{dT}{T} - R \ln \frac{p_2}{p_1} = \int_0^{T_2} c_p \frac{dT}{T} - \int_0^{T_1} c_p \frac{dT}{T} - R \ln \frac{p_2}{p_1} \\ &= s^0(T_2) - s^0(T_1) - R \ln \frac{p_2}{p_1} = \Delta s^0 - R \ln \frac{p_2}{p_1} \end{aligned}$$

Thermodynamics data

Mechanism development thus needs: enthalpy entropy and specific heat of reactants and products.

Tables

JANAF Thermochemical Tables 3rd ed., vols. 1-2, M.W. Chase, American Chemical Society, 1986, SELREF/QD516.D695 1986

Pedley, J. B.; Naylor, R. D.; Kirby, S. P. Thermochemical Data of Organic Compounds: Chapman & Hall, London, 1986.

Tables TRC (Thermodynamics Research Center) Thermodynamic Tables - Hydrocarbons - Department of Chemistry, Texas A&M University

On-line databases

NIST Webbook : <http://webbook.nist.gov>

Computational Chemistry Comparison and Benchmark Data Base <http://srdata.nist.gov/cccbdb/>

Third Millennium Ideal Gas and Condensed Phase Thermochemical Database for Combustion (Burcat) : <http://garfield.chem.elte.hu/Burcat/burcat.html>

Active Thermochemical Tables (ATcT) from Ruscic et al., Argonne National Lab <https://atct.anl.gov/>

Standard format

In the NASA 'format', seven coefficients are provided for two temperature ranges. Data are given in the following form, with the temperatures in Kelvin:

Name	Elements	T_{\min}	T_{\max}	T_{junction}			
N2	2N 0C 0H 0O 0G	0300.00	5000.00	1000.00	1		
		2.9266400E+00	1.4879770E-03	-5.6847603E-07	1.0097040E-10	-6.7533509E-15	2
		-922.76760E+00	5.9805290E+00	3.2986770E+00	1.4082399E-03	-3.9632218E-06	3
		5.6415148E-09	-2.4448340E-12	-1020.9000E00	3.9503720E+00		4

High temperature coefficients Low temperature coefficients

Two expressions for **high** ($T_{\text{junction}} - T_{\max}$) and **low** ($T_{\min} - T_{\text{junction}}$) temperatures

$$\frac{c_p}{R} = a_1 + a_2T + a_3T^2 + a_4T^3 + a_5T^4$$

$$\frac{c_p}{R} = a_8 + a_9T + a_{10}T^2 + a_{11}T^3 + a_{12}T^4$$

$$\frac{H_f^0}{RT} = a_1 + \frac{a_2T}{2} + \frac{a_3T^2}{3} + \frac{a_4T^3}{4} + \frac{a_5T^4}{5} + \frac{a_6}{T}$$

$$\frac{H_f^0}{RT} = a_8 + \frac{a_9T}{2} + \frac{a_{10}T^2}{3} + \frac{a_{11}T^3}{4} + \frac{a_{12}T^4}{5} + \frac{a_{13}}{T}$$

$$\frac{S^0}{R} = a_1 \ln(T) + a_2T + \frac{a_3T^2}{2} + \frac{a_4T^3}{3} + \frac{a_5T^4}{4} + a_7$$

$$\frac{S^0}{R} = a_8 \ln(T) + a_9T + \frac{a_{10}T^2}{2} + \frac{a_{11}T^3}{3} + \frac{a_{12}T^4}{4} + a_{14}$$

P.A. Glaude. COST- Milan Summer School 2013

Benson's group additivity theory

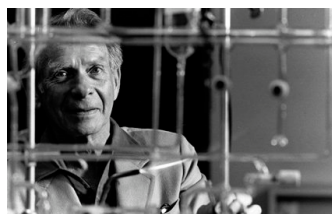
The Benson Group Additivity Method (1958, 1976) uses the experimental heat of formation for individual groups of atoms to calculate the heat of formation of new molecules.

This is a convenient way to determine theoretical heats of formation, when experimental data are not available.

Heats of formations are related to bond dissociation energies (BDE) and are important in understanding chemical structure and reactivity.

The theory is old, but still useful as one of the best methods aside from computational methods such as molecular mechanics.

Further developments also refer to Yoneda (1978), Joback (1984), Constantinou and Gani (1994).



Prof. Sidney W. Benson (1918-2011)

Benson's groups

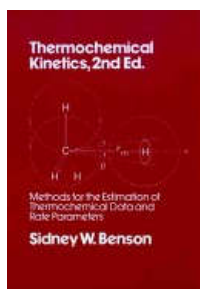


Table A.1. Group Values for ΔH_f° , S_{int}° , and C_p° , Hydrocarbons

Group	ΔH_f° 298	S_{int}° 298	C_p°					
			300	400	500	600	800	1000
C-(H) ₃ (C)	-10.20	30.41	6.19	7.84	9.40	10.79	13.02	14.77
C-(H) ₂ (C) ₂	-4.93	9.42	5.50	6.95	8.25	9.35	11.07	12.34
C-(H)(C) ₃	-1.90	-12.07	4.54	6.00	7.17	8.05	9.31	10.05
C-(C) ₄	0.50	-35.10	4.37	6.13	7.36	8.12	8.77	8.76
C _q -(H) ₂	6.26	27.61	5.10	6.36	7.51	8.50	10.07	11.27
C _q -(H)(C)	8.59	7.97	4.16	5.03	5.81	6.50	7.65	8.45
C _q -(C) ₂	10.34	-12.70	4.10	4.61	4.99	5.26	5.80	6.08
C _q -(C _q)(H)	6.78	6.38	4.46	5.79	6.75	7.42	8.35	8.99
C _q -(C _q)(C)	8.88	-14.6	(4.40)	(5.37)	(5.93)	(6.18)	(6.50)	(6.62)
[C _q -(C _q)(H)]	6.78	6.38	4.46	5.79	6.75	7.42	8.35	8.99
C _q -(C _n)(C)	8.64	(-14.6)	(4.40)	(5.37)	(5.93)	(6.18)	(6.50)	(6.62)
[C _q -(C _q)(H)]	6.78	6.38	4.46	5.79	6.75	7.42	8.35	8.99
C _q -(C _n) ₂	8.0							
C _q -(C _q) ₂	4.6							

These group contributions often need to be corrected for further interactions such as
 cis, trans interactions,
 ring-strain in cyclic molecules.....

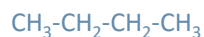
Values for these corrections are always discussed in Benson (1976).

Benson, Sidney William. Thermochemical Kinetics. Wiley, 1976.

Group additivity method: examples

Group	ΔH_f° 298	S_{int}° 298	C_p°					
			300	400	500	600	800	1000
C-(H) ₃ (C)	-10.20	30.41	6.19	7.84	9.40	10.79	13.02	14.77
C-(H) ₂ (C) ₂	-4.93	9.42	5.50	6.95	8.25	9.35	11.07	12.34
C-(H)(C) ₃	-1.90	-12.07	4.54	6.00	7.17	8.05	9.31	10.05
C-(C) ₄	0.50	-35.10	4.37	6.13	7.36	8.12	8.77	8.76

n-butane



2 groups C-(H)₃-C

2 groups C-(H)₂-(C)₂

$$\Delta H_{f,nC4H10}^0 = 2 \cdot (-10.2) + 2 \cdot (-4.93) = -30.26$$

Reference value -30.1 Kcal/mol

n-heptane



2 groups C-(H)₃-C

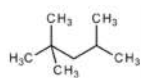
5 groups C-(H)₂-(C)₂

$$\Delta H_{f,nC7}^0 = 2 \cdot (-10.2) + 5 \cdot (-4.93) = -45.05$$

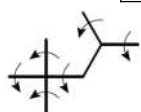
Reference value -45.0 Kcal/mol

Less simple example

Iso-octane: 2,2,4-tri-methyl-pentane



group	number	DH° (298K) kcal/mol	S° (298K) cal/mol/K	Cp° (298K) cal/mol/K
C-(H) ₃ (C)	5	-10.098	30.423	6.15
C-(H) ₂ (C) ₂	1	-4.930	9.357	5.47
C-(H)(C) ₃	1	-0.280	-12.808	4.80
C-(C) ₄	1	4.590	-35.720	3.95
CH ₃ q/t	5	-0.43	0	0
symmetries			-R ln729	
total		-53.26	99.85	44.97



Symmetries

$$3^{5+1}=729$$

P.A. Glaude. COST- Milan Summer School 2013

Benson's group additivity software

THERM Ritter and Bozzelli (1991)

Decomposition into groups and corrections done by the user

NIST database program Stein et al. (1991) Webbook

THERGAS C. Muller, V. Michel, G. Scacchi and G. M. Côme (1995)

CRANIUM : groups of Joback, estimation of other properties

(T_{eb} , T_{fus} , T_c , P_c ...)

P.A. Glaude. COST- Milan Summer School 2013

Problems with group additivity

While the group additivity method is intuitively simple, it has its drawbacks stemming from the need to consider higher-order correction terms for a large number of molecules. Take cyclopentane as an example, the addition of group contributions yields $H^{\circ} = -103$ kJ/mol, yet the experimental value is -76 kJ/mol. The difference is caused by the ring strain, which is not accounted for in the group value of C-(C2,H2) obtained from unstrained, straight-chain alkane molecules.

Cyclics are the biggest problem for group additivity, but some other species also do not work well, e.g. some halogenated compounds, and some highly branched compounds. Very small molecules are often unique (e.g. CO, OH), so group additivity does not help with those.

Species with different resonance forms can also cause problems, e.g. propargyl CH_2CCH can be written with a triple bond or two double bonds, which should be used when determining the groups?

From prof. Bill Green's notes

Thermodynamic properties correct evaluation

Thermodynamic properties (enthalpy, entropy and heat capacity) can be properly evaluated by performing ab initio calculations and the density-functional theory (DFT).

Ab initio methods allow determining the fundamental properties of materials based on the laws of quantum mechanics. The methods consist of the resolution of the many-body Schrödinger equation for atoms and their corresponding electrons.

We will be back about this, later...

Free Gibbs energy

Second law of thermodynamics can be expressed as “The entropy of an isolated system can only increase”

Specific Gibbs function (G) is defined as: $g = h - Ts$

A few thermodynamic manipulations allows to show that any process taking place at a specified temperature and pressure must occur in a way that:

$$dG|_{T,p} \leq 0$$

In particular, the **equilibrium state** is that with a minimum Gibbs energy

$$dG|_{T,p} = 0$$

Chemical Potential

Any extensive property of a single phase system is a function of two independent intensive properties and the size of the system

$G = G(T, p, n)$ Being n the number of moles, i.e. a measure of the size of the system

$G = G(T, p, n_1, \dots, n_S)$ In the case of a multicomponent system with n_S species

$$dG|_{T,p} = \sum_{i=1}^{n_S} \left(\frac{\partial G}{\partial n_i} \right)_{T,p,n_j} dn_i = \sum_{i=1}^{n_S} \mu_i dn_i$$

$\mu_i = \left. \frac{\partial G}{\partial n_i} \right|_{T,p,n_j} = \tilde{g}_i$ Chemical Potential is the partial molal Gibbs energy and plays a **central role in the criteria for chemical and phase equilibrium**

The **equilibrium state** $dG|_{T,p} = 0$

Can be written as $\sum_{i=1}^{n_S} \mu_i dn_i = 0$

Ideal gas mixture case

$$\mu_i = \left. \frac{\partial G}{\partial n_i} \right|_{T,p,n_j}$$

$$\left(\frac{\partial \mu_i}{\partial p} \right)_{T,n_j} = \frac{\partial}{\partial p} \left(\frac{\partial G}{\partial n_i} \right)_{T,p,n_j} = \frac{\partial}{\partial n_i} \left(\frac{\partial G}{\partial p} \right)_{T,p,n_j} = \left(\frac{\partial V}{\partial n_i} \right)_{T,p,n_j}$$

Being: $\left(\frac{\partial G}{\partial p} \right)_{T,p,n_j} = V$

In the case of **ideal gas**

$$V = \frac{RT}{p} \sum_{i=1}^{n_s} n_i$$

$$\left(\frac{\partial V}{\partial n_i} \right)_{T,p,n_j} = \frac{\partial}{\partial n_i} \left(\frac{RT}{p} \sum_{i=1}^{n_s} n_i \right)_{T,p,n_j} = \frac{RT}{p}$$

Evaluating the chemical potential of ideal gas

$$\left(\frac{\partial \mu_i}{\partial p} \right)_{T,n_j} = \frac{RT}{p} \quad \longrightarrow \quad d\mu_i = \frac{RT}{p} dp$$

Partial pressure of component p_i is $p_i = y_i p$ and, at constant composition, $dp_i = y_i dp$

Where y_i is the mole fraction of the component i in the mixture.

$$d\mu_i = \frac{RT}{p} dp = \frac{RT}{p_i} y_i dp = \frac{RT}{p_i} dp_i = RT d\ln(p_i)$$

Integrating this equation:

$$\mu_i = \mu_i^0 + RT \ln(p_i) = \mu_i^0 + RT \ln(py_i)$$

where $\mu_i^0 = \widetilde{g}_i^0$

Is the chemical potential (equal to the partial molal Gibbs energy) calculated at temperature T and pressure of 1 atmosphere

System component changes

Let's consider a closed system at T and p where a chemical reaction occurs



System composition can be expressed as a function of just one parameter (λ)

$$n_A = n_A^0 - \lambda v_A \quad n_B = n_B^0 - \lambda v_B \quad n_C = n_C^0 + \lambda v_C \quad n_D = n_D^0 + \lambda v_D$$

Or generically: $n_i = n_i^0 + \lambda v_i$

λ is the **extent** (or advancement) **of a reaction**, which measures the progress of the reaction and has units of moles

$$dn_i = v_i d\lambda$$

The **equilibrium state** $dG|_{T,p} = 0$ becomes

$$\sum_{i=1}^{n_S} \mu_i dn_i = \sum_{i=1}^{n_S} \mu_i v_i d\lambda = d\lambda \sum_{i=1}^{n_S} \mu_i v_i = \sum_{i=1}^{n_S} \mu_i v_i = 0$$

Equation of reaction equilibrium

Solving this equation is possible to determine the equilibrium composition at T and p

Equilibrium of ideal gas mixture

$$\sum_{i=1}^{n_S} \mu_i v_i = 0 \quad \text{In the case of ideal gas, we got} \quad \mu_i = \mu_i^0 + RT \ln(p_i)$$

$$\sum_{i=1}^{n_S} v_i \mu_i^0 + RT \sum_{i=1}^{n_S} v_i \ln(p_i) = 0 \quad \longrightarrow \quad \sum_{i=1}^{n_S} v_i \mu_i^0 = -RT \sum_{i=1}^{n_S} \ln p_i^{v_i} = -RT \ln \prod_{i=1}^{n_S} p_i^{v_i}$$

$$\sum_{i=1}^{n_S} v_i \mu_i^0 = \Delta G^0 \quad \text{Change in the Gibbs energy for the reaction at temperature T and pressure of 1 atm.}$$

$$\Delta G^0 = -RT \ln \prod_{i=1}^{n_S} p_i^{v_i}$$

$$e^{-\Delta G^0/RT} = \prod_{i=1}^{n_S} p_i^{v_i} = K_p = \frac{p_C^{v_C} p_D^{v_D}}{p_A^{v_A} p_B^{v_B}}$$

K_p is the **equilibrium constant** for partial pressures of the reaction, which can be evaluated from ΔG^0 and $\Delta G^0 = \Delta H^0 - T\Delta S^0$

Equilibrium constant for molar concentration

Ideal gas mixture:

$$c_i = \frac{n_i}{V} = RTp_i \quad c_i \text{ is the concentration (mol/m}^3\text{) of the species } i \text{ in the mixture}$$

$$K_p = \prod_{i=1}^{n_S} p_i^{\nu_i} = \prod_{i=1}^{n_S} \left(\frac{c_i}{RT}\right)^{\nu_i}$$

$$K_c = \prod_{i=1}^{n_S} (c_i)^{\nu_i} \quad K_c \text{ is the } \mathbf{equilibrium constant} \text{ for molar concentrations of the reaction}$$

$$K_c = K_p (RT)^{\sum_{i=1}^{n_S} \nu_i}$$

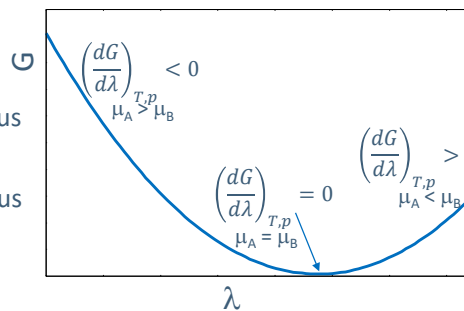
Spontaneous reactions



$$\left(\frac{dG}{d\lambda}\right)_{T,p} < 0 \quad \text{Reaction } A \rightarrow B \text{ is spontaneous}$$

$$\left(\frac{dG}{d\lambda}\right)_{T,p} > 0 \quad \text{Reaction } B \rightarrow A \text{ is spontaneous}$$

$$\left(\frac{dG}{d\lambda}\right)_{T,p} = 0 \quad \text{Equilibrium. Reaction stops}$$



In general, looking at the reaction:

$\Delta G < 0$: **spontaneous reactions.**

$\Delta G = 0$: Equilibrium conditions.

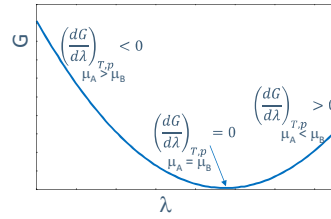
$\Delta G > 0$: Not spontaneous reactions.

Equilibrium composition

$$dG = \sum_{i=1}^{n_S} \mu_i dn_i = \sum_{i=1}^{n_S} (\mu_i^0 + RT \ln p_i) dn_i$$

$$dn_i = \nu_i d\lambda$$

$$dG = \sum_{i=1}^{n_S} (\nu_i \mu_i^0 + RT \nu_i \ln p_i) d\lambda$$



$$\frac{dG}{d\lambda} = \Delta G^0 + RT \sum_{i=1}^{n_S} \ln p_i^{\nu_i} = 0$$

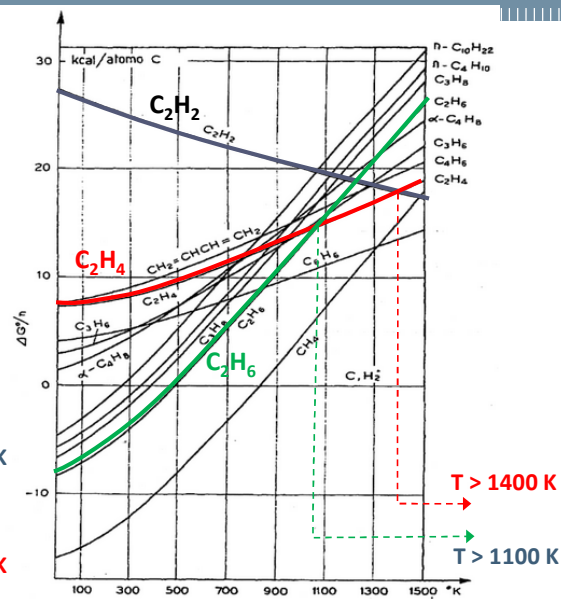
Equation of reaction equilibrium Solving this system of equations in p_i (or n_i) is possible to determine the equilibrium composition at T and p

It is more convenient from the numerical point of view to minimize the function, instead of solving the system

It is key to recognize that the n_i in equation are not independent variables. They are constrained such that the number of moles of each element in the system must remain constant. Specific algorithm can be conveniently adopted, like Lagrangian multipliers.

Codes are available to find the equilibrium composition: GASEQ, Cantera, OpenSMOKE++, CHEMKIN

An example: Francis diagram



Dehydrogenation reaction of ethane
 $C_2H_6 \leftrightarrow C_2H_4 + H_2$ is favored at $T > 1100$ K

Dehydrogenation reaction of ethylene
 $C_2H_4 \leftrightarrow C_2H_2 + H_2$ is favored at $T > 1400$ K

Vant'Hoff equation

$$d\left(\frac{G}{T}\right)_{p,n_i} = \frac{TdG - GdT}{T^2} = \frac{T(-SdT) - GdT}{T^2} = -\frac{(TS + G)dT}{T^2}$$

$$G = H - TS \quad H = G + TS$$

$$d\left(\frac{G}{T}\right)_{p,n_i} = -\frac{HdT}{T^2}$$

At assigned pressure and number of mole, the Gibbs energy is only function of the temperature, thus it is possible to evaluate the differential of its ratio with T

$$d\left(\frac{G}{T}\right)_{p,n_i} = \left(\frac{\partial(G/T)}{\partial T}\right)_{p,n_i} dT$$

From the two previous equations:

$$\left(\frac{\partial(G/T)}{\partial T}\right)_{p,n_i} dT = -\frac{HdT}{T^2} \longrightarrow \left(\frac{\partial(G/T)}{\partial T}\right)_{p,n_i} = -\frac{H}{T^2}$$

Vant'Hoff equation

Temperature effect on equilibrium constant

$$\left(\frac{\partial(\Delta G^0/T)}{\partial T}\right)_{p,n_i} = -\frac{\Delta H^0}{T^2}$$

$$\Delta G^0 = -RT \ln K_p$$

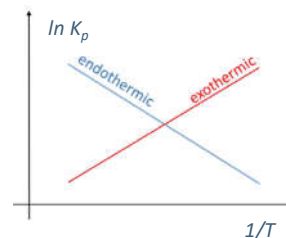
$$R \left(\frac{d \ln K_p}{dT}\right)_{p,n_i} = \frac{\Delta H^0}{T^2}$$

If it possible to assume that ΔH^0 is constant (generally not true)

$$\frac{\ln K_p(T_2)}{\ln K_p(T_1)} = \frac{\Delta H^0}{R} \left(\frac{1}{T_1} - \frac{1}{T_2}\right)$$

A more general case ΔH^0 not constant

$$R \ln K_p = -\frac{\Delta H^0(0K)}{T^2} + A \ln T + \frac{B}{2} T + \frac{C}{6} T^2 + \dots$$



For **endothermic reactions** the equilibrium constant increases with the temperature

For **exothermic reactions** the equilibrium constant decreases with the temperature

Le Chatelier Principle

If a dynamic equilibrium is disturbed by changing the conditions, the position of equilibrium moves to partially reverse the change.

- An **increase of temperature** decreases the equilibrium constant of *exothermic reactions*, whereas, increases the K value of *endothermic reactions*.
- An **increase of pressure** (due to decreasing volume) shifts the reaction to the side with the fewer moles of gas. A decrease of pressure due to increasing volume causes the reaction to shift to the side with more moles of gas.

Equilibrium tries to counteract the imposed changes in temperature and pressure!

At high T, the stable products from a C/H/O reaction system can dissociate. Endothermic dissociation reactions are favored at High Temperatures:

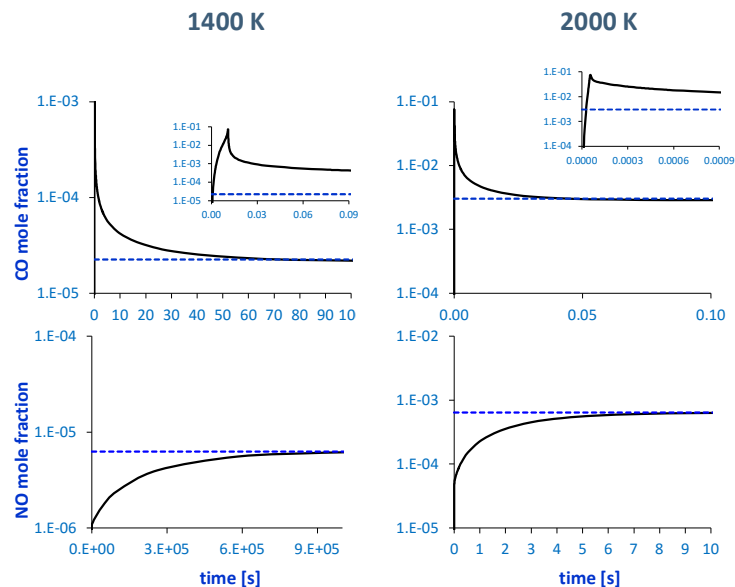
	T _{diss} (K)		T _{diss} (K)
CO ₂ ⇌ CO + 0.5 O ₂	1930	H ₂ ⇌ 2H	2430
H ₂ O ⇌ H + OH	2080	O ₂ ⇌ 2O	2570
H ₂ O ⇌ H ₂ + 0.5 O ₂	2120	N ₂ ⇌ 2N	3590

T_{diss} is the temperature where dissociation becomes higher than 1%, at 1 atm.

At higher pressures, dissociation reactions are less favored.

Approaching the equilibrium

Isothermal methane combustion at atmospheric pressure and stoichiometric conditions



Recap

- ✓ Enthalpy of formation: index of species stability
- ✓ Enthalpy of formation is a state function: independent of the transformation story
- ✓ Specific heat allows to move from the standard conditions to different temperature conditions
- ✓ Heat of reaction: opposite of the enthalpy change of a reaction
- ✓ Heating value: heat released from a fuel completely oxidized (LHV, HHV)
- ✓ Standard entropy: measure of the disorder of the system (atoms)
- ✓ Free Gibbs energy ($g = h - Ts$)
- ✓ Equilibrium state $dG = 0$
- ✓ Minimizing the constrained Free Gibbs energy allows to find the equilibrium composition
- ✓ Equilibrium constant can be determined from enthalpy and entropy
- ✓ Temperature, pressure and initial composition affect the equilibrium constant

Kinetics and reaction rates

Kinetics and time-dependent system

Species mass balance defines the species evolution in time.

In a closed, isothermal and isobaric system, the mass balance of i -th species can be written as:

$$\frac{dc_i}{dt} = R_i \quad i = 1, \dots, n_S$$

- c_i is the molar density (concentration)
- R_i is the rate of formation/disappearance of i
- n_S is the total number of species

$$R_i = \sum_{j=1}^{n_R} \nu_{ij} R_j \quad i = 1, \dots, n_S$$

- ν_{ij} is the stoichiometric coefficient of species i in reaction j
- R_j is the reaction rate of reaction j
- n_R is the total number of reactions

The kinetic system of ordinary differential equations (ODEs) defines the relationship between the production rates of the species and rates of the reaction steps.

From the numerical point of view, the solution of the system can be challenging because of the possible large number of species and of the stiffness (very different characteristic times among the species)

Combustion kinetics

Combustion is a high-temperature **exothermic** redox chemical **reaction** between a fuel (the reductant) and an oxidant, usually atmospheric oxygen, that produces oxidized, often gaseous products, in a mixture termed as smoke. Combustion does not always result in fire, because a flame is only visible ~~when substances~~ ~~undergoing combustion~~ ~~vaporize~~, but when it does, a flame is a characteristic indicator of the reaction. While the activation energy must be overcome to initiate combustion (e.g., using a lit match to light a fire), the heat from a flame may provide enough energy to make the reaction self-sustaining.

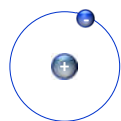
Combustion is ~~often~~ a complicated sequence of **elementary radical reactions**

[From Wikipedia](#)

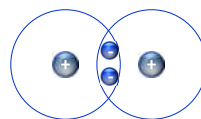
Radicals

Free **radical** is a molecule having **unpaired electrons**:

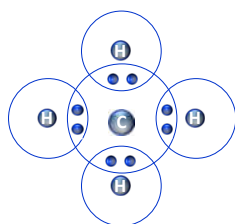
- are unstable
- react quickly with other compounds
- a single molecule can have several unpaired electrons, notably oxygen which can be thought of as a bi-radical
- rarely occur in nature



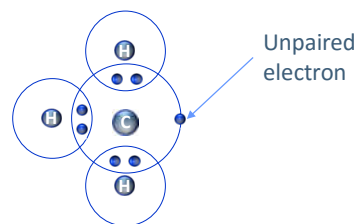
H atom: radical



H₂ molecule: stable species



Methane (CH₄) molecule: stable species



Methyl (CH₃) radical

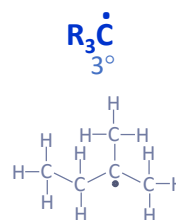
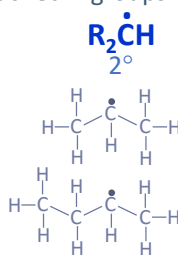
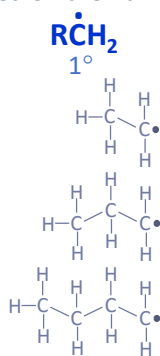
Radical types

Homolytic bond cleavage leads to the formation of radicals

Single headed arrows are usually used to show the movement of single electrons

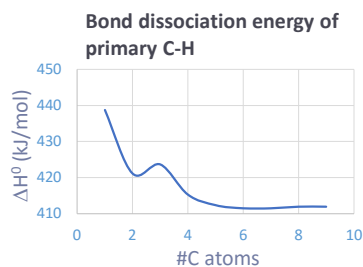
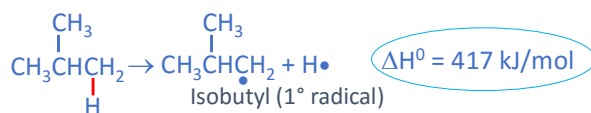
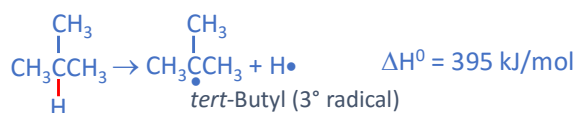
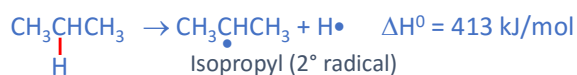
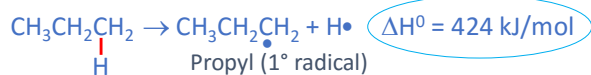


Alkane radicals (alkyl) are categorized as primary (1°), secondary (2°) and tertiary (3°) based on the number of attached R groups.

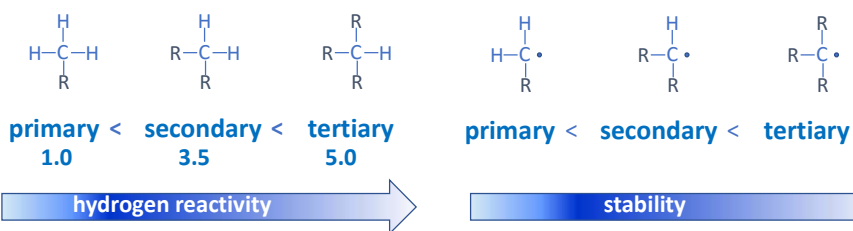


Radical stability

Bond dissociation energy is used as a measure of radical stability.



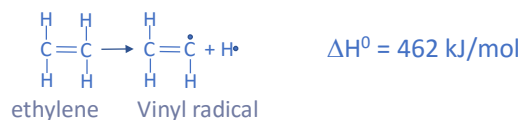
Radical reactivity



Relative bond energy reactivity reflects the radical stability

Vinyl radical

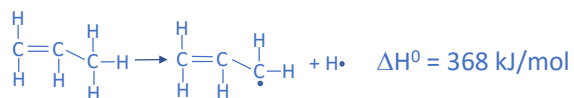
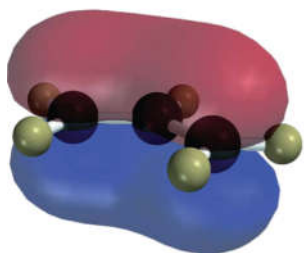
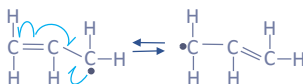
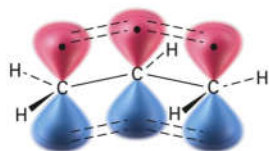
Presence of double bonds significantly affects the formed radicals and their stability



C-atoms involved in double bonds present a sp^2 hybridization (instead of the sp^3 of alkane). As the s -character of the orbital containing the free radical is increased, the half-filled orbital containing the free radical is held more closely to the nucleus. This actually *destabilizes* the species, because being closer to the nucleus, the electron affinity of the orbital will increase.

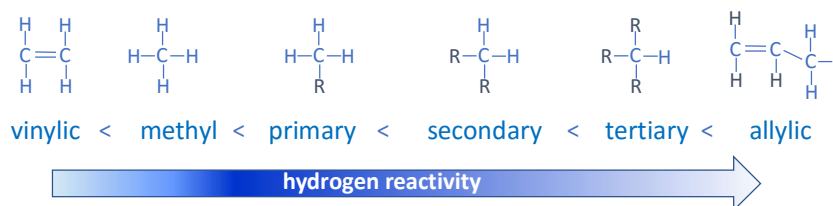
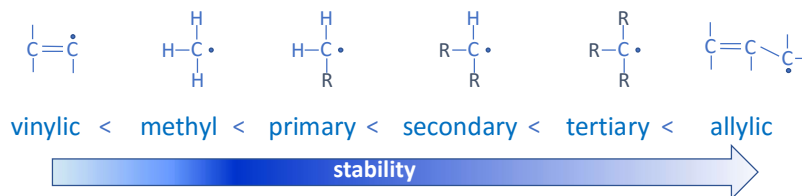
Allyl radical

- Three electrons are delocalized over three carbons. Allyl radicals are more stable than alkyl radicals due to resonance effects - an unpaired electron can be delocalized over a system of conjugated pi bonds.
- Spin density surface shows single electron is dispersed

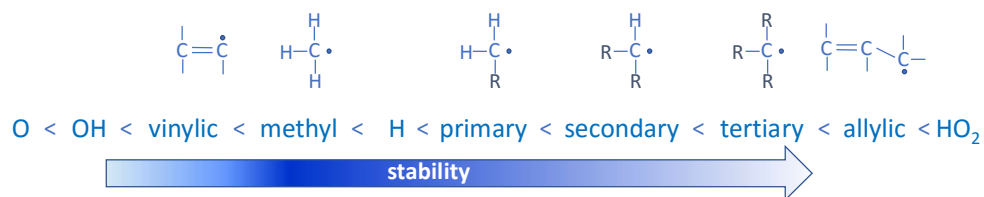


Radical stability

Summarizing previous slides:



Inorganic radical stability



Typical bond energies (kJ/mol)

atom or group	methyl CH ₃	ethyl C ₂ H ₅	<i>i</i> -propyl (CH ₃) ₂ CH	<i>n</i> -butyl (CH ₂) ₃ C	phenyl C ₆ H ₅	benzyl C ₆ H ₅ CH ₂	allyl C ₃ H ₅	acetyl CH ₃ CO	vinyl C ₂ H ₃	ethynyl C ₂ H
H	439	420	413	400	474	375	369	377	465	547
OH	384	392	400	398	473	339	332		464	552
CH ₃	375	369	370	362	435	323	317	352	424	516
C ₂ H ₅	369	364	363	353	428	318		346	419	510
(CH ₃) ₂ CH	370	363	358	343	425	319		341		510
(CH ₃) ₃ C	362	353	343	322	410			327		498
C ₆ H ₅	435	428	425	410	496	381		414	491	588
C ₆ H ₅ CH ₂	323	318	319		381	278		290		

Radical mechanism

Initiation reactions from stable species initially create radical species. In most cases, this is a homolytic cleavage event, and takes place rarely due to the high energy barriers involved

Propagation reactions are the 'chain' part of chain reactions. Once a reactive free radical is generated, it can react with stable molecules to form new free radicals.

Chain termination reactions occur when two free radicals react with each other to form a stable, non-radical adduct. This is a very thermodynamically favored event, it is also rare due to the low concentration of radical species, which hardly collide with one another

Initiation reactions

Homolytic bond cleavage



Symmetrical bond-cleavage forming two free radicals. One unpaired bonding electron stays with each product



H-abstraction from a stable molecule



A stable molecule abstracts a hydrogen from another stable molecules forming two free radicals.



Propagation reactions

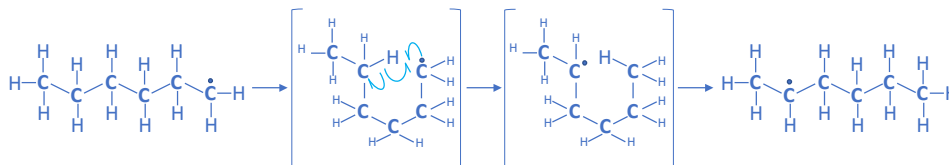
Radical transfer: H abstraction



A radical can break a bond in another molecule and abstract a partner with an electron, giving substitution in the original molecule



Radical inter-transfer: isomerization



A radical can break a bond in the same molecule and abstract a partner with an electron, moving the free radical position



Propagation reactions

β -decomposition



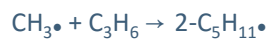
A radical can break a bond in β position forming a smaller radical and an unsaturated molecule



Radical addition

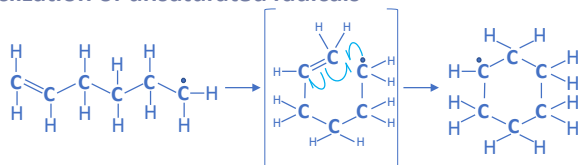


A radical can add on a double bond forming a new larger radical (reverse reaction of β -decomposition)



Propagation reactions

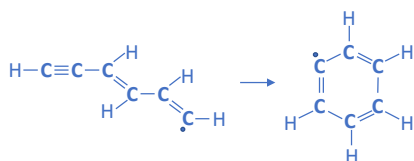
cyclization of unsaturated radicals



A radical can add on an internal double bond forming a cyclic species

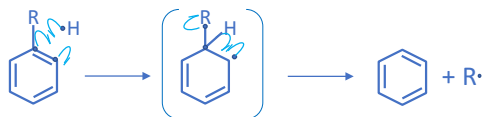


In some cases this reaction can be very important and favored, like in the formation of aromatic radicals



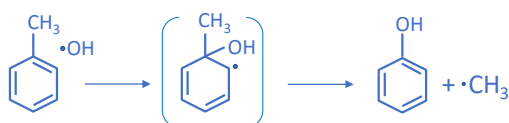
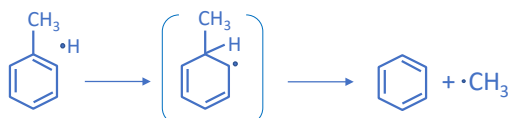
Propagation reactions

Ipso-addition



This reaction class occurs on aromatics. It is the sum of an addition reaction on double bonds, directly followed by a β -scission.

Examples

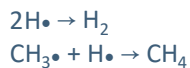


Termination reactions

Recombination



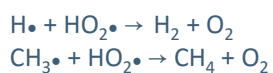
Symmetrical bond-making from two radicals. One unpaired bonding electron is donated by each reactant (reverse reaction of homolytic bond-cleavage)



Disproportionation



One radical abstracts a hydrogen atom from a second radical, which forms a double bond (reverse reaction of H-abstraction from a stable molecule)



Branching reactions

Radicals in reaction products are more than those in reactants

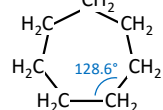
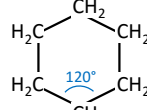
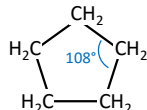
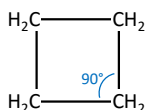
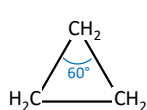
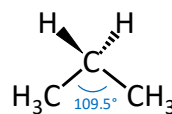


Most important **Chain Branching Reaction** in combustion



Isomerization reactions: cyclic structure stability

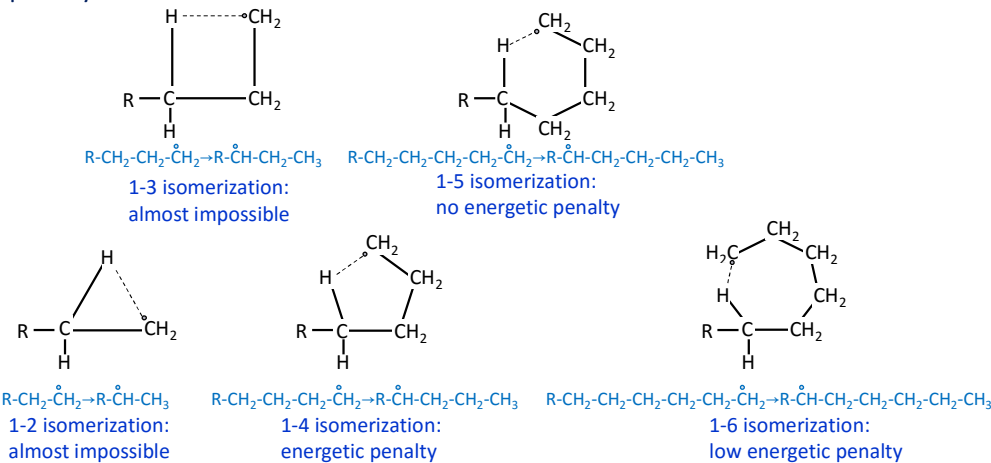
Carbon atoms sp^3 hybridized have bond angles of 109.5°



Bond angles of most of cyclic hydrocarbons are too different from the optimal one. This induces extra strains in the molecules and moves their atoms by puckering the ring, adopting non planar configurations, to reduce the angle strain.

Isomerization reactions: energetic view point

Internal isomerization are not equivalent from the energetic point of view. Some of them, those including 3, 4 member ring cyclic structure are negligible, the 5 membered ring can occur, but it is penalized. From 6 membered ring and up the penalty is low.



Isomerization reactions: entropic view point

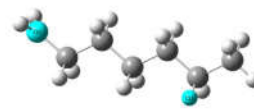
5 membered ring isomerization



6 membered ring isomerization



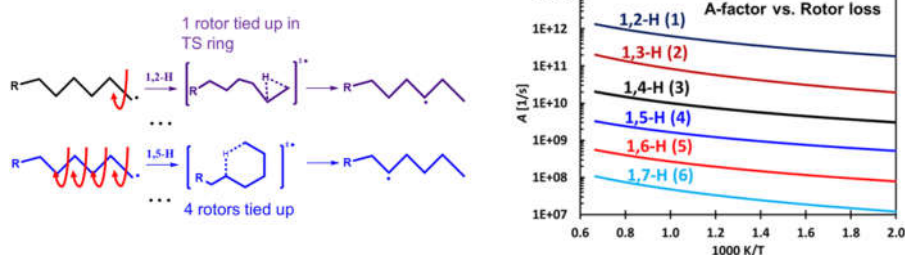
7 membered ring isomerization



Larger rings have an entropic disadvantage: a larger number of rotors must be blocked in the transition state to allow a proper configuration of the radicals. The rate coefficient gradually decreases as the cyclic chain becomes longer.

Isomerization reactions: entropic view point

The A-factors can be estimated by accounting for the number of rotors that are lost in the cyclic TS. There is a systematic decrease in the A-factor as the size of the TS ring increases and more rotors are tied up in the cyclic TS.



Following the ideas of Benson, the activation energy for the hydrogen shift reactions is the sum of the activation energy of H-abstraction reaction plus the ring strain associated with the cyclic TS.

The strain for a 3- and 4-member rings are 24-26 kcal/mol.

Mainly 1,4-H, 1,5-H, and 1,6-H shift reactions are effective

Wang and Dean (2018). Rate Rules and Reaction Classes.

Reaction rate definition

The **reaction rate** of the reaction j (R_j) is the speed at which a chemical reaction takes place.

It is proportional to the increase in the concentration of a product per unit time and to the decrease in the concentration of a reactant per unit time.

$$R = \frac{\Delta[\text{concentration}]}{\Delta[\text{time}]}$$

$\Delta(\text{time})$ large \Rightarrow average reaction rate
 $\Delta(\text{time})$ small \Rightarrow instantaneous reaction rate.
The difference quotient becomes the derivative



$$R = -\frac{\Delta[A]}{\Delta t} = -\frac{\Delta[B]}{\Delta t} = \frac{\Delta[C]}{\Delta t} = \frac{\Delta[D]}{\Delta t}$$

Reaction rate evaluation

Reaction rate is generally evaluated from:

$$R = k(T, p) \prod_{i=1}^{n_{Sr}} c_i^{\alpha_i}$$

n_{Sr} is the number of reactants of the reaction

c_i is the molar concentration of i-th reactant (equivalent to [i])

Elementary reaction



$$R = k(T, p) c_A c_B$$

α_i is called the reaction order with respect to species i (generally experimentally determined).

For **elementary reactions**, the reaction order corresponds to the absolute value of the stoichiometric coefficient of the species i

k is the reaction rate constant (it should better to call it reaction rate coefficient).
 k may depend on T, P, and the quality and quantity of the nonreactive species present (for example an inert dilution gas or solvent).

Reaction molecularity

The molecularity of a single chemical reaction is defined as the minimum number of molecules which must interact.

The rate expression for unimolecular reactions is:

Unimolecular



$$R = k_c(T) [A]$$

$$R = \frac{\text{concentration}}{\text{time}} \quad [A] = \text{concentration}$$

units of k_c are [1/time]

Bimolecular



$$R = k_c [A]^2$$



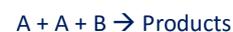
$$R = k_c [A][B]$$

units of k_c are [1/time/concentration]

Trimolecular



$$R = k_c [A]^3$$



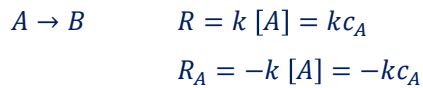
$$R = k_c [A]^2 [B]$$



$$R = k_c [A][B][C]$$

units of k_c are [1/time/concentration²]

First order reactions



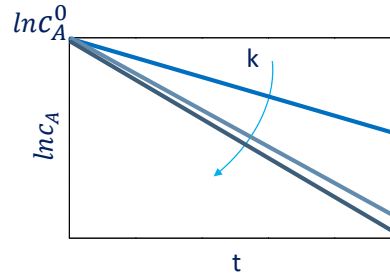
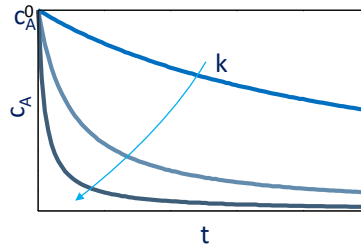
$$\frac{dc_A}{dt} = -kc_A \quad \text{Initial condition } t = 0 \quad c_A = c_A^0$$

$$\frac{dc_A}{c_A} = -kdt \quad \Rightarrow \quad \int_{c_A^0}^{c_A} \frac{dc_A}{c_A} = -k \int_0^t dt$$

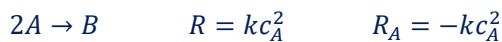
$$\ln \frac{c_A}{c_A^0} = -kt \quad \Rightarrow \quad c_A = c_A^0 e^{-kt}$$

Complete conversion only when $t \rightarrow \infty$

$$\text{Conversion: } \xi = \frac{c_A^0 - c_A}{c_A^0} \begin{cases} c_A = c_A^0 & \xi = 0 \\ c_A = 0 & \xi = 1 \end{cases}$$



Second order reactions



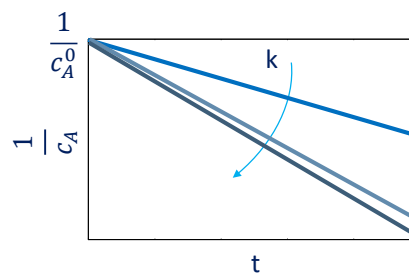
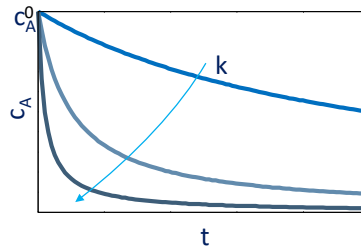
$$\frac{dc_A}{dt} = -2kc_A^2 \quad \text{Initial condition } t = 0 \quad c_A = c_A^0$$

$$\frac{dc_A}{c_A^2} = -2kdt \quad \Rightarrow \quad \int_{c_A^0}^{c_A} \frac{dc_A}{c_A^2} = -2k \int_0^t dt$$

$$-\left[\frac{1}{c_A} \right]_{c_A^0}^{c_A} = -2kt \quad \Rightarrow \quad \frac{1}{c_A} - \frac{1}{c_A^0} = 2kt$$

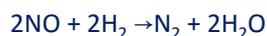
$$\Rightarrow \quad c_A = \frac{c_A^0}{1 + 2c_A^0 kt}$$

Complete conversion only when $t \rightarrow \infty$



Experimental reaction order evaluation

$$R = k[\text{NO}]^\alpha [\text{H}_2]^\beta$$



Expt.	$[\text{NO}]_0$	$[\text{H}_2]_0$	R
- 1	25	10	2.4×10^{-3}
- 2	25	5	1.2×10^{-3}
- 3	12.5	10	0.6×10^{-3}

- $R = k[\text{NO}]^\alpha [\text{H}_2]^\beta$
- $R_1 = k[25]^\alpha [10]^\beta = 2.4 \times 10^{-3}$
- $R_2 = k[25]^\alpha [5]^\beta = 1.2 \times 10^{-3}$
- $\frac{R_1}{R_2} = \left(\frac{10}{5}\right)^\beta = \frac{2.4 \times 10^{-3}}{1.2 \times 10^{-3}}$
- $(2)^\beta = 2$
- $\beta = 1$
- $R = k[\text{NO}]^\alpha [\text{H}_2]^\beta$
- $R_1 = k[25]^\alpha [10]^\beta = 2.4 \times 10^{-3}$
- $R_3 = k[12.5]^\alpha [10]^\beta = 0.6 \times 10^{-3}$
- $\frac{R_1}{R_3} = \left(\frac{25}{12.5}\right)^\alpha = \frac{2.4 \times 10^{-3}}{0.6 \times 10^{-3}}$
- $(2)^\alpha = 4$
- $\alpha = 2$

Courtesy prof. Henry Curran

Rate constant

Rate constant (k) depends on two main factors: the probability of the molecules to collide and the energy of the molecules, which has to be enough to allow the reaction to occur

The Arrhenius equation

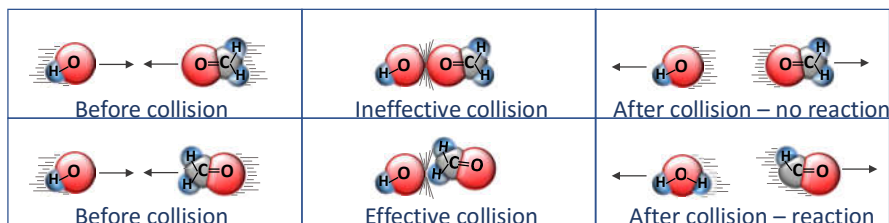
$$k = A e^{-\frac{E_a}{RT}}$$

A is the frequency factor, also called pre-exponential factor, which, according to collision theory, depends on how often molecules collide and on whether the molecules are properly oriented when they collide. It is a measure of the frequency of effective collisions among the reactants

E_a is the activation energy, which is the kinetic energy that the molecules must have to react

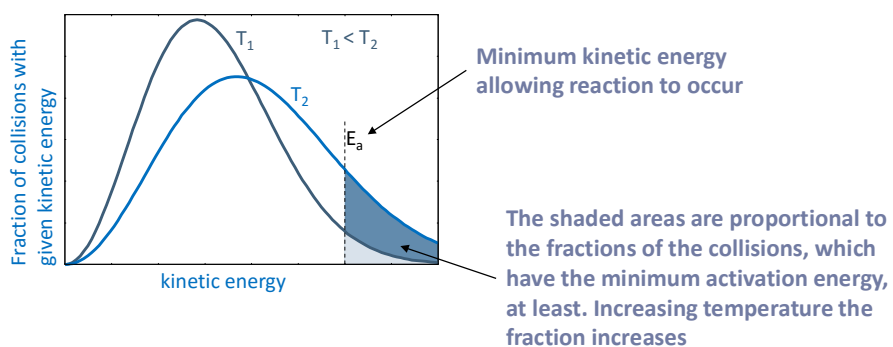
Frequency factor

molecule orientation



Activation energy

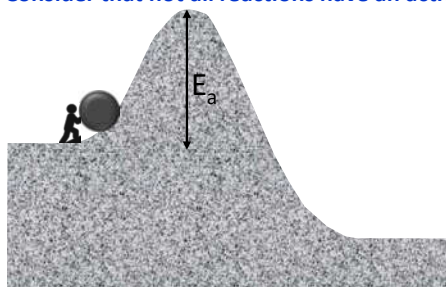
Together with proper orientation, molecules requires the proper energy.
By assuming a Boltzmann distribution of molecule kinetic energy, we know that the fraction of collisions which will have a kinetic energy high enough is $e^{-\frac{E_a}{RT}}$



Activation energy concept

According to the ancient Greek mythology, Sisyphus was a very evil king. As a punishment for his misdoings, he was supposed to roll a large stone up to the top of a long hill. A spell had been placed on the stone so that it would roll back down before reaching the top, never to complete the task. Sisyphus was condemned to an eternity of trying to get to the top of the hill, but never succeeding.

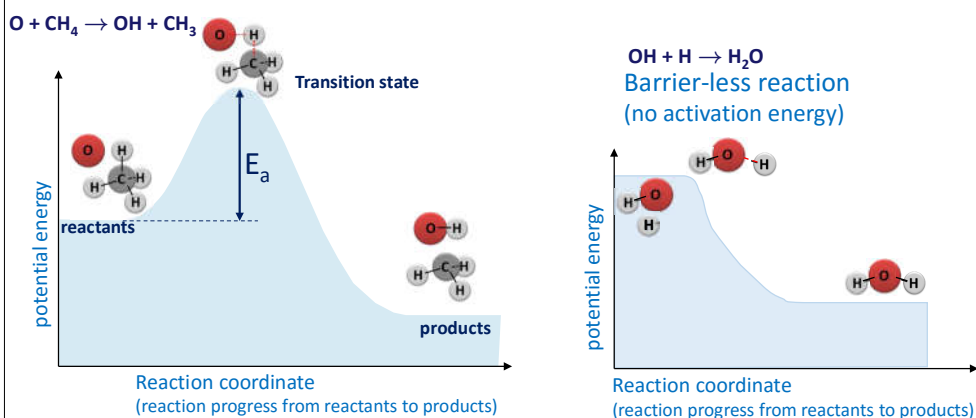
This myth (without the spell of rolling back) is sometimes used to explain the concept of the activation energy: molecules have to overcome a hill (not always long). The height of the hill is the activation energy. Contrary to Sisyphus, some molecules reach the top. Only those molecules (reactants) which have energy enough to be successful can then arrive to their final destination: the products. **Consider that not all reactions have an activation energy!**



Potential energy diagram

Potential energy diagram shows the change in potential energy of a system as reactants are converted into products.

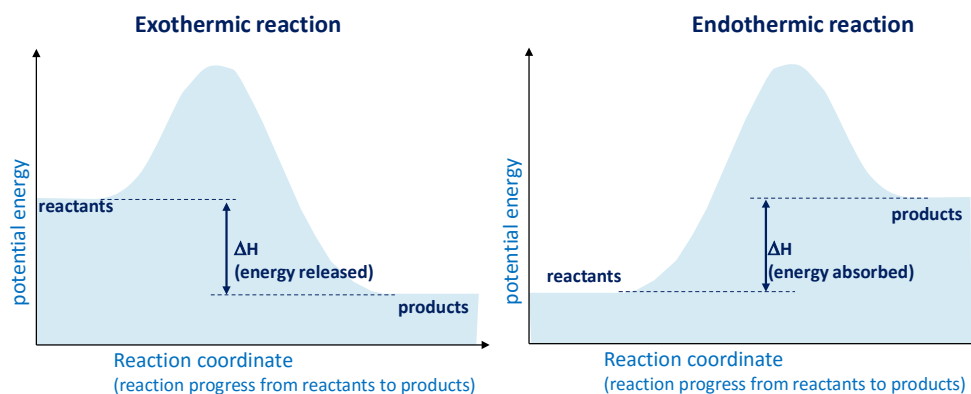
In transition-state theory, there is the formation of a state, where an activated complex in between reactants and products is formed.



Potential energy diagram and heat of reaction

The enthalpy change from reactants to products (ΔH) is negative for an exothermic reaction and positive for an endothermic reaction.

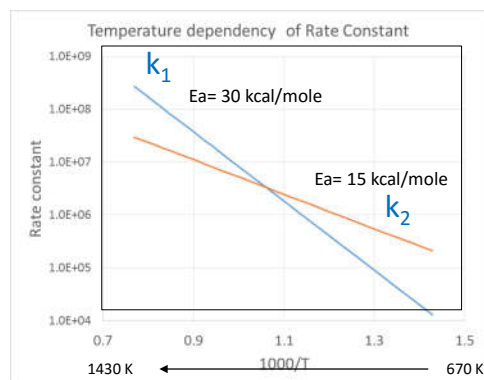
The total potential energy of the system decreases for the exothermic reaction as the system releases energy to the surroundings. The total potential energy of the system increases for the endothermic reaction as the system absorbs energy from the surroundings.



Activation Energy and Temperature Dependency

The activation energy determines the temperature dependency of reaction rates.

Arrhenius' law: $k_c = k_0 \times \exp(-E_a/RT)$ $\implies \ln k_c = \ln k_0 - (E_a/R) (1/T)$
 the plot of $\ln k$ vs $1000/T$ gives a **straight line**, where the slope is the activation energy (multiplied by gas constant).

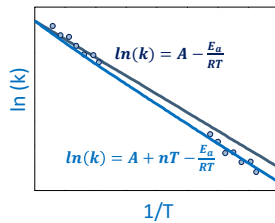


Reactions with high activation energies are very temperature-sensitive.
 All the reactions are more temperature-sensitive at low temperatures.

Modified Arrhenius equation

On relatively small temperature ranges, the classical Arrhenius equation works

$$k = Ae^{-\frac{E_a}{RT}}$$



The assumption of a frequency factor temperature independent does not allow to describe the rate constant on large temperature ranges (combustion). Moreover, it disagrees with the transition state theory, where the frequency factor depends primarily on the entropy of activation, which is slowly temperature dependent.

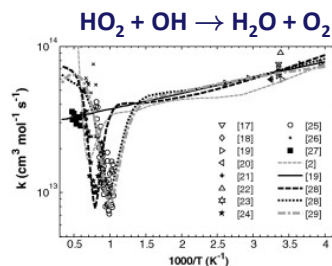
A modified Arrhenius equation is then more correctly proposed:

$$k = AT^n e^{-\frac{E_a}{RT}}$$

Where n is a parameter, which accounts for the temperature effect on the frequency factor

Duplicate reactions

Sometimes, rate constants show very unusual behaviors, which cannot be easily explained with a modified Arrhenius equations.



Burke et al., Proc. Comb. Inst., 34, 2013

In this case, the rate constant is assumed as the sum of two Arrhenius expressions

$$k = A_1 T^{n_1} e^{-\frac{E_{a1}}{RT}} + A_2 T^{n_2} e^{-\frac{E_{a2}}{RT}}$$

Brief recap

Three things must happen for a reaction to occur

- 1) Molecules must **collide**.
- 2) Molecules must collide with **enough energy**.
- 3) Molecules must collide with the **correct orientation**.

How can we modify the reaction rate?

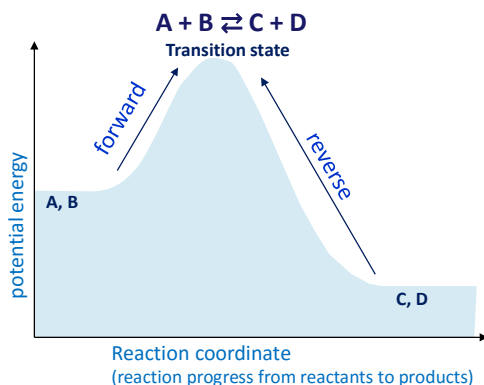
- 1) Modify **concentration**. Increasing/decreasing the concentration increases/decreases the number of collisions. The more/lesser collisions per second, the faster/slower the reaction.
- 2) Modify **temperature**. Increasing/decreasing the temperature increases/decreases the number of collisions because the molecules are moving faster/slower. It also means that more/less of the collisions have/don't have enough energy for a reaction to occur. A higher/smaller % of collisions will have enough energy

Reversible reactions

All thermal elementary reactions are **reversible**: the reaction products may react with each other to re-form the reactants.

Forward and reverse rate constants are not independent.

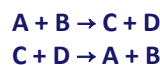
The **Micro-Reversibility Principle** states that given an elementary reaction, the reverse reaction follows the same path on the potential energy surface.



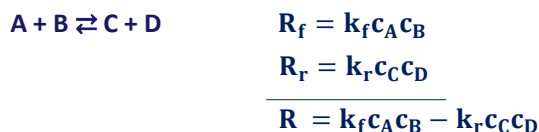
Irreversible reaction means that either the reverse reaction has been neglected



or that the reactions have been separated into forward and backwards rates.



Forward and reverse rate constants



At the equilibrium, the reaction rate is zero: composition does not change

$$\mathbf{R} = \mathbf{k}_f \mathbf{c}_A \mathbf{c}_B - \mathbf{k}_r \mathbf{c}_C \mathbf{c}_D = 0 \quad \Rightarrow \quad \frac{\mathbf{k}_f}{\mathbf{k}_r} = \frac{\mathbf{c}_C \mathbf{c}_D}{\mathbf{c}_A \mathbf{c}_B} = \mathbf{K}_c$$

From thermodynamics: $K_c = K_p (RT)^{\sum_{i=1}^{n_S} \nu_i} = e^{-\Delta G^0 / RT} (RT)^{\sum_{i=1}^{n_S} \nu_i}$

Forward and reverse rate constants are related by thermodynamics:

$$\mathbf{k}_r = \frac{\mathbf{k}_f}{\mathbf{K}_c} = \frac{\mathbf{k}_f}{e^{-\Delta G^0 / RT} (RT)^{\sum_{i=1}^{n_S} \nu_i}}$$

Pressure dependent reaction



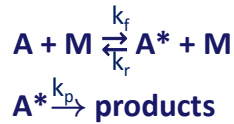
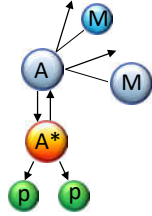
https://chem.libretexts.org/Courses/University_of_Arkansas_Little_Rock/Chem_1403%3A_General_Chemistry_2/Text/14%3A_Rates_of_Chemical_Reactions/14.07%3A_Reaction_Mechanisms

Originally, unimolecular reactions were thought to do not depend on molecular collisions and hence occur only by absorbing energy and forming an activated complex. This was later disproven by showing that believed unimolecular reactions do not remain first order at low pressures.

Although a unimolecular reaction is supposed by definition to involve one molecule of the reactant species only, and proceed in one step, the definition was broadened to allow mechanisms for explanation of unimolecular reactions.

Lindemann mechanism (1922)

Lindemann proposed that first-order processes occur as a result of a two-step sequence where **the reacting molecule A is first activated (A*) by collision**, then A* can decompose or could be deactivated by another collision.



M is the collision partner (generally named "third body"), which can be any of the other molecules present in the system

The rate of formation of A and A* are:

$$\begin{aligned} \frac{dc_A}{dt} &= -k_f c_A c_M + k_r c_{A^*} c_M \\ \frac{dc_{A^*}}{dt} &= k_f c_A c_M - k_r c_{A^*} c_M - k_p c_{A^*} \end{aligned}$$

Third Body

c_M is the **third body concentration** and is generally indicated as [M]
In the case of ideal gas

$$c_M = [M] = \frac{P}{RT}$$

Not all the molecules show the same effectiveness as collisional partner. Some are more effective other less effective.

Thus, when calculating the effective concentration of the third body, the collision efficiencies ε_i should also be taken into account:

$$[M] = \sum_{i=1}^{n_s} \varepsilon_i c_i$$

Steady state approximation

The **steady-state approximation** is a method, which assumes that one intermediate in the reaction mechanism is consumed as quickly as it is generated. As a consequence, its concentration remains the same in a duration of the reaction.



If A^* consumption is much faster than its formation, it cannot accumulate: its accumulation is negligible

$$\frac{dc_{A^*}}{dt} = 0$$

$$\frac{dc_{A^*}}{dt} = k_f c_A c_M - k_r c_{A^*} c_M - k_p c_{A^*} = 0$$

Overall reaction rate constant

$$\frac{dc_{A^*}}{dt} = k_f c_A c_M - k_r c_{A^*} c_M - k_p c_{A^*} = 0$$

$$c_{A^*} = \frac{k_f c_A c_M}{k_r c_M + k_p}$$

Substituting this value in the A balance: $\frac{dc_A}{dt} = -k_f c_A c_M + k_r c_{A^*} c_M$

$$\frac{dc_A}{dt} = -k_f c_A c_M + k_r \frac{k_f c_A c_M}{k_r c_M + k_p} c_M = -\frac{k_f k_p c_A c_M}{k_r c_M + k_p} = -k_{over} c_A$$

According to the Lindemann approach the overall reaction rate constant of A depletion is then:

$$k_{over} = \frac{k_f k_p c_M}{k_r c_M + k_p}$$

Pressure dependence

$$\frac{dc_A}{dt} = -k_{over}c_A$$

$$k_{over} = \frac{k_f k_p c_M}{k_r c_M + k_p}$$

At **high pressures** there are a lot of molecules around, $[M]$ is high: $k_r[M] \gg k_p$ thus:

$$k_{\infty} = \frac{k_f k_p}{k_r} = K \cdot k_p$$

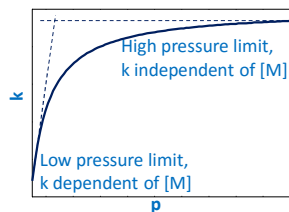
where k_{∞} is the **high-pressure-limit** rate constant and K is the equilibrium constant (k_f/k_r). Thus at high pressures the decomposition process becomes overall first-order.

At **low pressures**, the concentrations drop (not many molecules around) and $k_r[M] \ll k_p$, then reaction is of second-order and the **low-pressure limit** rate constant (k_0) becomes:

$$k_0 = k_f[M].$$

Fall-off region

The fall-off region is the transition between linear dependence on pressure and no dependence on pressure. Many reaction systems, combustion too, fall in this region



Lindemann simply proposed to account for the whole pressure range, using the sum of the reciprocals of low and high pressure limits

$$\frac{1}{k} = \frac{1}{k_0} + \frac{1}{k_{\infty}}$$

Troe formulation

Troe formulation is a more precise expression for the fall-off region.

the apparent first-order rate coefficient at any pressure can be calculated by:

$$k = k_{\infty} \left(\frac{P_r}{1+P_r} \right) F \quad \text{where} \quad P_r = \frac{k_0 M}{k_{\infty}} \quad \text{If } F = 1, \text{ this is the Lindemann expression again}$$

$$\log F = \log F_{cent} \left[1 + \left[\frac{\log P_r + c}{n - 0.14(\log P_r + c)} \right]^2 \right]^{-1}$$

$$c = -0.4 - 0.67 \log F_{cent} \quad n = -0.75 - 1.271 \log F_{cent}$$

$$F_{cent} = (1 - \alpha) \exp\left(-\frac{T}{T^{***}}\right) + \alpha \exp\left(-\frac{T}{T^*}\right) + \exp\left(-\frac{T^{**}}{T}\right)$$

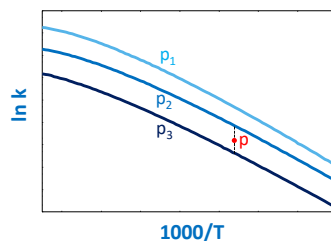
four extra parameters α , T^{***} , T^* , T^{**} must be defined to describe the fall-off curve!!

LOGP formulation

Troe fitting is not always accurate. Errors up to 30-40% can be found for some reactions.

Current best option is to evaluate rate constants (k_i) for a specific reaction at different pressures (p_i) and to tabulate them.

The actual rate constant (k) at the pressure p , is obtained by the linear interpolation in $\ln(p)$



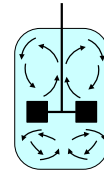
$$\ln k = \ln k_i + (\ln k_{i+1} - \ln k_i) \frac{\ln p - \ln p_i}{\ln p_{i+1} - \ln p_i}$$

Being p_i and p_{i+1} the closest lower higher pressure values of p and k_i and k_{i+1} the corresponding rate constants

Kinetic equations

Simplest system to study kinetics is the isothermal Batch Reactor (BR) at constant volume.

BR is an ideal closed reactor, where the reactants are initially charged into a container, are well ('perfectly') mixed (i.e. mixing is much faster than reaction time) and left to react for a certain period



The material balance of any component i is quite simple, because the composition is uniform throughout at any instant and no flows enter in or exit from the reactor.

$$\frac{dN_i}{dt} = R_i V \quad \text{Initial condition } t = 0 \quad N_i = N_i^0$$

being N_i the moles of i

If the volume is constant.

$$\frac{dc_i}{dt} = R_i \quad \text{Initial condition } t = 0 \quad c_i = c_i^0$$

where c_i is the molar concentration of i $c_i = \frac{N_i}{V}$

A simple example

Two successive first order reactions



Balance Equations

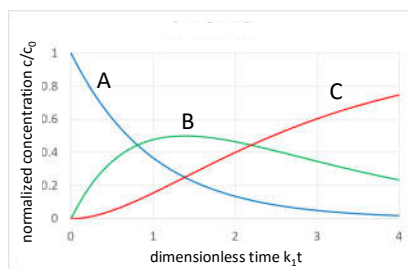
-isothermal system

Initial values (t=0)

$$[A] = [A]_0$$

$$[B]_0 = [C]_0 = 0$$

$$\begin{cases} \frac{d[A]}{dt} = -k_1[A] \\ \frac{d[B]}{dt} = +k_1[A] - k_2[B] \\ \frac{d[C]}{dt} = +k_2[B] \end{cases}$$

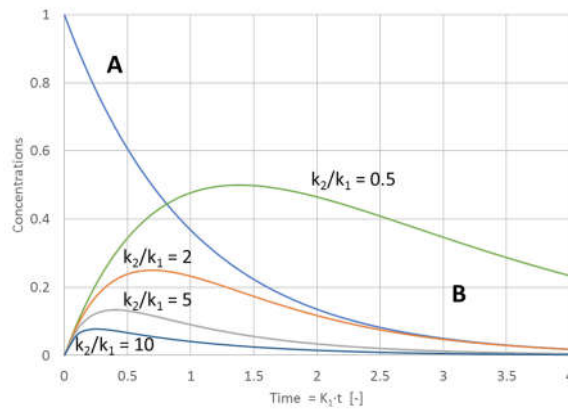


Temporal behavior of species concentrations

Analytical solution

$$\begin{cases} [A] = [A]_0 \exp(-k_1 t) \\ [B] = [A]_0 \frac{k_1}{k_1 - k_2} [\exp(-k_2 t) - \exp(-k_1 t)] \\ [C] = [A]_0 \left[1 - \frac{k_1}{k_1 - k_2} \exp(-k_2 t) + \frac{k_2}{k_1 - k_2} \exp(-k_1 t) \right] \end{cases}$$

Rate constant effect



Temporal behavior of species concentrations at different values of $[k_2/k_1]$

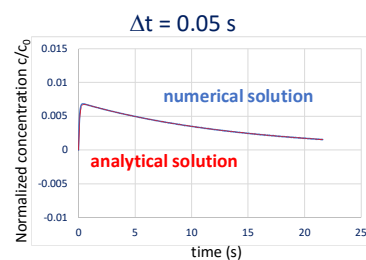
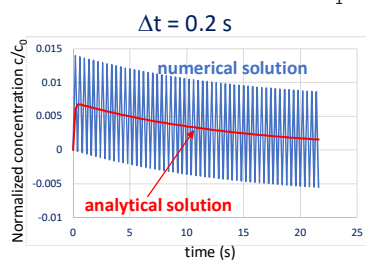
Stiffness problem

An ODE system is **stiff** if the ratio between the real parts of maximum and the minimum eigenvalues of the local Jacobian matrix is very large: $\frac{Re[\lambda_{max}]}{Re[\lambda_{min}]} \gg 1$

Stiffness refers to multiple time scales. If the problem has widely varying time scales, and the phenomena that change on fast scales are stable, then the problem is stiff.

In the previous example (two successive first order reactions), the eigenvalues correspond to the rate constants (k_1 and k_2), which are the characteristic chemical times. If they significantly differ, the system can be stiff and a numerical solution (i.e. the explicit Euler method) can fail if the integration step is too large.

$$k_1 = 0.07 \text{ s}^{-1} \quad k_2 = 10 \text{ s}^{-1}$$

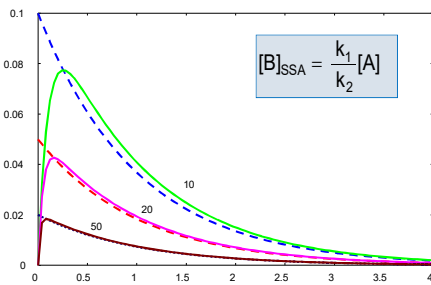


Steady state approximation

Possible solution to stiffness can be the steady state approximation of fast (short life time) intermediates. Thus, the largest eigenvalues are removed from the ODE system.

For $[k_2 / k_1] \gg 1$, $\text{Max } B \rightarrow 0$
(as soon as formed B is consumed by the second reaction)

$$\begin{cases} \frac{d[A]}{dt} = -k_1[A] \\ \frac{d[B]}{dt} = +k_1[A] - k_2[B] \approx 0 \quad \leftarrow \text{Steady State Approximation (SSA)} \\ \frac{d[C]}{dt} = +k_2[B] \end{cases}$$



$$\begin{cases} [A] = [A]_0 \exp(-k_1 t) \\ [B]_{\text{SSA}} = \frac{k_1}{k_2} [A] = \frac{k_1}{k_2} [A]_0 \exp(-k_1 t) \quad \leftarrow \text{(SSA)} \\ [C] = [A]_0 [1 - \exp(-k_1 t)] \end{cases}$$

Comparison of SSA (dashed lines) and analytical solution (solid lines)
Temporal behavior of $[B]/[A]_0$ versus t at different values of $[k_2/k_1]$

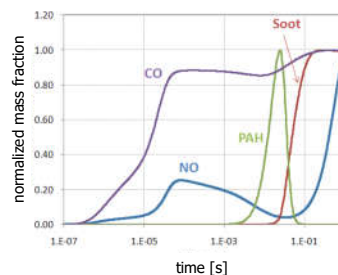
Kinetic equations

Summarizing: the reacting gas mixture is usually governed by an ODE system:

$$\frac{d\omega}{dt} = f(\omega, \xi)$$

where ω is the vector of unknowns (concentrations, temperature, pressure, etc.), ξ is the independent variable (time or spatial coordinate) and $f(\omega, \xi)$ is a non-linear function of the unknowns.

For large kinetic mechanisms, the ODE system contains a **large number** (large number of species) of **non-linear** (product of concentrations and exponential with temperature), **stiff equations** (the chemistry involves a wide range of characteristic times).



Sensitivity analysis

Given the ODE governing the reacting system, **sensitivity analysis** allows a quantitative understanding of how the simulation results depends on the various model parameters. The first-order sensitivity coefficients, with respect to the reaction rate coefficients (pre-exponential factor, activation energy or kinetic constant), can be easily obtained starting from the ODE system describing the reacting system:

$$\frac{d\omega}{dt} = f(\omega, \xi, \alpha)$$

where α is the vector of kinetic parameters.

The **first-order sensitivity matrix** is defined as:

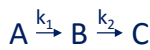
$$S = \frac{\partial \omega}{\partial \alpha} \quad \text{whose coefficients are: } s_{ij} = \frac{\partial \omega_i}{\partial \alpha_j}$$

Sensitivity coefficients are conveniently normalized in the form of logarithmic derivatives:

$$\tilde{S} = \frac{\partial \ln \omega}{\partial \ln \alpha} \quad \text{whose coefficients are: } \tilde{s}_{ij} = \frac{\partial \ln \omega_i}{\partial \ln \alpha_j} = \frac{\alpha_j}{\omega_i} \frac{\partial \omega_i}{\partial \alpha_j}$$

For large mechanisms, the sensitivity matrix is very large

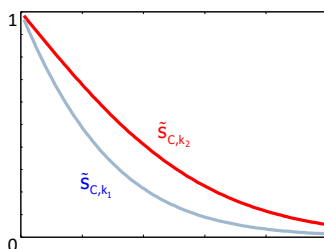
A simple example



$$\begin{cases} [A] = [A]_0 \exp(-k_1 t) \\ [B] = [A]_0 \frac{k_1}{k_1 - k_2} [\exp(-k_2 t) - \exp(-k_1 t)] \\ [C] = [A]_0 \left[1 - \frac{k_1}{k_1 - k_2} \exp(-k_2 t) + \frac{k_2}{k_1 - k_2} \exp(-k_1 t) \right] \end{cases}$$

sensitivity of species C to the kinetic constants k_1 and k_2

$$\begin{cases} s_{C,k_1} = \frac{\partial [C]}{\partial k_1} = \frac{[A]_0 k_2}{(k_1 - k_2)^2} \{ e^{-k_2 t} + e^{-k_1 t} (k_2 t - k_1 t - 1) \} \\ s_{C,k_2} = \frac{\partial [C]}{\partial k_2} = \frac{[A]_0 k_1}{(k_1 - k_2)^2} \{ e^{-k_1 t} + e^{-k_2 t} (k_1 t - k_2 t - 1) \} \end{cases} \quad \left\{ \begin{array}{l} \tilde{s}_{C,k_1} = \frac{k_1}{[C]} s_{C,k_1} \\ \tilde{s}_{C,k_2} = \frac{k_2}{[C]} s_{C,k_2} \end{array} \right.$$

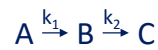
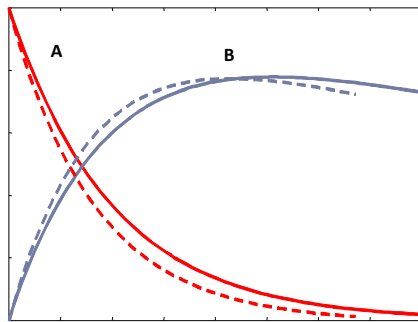


This result was obtained when $k_1 = 2k_2$.
C is more sensitive to the reaction 2, because it is slower, thus it is the rate controlling step.

Sensitivity coefficient evaluation: Brute Force

$$\frac{\partial \omega_i}{\partial \alpha_j} \cong \frac{\omega_i(\alpha_j + \Delta \alpha_j) - \omega_i(\alpha_j)}{\Delta \alpha_j} \quad (\text{Finite difference approximation})$$

Evaluation of the different parameter effects (sensitivity) requires to carry out many simulations (as many as the parameters whose effect has to be estimated)



Change of A and B profiles, when k_1 is increased.

Sensitivity coefficients can be then estimated, either locally or globally

Sensitivity coefficient evaluation: Direct method

$$\frac{d\omega}{dt} = f(\omega, \alpha)$$

Let's consider the α_j derivative of ω_i :

$$\frac{\partial}{\partial \alpha_j} \left(\frac{d\omega_i}{dt} \right) = \frac{\partial f_i(\omega, \alpha)}{\partial \alpha_j} \implies \frac{d}{dt} \left(\frac{\partial \omega_i}{\partial \alpha_j} \right) = \frac{\partial f_i}{\partial \alpha_j} + \sum_k \left(\frac{\partial f_i}{\partial \omega_k} \frac{\partial \omega_k}{\partial \alpha_j} \right)$$

$$\implies \frac{d}{dt} (s_{ij}) = \frac{\partial f_i}{\partial \alpha_j} + \sum_k \left(\frac{\partial f_i}{\partial \omega_k} s_{kj} \right) \quad \begin{cases} s_{ij}^0 = 0 & \text{if } \alpha_j \neq \omega_i^0 \\ s_{ij}^0 = 1 & \text{if } \alpha_j = \omega_i^0 \end{cases}$$

$$\text{equivalently: } \frac{dS}{dt} = J_\alpha + J_\omega S$$

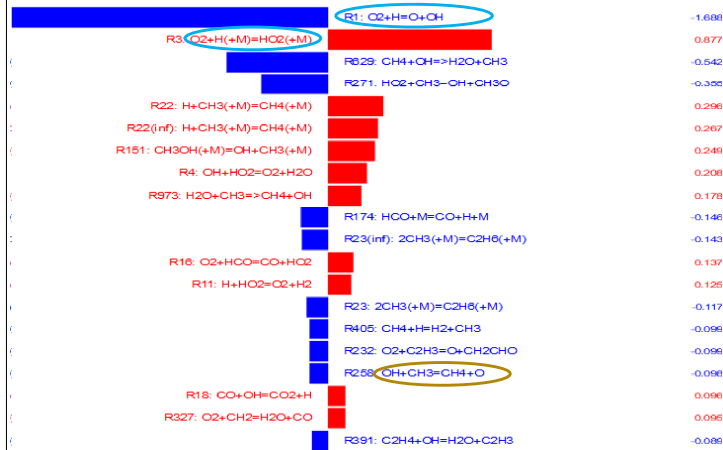
J_ω is the Jacobian of the kinetic equations, thus it is possible to integrate simultaneously the kinetic equations and the sensitivity coefficients.

The problem dimension can become quite huge, because it includes $n \times m$ new equations of the sensitivity coefficient variables, with n number of species and m number of parameters (reactions)

Sensitivity coefficient: bar plot

CH₄ stoichiometric combustion in PSR @ 1200 K and 1 atm

Sensitivity Analysis - CH₄



If CH₄ reacts too fast (or too slow,) we could work on the first two reactions (if we know their values are uncertain), decreasing (increasing) the former or increasing (decreasing) the latter. It is useless to work on reaction CH₄ + O for example

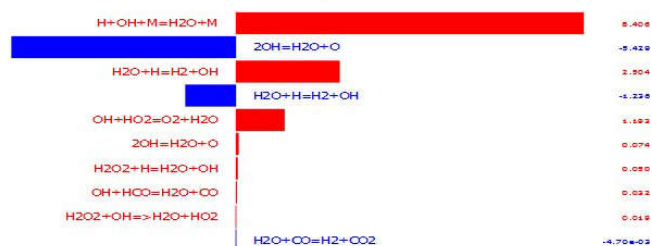
Rate of production analysis (RoPA)

The **rate of production analysis (RoPA)** determines the contribution of each reaction to the production or depletion rates of a species.

For each species *i* and each reaction *j* it is possible to define a normalized production contribution CP_{ij} and a normalized depletion contribution CD_{ij} .

The **normalized contributions** to production and depletion sum to 1.

Rate of Production Analysis - H₂O



Rate constant estimation

Rate constant estimation

- Large number of reactions in a combustion mechanism
- Direct experimental determination often difficult for elementary reactions over a wide range of temperature and pressure
- Few experimental data, limited to light species

- Estimation methods:
 - Collision theory (kinetic theory gas) pre-exponential A, radical combination
 - correlations between structure and reactivity
 - methods based on the Transition State Theory (estimation of the TS)
 - quantum calculation and TST

Databases

➤ On-line databases

NIST Chemical Kinetics Database, Standard Reference Database 17

<http://kinetics.nist.gov/kinetics/index.jsp>

➤ Review

- D.L. Baulch, C.T. Bowman, C.J. Cobos, Th. Just, J.A. Kerr, M.J. Pilling, D. Stocker, J. Troe, W. Tsang, R.W. Walker and J. Warnatz, *Phys. Chem. Ref. Data*, **34**, 757 (2006)
- Tsang, W., Hampson, R. F., *J. Phys. Chem. Ref. Data* **15**:3 (1986)
- Tsang, W., *J. Phys. Chem. Ref. Data* **20**:221 (1991)

➤ On-line mechanisms:

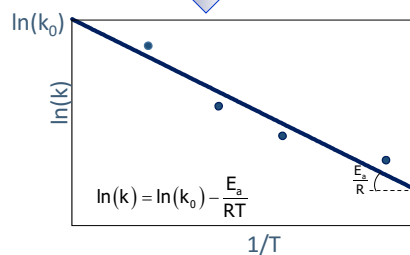
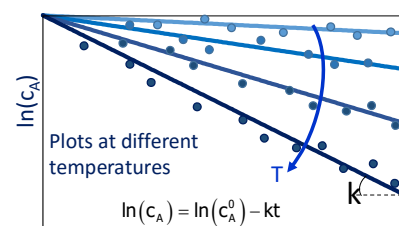
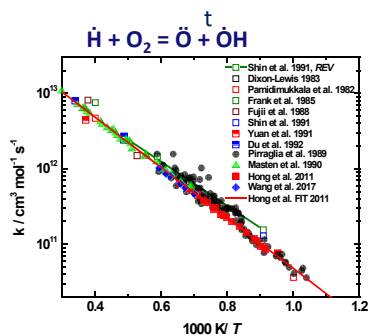
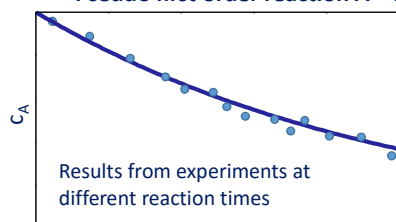
- Estimated rate constants for most reactions, to handle and mix carefully
- GRI-mech, LLNL, Leeds, Konnov, NUIG, POLIMI, Jet-Surf, UCSD...

➤ Good website for general links: <https://c3.nuigalway.ie/links/#>

Courtesy of Henry Curran

Direct experimental determination

Pseudo first order reaction A + B

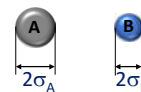


Collision theory

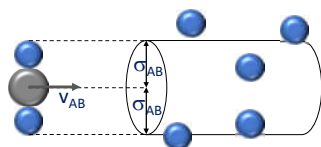
Reaction: $A + B \rightarrow \text{products}$

Assumptions:

1. molecules are rigid spheres
2. every collision results in reactions



the coordinate system is such that molecule B is stationary with reference to molecule A so that molecule A moves towards molecule B with a relative velocity v_{AB} . Molecule A moves through space and collides with all B's within a collision cylinder, whose cross section is $\pi\sigma_{AB}^2$



Collision radius is $\sigma_{AB} = \sigma_A + \sigma_B$

when the center of a "B" molecule comes within a distance σ_{AB} of the center of "A", they collide.

The single collision of A with B per unit time, or collision frequency (Z_A) is:

$$Z_A = \widetilde{C}_B \pi (\sigma_A + \sigma_B)^2 v_{AB}$$

Being \widetilde{C}_B the molecular concentration of B (molecules/ m^3), i.e. the number of B molecules per unit volume and $(\pi\sigma_{AB}^2 v_{AB} t)$ the volume of the cylinder, whose length is just $v_{AB} t$

Collision theory

Total collision rate (Z_{AB}) of all A molecules with all B molecules results:

$$Z_{AB} = \widetilde{C}_A \widetilde{C}_B \pi \sigma_{AB}^2 v_{AB}$$

The relative velocity can be expressed in terms of the Maxwell-Boltzmann distribution of velocity

$$v_{AB} = \sqrt{\frac{8k_B T}{\pi \mu}}$$

k_B = Boltzmann's constant = 1.381×10^{-23} J/K/molecule
 μ is the reduced mass: $\mu = \frac{m_A m_B}{m_A + m_B}$

In usual units (SI): $v_{AB} = 4.6 \sqrt{\frac{T(m_A + m_B)}{m_A m_B}}$ T in [K]; m in [kg/mol]

Being any collision a reacting act, the reaction rate corresponds to the collision rate:

$$R = Z_{AB} = C_A C_B \pi \sigma_{AB}^2 v_{AB}$$

Avogadro number allows to pass from \widetilde{C}_i to C_i

In the usual Arrhenius format $R = k C_A C_B$

From which: $k = \pi \sigma_{AB}^2 v_{AB}$

Collision theory: application example



$$m_{\text{H}} = 1 \text{ kg/mol} \quad m_{\text{O}_2} = 32 \text{ kg/mol} \quad T = 300 \text{ K}$$

$$\sigma_{\text{H}} = 0.61 \times 10^{-10} \text{ m} \quad \sigma_{\text{O}_2} = 1.5 \times 10^{-10} \text{ m}$$

$$v_{\text{AB}} = 4.6 \sqrt{\frac{T(m_{\text{A}} + m_{\text{B}})}{m_{\text{A}}m_{\text{B}}}} = 2559 \text{ m/s} \quad \text{About 7 times the speed of sound!}$$

$$k = \pi \sigma_{\text{AB}}^2 v_{\text{AB}} = 3.6 \times 10^{-16} \text{ m}^3/\text{molecule/s}$$

Convert to $\text{cm}^3/\text{mol/s}$

$$k = 2.15 \times 10^{14} \text{ m}^3/\text{mol/s} \quad \text{Experimental: } k = 1.91 \times 10^{13} \text{ m}^3/\text{mol/s}$$

Reasonable estimation (anyway too large error). Above all, T-dependence all wrong

Collision theory: hypothesis relax

Assumptions:

- ~~1. molecules are rigid spheres~~
- ~~2. every collision results in reactions~~

Introducing a parameter ε and a critical value ε_c . Only if $\varepsilon \geq \varepsilon_c$ the reaction occurs.

Fraction f of collisions having $\varepsilon \geq \varepsilon_c$ can be derived from Maxwell-Boltzmann theory

$$f = \exp\left(-\frac{\varepsilon_c}{k_{\text{B}}T}\right) = \exp\left(-\frac{E_c}{RT}\right)$$

$$k = \pi \sigma_{\text{AB}}^2 v_{\text{AB}} \exp\left(-\frac{E_c}{RT}\right)$$

Rate Constant is smaller now and is T-dependent.

New problem: how E_c

Collision theory: hypothesis relax

Collision theory rate constant vs. Arrhenius rate constant:

$$k_{\text{coll}} = \pi \sigma_{\text{AB}}^2 v_{\text{AB}} \exp\left(-\frac{E_{\text{C}}}{RT}\right) \qquad k_{\text{Arr}} = k_0 \exp\left(-\frac{E_{\text{A}}}{RT}\right)$$

$$k_{\text{coll}} = \pi \sigma_{\text{AB}}^2 v_{\text{AB}} \exp\left(-\frac{E_{\text{C}}}{RT}\right) = \pi \sigma_{\text{AB}}^2 4.6 \sqrt{\frac{T(m_{\text{A}} + m_{\text{B}})}{m_{\text{A}} m_{\text{B}}}} \exp\left(-\frac{E_{\text{C}}}{RT}\right) = \alpha T^{1/2} \exp\left(-\frac{E_{\text{C}}}{RT}\right)$$

$$\ln k_{\text{coll}} = \ln \alpha + \frac{1}{2} \ln T - \frac{E_{\text{C}}}{RT} = \ln \alpha - \frac{1}{2} \ln\left(\frac{1}{T}\right) - \frac{E_{\text{C}}}{RT}$$

$$\frac{d(\ln k_{\text{coll}})}{d(1/T)} = -\frac{1}{2} T - \frac{E_{\text{C}}}{RT} \qquad \frac{d(\ln k_{\text{Arr}})}{d(1/T)} = -\frac{E_{\text{A}}}{RT}$$

Equating the two derivatives: $-\frac{1}{2} T - \frac{E_{\text{C}}}{RT} = -\frac{E_{\text{A}}}{RT}$ $E_{\text{C}} = E_{\text{A}} - \frac{RT}{2}$

(RT is generally *small* in comparison with most E_{A} 's)

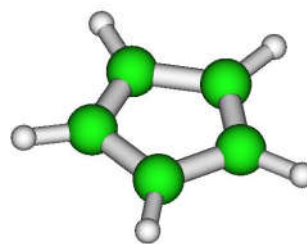
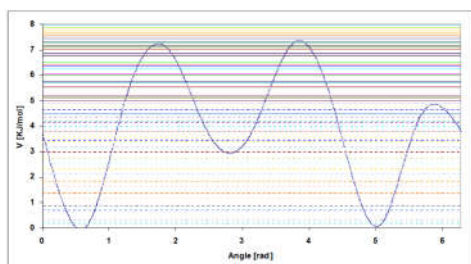
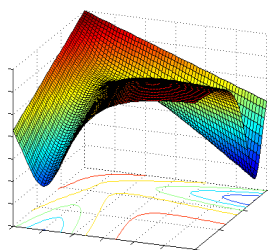
$$k_{\text{coll}} = \pi \sigma_{\text{AB}}^2 v_{\text{AB}} \exp\left(-\frac{E_{\text{C}}}{RT}\right) = \pi \sigma_{\text{AB}}^2 v_{\text{AB}} \left(-\frac{E_{\text{A}}}{RT}\right) e^{1/2}$$

Simulation of Molecular systems for Chemistry, Materials and Biology

Chemical Kinetics

Carlo Cavallotti

*Dip. Chimica, Materiali, Ing Chimica
Politecnico di Milano*



Outline

- molecular partition functions
- transition state theory
- where to get data: ab initio simulations
- limits of TST: degeneration of internal degrees of freedom into hindered rotations
- beyond TST: RRKM + master equation theory
- beyond TST: quantum tunneling
- beyond TST: spin forbidden reactions

transition state theory

Statistical Thermodynamics

main results (macrocanonic ensemble)

$$Z = \sum_j \exp\left(-\frac{E_j}{k_b T}\right) \quad \begin{array}{l} \text{Partition function} \\ E_j = \text{energy of } j \text{ state} \end{array}$$

$$U = \sum_r w_r E_r = \sum_r E_r \exp(-E_r / k_b T) / Z$$

$$S = -k_B \sum_r w_r \ln w_r = k \ln Z + k\beta U = \frac{U}{T} + k \ln Z$$

$$F = -k_B T \ln Z \quad \begin{array}{l} \text{From} \\ \text{which} \end{array} \quad P = -(\partial F / \partial V)_T$$

Molecular Partition Functions

$$Z = \frac{(\sum z_i)^N}{N!} = \frac{(\sum \exp(-\varepsilon_i / k_b T))^N}{N!} = \frac{(z_{\text{mol}})^N}{N!}$$

z_{mol} is called molecular partition function as it is a function only of molecular properties (structure, bond energies, molecular weight, ...). It can be decomposed into 4 parts:

$$z_{\text{mol}} = z_{\text{trans}} \cdot z_{\text{rot}} \cdot z_{\text{vib}} \cdot z_{\text{el}} \quad \text{with} \quad z_{\text{trans}} = \sum \exp(-\varepsilon_i^{\text{trans}} / k_B T) \quad z_{\text{rot}} = \dots$$

The accessible energetic levels can be computed through the solution of the Schrodinger equation:

$$H\Psi = E\Psi \quad \text{where } H \text{ is the Hamiltonian, } E \text{ the energy and } \Psi \text{ the wave function}$$

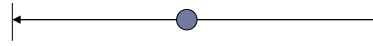
$$H \text{ expressed as:} \quad \hat{H} = -\frac{\hbar^2}{2m} \nabla^2 + V(\mathbf{r})$$

Schrodinger equation

For translational, vibrational and some rotational motions the Schrodinger equation has an analytic solution. In particular for a particle confined in a box the Schrodinger equation assumes the form:

$$\left[-\frac{\hbar^2}{2m} \frac{d^2}{dx^2} + V \right] \Psi(x) = E\Psi$$

$$V = \begin{cases} 0 & \text{for } 0 < x < a \\ \infty & \text{for } x < 0 \text{ or } x > a \end{cases}$$



Boundary conditions

$$\Psi_n(x) = C_n \sin\left(\frac{n\pi x}{a}\right)$$

Wave function

With eigenvalues $E_n = \frac{n^2 \hbar^2}{8ma^2} \quad n = 1, 2, 3, \dots$

z_{trasl} can thus be expressed as:

$$z_{\text{trasl}} = \sum \exp\left(\frac{-\hbar^2 n^2}{8mL^2 k_b T}\right) \approx \int \exp\left(\frac{-\hbar^2 n^2}{8mL^2 k_b T}\right) dn = \left(\frac{2\pi m k_b T}{\hbar^2}\right)^{3/2} V$$

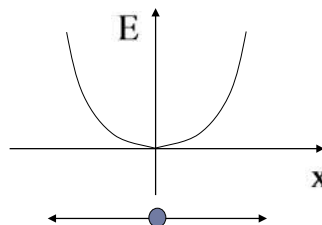
vibrational and rotational motions

For vibrational and rotational motions the analytic solution of Schrödinger equation is a bit more complex and we report only the main equations of the vibrational problem.

The Schrödinger equation associated to the motion of a particle subject to an elastic strength $F = -kx$ can be expressed as:

$$-\frac{\hbar}{2m} \frac{\partial^2 \Psi}{\partial x^2} + \frac{kx^2}{2} \Psi = E\Psi$$

$$E = \left(\frac{1}{2} + n\right) \sqrt{\frac{k\hbar^2}{m}} = \left(\frac{1}{2} + n\right) h\nu$$



The vibrational partition function can then be calculated as:

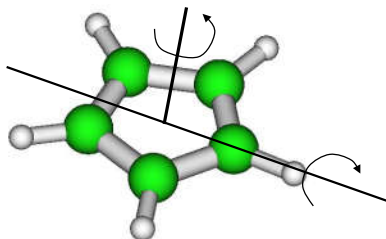
$$z_{\text{vib}} = \sum \exp\left(\frac{-\varepsilon_i}{k_b T}\right) = \sum \exp\left(\frac{-(1/2 + n)h\nu}{k_b T}\right) = \frac{e^{-\frac{h\nu}{2k_b T}}}{1 - e^{-\frac{h\nu}{k_b T}}}$$

rotational symmetry

The rotational partition function is obtained using a similar procedure and can be expressed as:

$$z_{\text{rot}} = \sum \exp\left(\frac{-\varepsilon_i}{k_b T}\right) = \sum (2J+1)^2 \exp\left(\frac{-J(J+1)h^2}{8\pi^2 I k_b T}\right) = \frac{8\pi^2 (2\pi k_b T)^{3/2} \sqrt{I_x I_y I_z}}{\sigma h^3}$$

Where I is the molecule inertia moment and σ the rotational symmetry number (number of identical configurations that can be obtained rotating the molecule around symmetry axes).



For example C_5H_5 has a 5 fold degenerate rotational axis and 5 2 fold degenerate axes \rightarrow rotational symmetry number = $5 + 5 = 10$

RIGID ROTOR HARMONIC OSCILLATOR

Finally, for non excited molecules, the electronic partition function is simply:

$$z_{\text{el}} = \exp\left(\frac{-\varepsilon_{\text{el}}}{k_b T}\right)$$

Where ε_{el} is related to the energy of interaction of electrons with nuclei, and is defined by the solution of the Schrödinger equation for a multi-nuclear-multielectronic Hamiltonian

Summarizing:

$$F = -k_b T \ln Z \quad Z = \frac{(z_{\text{mol}})^N}{N!} \quad z_{\text{mol}} = z_{\text{trasl}} z_{\text{vib}} z_{\text{rot}} z_{\text{el}}$$

$$z_{\text{trasl}} = \left(\frac{2\pi m k_b T}{h^2}\right)^{3/2} V \quad z_{\text{rot}} = \frac{8\pi^2 (2\pi k_b T)^{3/2} \sqrt{I}}{\sigma h^3} \quad z_{\text{vib}} = \frac{e^{-\frac{h\nu}{2k_b T}}}{1 - e^{-\frac{h\nu}{k_b T}}} \quad z_{\text{el}} = \exp\left(\frac{-\varepsilon_{\text{el}}}{k_b T}\right)$$

To calculate z_i it is thus necessary to know: m , I , ν_i , ε_{el}

THIS IS THE RIGID ROTOR HARMONIC OSCILLATOR APPROXIMATION (RRHO)

How can I exploit this knowledge?

Application of molecular partition functions

Which state equation is predicted?

$$P = -\left(\frac{\partial F}{\partial V}\right)_T$$

$$F = -k_B T \ln Z = -k_B T \ln \frac{z_{\text{mol}}^N}{N!} \approx -k_B T \cdot (N \ln z_{\text{mol}} - N \ln N + N)$$

Since the only z_{mol} with a functional dependence from V is z_{trasl} , then

$$P = -\left(\frac{\partial F}{\partial V}\right)_T = k_B T N \left(\frac{\partial \ln z_{\text{trasl}}}{\partial V}\right)_T = k_B T N \left(\frac{\partial \ln \alpha V}{\partial V}\right)_T = k_B T N V$$

Which is the state equation of a perfect gas. This is consistent with the hypothesis of non interacting molecules that is at the basis of the z_{mol} expression derivation.

The perfect gas state equation had already been known for some time, which other predictions are possible?

Which thermodynamic state functions are predicted?

$$S = \frac{U}{T} + k_B \ln Z = k_B \ln z_{\text{mol}} + k_B T \left(\frac{\partial \ln z_{\text{mol}}}{\partial T}\right)_V$$

known z_{mol} , thus mass, geometry and molecular vibrational frequencies (z_{el} becomes 0), it is possible to calculate the entropy of any gas. The necessary data can either be determined experimentally or calculated through quantum mechanics simulations.

A comparison between computational predictions based on QM calculations and experimental data is reported below (in cal/molK):

	S° trasl	S° vibr	S° rot	S° calc	S° exp	CPU
CH ₄	34.3	0.09	10.2	44.5	44.51	60 s
H ₂ O	34.6	0.01	10.5	45.1	45.11	20 s
C ₆ H ₆	39.0	4.4	20.7	64.1	64.34	20 s

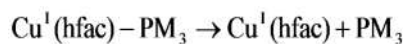
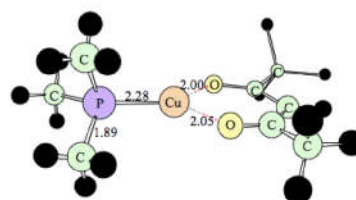
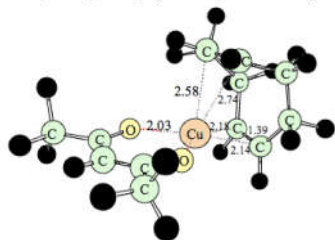
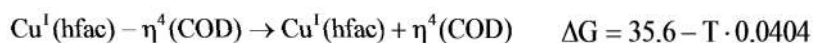
Comparison with experimental data

	S° trasl	S° vibr	S° rot	S° calc	S° exp	CPU
C ₆ H ₁₄	39.3	21.9	27.3	88.5	92.9	108 min
1,3C ₄ H ₆	37.9	5.9	23.6	67.4	66.6	78 min
C ₂ H ₅ NH ₂	38.3	5.8	23.6	67.8	70.8	16 min

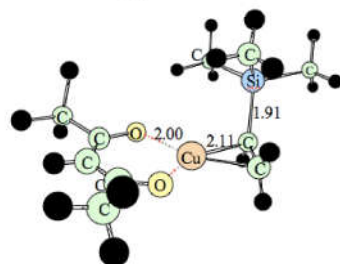
The disagreement is due to the degeneration of some vibrational motions with low frequencies into rotational motions, which are usually referred to as hindered rotational motions, as they are restrained by a potential energy field.

The proposed approach has general validity and can be used to study systems for which no thermodynamic data are available.

An example of its application to the study of the gas phase chemistry of Cu precursors to the deposition of Cu thin films is reported below:

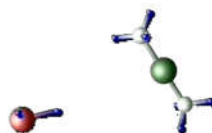
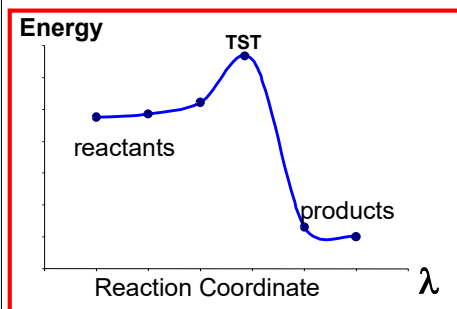


$$\Delta G = 38.4 - T \cdot 0.0323$$



Transition State Theory (TST)

Transition state theory has the aim of predicting the rate at which a chemical reaction takes place. The basic idea is that molecules react following a well defined reaction coordinate, λ , which connects reactants to products



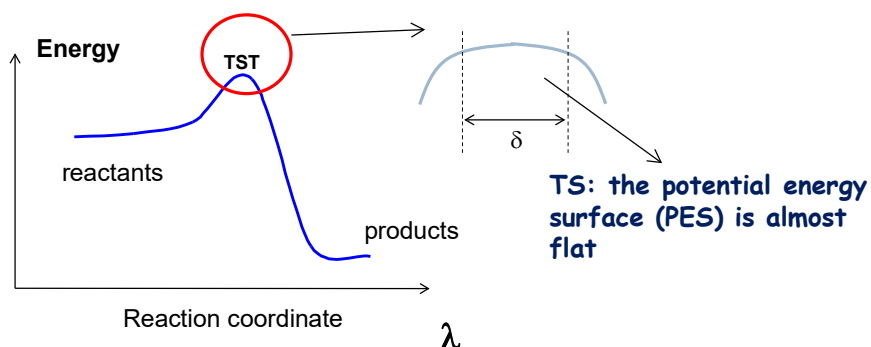
Fundamental hypotheses (almost always satisfied)

- Separability of electronic and nuclear motions (Born-Oppenheimer)
- Maxwell-Boltzmann velocity distribution

Hypotheses

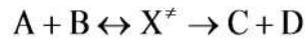
Restrictive hypotheses

- 1) molecules that have crossed the TS once cannot cross it again (non recrossing)
- 2) in the TS the motion along the reaction coordinate can be separated from the other internal motions and be considered as a translation
- 3) there is equilibrium between the transition state and the reactants



Reaction rate

The equilibrium hypotheses (3) between reactant and TS for a generic reaction $A+B \rightarrow C+D$ translates into:



where X^\ddagger is the concentration of molecules at the TS

$$\frac{C_{X^\ddagger}}{C_A C_B} = K_{eq} = \exp(-\Delta G^\circ / RT) = \prod z_i^{v_i}$$

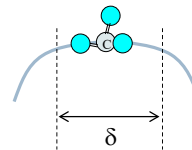
Can be deduced from $F = -k_B T \ln(z_{mol})^N / N!$

where z_i is the molecular partition function.

The reaction rate can then be defined as the flux of molecules crossing the TS, which can be expressed as (1):

$$R = \frac{1}{2} C_{X^\ddagger} \frac{v^\ddagger}{\delta}$$

Speed of molecules at the TS
Distance to travel



Statistical factor

Reaction rate

assuming a Maxwellian velocity distribution function, v^\ddagger can be expressed as:

$$v^\ddagger = \sqrt{\frac{2k_B T}{\pi M}}$$

Thus the rate constant expression becomes:

$$k_{cin} = \frac{1}{2} C_{X^\ddagger} \cdot \frac{v^\ddagger}{\delta} = \frac{1}{2} \sqrt{\frac{2k_B T}{\pi M}} \frac{C_{X^\ddagger}}{\delta} = \frac{1}{2\delta} \sqrt{\frac{2k_B T}{\pi M}} \prod z_i^{v_i} = \frac{1}{2\delta} \sqrt{\frac{2k_B T}{\pi M}} \frac{z_i^\ddagger}{\prod z_i^{reactants}}$$

Remembering that $Z_{mol} = Z_{trasl} Z_{vib} Z_{rot} Z_{el}$

And that according to hypothesis 2 one vibrational motion becomes translational, z_{mol} at the TS can be expressed as:

$$Z_{mol}^\ddagger = Z_{trasl}^\ddagger Z_{vib(3N-7)}^\ddagger Z_{rot}^\ddagger Z_{el}^\ddagger Z_{trasl}^{ID-TST} = Z_{trasl}^\ddagger Z_{vib(3N-7)}^\ddagger Z_{rot}^\ddagger Z_{el}^\ddagger \sqrt{\frac{2\pi M k_B T}{h^2}} \delta$$

Reaction rate

The final expression is thus

$$k_{cin} = \frac{1}{2\delta} \sqrt{\frac{2k_B T}{\pi M}} \frac{z_i^\ddagger}{\prod z_i^{reactants}} = \frac{1}{2\delta} \sqrt{\frac{2k_B T}{\pi M} \frac{z_{trans}^\ddagger z_{rot}^\ddagger z_{vib(3N-7)}^\ddagger z_{el}^\ddagger \sqrt{2\pi M k_B T / h^2 \delta}}{\prod z_i^{reactants}}}$$

Which leads to

$$k_{cin} = \frac{k_B T}{h} \frac{z_{trans}^\ddagger z_{rot}^\ddagger z_{vib(3N-7)}^\ddagger z_{el}^\ddagger}{\prod z_i^{reactants}}$$

Making the electronic partition function explicit and grouping the vibrational ZPE we obtain:

$$k_{cin} = \frac{k_B T}{h} \frac{z_{trans}^\ddagger z_{rot}^\ddagger z_{vib(3N-7)}^\ddagger z_{el}^\ddagger}{\prod z_i^{reactants}} \exp\left(\frac{\sum(\varepsilon_i + ZPE)v_i}{k_B T}\right) \approx (H_{tst} - H_{reactants})_{OK}$$

Reaction rate example

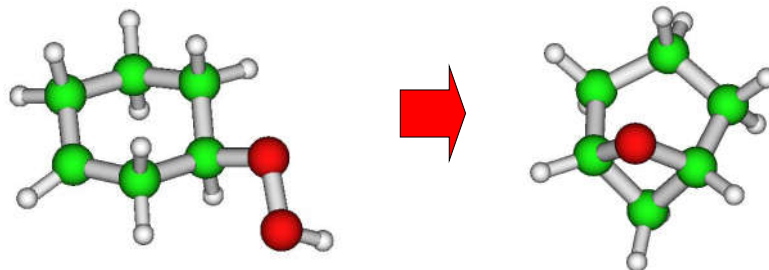
The data required for applying TST in the RRHO approximation are:

- structure and energy of reactants
- structure and energy of TS
- vibrational frequencies of TS and reactants

Two approaches are possible to determine the required data:

- approximated methods (BEBO, Benson, ...)
- quantum mechanical calculations

Example: $C_6H_{10}OOH \rightarrow C_6H_{10}O + OH$



Reaction rate example

The TS and reactant data calculated using DFT at 300 K are:

Reactant:

zvib: 67.2

zrot: $3.5 \cdot 10^5$

Eel+ZPE: -385.411 Hartree

5 low vibrational frequencies
103; 141; 175; 208; 235

TS:

zvib: 39.8

zrot: $2.9 \cdot 10^5$

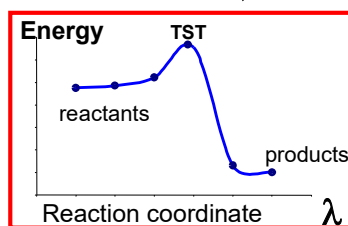
Eel+ZPE: -385.380

5 low vibrational frequencies
-732; 106; 142; 192; 229

$$k_{cin} = \frac{k_B T}{h} \frac{z_{rot}^\ddagger z_{vib}^\ddagger (3N-7)_{rid}}{z_{rot}^{reactant} z_{vib}^{reactant}} \exp\left(-\frac{(\varepsilon^\ddagger + ZPE^\ddagger - \varepsilon^{react} - ZPE^{react})}{k_B T}\right)$$

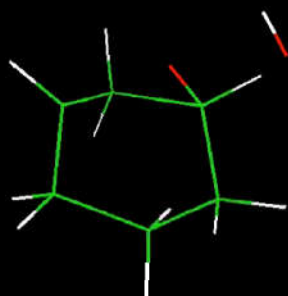
$$= 3.110^{12} \exp(-19.3/RT)$$

NB: for unimolecular reactions Q translational of TS and reactant are the same, and thus cancel out



Structure of the reaction TS

MOLDEN



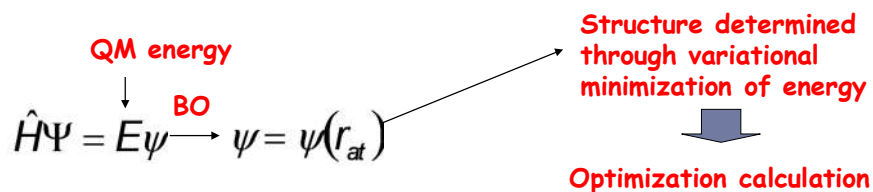
The negative vibrational frequency corresponds to a translational motion

Quantum Mechanical computation of TST data

The data necessary to compute the partition functions are:

- **Translational**: mass \rightarrow Molecular Weight
- **Rotational**: principal inertia moments \rightarrow geometry
- **Vibrational**: vibrational frequencies: \rightarrow normal mode analysis
- **Electronic**: QM energy + spin number

\rightarrow Geometry + Vibrational Frequencies + Energy possible through ab initio (QM) calculations



Quantum Mechanical computation of TST data

Energy of molecular system: key quantity to define reactivity. It is a multidimensional surface: the Potential Energy surface

$$E: \mathbb{R}^N \rightarrow \mathbb{R}$$

For a system containing two molecules of Na and Nb atoms, the potential energy surface (PES) dimension is:

$$N = 3N_a + 3N_b - 6 = 3(N_{\text{tot atoms}}) - 6$$

6 as independent of rotation of frame of reference

For $\text{H}_2 + \text{OH}$ the PES is 6 dimensional.

Quantum Mechanical computation of TST data

If a PES is fully known at a high level of detail than kinetics is a solved problem:

$$F = -\nabla E$$

Possible Approaches:

- Born Oppenheimer Molecular **Dynamics** (BOMD): trajectories over PES integrating Newton equation
- Ring Polymer **Dynamics** or Quantum Scattering: full quantum calculations

Problems:

- Dimension of PES explodes with number of atoms
- PES sometimes necessary also for excited states
- High accuracy is not simply attainable

Alternative:

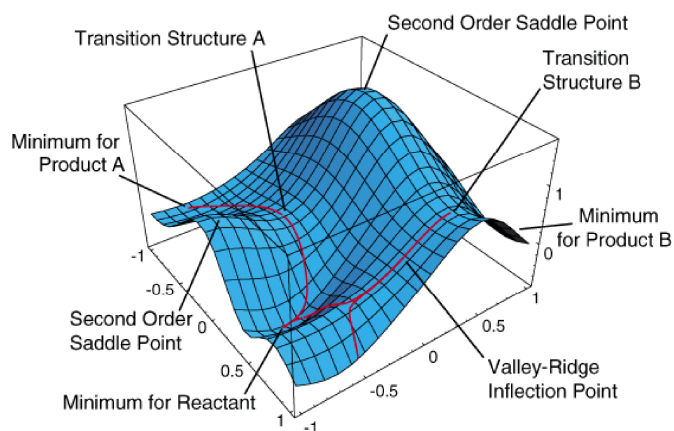
Limit study of PES to stationary points (minima and saddle points) and use Transition State Theory (**Kinetics**).

Key info from ab initio calculations

Key quantities:

- Energy at minimum energy structures (Optimization)
- Geometries at minimum energy structures
- Minimum energy paths (Intrinsic Reaction Paths)
- Gradients (first derivatives)
- Hessians (second derivatives) → frequency calculations

The Potential Energy surface



ab initio calculations

FCI	FCI/ STO-3G	FCI/ 3-21G	FCI/ 6-31G*	FCI/ 6-311G(2df)	exact
...					
CCSD(T)	CCSD(T)/ STO-3G	CCSD(T)/ 3-21G	CCSD(T)/ 6-31G*	CCSD(T)/ 6-311G(2df)	CCSD(T) limit
CCSD	CCSD/ STO-3G	CCSD/ 3-21G	CCSD/ 6-31G*	CCSD/ 6-311G(2df)	CCSD limit
MP2	MP2/ STO-3G	MP2/ 3-21G	MP2/ 6-31G*	MP2/ 6-311G(2df)	MP2 limit
HF	HF/ STO-3G	HF/ 3-21G	HF/ 6-31G*	HF/ 6-311G(2df)	HF limit
	STO-3G	3-21G	6-31G*	6-311G(2df)	... complete

↑
Correlation

→
AO Basis Set

$$H(\mathbf{r};\mathbf{R}) \Psi(\mathbf{r};\mathbf{R}) = E(\mathbf{R}) \Psi(\mathbf{r};\mathbf{R})$$

J. Phys. Chem., Vol. 100, No. 31, 1996

$$H(\mathbf{r};\mathbf{R}) = -\frac{1}{2} \sum_i^n \left(\frac{\partial^2}{\partial x_i^2} + \frac{\partial^2}{\partial y_i^2} + \frac{\partial^2}{\partial z_i^2} \right) - \sum_i^n \sum_{\alpha}^A \frac{Z_{\alpha}}{|\mathbf{r}_i - \mathbf{R}_{\alpha}|} + \frac{1}{2} \sum_i^n \sum_j^n \frac{1}{|\mathbf{r}_i - \mathbf{r}_j|} + \frac{1}{2} \sum_{\alpha}^A \sum_{\beta}^A \frac{Z_{\alpha} Z_{\beta}}{|\mathbf{R}_{\alpha} - \mathbf{R}_{\beta}|}$$

Analysis of a PES: Normal mode analysis 1/2

The energy associated with the translational motions of a non linear polyatomic molecule that moves by x_i with respect to equilibrium can be expressed as:

$$V = V(0) + \sum_i \left(\frac{\partial V}{\partial x_i} \right)_0 x_i + \frac{1}{2} \sum_{i,j} \left(\frac{\partial^2 V}{\partial x_i \partial x_j} \right)_0 x_i x_j$$

For small movements we have:

$$V = \frac{1}{2} \sum_{i,j} \left(\frac{\partial^2 V}{\partial x_i \partial x_j} \right)_0 x_i x_j = \frac{1}{2} \sum_{i,j} k_{ij} x_i x_j$$

Generalized force constant

Introducing $q_i = m_i^{1/2} x_i$ $K_{ij} = \frac{k_{ij}}{(m_i m_j)^{1/2}} = \left(\frac{\partial^2 V}{\partial q_i \partial q_j} \right)_0$

We obtain $T = \frac{1}{2} \sum_i m_i \dot{x}_i^2 = \frac{1}{2} \sum_i \dot{q}_i^2$ $V = \frac{1}{2} \sum_{i,j} K_{ij} q_i q_j$

Analysis of a PES: Normal mode analysis 2/2

From which
$$E = T + V = \frac{1}{2} \sum_i \dot{q}_i^2 + \frac{1}{2} \sum_{i,j} K_{ij} q_i q_j$$

The normal mode analysis consists in determining the transformation of coordinates $q_i \rightarrow Q_i$, with Q_i linear function of q_i , for which $K_{ij}(i \neq j) = 0$. The problem can be solved by diagonalizing the K_{ij} matrix.

The result is a set of constants K_{ii} , of which 6, corresponding to external rotational and translation motions, become 0.

In practice, the evaluation of the normal vibrational modes requires the evaluation of the second derivatives of the energy.

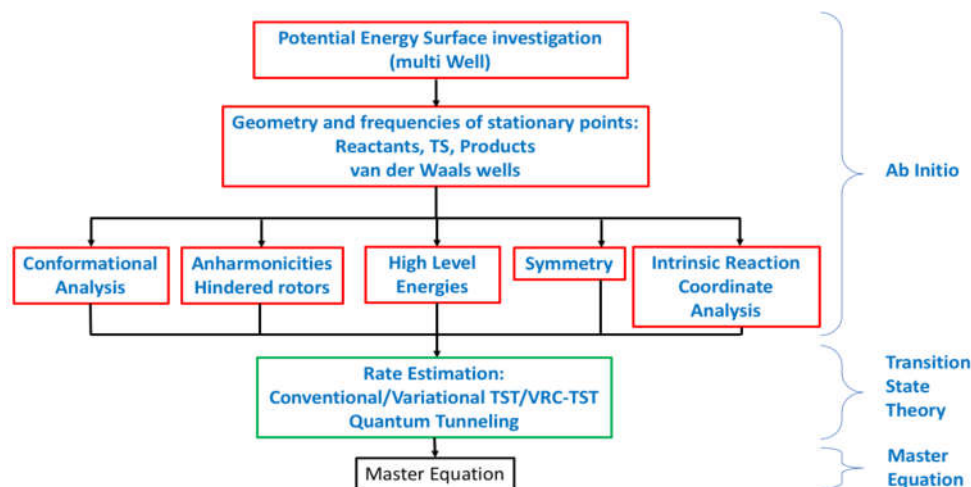
Problems with Harmonic Approximation

	S° trasl	S° vibr	S° rot	S° calc	S° exp	CPU
<chem>C6H14</chem>	39.3	21.9	27.3	88.5	92.9	108 min
<chem>1,3C4H6</chem>	37.9	5.9	23.6	67.4	66.6	78 min
<chem>C2H5NH2</chem>	38.3	5.8	23.6	67.8	70.8	16 min

The disagreement is due to the degeneration of some vibrational motions with low frequencies into rotational motions, which are usually referred to as hindered rotational motions, as they are restrained by a potential energy field.

The approach

Steps involved in accurate calculation of rate constant in the *ab initio* Transition State Theory based master equation approach



Degeneration of low vibrational frequencies in hindered rotors

If low vibrational frequencies ($< 150 \text{ cm}^{-1}$) can “degenerate” in *free or hindered internal rotors*, they must be excluded from the calculation of Q_{vibr} and treated adopting a suitable theory, for example as rotors:

$$z_{\text{rot}}^{\text{1D}} = \frac{1}{\sigma_{\text{rot,int}}} \cdot \left(\frac{8\pi^2 \cdot I_{\text{rid}} \cdot k_B \cdot T}{h^2} \right)^{\frac{1}{2}} \quad \text{vs} \quad z_{\text{vib}}^{\text{int}} = \frac{1}{1 - \exp(-h\nu/k_B T)}$$

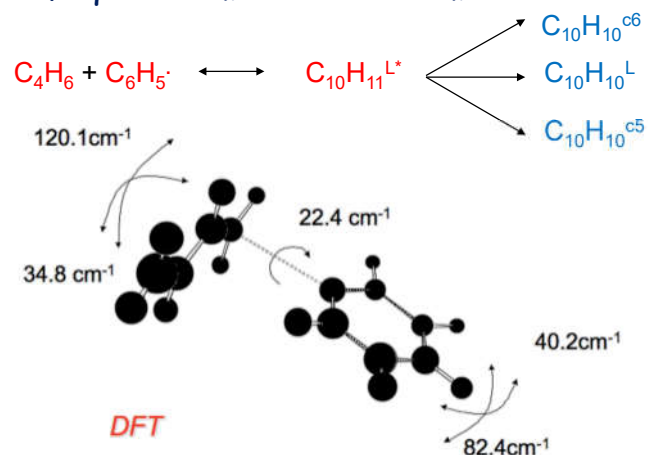
Considering an internal motion as a vibration or a rotation can affect significantly both the rate constant estimation and the estimation of the entropy.

⇒ how can it be determined if an internal motion can be treated as vibration or not?

A first indication is the analysis of the low vibrational frequencies, which indicate that the energetic barrier for the corresponding internal motion is small. In particular it is quite common to find low vibrational frequencies in the TS corresponding to the formation or rupture of chemical bonds

Small vibrational frequencies

For example, in the case of butadienylphenyl dissociation, we can find 5 vibrational frequencies smaller than 150 cm^{-1}



An approach to treat these 5 small vibrational frequencies has been suggested by Gilbert

Gilbert method

The decomposition of a AB molecule in the fragments A and B correspond to the loss of 6 vibrational frequencies, which transform into 6 new degrees of freedom, 3 rotational and 3 translational. These are usually called **transitional modes**.

Gilbert proposes that in the TS the disappearing vibrational frequencies become:

- 2 bi-dimensional rotors (4 vibr. freq)
- 1 mono-dimensional rotor (1 torsional vibr. Freq.)
- 1 imaginary frequency (translation along TS coordinate)

At a first level of approximation, they can be calculated using 2D and 1D rotational partition functions as:

$$z_{\text{rot}}^{2\text{D}} = \frac{k_{\text{B}}T}{\sigma_{\text{rot}}} \cdot \left(\frac{8\pi^2 \cdot I_{\text{rid}}}{h^2} \right) \frac{1 - \cos \vartheta}{2}$$

$$z_{\text{rot}}^{\text{tors}} = \frac{1}{\sigma_{\text{rot}}^{\text{int}}} \cdot \left(\frac{8\pi^2 \cdot I_{\text{rid}} \cdot k_{\text{B}} \cdot T}{h^2} \right)^{\frac{1}{2}}$$

The pre-exponential factor of the reaction calculated with Gilbert method changes significantly from that determined with vibrational TST, going from 10^{10} to 10^{14} .

Gilbert method

Gilbert approach is based on the assumption that the two molecular moieties moves freely around the pivot points and are blocked only by steric impediments. In reality the moving moieties are restrained by a multidimensional potential, function of the transitional modes. To correctly account for such motions it is possible to refer to the 1D rotational Schrödinger equation:

$$H\psi = E\psi \quad \longrightarrow \quad -\frac{\hbar^2}{2I_m} \frac{\partial^2 \psi}{\partial \phi^2} + V(\phi)\psi(\phi) = E\psi(\phi)$$

$V(\phi)$ is the potential, which can be expressed through a Fourier expansion as:

$$V_m(\phi_m) = \sum_{k=1}^{k_{\max}} \frac{1}{2} V_{mk} \cdot (1 - \cos(k\phi_m))$$

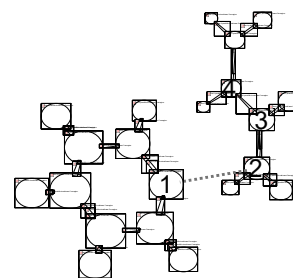
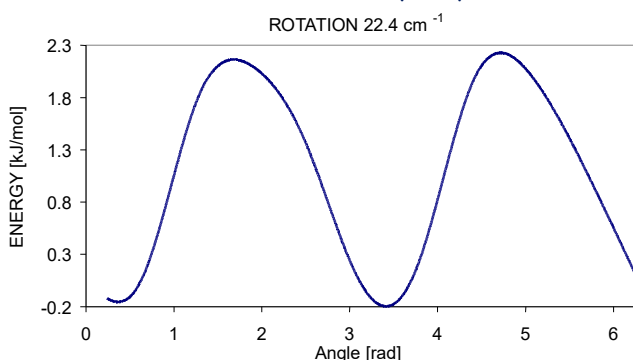
Not easily defined!
2 possibilities \rightarrow average values or I of the rotational moiety

The solution of the 1D Schrödinger equation allows to determine the eigenvalues ε_i , from which the rotational partition function can be computed as:

$$q_{\text{rot,int,m}} = \frac{1}{\sigma_m} \sum_k g_k(m) \cdot \exp\left(-\frac{\varepsilon_k(m)}{k_B \cdot T}\right)$$

Gilbert method

The QM estimation of the rotational energy associated to the rotation of C₄H₆ around the butadiene-phenyl bond lead to:

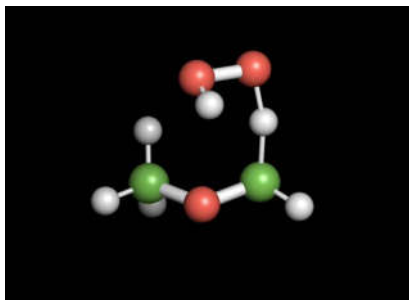


$$\nu = 22.4 \text{ cm}^{-1}$$

The energy barrier is small, only 1.8 Kcal/mol. At 300 K the pre-exponential factor becomes

K vibrational	K int rot QM	K Gilbert
6.8×10^{10}	1.5×10^{12}	1.8×10^{14}

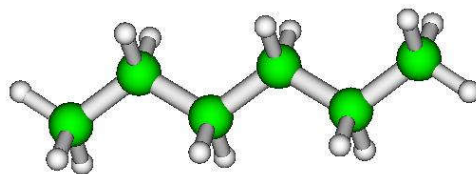
Gilbert method



Entropy correction

This type of correction can be relevant also for the evaluation of the entropy. For C_6H_{14} we found using the HA:

	S° transl	S° vibr	S° rot	S° calc	S° exp
C_6H_{14}	39.3	21.9	27.3	88.5	92.9

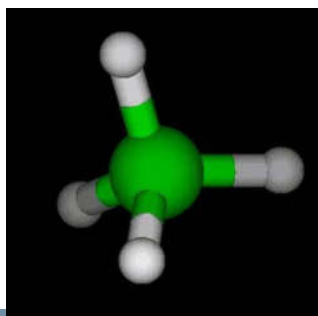


But this molecule has 3 very low vibrational frequencies: 73, 98 and 131 cm^{-1} , which are better described as internal torsional rotors rather than vibration. A QM calculation of the corresponding PES and of the associated Qrot, allows to correct the rotational and vibrational partition functions, increase by 3 cal/mol/K, thus significantly improving the agreement with experimental data

Estimation of TS symmetry/degeneracy

It is the number of equal reaction channels. Usually indicated as σ :

$$k_{cin} = \sigma \frac{k_B T}{h} \frac{z_{trasl}^\ddagger z_{rot}^\ddagger z_{vib}^\ddagger (3N-7)_{rid}}{\prod z_i^{reactants}} \exp\left(-\frac{\sum(\epsilon_i + ZPE)v_i}{k_B T}\right)$$

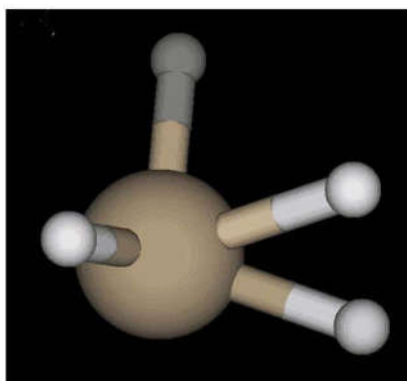


Es.: $\text{CH}_4 \rightarrow \text{CH}_3 + \text{H}$ has a degeneracy factor of 4.

The estimation of σ can get rapidly complicated

Es.: $\text{SiH}_4 \rightarrow \text{SiH}_2 + \text{H}_2$

Estimation of TS symmetry/degeneracy



The degeneracy factor is directly related to the rotational symmetry number

Estimation of TS symmetry/degeneracy

From a rigorous standpoint, it is defined as:

$$\sigma = \frac{\sigma_R m_{ts}}{\sigma_{TS} m_R}$$

Where:

- σ of r and ts are the rotational degrees of symmetry of reactant and TS

- m is the number of optical isomers

for CH₄ decomposition:

$$\sigma_{\text{st}} = 3 \quad \sigma_{\text{CH}_4} = 12 \quad m_{\text{CH}_4/\text{TST}} = 1 \quad \sigma = 4$$

For SiH₄ decomposition :

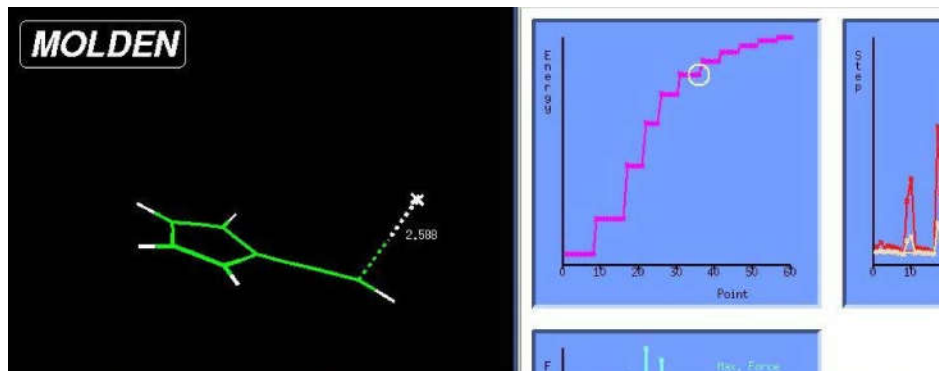
$$\sigma_{\text{st}} = 1 \quad \sigma_{\text{SiH}_4} = 12 \quad m_{\text{SiH}_4/\text{TST}} = 1 \quad \sigma = 12$$

Reactions without a distinct TS

It happens when the PES, scanned as a function of the reaction coordinate, shows that the transition from reactants to products takes place without passing from a maximum.

→ How can we determine a rate constant for such reactions?

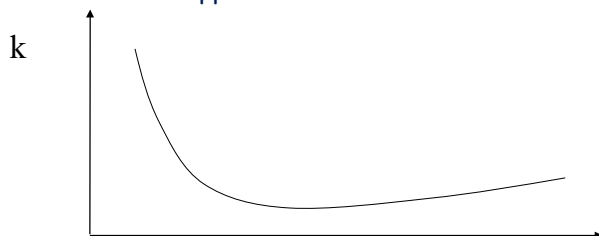
Es: C₅H₄_CCH₂ → C₅H₄_CCH + H



Variational TST

TS variational theorem

The rate constant calculated applying TST as a function of the reaction coordinate is an upper limit of the 'real' rate constant



Procedure:

Reaction Coordinate

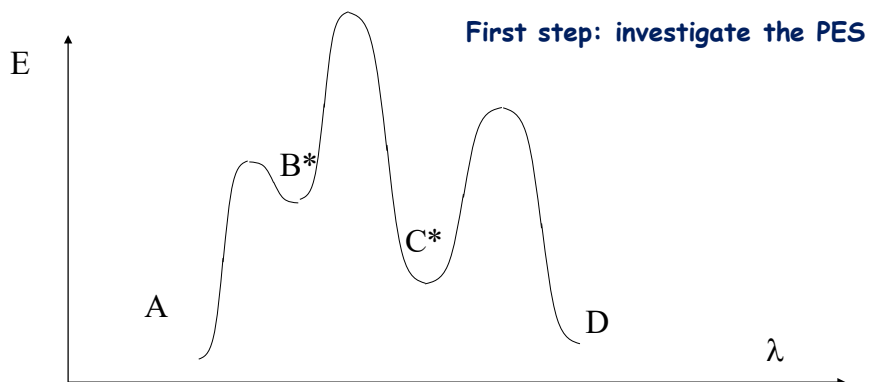
- 1) Scan PES as a function of reaction coordinate
- 2) Frequency calculation for each scan point
- 3) determine k_{cin} at different Temperatures
- 4) problem: large amplitude motions \rightarrow Variable Reaction Coordinate TST

Ab initio kinetics for pyrolysis and combustion systems. SJ Klippenstein, C Cavallotti
Computer Aided Chemical Engineering 45, 115-167

MultiWell reacting systems

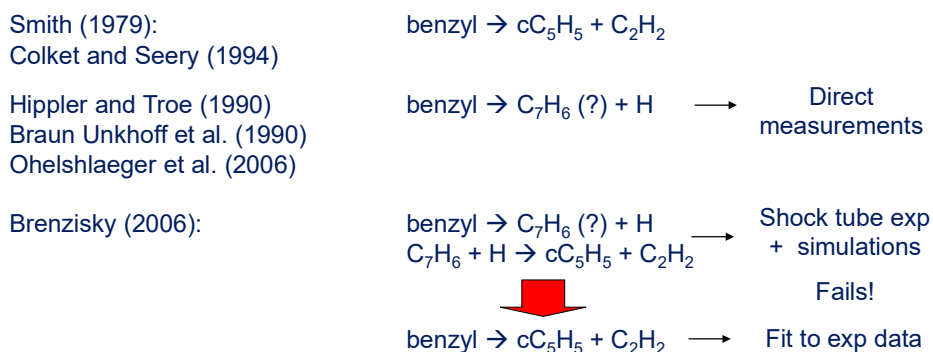
Often happens that multiple wells can be present on the same PES \rightarrow it is necessary to pass through several intermediates before reaching the reaction bottleneck

\rightarrow How to study such reactions?



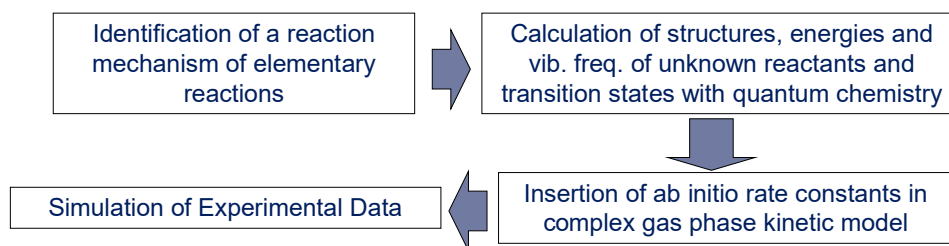
Example: benzyl decomposition

High temperature (unimolecular)



Specific AIM: determine benzyl decomposition mechanism, nature of C7H6 product and successive reactivity of C7H6

Approach and Computational Protocol



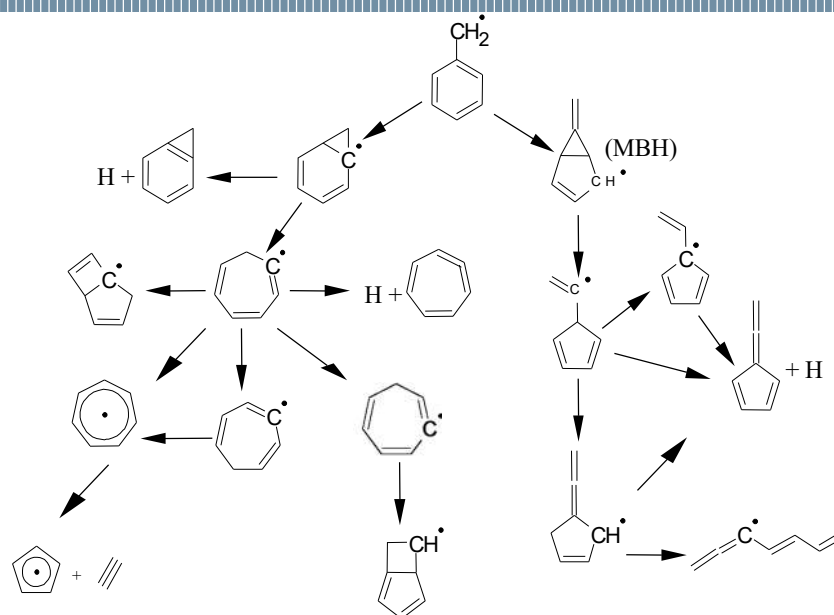
Ab Initio Calculations details

- Structures and energies of reactants and TST optimized at the B3LYP/6-31g(d,p) level
- Vibrational Frequencies at B3LYP/6-31g(d,p) level
- TST structures located using synchronous transit method
- Explicitly account of degeneration of low vibrational frequencies in internal rotors
- Energy refined at G2MP2 level on B3LYP/6-31g(d,p) structures

$$\text{EG2MP2} = \text{E}(\text{QCISD}(\text{T})/6-311+\text{g}(\text{d},\text{p})) + \text{E}(\text{MP2}/6-311+\text{g}(3\text{df},2\text{p})) - \text{E}(\text{MP2}/6-311+\text{g}(\text{d},\text{p})) + \text{ZPE} + \text{HLC}$$

Accuracy of 1-2 kcal/mol. e.g. toluene \rightarrow benzyl + H $\Delta H_{\text{exp}} = 89.6 \pm 1$ kcal/mol $\Delta H_{\text{calc}} = 90.7$ kcal/mol

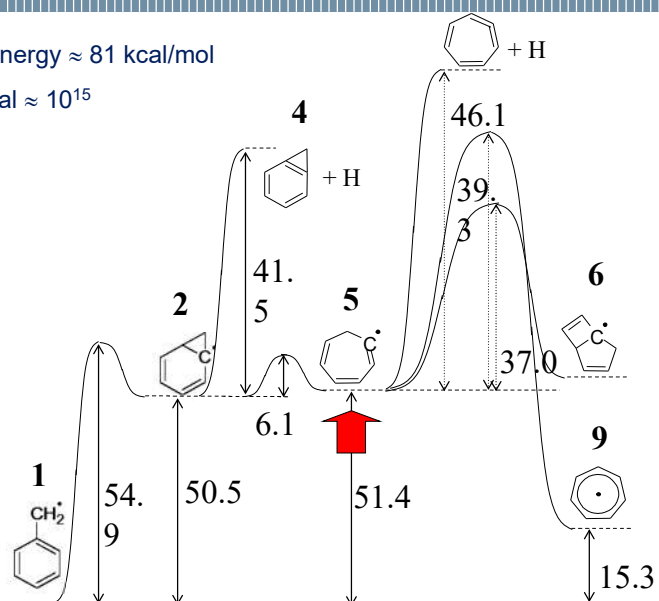
Investigated C7H7 Mechanism



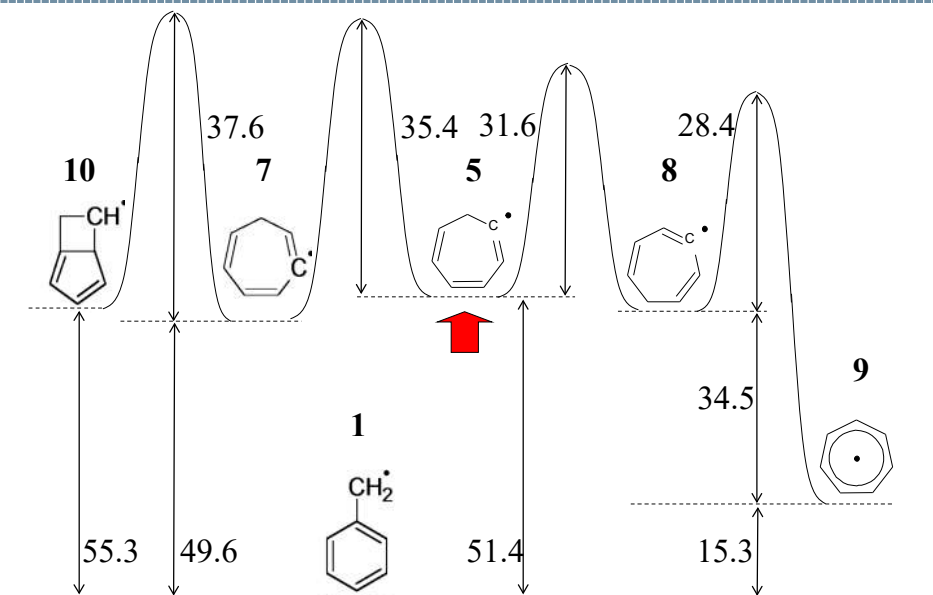
Potential Energy Surface 1

Exp activation energy ≈ 81 kcal/mol

Pre-exponential $\approx 10^{15}$



Potential Energy Surface 2

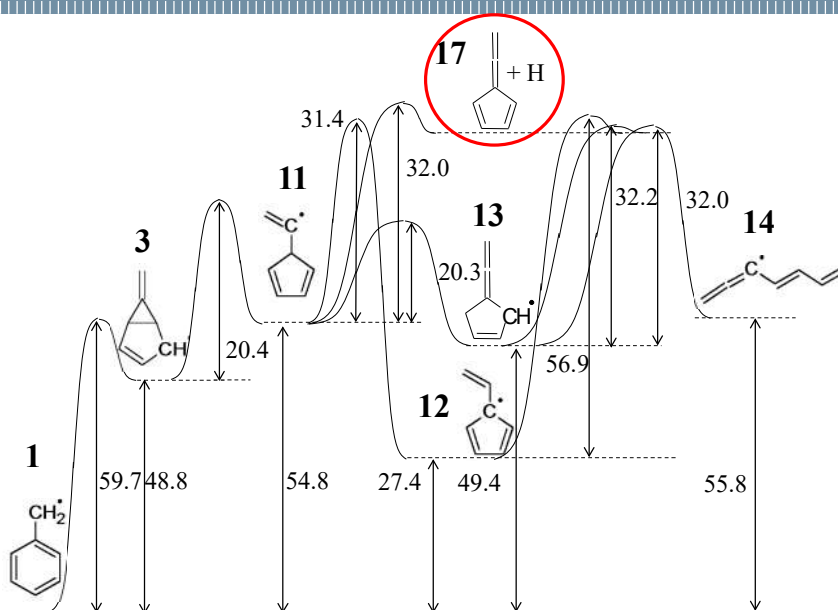


59

Tsinghua Summer School

POLITECNICO MILANO 1863

Potential Energy Surface 3

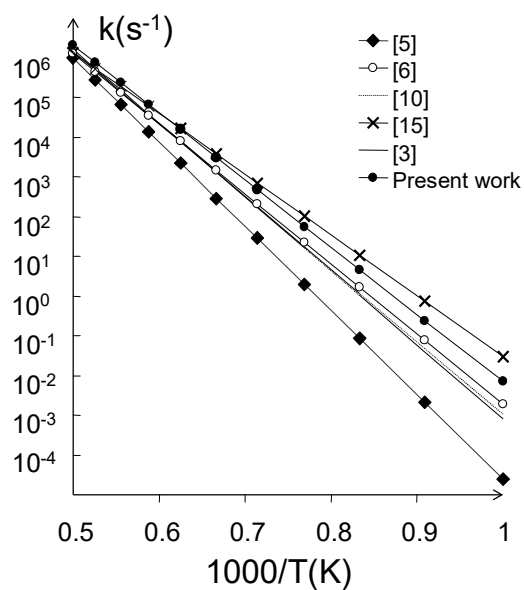


60

Tsinghua Summer School

POLITECNICO MILANO 1863

Calculated Rate Constant



Rate constant determined assuming equilibrium between reactant and bottleneck TS. But... What if this hypothesis is not valid?

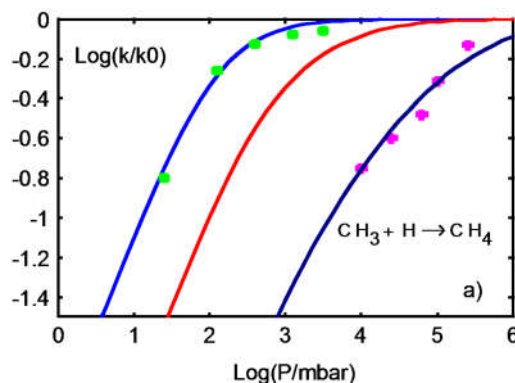
Violation of classic TS Theory Hypotheses 1

Equilibrium between reactants and transition state not valid.

The violation consists essentially in a decrease of the population of molecules at elevated internal energies. In this sense, what is violated is the Boltzmann energy distribution function. When this happens, the rate constant exhibits a marked pressure dependence. These reactions, that have been known for some time, are called **fall-off reactions**.

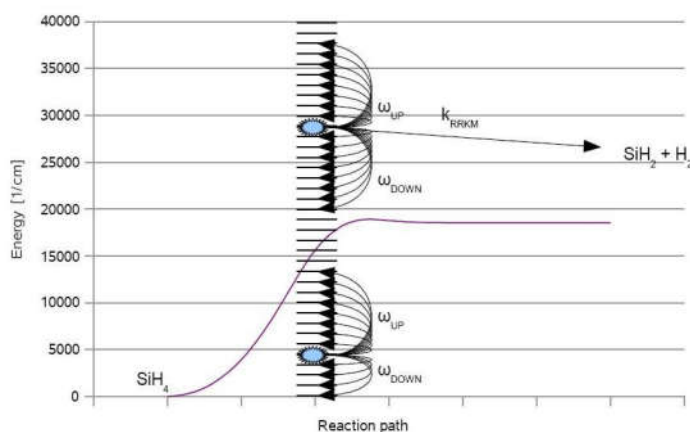
Fall off Reactions - experimental evidences

Experimentally, it is found that for some reactions a decrease of the pressure leads to a decrease of the rate constant, up to the point at which the rate constant becomes linearly dependent from the pressure. The transition to the linear dependence regime is called fall off regime.



Fall off – physical origin

The pressure dependence of the rate constant is determined by the decrease of the population of the excited vibrational energy levels. To describe this behavior adequately it is thus necessary to treat explicitly the molecular vibrational excitation dynamics.



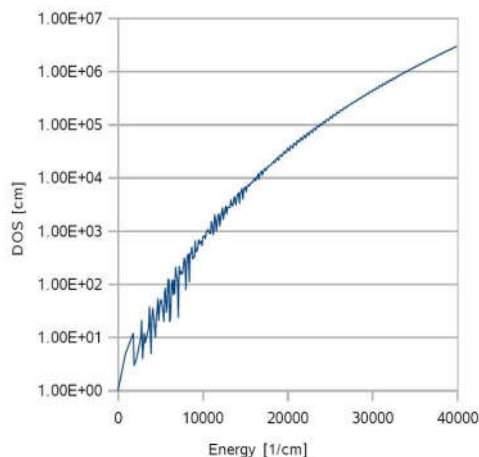
Density of states

To introduce a correct description of the vibrational states dynamics, it is necessary to introduce the concept of Density of States. For a molecule with energy E , the DOS is the number of different ways in which the energy can be partitioned among the S harmonic oscillators (vibrations) of the molecule

DOS = number of states between energy E and $E+dE/dE$

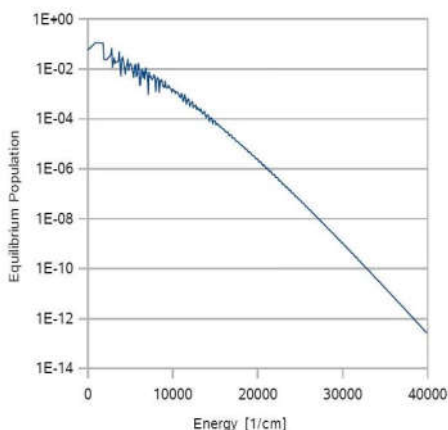
The DOS can be readily calculated with the Beyer - Swinehart algorithm, remembering that each oscillator can contain only quanta of energy proportional to $h\nu_i$

The minimum vibrational energy level is the Zero Point Energy



Vibrational energy distribution function

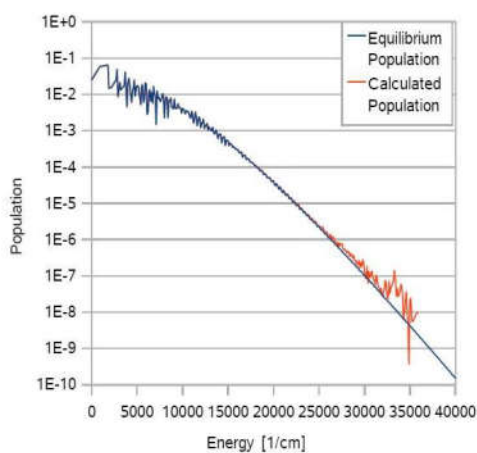
The vibration energy excitation takes place through the collision made by each molecule with the surrounding bath gas. At the equilibrium the vibrational energy population is described by the exponential law known as Boltzmann distribution function. This is the law that is violated and that invalidates the TS assumptions.



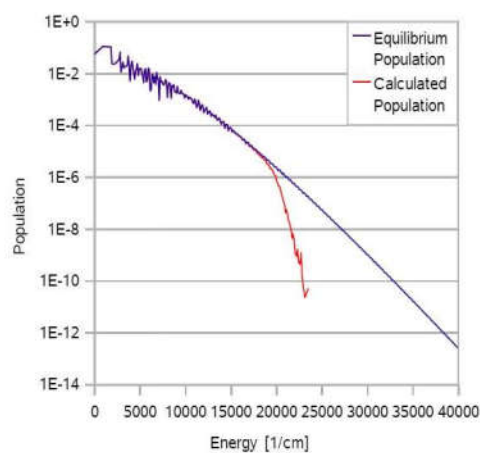
$$f(E) = \frac{DOS(E)}{Q} e^{-\frac{E}{k_B T}}$$

$$Q = \sum_{E=0}^{\infty} DOS(E) e^{-\frac{E}{k_B T}}$$

Low Pressure Effect



High pressure reacting molecules



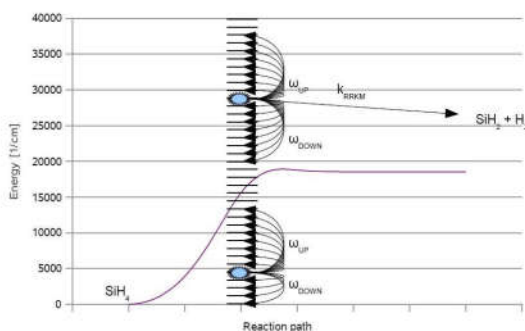
Low pressure reacting molecules

Master Equation

In order to determine the dynamics of a system that it is not in Boltzmann equilibrium, it is necessary to study explicitly the population of each vibrational energy level. This is accomplished through the integration of the master equation:

$$\frac{\partial n(E)}{\partial t} = Z \cdot \sum_{E'=0}^{\infty} (P(E, E') \cdot n(E') - P(E', E) \cdot n(E)) - k(E)n(E)$$

It is a population balance of the generic energy level E , which population is assumed to be $n(E)$:



$P(E, E^I)$: probability that a molecule at energy E^I goes to energy E through a collision

$K(E)$ rate constant for the reaction of a molecule with energy E

Master Equation: parameters determination

To solve the master equation it is necessary to know $k(E)$ and $P(E, E')$. Several possibilities exist to calculate $P(E, E')$:

$$P(E, E') = \frac{1}{N(E')} e^{-\frac{E'-E}{\alpha}} \quad (E \leq E') \quad \text{exponential down model}$$

$$P(E, E') = \frac{1}{N(E')} e^{-\left(\frac{E'-E}{\alpha}\right)^2} \quad (E \leq E') \quad \text{Gaussian model}$$

$$P(E, E') = \frac{1}{N(E')} \left[(1-f) e^{-\frac{E'-E}{\alpha_1}} + f e^{-\frac{E'-E}{\alpha_2}} \right] \quad (E \leq E') \quad \text{double exponential down model}$$

$$P(E, E') = \frac{1}{N(E')} e^{-\frac{E'-E}{\alpha}} \quad (E \leq E') \quad \text{Exponential model}$$

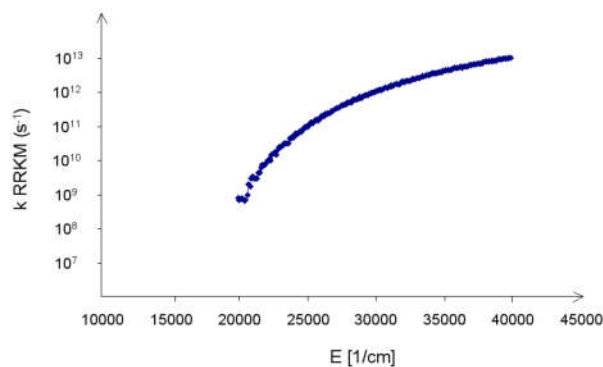
$$P(E, E') = \frac{1}{N(E')} e^{-\frac{E'-E}{\beta}} \quad (E > E') \quad N(E^I) \text{ is a normalization factor}$$

Master Equation: parameters determination

The microcanonical reaction rate constant of a molecule excited at energy level E can be calculated through Marcus theory as:

$$k(E) = \frac{\int_{E_0}^E \rho_{vib}^{\ddagger}(E - E^*) dE^*}{h \rho_{vib}(E)}$$

Where $\rho(E)$ is the density of vibrational states



$k(E)$ is known as RRKM rate constant and gives the TST classic expression if the molecules are at the Boltzmann equilibrium

Master Equation + RRKM: integration

3 possibilities:

MESS: from chemical significant eigenvalues: <https://github.com/Auto-Mech/MESS>

Mesmer: (<https://pubs.acs.org/doi/abs/10.1021/jp3051033>)

(<https://www.chem.leeds.ac.uk/mesmer/introduction.html>)

Mixed stochastic/numeric: Multiwell (Barker)

Example: stochastic code

- single molecule dynamic directly tracked
- the possible transitions are NR and can either be transitions between different energy levels or reactions (all frequencies)

Transition probability

$$P_i = \frac{R_i}{\sum_i^{NR} R_i}$$

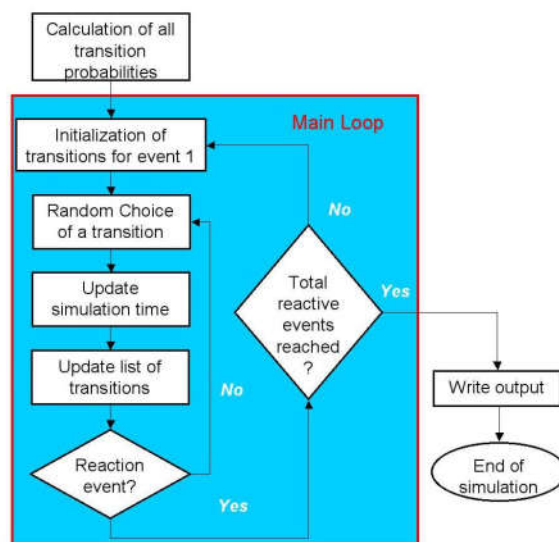
- a transition is chosen determining a random number U_1 , which satisfies the condition:

$$\sum_1^{j-1} R_i < U_1 \cdot \sum_1^{\infty} R_i < \sum_1^j R_i$$

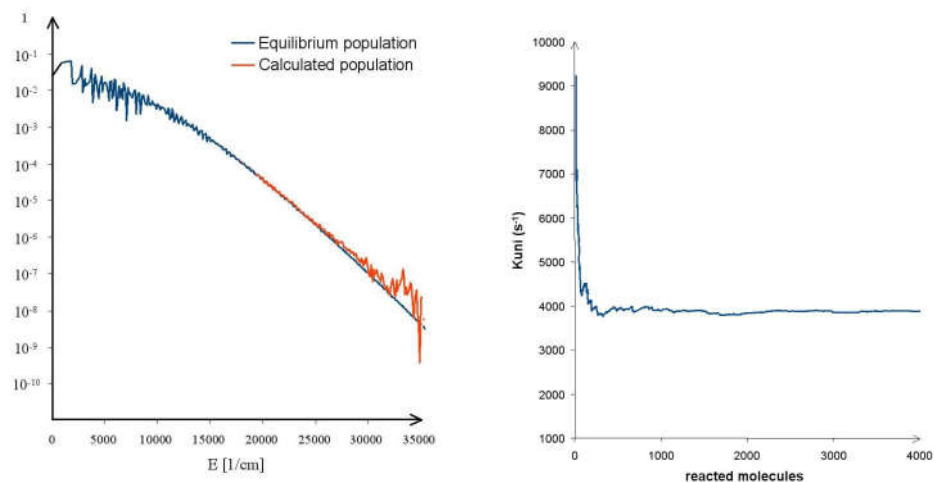
The time is incremented by

$$\Delta t = -\ln(U_2) / \sum_1^{\infty} R_i$$

Master Equation + RRKM: KMC solution

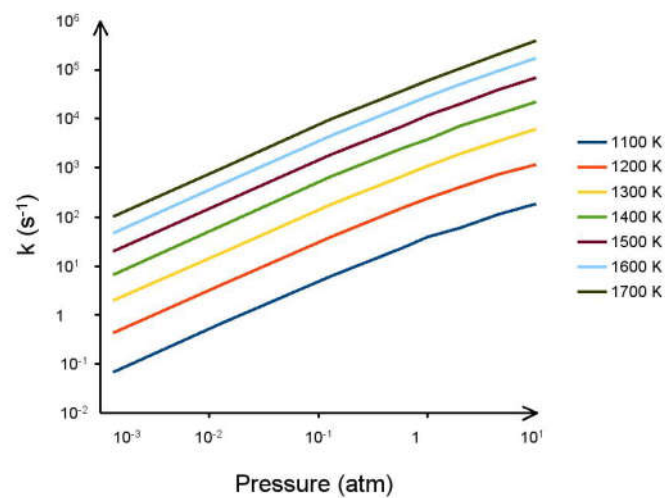


Master Equation + RRKM: $\text{SiH}_4 \rightarrow \text{SiH}_2 + \text{H}_2$

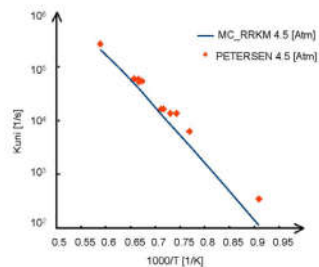
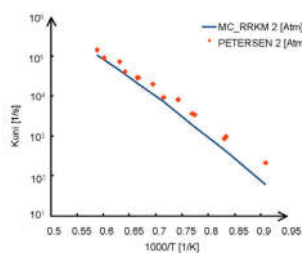
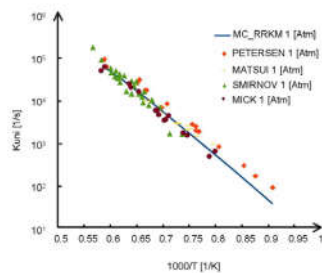
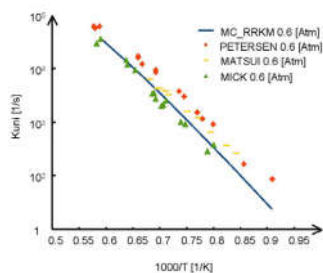


Rate constant calculated as $k = \text{number of reactive events}/\text{total time}$

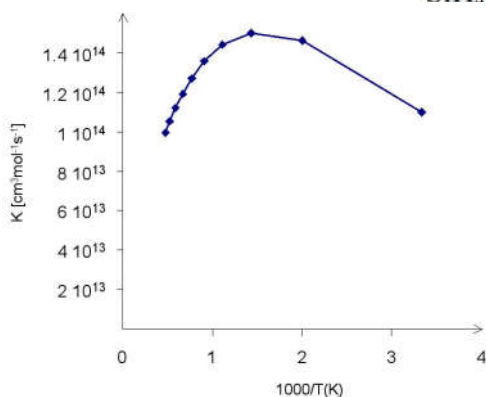
Master Equation + RRKM: Results



Master Equation + RRKM: Results



Master Equation + RRKM: bimolecular reactions



Procedure:

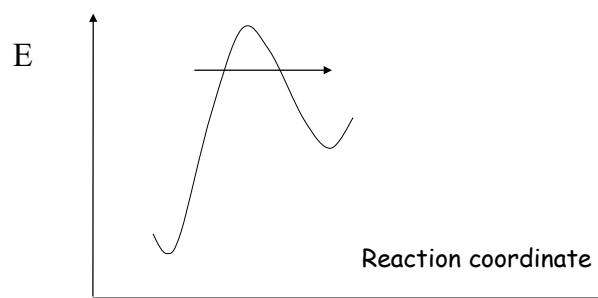
- time 0 it is generated a molecule at energy E given by the sum of the vibration energies of the reactants, estimated through 2 random numbers assuming Boltzmann equilibrium
- same simulation protocol as unimolecular reaction
- k_{cin} determined as reaction probability with respect to stabilization and multiplied by the association constant between SiH₃ + H

Violation of TS Theory Hypotheses 2

**Maxwell velocity distribution not valid
(i.e. non classic description of nuclei motion).**

In some conditions, it is possible that some quantum effects influence the rate of a chemical reaction. This is for example the case of tunneling

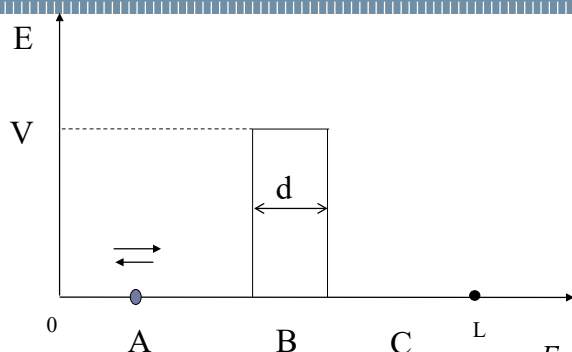
Quantum Tunneling



From a quantum standpoint, a particle moving along a PES tunnels through energetic barriers even if its kinetic energy is smaller than the height of the barrier.

This effect is known as quantum tunneling

Tunnel effect for barrier of fixed width and height



$$\left[-\frac{\hbar^2}{2m} \frac{d^2}{dx^2} + V \right] \Psi(x) = E\Psi$$

The probability to cross the barrier is:

$$p = 4 \frac{E}{V} \left(1 - \frac{E}{V} \right) \exp\left(-\frac{2d}{\hbar} (2m(V-E))^{1/2} \right)$$

The crossing probability increases with the decrease of mass of the moving particle and of the width d of the barrier. At very high T it is usually negligible.

An indirect estimate of the width d is given by the value of the imaginary frequency. Q_{tunnel} becomes important $\nu > 1500i \text{ cm}^{-1}$

Quantum Tunneling

Extending the theory to molecular system complicates the problem significantly since:

- multi atomic reacting system \rightarrow complex PES
- the PES has not a rectangular shape

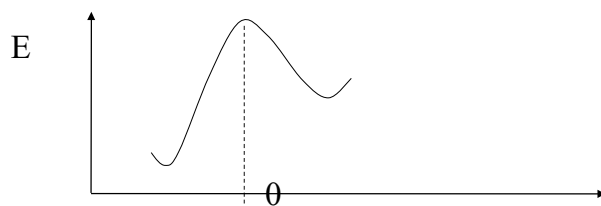
The tunneling contribution is usually indicated as z_{tunnel} :

$$k_{\text{cin}} = \frac{k_B T}{h} \frac{z_{\text{tunnel}} z_{\text{trans}}^{\ddagger} z_{\text{rot}}^{\ddagger} z_{\text{vib}}^{\ddagger(3N-7)} z_{\text{rid}}}{\prod z_i^{\text{reactants}}} \exp\left(-\frac{\sum(\varepsilon_i + ZPE)v_i}{k_B T} \right)$$

Among the approximate solutions proposed in the literature, the Shavitt proposal is remarkably simple:

$$z_{\text{tunnel}} = 1 - \frac{1}{24} \left(\frac{h\nu}{k_B T} \right)^2 \left(1 + \frac{k_B T}{Ea} \right)$$

Quantum Tunneling



More complex approaches are reported in the literature. To use such theories the procedure is usually the following:

- The reaction coordinate s , is centered on the TS
- the PES must be determined as a function of s , which is defined as the length of the bond formed before the TS and of that broken after
- the possible theory level are then classified as:
 - Wigner Shavitt: only geometry of TS and ν_{imm}
 - Eckart: only E_{act} , ν_{imm} , and barrier width are necessary
 - Post-Eckart: SCT, ...: PES as A function of s , ν_{imm} + all vibr. freq along PES

Recommended: Polyrate code from Truhlar/ EStokTP

Quantum Tunnel - examples

Table 2 Calculated transmission coefficients for $H + CH_3F$ reaction

T/K	κ_{SCT}	κ_{ZCT}	κ_w	κ_{Eckart}	$\kappa_{RC-\mu V}$	$\kappa_{RC-\mu I}$
250	151.69	12.64	4.41	49.50	32.47	200.45
300	32.85	5.14	3.36	12.04	10.77	39.43
400	6.72	2.17	2.33	3.36	3.47	7.36
500	3.16	1.45	2.05	1.93	2.02	3.33
600	2.06	1.15	1.59	1.42	1.48	2.14
800	1.31	0.90	1.33	1.03	1.06	1.34

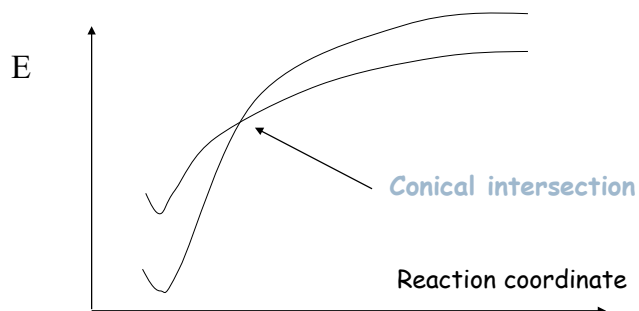
Violation of TS Theory Hypotheses 3

Born Oppenheimer non valid

This happens when the crossing between different PES (i.e. with different electronic configurations) becomes necessary. Such reactions are usually called spin forbidden.

Spin Forbidden Reactions

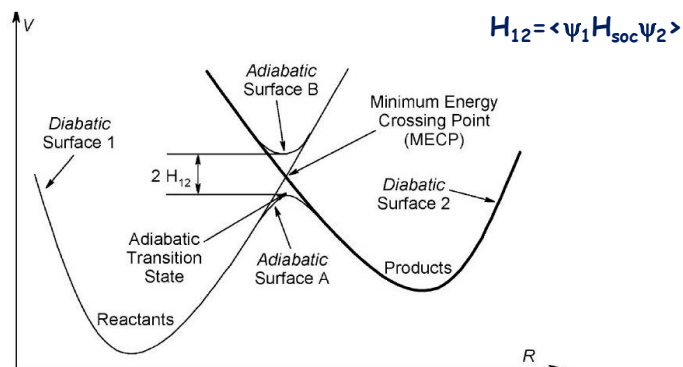
Sometimes it happens that, along the reaction coordinates, the energy decreases if a change of spin takes place (spin flip). This might happen when the spin state of the product is different from that of the reactants.



In the standard BO approximation it is not possible to hop from one surface to the other, as they do not cross because of spin-orbit interactions.

Spin Forbidden Reactions

In reality the two wave functions are coupled by the interaction between the electron spin and the orbital angular momentum (H_{so}). Adding H_{so} to the energy calculated in the BO approximation the intersection between the two PES of different spin is avoided (in general singlet and triplet).



Spin Forbidden Reactions – Rate constant

The evaluation of the rate constants of spin forbidden reaction is a complex problem. However, often the PES crossing takes place before the TS, so that classic TS Theory can still be applied.

The most reasonable approach to calculate the rate constant is to use microcanonical theory, as in RRKM, with:

$$k(E) = \frac{N_{\alpha}(E)}{h\rho(E)}$$

$$N_{\alpha}(E) = \int dE_h \rho_{\alpha}(E - E_h) \rho_{hop}(E_h) \quad \rho_{hop}(E) = (1 - P_{LZ})(1 + P_{LZ})$$

N_{α} is the effective density of states at the conical intersection

P_{sh} is the intersystem hopping probability

P_{LZ} can be expressed through Landau Zener theory as a function of H_{so} (ref. J.N. Harvey, Phys. Chem. Chem. Phys. (2007), 9, 331-343)

$$P_{LZ} = \exp\left(-\frac{2\pi H_{SO}^2}{\hbar\Delta F} \sqrt{\frac{\mu}{2E}}\right)$$

References

Chemical Kinetics, Leidler

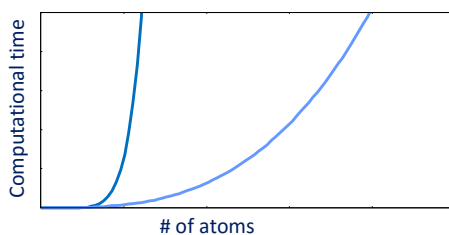
Chemical Kinetics and Dynamics, Steinfeld, Francisco, Hase

Theory of Unimolecular and Recombination Reactions, Gilbert and Smith

Molecular theory of gases and liquids, Hirschfelder, Curtiss, Bird

- Ab initio kinetics for pyrolysis and combustion systems. SJ Klippenstein, C Cavallotti *Computer Aided Chemical Engineering* 45, 115-167 (I general the whole book is a good reference)
- Spiers Memorial Lecture: theory of unimolecular reactions. DOI: 10.1039/D2FD00125J (Paper) *Faraday Discuss.*, 2022, Accepted Manuscript
- From Theoretical Reaction Dynamics to Chemical Modeling of Combustion Stephen J. Klippenstein *Proceedings of the Combustion Institute* 36 (1), 77-111
- Variational transition state theory: theoretical framework and recent developments. *Chem. Soc. Rev.*, 2017, 46, 754

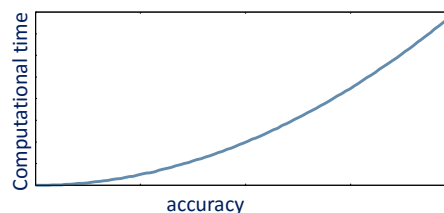
Quantum chemistry computational cost



Problem of computational chemistry is that the computational effort increases exponentially with the number of electrons (i.e. the number of atoms) of the system.

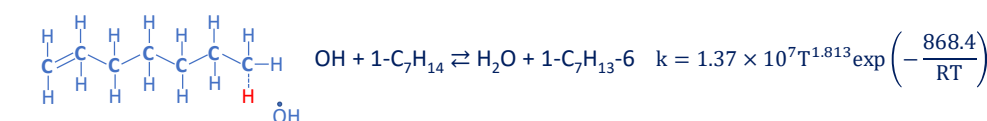
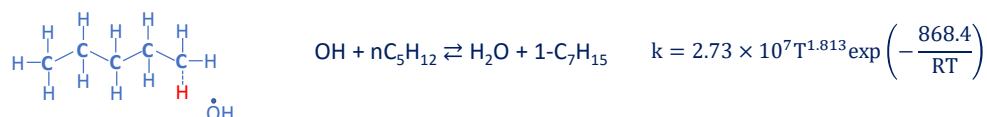
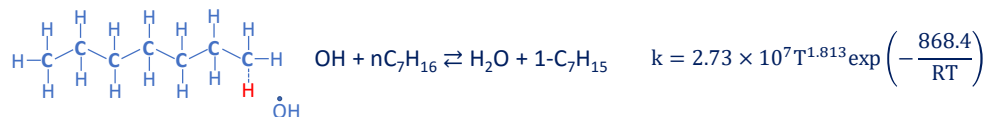
Chemistry of real fuels, like in the case of diesels or jet fuels, or formation of pollutant like soot involves large molecules, which prevent the use of the theoretical estimation of the rate constants.

This increase depends on the accuracy of the estimation. Small errors require larger computational time

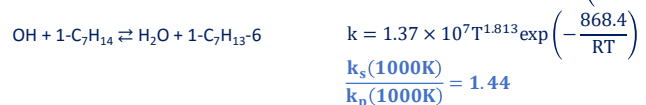
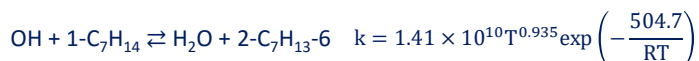
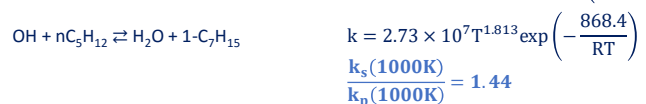
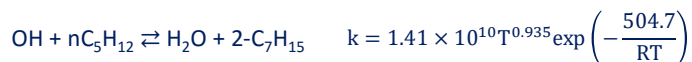
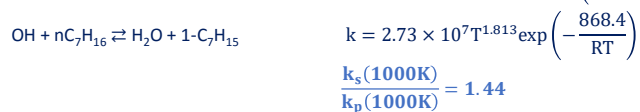
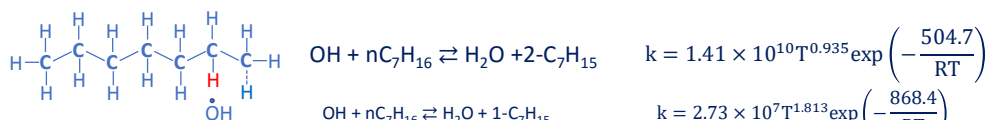


Analogy rules

The forces between atoms are generally very short range (Benson, 1976), i.e. in the order of magnitude of the bond lengths: each atom contributes constant amounts to the molecule properties.

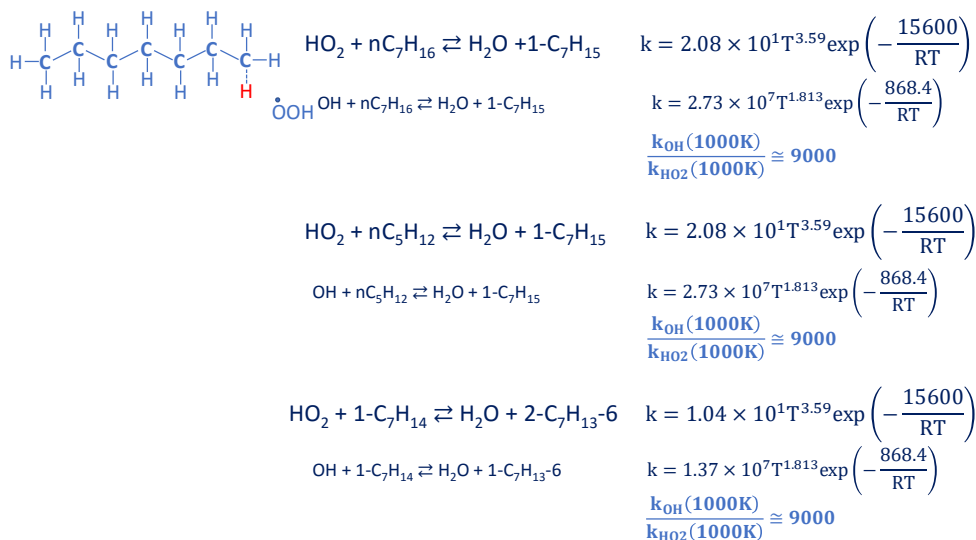


Analogy rules



Ratio between abstracting a secondary and a primary H atom is the same

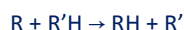
Analogy rules



OH abstracts about 9000 times faster than HO₂ (at 1000 K)

H-abstraction reactions

Generalizing the Habstraction reactions:



It is possible to roughly and simply estimate the rate constant:

$$k_{\text{Habstr}} = k_{\text{ref,R}}^0 C_{\text{R}'\text{H}} \quad \text{Ranzi et al., Comb. Sci., Tech., 95, 1993}$$

where $k_{\text{ref,R}}^0$ represents the intrinsic reactivity of the abstracting radical R radical and $C_{\text{R}'\text{H}}$ is the relative reactivity of the removed H-atom.

This assumption simply means that the contributions for evaluating the rate constant only come from properties related to the abstracting radical and to the type of the hydrogen atom to be abstracted.

Theoretical basis for this simplification can be partially found in the assumption of short range forces among atoms (Benson, 1976).



This estimation is quite approximated and should be used only when no theoretical or experimental data are available, like for large molecules

Summary of analogy rules

A few reference kinetic parameters allow to estimate a large number of rate constants, laying the foundation for possible automatic mechanism generation

H-Abstraction Reactions			
	Primary H atom	Secondary H atom	Tertiary H atom
Primary radical	$10^{8.0} \exp(-13.5/RT)$	$10^{8.0} \exp(-11.2/RT)$	$10^{8.0} \exp(-9/RT)$
Secondary radical	$10^{8.0} \exp(-14.5/RT)$	$10^{8.0} \exp(-12.2/RT)$	$10^{8.0} \exp(-10/RT)$
Tertiary radical	$10^{8.0} \exp(-15/RT)$	$10^{8.0} \exp(-12.7/RT)$	$10^{8.0} \exp(-10.5/RT)$
Isomerization Reactions (Transfer of a Primary H-atom)			
	1-4 H Transfer	1-5 H Transfer	1-6 H Transfer
Primary radical	$10^{11.0} \exp(-20.6/RT)$	$10^{10.2} \exp(-14.5/RT)$	$10^{9.7} \exp(-14.5/RT)$
Alkyl Radical Decomposition Reactions to form Primary Radicals			
Primary radical	Secondary radical	Tertiary radical	
$10^{14.0} \exp(-30/RT)$	$10^{14.0} \exp(-31/RT)$	$10^{14.0} \exp(-31.5/RT)$	
Corrections in Activation Energy to form:			
Methyl radical	Secondary radical	Tertiary radical	
+ 2.	- 2.	- 3.	

Ranzi et al., Comb. Flame, 102, 1995

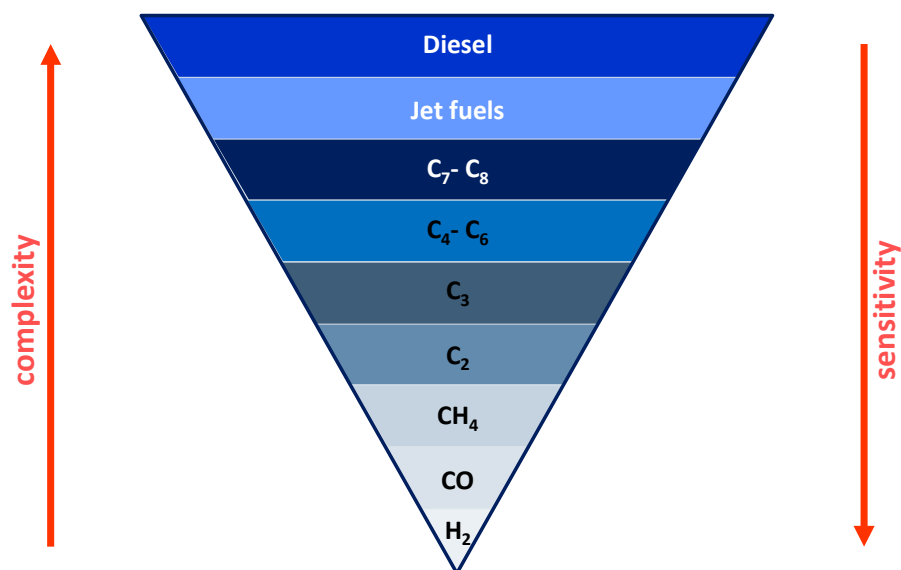
RECAP

Combustion consists of radical chain reactions. Rate constant can be estimated from:

- ✓ Experimental measurement
- ✓ Collision theory
- ✓ Quantum calculations
 - kinetic theory of gases
 - Rate constant expression and limitations
 - transition state theory
 - formulation
 - RRHO approximation
 - potential energy surfaces
 - limits of TST: degeneration of internal degrees of freedom into hindered rotations
 - beyond TST: RRKM + master equation theory
 - beyond TST: quantum tunneling
 - beyond TST: spin forbidden reactions
- ✓ Analogy rules

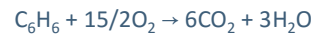
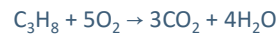
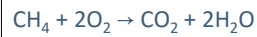
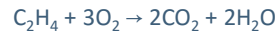
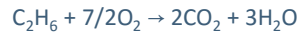
Combustion mechanisms

The mechanism hierarchical structure



An important combustion parameter

Stoichiometric combustion is the ideal combustion process where fuel is burned completely. A complete combustion is a process burning all the carbon (C) to CO_2 and all the hydrogen (H) to H_2O



Equivalence ratio:
$$\Phi = \frac{F_{\text{uel}}/O_{\text{xidizer}}}{(F_{\text{uel}}/O_{\text{xidizer}})_{\text{stoich}}}$$

$\Phi = 1$ **stoichiometric conditions**

$\Phi < 1$ **Lean conditions**: more oxygen than needed

$\Phi > 1$ **Rich conditions**: less oxygen than needed

$\Phi = 0$ no fuel (i.e. no combustion)

$\Phi = \infty$ no oxygen: **Pyrolysis**

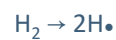
Equivalence ratio equivalent in mass or in moles

$$\Phi = \frac{F/O}{(F/O)_{\text{stoich}}} = \frac{m_F/m_O}{(m_F/m_O)_{\text{stoich}}} = \frac{n_F/n_O}{(n_F/n_O)_{\text{stoich}}}$$

Sometimes air–fuel equivalence ratio (λ) or air excess is used
$$\lambda = \frac{O_{\text{xidizer}}/F_{\text{uel}}}{(O_{\text{xidizer}}/F_{\text{uel}})_{\text{stoich}}} = \frac{1}{\Phi}$$

H₂ mechanism

Homolytic bond cleavage



H-abstraction from a stable molecule



Radical transfer: H abstraction



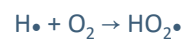
Homolytic bond cleavage



Radical transfer: H abstraction



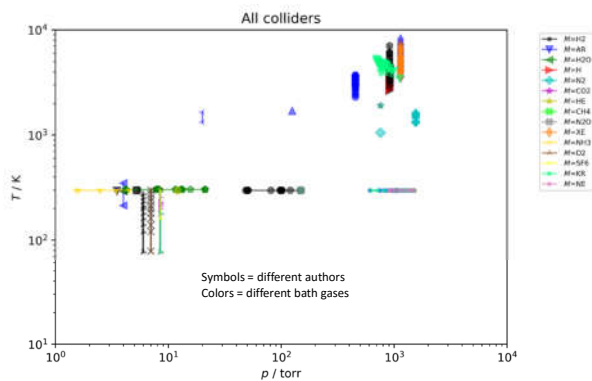
Radical addition



Branching reaction



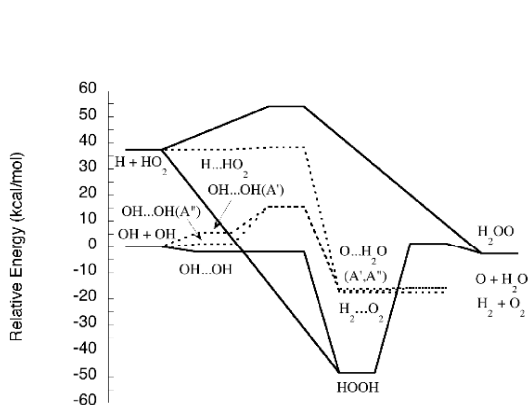
Homolytic bond cleavage $\text{H}_2 \rightarrow 2\text{H}\cdot$



$$k = 4.577 \times 10^{19} T^{-1.4} e^{\frac{104400}{RT}}$$

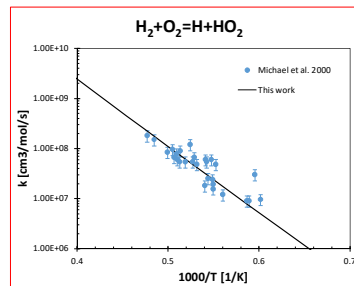
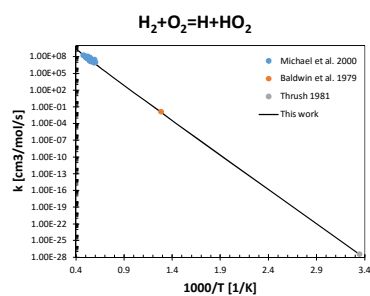
Third body efficiencies: HE 0.83/ CO 1.90/ CH₄ 2.00/ H₂ 2.50/ C₂H₆ 3.00/ CO₂ 3.80/ H₂O 12.00/

H-abstraction from oxygen $\text{H}_2 + \text{O}_2 \rightarrow \text{H}\cdot + \text{HO}_2\cdot$

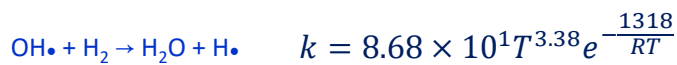
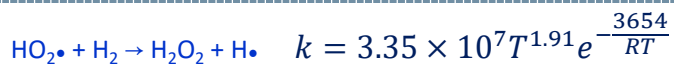


Courtesy of Stephen Klippenstein

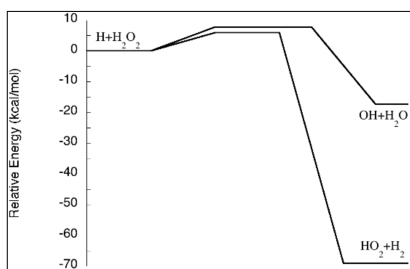
$$k = 1.13 \times 10^7 T^{1.94} e^{\frac{644}{RT}}$$



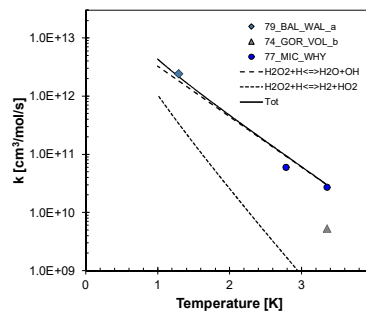
Radical transfer: H abstraction $\text{HO}_2\bullet + \text{H}_2 \rightarrow \text{H}_2\text{O}_2 + \text{H}\bullet$



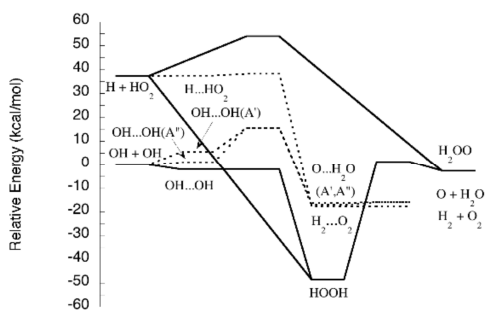
In principle two channels available, but it is inappropriate to treat separately



Courtesy of Stephen Klippenstein



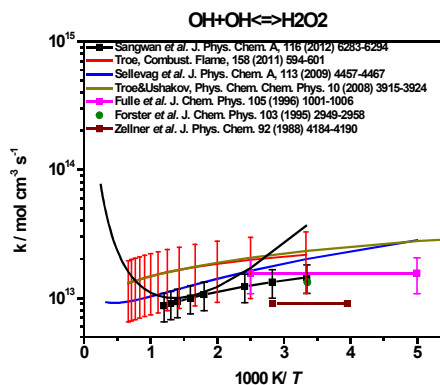
Homolytic bond cleavage $\text{H}_2\text{O}_2 \rightarrow 2\text{OH}\bullet$



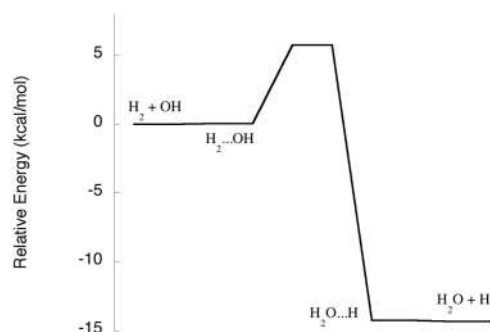
Courtesy of Stephen Klippenstein

$$k = 1.11 \times 10^{12} T^{0.52} e^{-\frac{763}{RT}}$$

(High pressure limit)

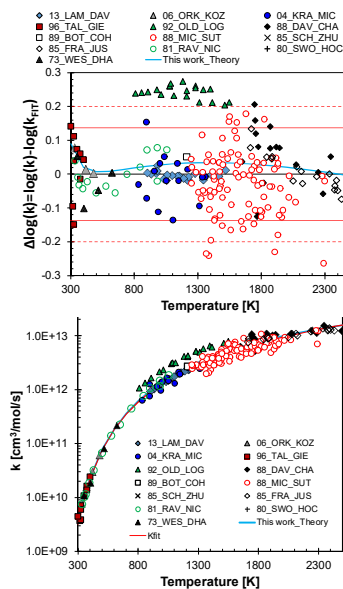


Radical transfer: H abstraction OH + H₂ → H₂O + H•



Courtesy of Stephen Klippenstein

$$k = 1.85 \times 10^8 T^{1.54} e^{-\frac{3553}{RT}}$$

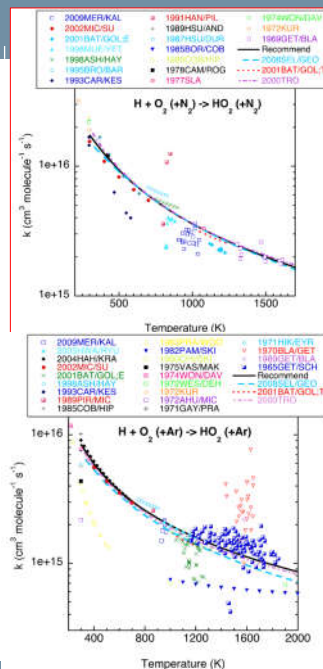
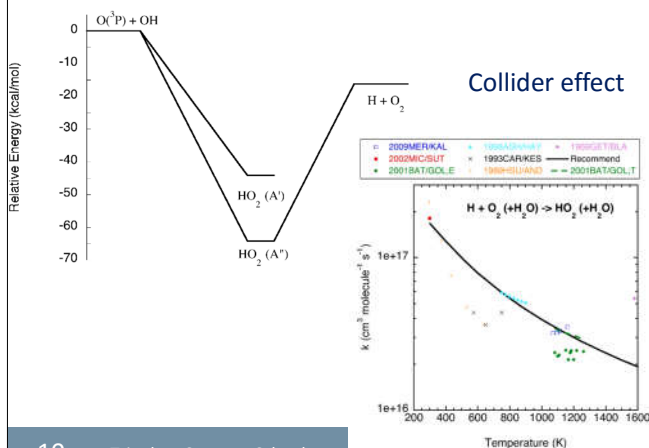


Radical addition: H• + O₂ → HO₂•

$$k_{HPL} = 1.31 \times 10^{12} T^{0.57} e^{-\frac{203}{RT}}$$

$$k_{LPL} = 8.00 \times 10^{21} T^{-1.73} e^{-\frac{536}{RT}} \quad \text{Collider H}_2\text{O}$$

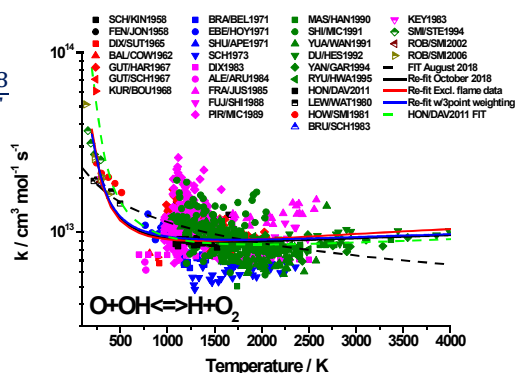
$$k_{LPL} = 1.90 \times 10^{20} T^{-1.56} e^{-\frac{254}{RT}} \quad \text{Collider Ar}$$



Branching reaction: $\text{H}\cdot + \text{O}_2 \rightarrow \text{OH}\cdot + \text{O}\cdot$

$$k_{rev} = 5.34 \times 10^{13} T^{-0.25} e^{\frac{238}{RT}}$$

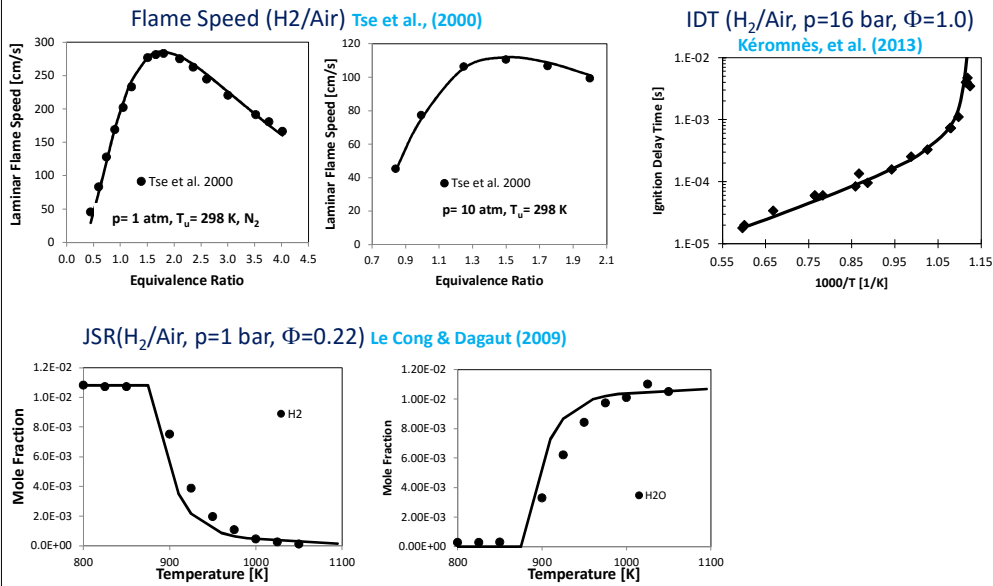
$\text{OH}\cdot + \text{O}\cdot \rightarrow \text{H}\cdot + \text{O}_2$



H₂ whole mechanism

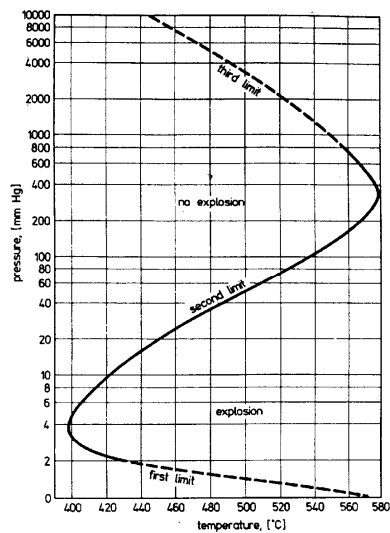
H2+M=2H+M	4.5770e+19	-1.400	104400.00				
H2/ 2.50/ H2O/ 12.00/ CO/ 1.90/ CO2/ 3.80/ HE/ 0.83/							
H2+O=H+OH	5.0800e+04	2.670	6292.00				
H2+OH=H+H2O	4.3800e+13	0.000	6990.00				
2O+M=O2+M	6.1650e+15	-0.500	0.00				
H2/ 2.50/ H2O/ 12.00/ AR/ 0.83/ CO/ 1.90/ CO2/ 3.80/ HE/ 0.83/							
H+O2=O+OH	1.1400e+14	0.000	15286.00				
H+OH+M=H2O+M	3.5000e+22	-2.000	0.00				
H2/ 0.73/ H2O/ 3.65/ AR/ 0.38/							
O+H2O=2OH	6.7000e+07	1.704	14986.80				
H+O+M=OH+M	4.7140e+18	-1.000	0.00				
H2/ 2.50/ H2O/ 12.00/ AR/ 0.75/ CO/ 1.50/ CO2/ 2.00/ HE/ 0.75/							
H2O2 (+M)=2OH (+M)	2.0000e+12	0.900	48749.00				
LOW/ 2.49e+24 -2.300 48749.0/							
TROE/ 0.4300 1.000e-30 1.000e+30/							
H2O/7.65/ CO2/1.60/ N2/1.50/ O2/1.20/ HE/0.65/							
H2O2/7.70/ H2/3.70/ CO/2.80/							
H+H2O2=H2O+OH	2.4100e+13	0.000	3970.00				
H+H2O2=H2+HO2	2.1500e+10	1.000	6000.00				
O+H2O2=OH+HO2	9.5500e+06	2.000	3970.00				
OH+H2O2=H2O+HO2	1.7400e+12	0.000	318.00				
DUPLICATE							
OH+H2O2=H2O+HO2	7.5900e+13	0.000	7269.00				
DUPLICATE							
H+HO2=2OH	7.0790e+13	0.000	295.00				
H+HO2=H2+O2	1.1402e+10	1.083	553.78				
O+HO2=O2+OH	3.2500e+13	0.000	0.00				
OH+HO2=O2+H2O	7.0000e+12	0.000	-1092.96				
DUPLICATE							
OH+HO2=O2+H2O	4.5000e+14	0.000	10929.60				
DUPLICATE							
2HO2=O2+H2O2	1.0000e+14	0.000	11040.88				
DUPLICATE							
2HO2=O2+H2O2	1.9000e+11	0.000	-1408.92				
DUPLICATE							
H+O2 (+M)=HO2 (+M)	4.6500e+12	0.440	0.00				
LOW/ 1.74e+19 -1.230 0.0/							
TROE/ 0.6700 1.000e-30 1.000e+30 1.000e+30/							
H2/1.30/ CO/1.90/ CO2/3.80/ HE/0.64/							
H2O/10.00/ AR/0.50/							
O+OH+M=HO2+M	1.0000e+16	0.000	0.00				

Mechanism works



Explosion diagram

Hydrogen/oxygen explosion diagram



Lewis, B., von Elbe, G.
 'Combustion Flames and Explosion of Gases' Academic Press New York 1961

Chemical system ignition

Skeletal mechanism of chain reactions suitable for the combustion of a generic fuel S:



R• generic radical
 P stable products
 α > 1 propagation → branching

Lower ignition limit

Lower limit of the explosion diagram: wall termination rules the radical depletion, being the radical termination negligible, because of the low pressures which make less probable an event proportional to the square of pressure: reactions 3 and 5 can be neglected

Radical conservation:

$$\frac{d[R\bullet]}{dt} = 2k_1[S] + (\alpha - 1)k_2[S][R\bullet] - k_4[R\bullet]$$

1. S → 2R•
2. S + R → αR• + P
3. R• + S + [M] → P + [M]
4. R• + wall → P
5. R• + R• + [M] → P + [M]

First ignition occurs when only a few reactant is consumed, then:

$$[S] = [S]_0 = \text{constant}$$

$$\int_0^{[R\bullet]} \frac{d[R\bullet]}{2k_1[S]_0 + \{(\alpha - 1)k_2[S]_0 - k_4\}[R\bullet]} = \int_0^{[R\bullet]} \frac{d[R\bullet]}{2k_1[S]_0 + B[R\bullet]} = \int_0^{[R\bullet]} dt$$

$$B = (\alpha - 1)k_2[S]_0 - k_4$$

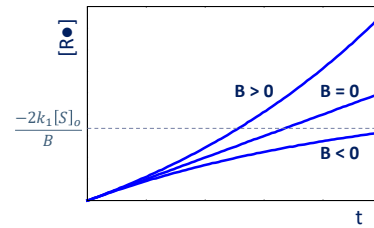
$$\frac{\ln(2k_1[S]_0 + B[R\bullet])}{B} = t \quad \Rightarrow \quad [R\bullet] = \frac{2k_1[S]_0(e^{Bt} - 1)}{B}$$

Lower ignition limit

$$[R\bullet] = \frac{2k_1[S]_0(e^{Bt} - 1)}{B}$$

Case 1: $B = (\alpha - 1)k_2[S]_0 - k_4 < 0$

$$\lim_{t \rightarrow \infty} [R\bullet] = \frac{-2k_1[S]_0}{B} \quad \text{Stationary state solution}$$



Case 2: $B = (\alpha - 1)k_2[S]_0 - k_4 > 0$

$$\lim_{t \rightarrow \infty} [R\bullet] = \infty \quad \text{Radical concentration continuously increases}$$

Case 3: $B = (\alpha - 1)k_2[S]_0 - k_4 = 0$

Critical limit between stable stationary solution and explosion

Radical conservation: $\frac{d[R\bullet]}{dt} = 2k_1[S] + \{(\alpha - 1)k_2[S] - k_4\}[R\bullet] = 2k_1[S]_0$

➔ $[R\bullet] = 2k_1[S]_0 t$

Lower ignition limit

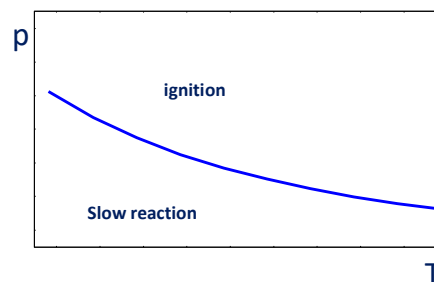
Case 3: Critical limit between stable stationary solution and explosion

$$B = (\alpha - 1)k_2[S]_0 - k_4 = 0$$

Ideal gas behavior:

$$(\alpha - 1)k_2 \frac{p}{RT} x_{S_0} - k_4 = 0$$

$$p = \frac{k_4(T)RT}{(\alpha - 1)k_2(T)x_{S_0}}$$



Hydrogen case

2. propagation $O_2 + H \rightarrow OH + O$ $\alpha = 3$: from 1 to 3 radicals: => branching

4. wall termination $H + wall \rightarrow P$

$$k_2 = 1.14 \times 10^{14} e^{-\frac{15286}{RT}}$$

Units are: cal, mol, cm³, s

Wall termination reactions of radicals is the result of two consecutive processes:

- diffusion of the radicals to the wall
- interaction of the radical with the surface.

We assume that first process is the rate limiting step (diffusion is slower).

Diffusion rate constant which for the cell with characteristic size d can be derived from the Einstein diffusion equation:

$$k_4 = k_{diff} = \frac{AD}{d^2}$$

Where the coefficient A depends on the shape of the cell ($A=39.6$ for a sphere, and $A=23.3$ for a very long cylinder). The diffusion coefficient \mathcal{D} depends on the temperature and pressure:

$$\mathcal{D} = \mathcal{D}_0 \left(\frac{T}{T_0} \right)^{0.5} \left(\frac{p}{p_0} \right)$$

\mathcal{D}_0 is the diffusion coefficient at normal conditions, T_0 and p_0

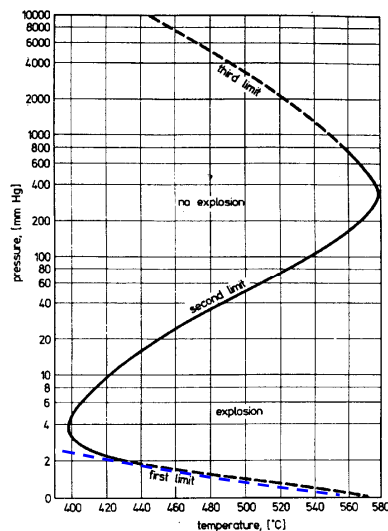
H₂ first limit estimation

$$(\alpha - 1)k_2 \frac{p}{RT} x_{S_0} - k_4 = 0$$

Substituting the expressions of k_2 and k_4 and recalling that $\alpha = 3$

$$2A_2 e^{-\frac{E_2}{RT}} \frac{p}{RT} x_{0O_2} - \frac{A}{d^2} \mathcal{D}_0 \left(\frac{T}{T_0} \right)^{0.5} \left(\frac{p}{p_0} \right) = 0$$

$$p = \sqrt{\frac{A}{d^2} \mathcal{D}_0 \left(\frac{T}{T_0} \right)^{0.5} p_0 \frac{RT}{2A_2 x_{0O_2}} e^{\frac{E_2}{RT}}}$$

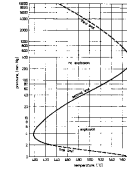


Second ignition limit

At assigned T, pressure increase inhibits the ignition reactions.

Higher pressures make less important wall termination reactions. Pressure affects more the termination

1. **initiation** S $\rightarrow 2R\bullet$
2. **propagation** S + R $\rightarrow \alpha R\bullet + P$
3. **termination** $R\bullet + S + [M]$ $\rightarrow P + [M]$
4. **wall termination** $R\bullet + \text{wall}$ $\rightarrow P$
5. **termination** $R\bullet + R\bullet + [M]$ $\rightarrow P + [M]$



Radical conservation:

$$\frac{d[R\bullet]}{dt} = 2k_1[S] + (\alpha - 1)k_2[S][R\bullet] - k_3[R\bullet][S][M]$$

First ignition occurs when only a few reactant is consumed, then: $[S] = [S]_0 = \text{constant}$

$$\int_0^{[R\bullet]} \frac{d[R\bullet]}{2k_1[S]_0 + \{(\alpha - 1)k_2[S]_0 - k_3[S]_0[M]\}[R\bullet]} = \int_0^{[R\bullet]} \frac{d[R\bullet]}{2k_1[S]_0 + B[R\bullet]} = \int_0^{[R\bullet]} dt$$

$$[R\bullet] = \frac{2k_1[S]_0(e^{Bt} - 1)}{B}$$

$$B = (\alpha - 1)k_2[S]_0 - k_3[S]_0[M]$$

Second ignition limit

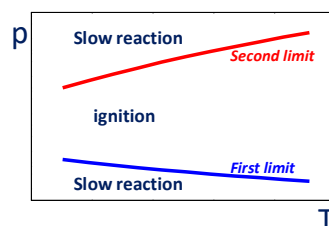
Critical limit between stable stationary solution and explosion

$$B = (\alpha - 1)k_2[S]_0 - k_3[S]_0[M] = 0$$

Ideal gas behavior:

$$(\alpha - 1)k_2 \frac{p}{RT} x_{S0} - k_3 \frac{p}{RT} x_{S0} \frac{p}{RT} = 0$$

$$p = (\alpha - 1)RT \frac{k_2}{k_3} = (\alpha - 1)RT \frac{A_2 e^{-\frac{E_2}{RT}}}{A_3 e^{-\frac{E_3}{RT}}} = (\alpha - 1)RT \frac{A_2}{A_3} e^{-\frac{(E_2 - E_3)}{RT}}$$



Hydrogen case

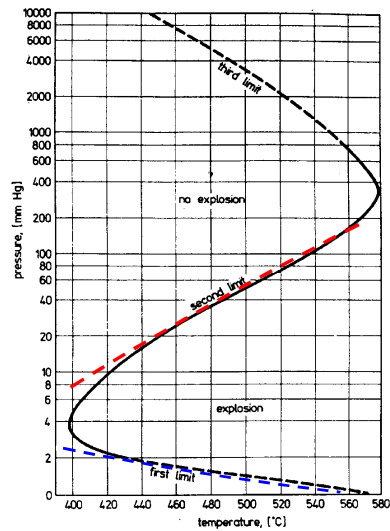


Even though second reaction appears as a propagation (radical H, is transformed in another radical HO_2), it can be considered a termination: HO_2 is a very stable radical, less reactive than all the other radicals and during its long life could also diffuse to walls.

$$k_2 = 1.14 \times 10^{14} e^{\frac{-15286}{RT}} \quad \text{Units are: cal, mol, cm}^3, \text{ s}$$

$$k_4 = 1.74 \times 10^{19} T^{-1.23} \quad \text{Low pressure limit of the falloff expression}$$

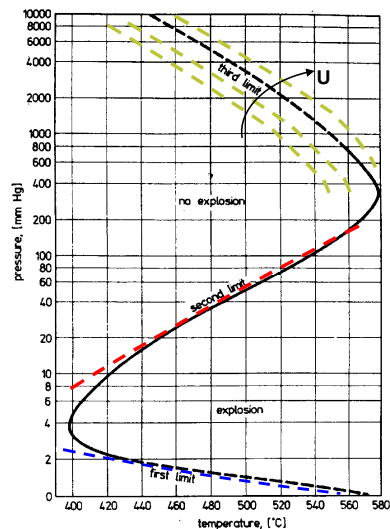
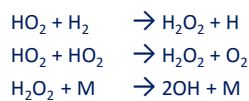
$$p = 2RT \frac{A_2}{A_3} e^{\frac{-(E_2 - E_3)}{RT}}$$



Third ignition limit

Third limit is at quite high pressures. In these conditions, the system cannot be considered almost isothermal up to ignition, as in the case of first and second limit. Thus, the heat loss plays a fundamental role and the thermal ignition (Semenov equation in its simplest form) competes with the branching ignition.

From the chemical point of view: at high pressures, HO_2 becomes more reactive, abstracting and forming H radical or recombining and later forming two reactive OH radicals, through a very fast hydrogen peroxide decomposition:



Summarizing

- **1st limit**

(sensitive to surface, vessel shape, heat transfer & added inert gas)

- Competition between branching and diffusion to wall of H•

- **no explosion wall** $\leftarrow \text{H}^\bullet + \text{O}_2 \rightarrow \text{O}^\bullet + \text{OH}^\bullet$ **explosion**

- **2nd limit** (dependent on intrinsic kinetics)

- Competition:

- $\text{H}^\bullet + \text{O}_2 + \text{M} \rightarrow \text{HO}_2^\bullet + \text{M}$ **no explosion** third order

- $\text{H}^\bullet + \text{O}_2 \rightarrow \text{O}^\bullet + \text{OH}^\bullet$ **explosion** second order

- hydroperoxyl radical HO_2^\bullet much less reactive than $\text{H}^\bullet, \text{OH}^\bullet$

- **3rd limit** (sensitive to vessel shape/size/inert gases)

- rate very fast ($\text{H}^\bullet + \text{O}_2 \rightarrow \text{O}^\bullet + \text{OH}^\bullet$), faster than can be conducted away
 \Rightarrow **thermal explosion**

- added gases have effect **because of** their heat transport properties, as well as of their third body effect.

Carbon Monoxide Oxidation

The direct oxidation $\text{CO} + \text{O}_2 \rightarrow \text{CO}_2 + \text{O}$

has a high activation energy (48 kcal/mol) and is a very slow process even at high T.

However, in the presence of ppm of $\text{H}_2/\text{H}_2\text{O}$, OH radicals are formed, then the effective conversion proceeds via the reaction



The H atoms produced feed the chain-branching reactions $\text{H} + \text{O}_2$, and thereby accelerate the CO oxidation rate.

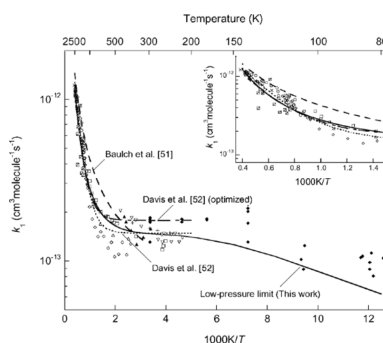
At **high pressures**, it is also important the reaction



OH+CO=H+CO2 7.015e+04 2.053 -355.7
 DUPLICATE

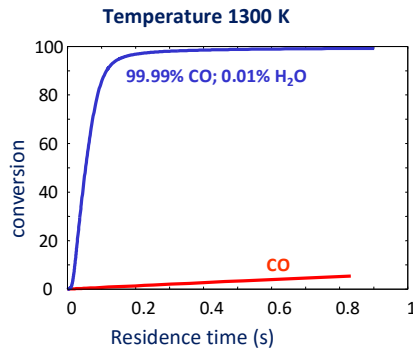
OH+CO=H+CO2 5.757e+12 -0.664 331.8
 DUPLICATE

Very low temperature dependence

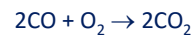
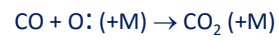
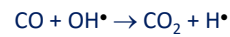


A.V. Joshi, H. Wang Int. J. Chem. Kinet. 38 (1) (2006) 57–73.

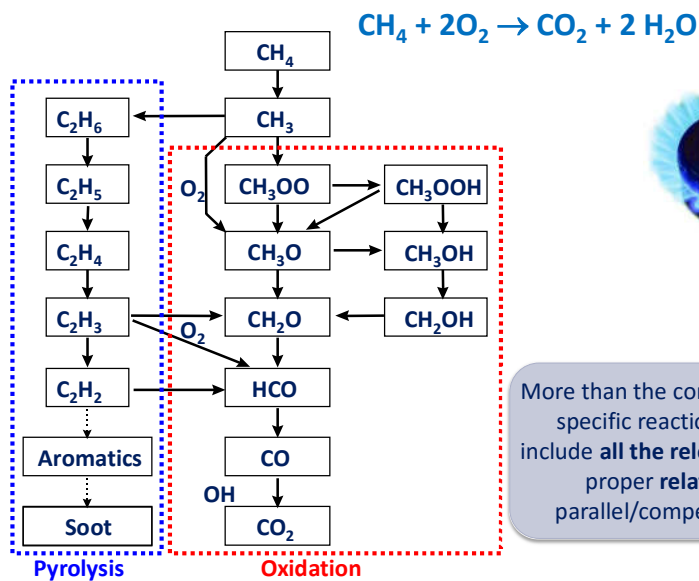
Water effect



Traces of water are sufficient to form H atoms, whose effect is purely catalytic, through the OH formation:

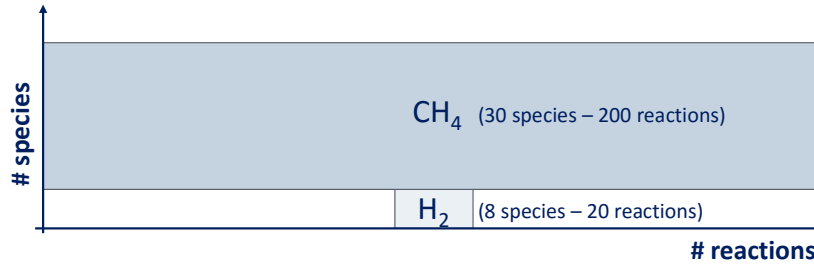
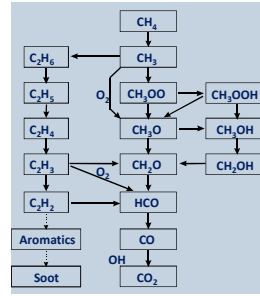
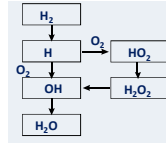
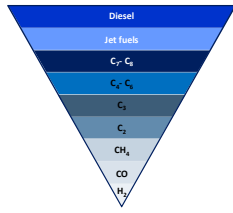


Methane Oxidation: complexity increases

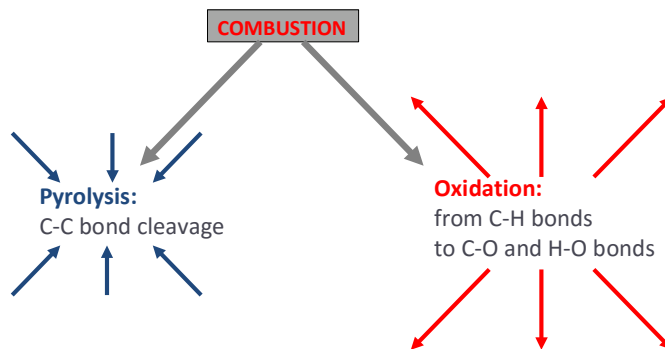
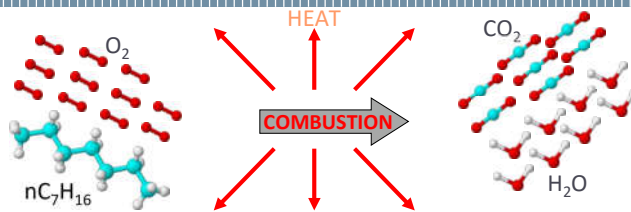


More than the correct rate parameters of specific reaction, it is important to include **all the relevant reactions** and the proper **relative selectivity** of parallel/competing reaction paths.

Mechanism growth

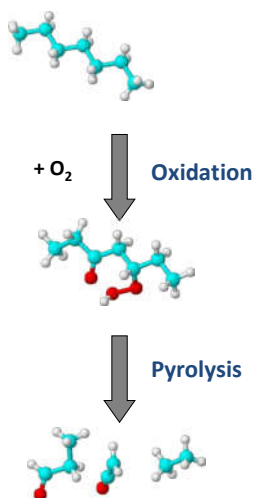


Larger molecules

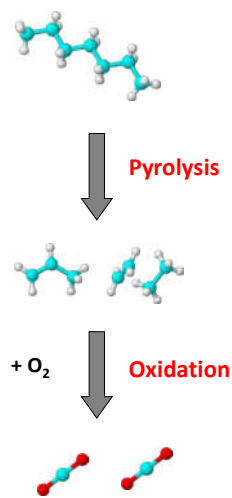


Larger molecules combustion complexity

Low temperature

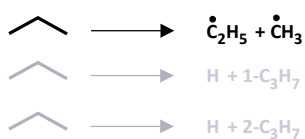


High temperature



Propane Pyrolysis

Chain Initiation Reactions

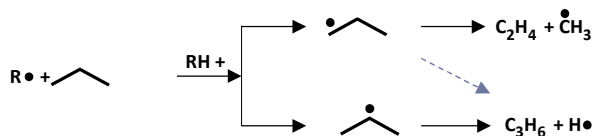


The chemical bonds with a smaller BDEs are more prone to dissociate than those with larger BDEs. Dehydrogenation are less favored than pyrolysis reactions.

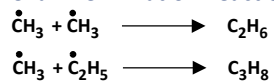


Chain Propagation Reactions:

- H-Abstraction Reactions & Radical Decomposition Reactions



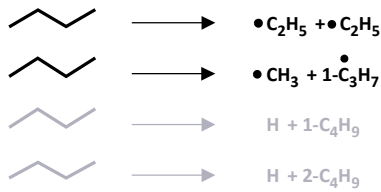
Chain Termination Reactions



H radicals are not effective in recombination reactions.

n-butane Pyrolysis

Chain Initiation Reactions



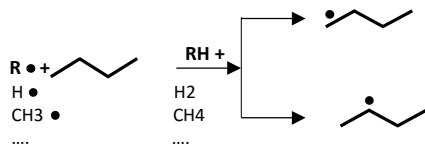
n-butane pyrolysis is similar to the pyrolysis of propane.

Always the **same reaction classes** are present:

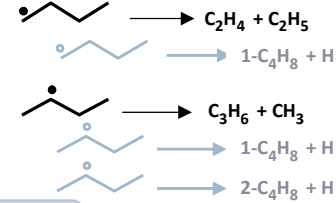
- Chain initiation
- H-abstraction
- H-radical decomposition
- Radical recombination.

Chain Propagation Reactions:

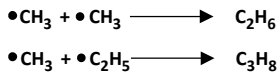
- H-Abstraction Reactions



- Radical Decomposition Reactions



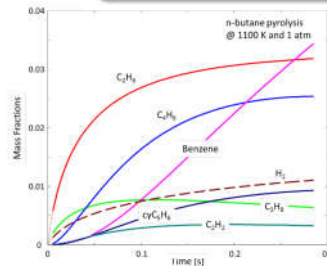
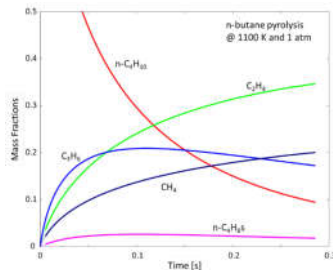
Chain Termination Reactions



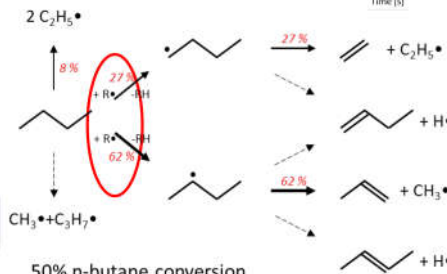
H• radicals are not effective in recombination reactions.

n-butane Pyrolysis

Butadiene, Benzene and heavier species are due to successive addition and condensation reactions



Reaction Path Analysis (RPA)



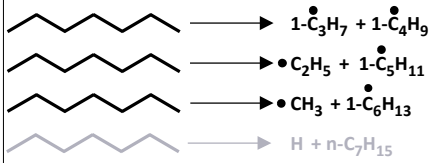
H-Abstractions prevail on Initiation Reactions.

Dehydrogenation reactions of alkyl radicals are of limited importance

50% n-butane conversion @ 1100 K, 1 atm, and .04 s

n-heptane Pyrolysis

Chain Initiation Reactions

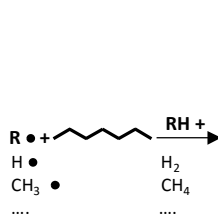


n-heptane pyrolysis is similar too, Always the **same reaction classes** are present, but their number increases:

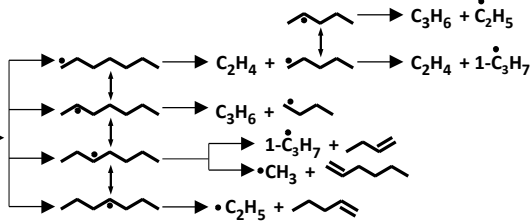
- Chain initiation
- H-abstraction
- H-radical decomposition
- Radical recombination.

Chain Propagation Reactions:

- H-Abstraction Reactions

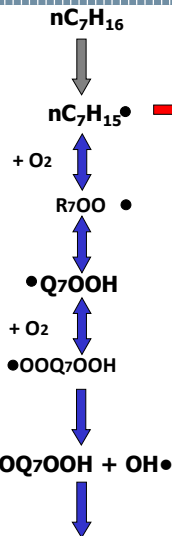


- Radical Decomposition Reactions



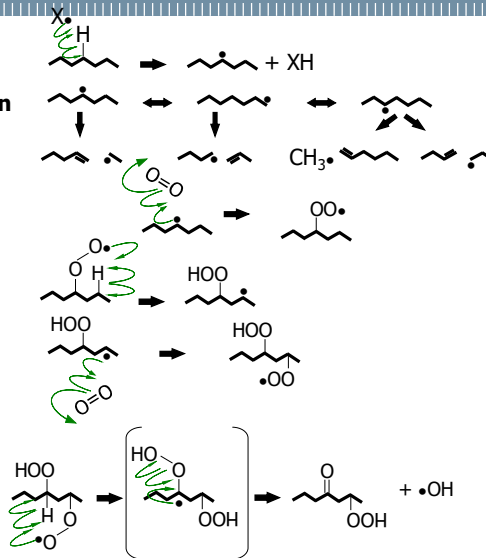
Radical decomposition reactions forming hydrogen and the different heptenes (1-, 2-, 3- C₇H₁₄) are not shown, being of lower importance because of the higher energy of C-H bonds compared with the C-C bonds

Oxidation of alkanes

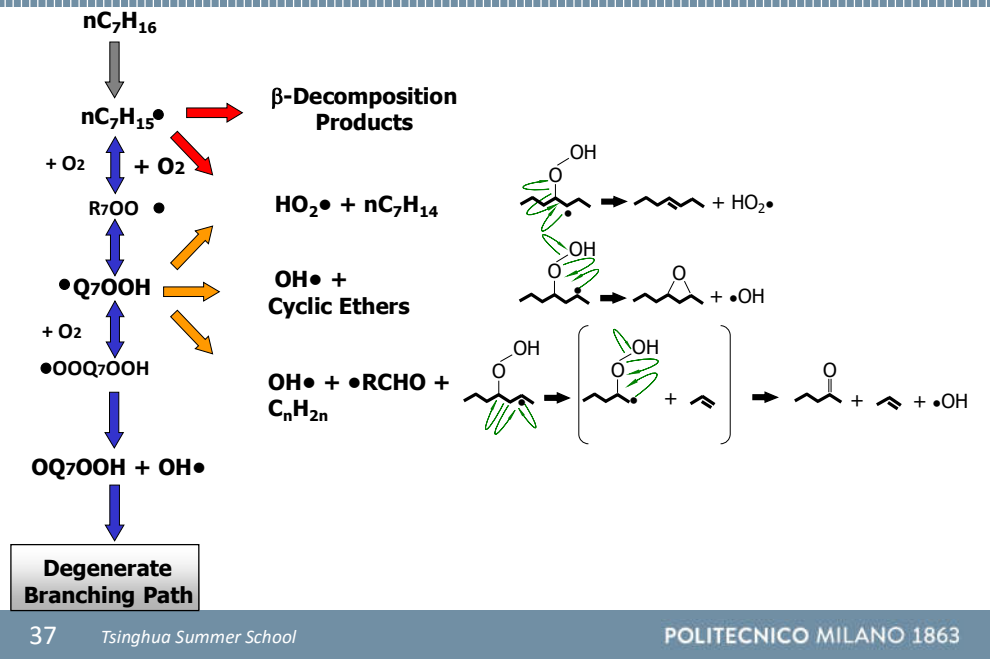


Degenerate Branching Path

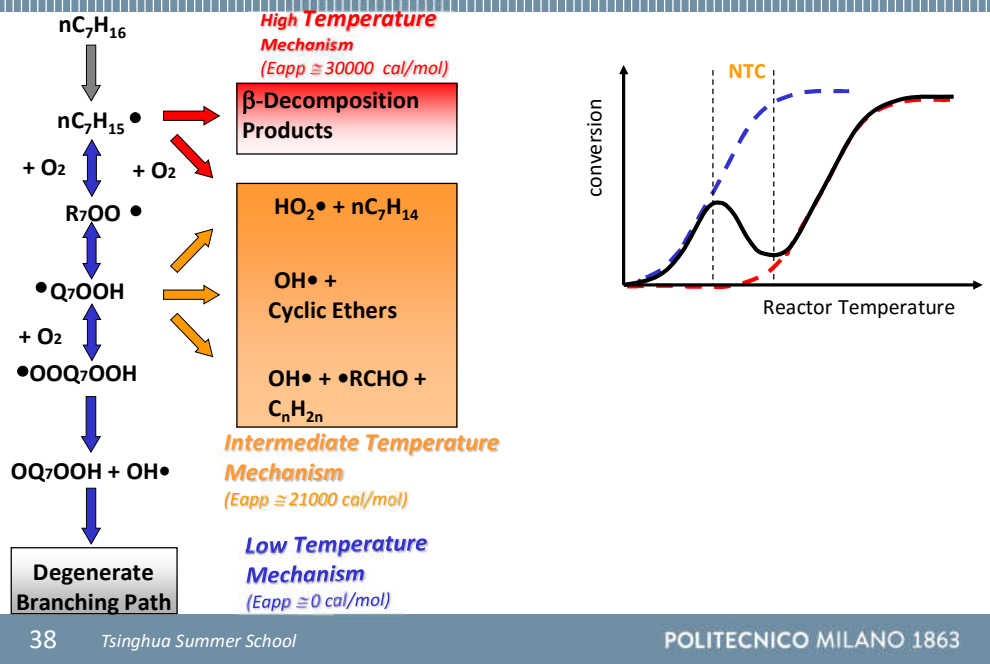
β-Decomposition Products



Oxidation of alkanes



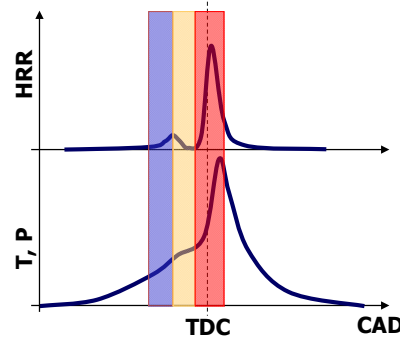
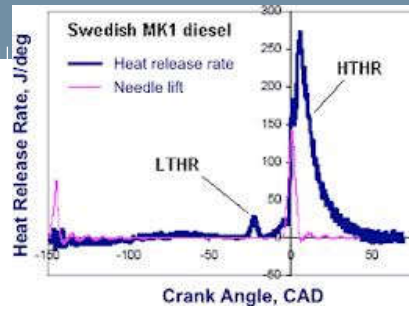
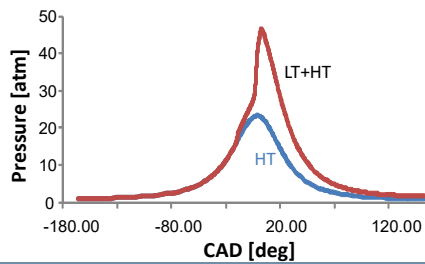
Oxidation of alkanes



Is low T true and significant?

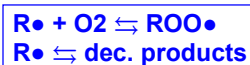
When valves are close, the cylinder is a close system with heat exchange

Neglecting low T mech. can result in a dramatic error



Mechanism competition

Transition from the LT to the HT mechanism ruled by the competition between decomposition of alkyl radicals (**pyrolysis**) and formation of peroxy radicals (**oxidation**)



Addition (oxidation): $k_{\text{add}} = 10^9$ [l/mol/s]
Decomposition (pyrolysis): $k_{\text{dec}} = 10^{13} \exp(-30000/RT)$ [1/s]

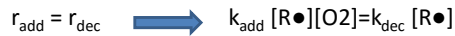
Competitive pathways: at high temperatures alkyl radicals are favored over the peroxy radicals, or pyrolysis is favored over oxidation.

Ceiling Temperature is the transition temperature from one mechanism to the other

At the equilibrium the addition and the decomposition reaction rates are equal:

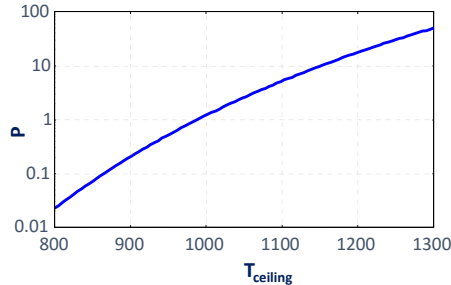
$$r_{\text{add}} = r_{\text{dec}} \quad \longrightarrow \quad k_{\text{add}} [R\bullet][O_2] = k_{\text{dec}} [R\bullet]$$

Ceiling temperature vs. pressure



$$1 = \frac{r_{\text{dec}}}{r_{\text{add}}} = \frac{k_{\text{dec}}}{k_{\text{add}} [\text{O}_2]} \cong \frac{10^{13} \exp\left(-\frac{30000}{RT}\right)}{10^9 \frac{P}{RT} x_{\text{O}_2}}$$

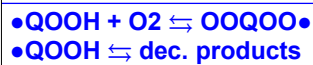
$$P \cong \frac{RT}{x_{\text{O}_2}} \frac{10^{13} \exp\left(-\frac{30000}{RT}\right)}{10^9}$$



Ceiling temperature increases with the pressure: higher oxygen concentration favors direct reaction of peroxy radical formation: NTC region moves toward higher temperatures

Mechanism competition: LT vs. intermediate T

Transition from the LT to the intermediate mechanism ruled by the decomposition of peroxy radicals



Addition (oxidation): $k_{\text{add}} = 10^9$ [l/mol/s]
 Decomposition (pyrolysis): $k_{\text{dec}} = 10^{13} \exp(-21000/RT)$ [1/s]

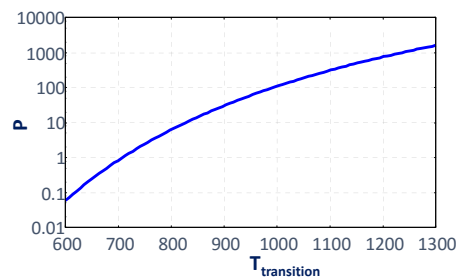
Transition Temperature is the transition temperature from one mechanism to the other one

At the equilibrium the addition and the decomposition reaction rates are equal:

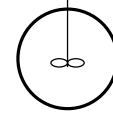
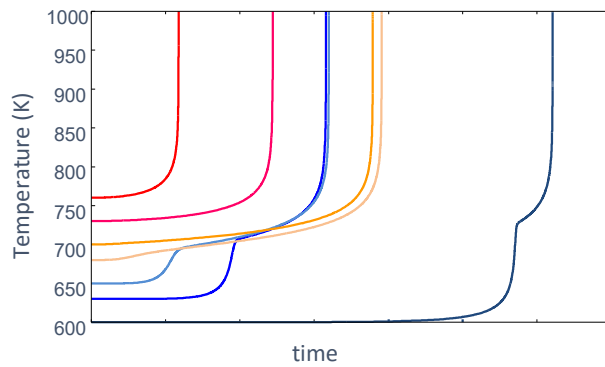


$$1 = \frac{r_{\text{dec}}}{r_{\text{add}}} = \frac{k_{\text{dec}}}{k_{\text{add}} [\text{O}_2]} \cong \frac{10^{13} \exp\left(-\frac{21000}{RT}\right)}{10^9 \frac{P}{RT} x_{\text{O}_2}}$$

$$P \cong \frac{RT}{x_{\text{O}_2}} \frac{10^{13} \exp\left(-\frac{21000}{RT}\right)}{10^9}$$



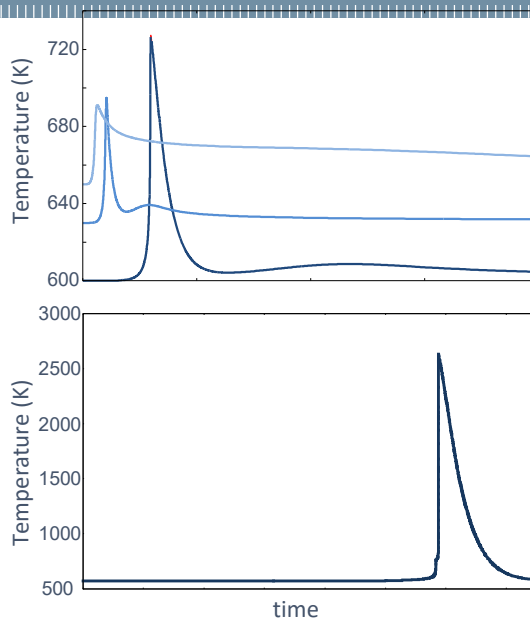
C₃H₈/O₂ ignition in closed adiabatic system



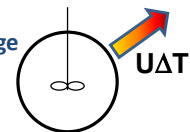
No heat exchange
No mass exchange

- One or two stage ignition.
- NTC between 650-700 K

C₃H₈/O₂ ignition in closed non adiabatic system



Heat exchange
No mass exchange

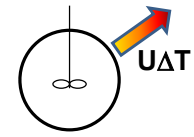
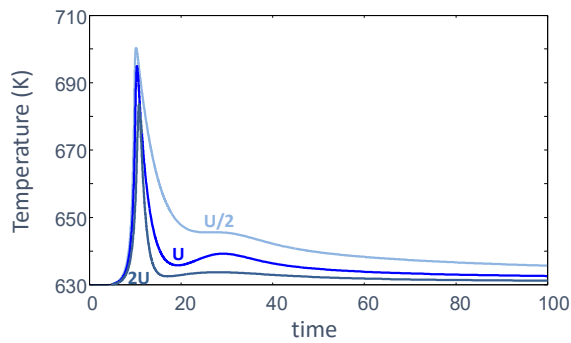


At lower temperatures first flame occurs later (even minutes). More time to accumulate reactive species, thus higher heat release.

Second flame less exothermic, because part of the fuel already consumed during the first flame and not replaced.

At very low T (~ 550 K) the first flame is so exothermic that it allows the high T mech. to start (two stage ignition) and no other flames occur.

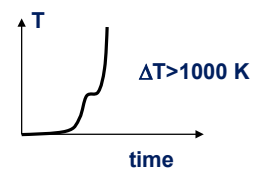
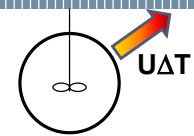
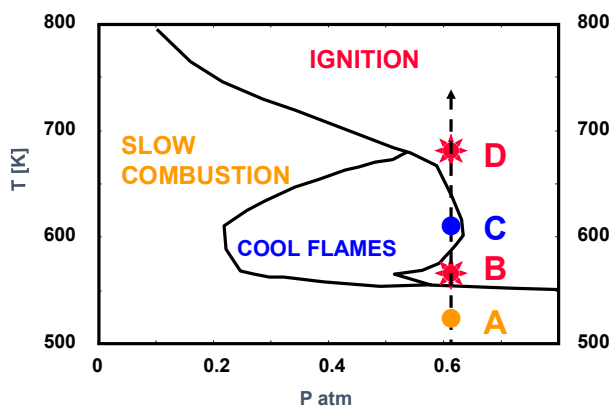
Heat exchange effect



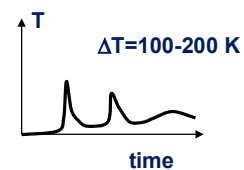
Heat exchange
No mass exchange

- High heat transfer coefficient reduces both the first flame peak and the second flame peak
- Low heat transfer coefficient does not cool the system enough after the first flame. The temperature is not low enough to allow the low T mech to express an evident second flame

Explosion diagram of C_3H_8/O_2 system

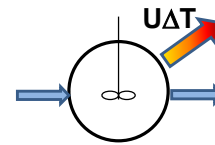
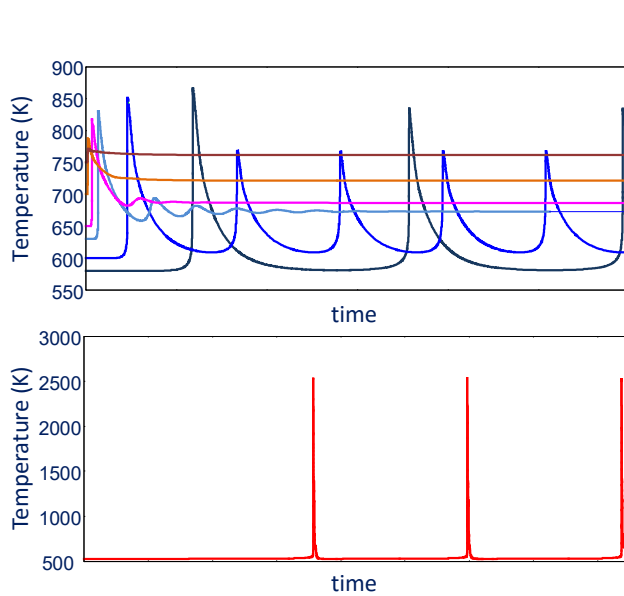


B – D: Hot Ignition



C : Cool Flames

C₇H₁₆/O₂ ignition in open non-adiabatic system

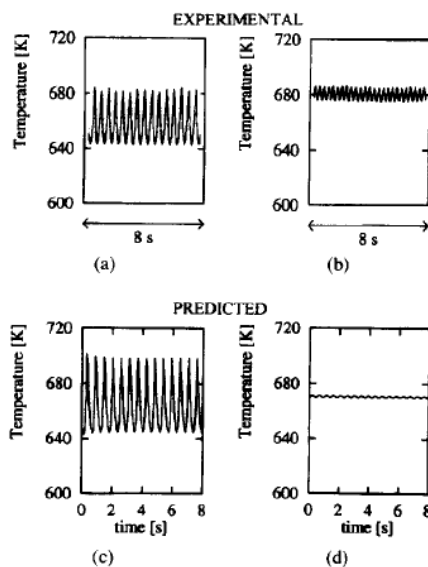


At lower temperatures flame occurs later. More time to accumulate reactive species, thus higher heat release.

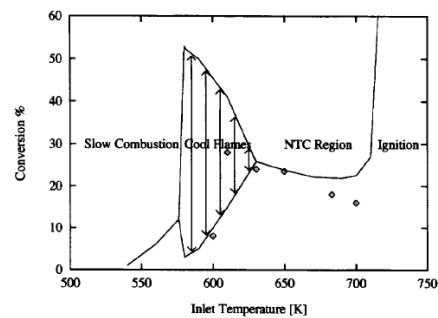
Moving toward intermediate T, dumped cool flames first and no cool flames then

At very low inlet T, the reactivity drives the system to high T which allows high T mech to occur

Cool flames observed in experiments

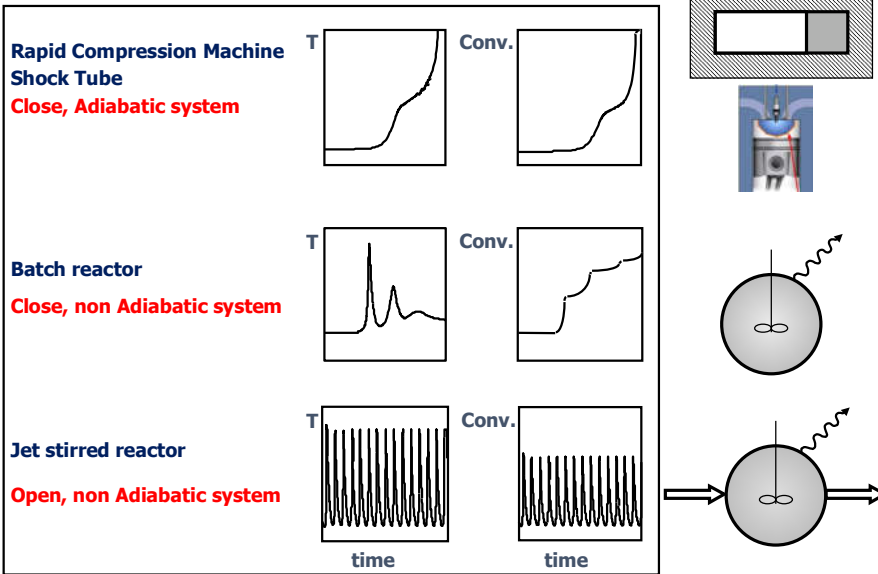


i-C₈H₁₈/air mixture in a JSR at 7 bar.

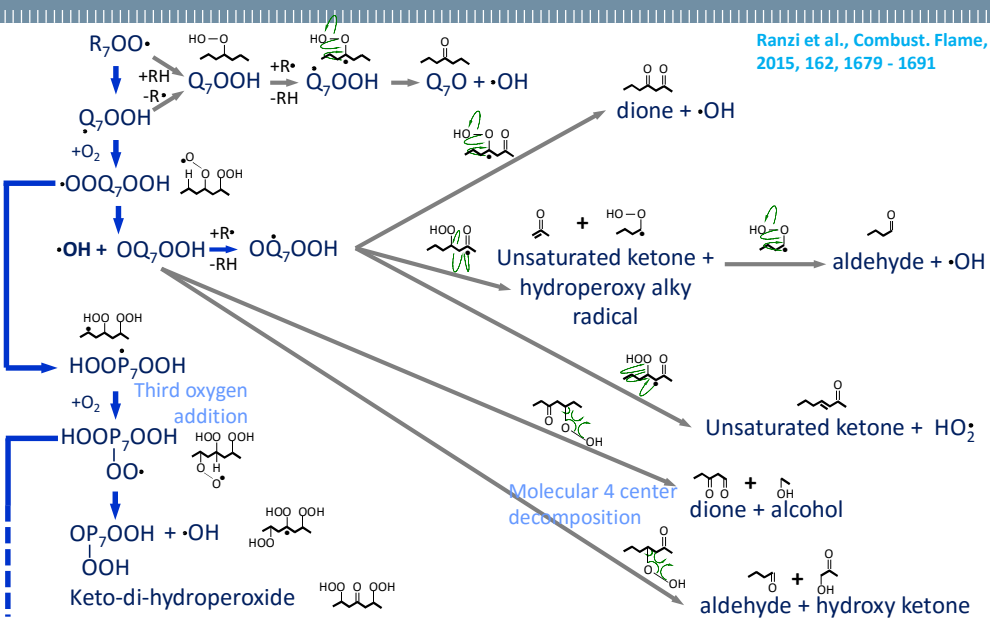


E. Ranzi, T. Faravelli, P. Gaffuri, A. Sogaro, A. D'anna, A. Ciajolo, *Combustion Flame*, 108: 24-42 (1997)

Low T pathologies

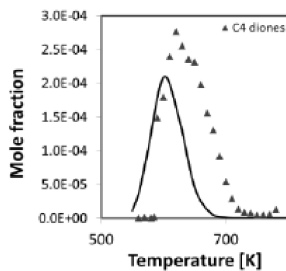
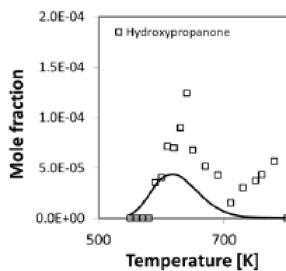
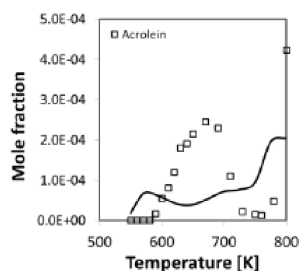
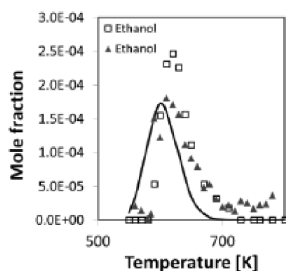


Peroxy and hydroperoxy alternative pathways



Products found from low T oxidation

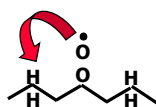
n-butane oxidation in jet stirred reactor (*n*-C₄H₁₀/O₂/Ar = 4/26/70 mol%)



Exp. data:
Herbinet et al., *Phys. Chem. Chem. Phys.*, 2011, 13, 296-308.

Oxidation of iso-alkanes

n-heptane ON=0

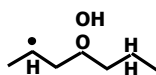


Peroxy radicals

4 secondary H atoms

Isomerization (1-5):
six membered ring

$$k = 4 \times 10^{11.0} \exp(-20000/RT) \text{ [s}^{-1}\text{]}$$



Alkyl-hydroperoxy radicals

$$k(700) = 10^{5.4} \text{ [s}^{-1}\text{]}$$

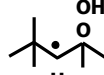
iso-octane ON=100



2 secondary H atoms

Isomerization (1-4):
five membered ring

$$k = 2 \times 10^{11.8} \exp(-26000/RT) \text{ [s}^{-1}\text{]}$$

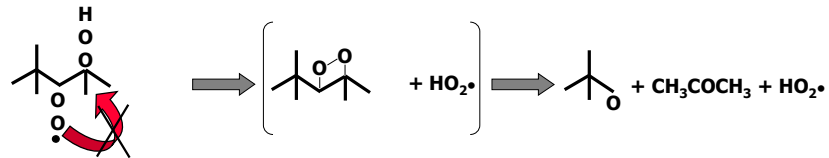
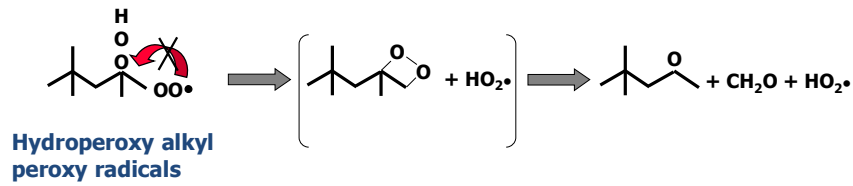


$$k(700) = 10^{4.0} \text{ [s}^{-1}\text{]}$$

Isomerization reactions of peroxy radicals contribute explaining lower reactivity of different primary reference fuels

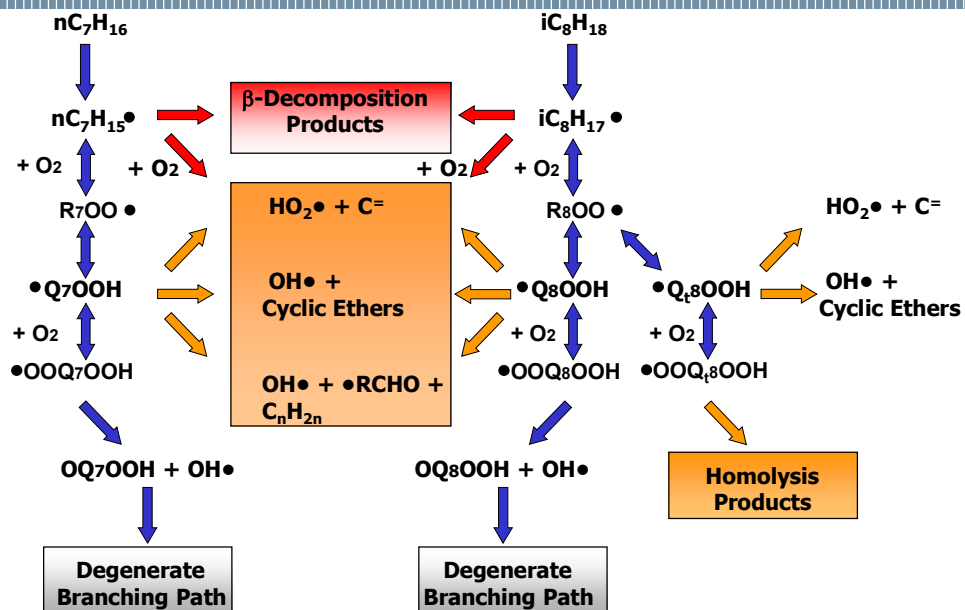
Oxidation of iso-alkanes

Homolysis Reactions

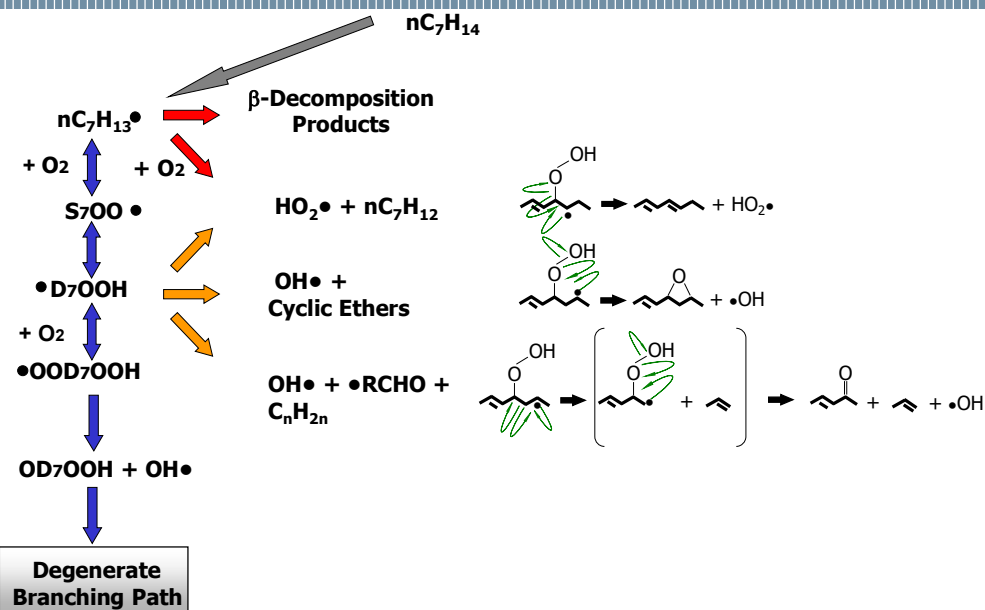


Not all the hydroperoxy alkyl peroxy radicals can undergo degenerate branching paths. This contributes explaining lower reactivity of different primary reference fuels

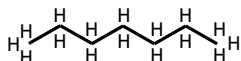
Oxidation of iso-alkanes



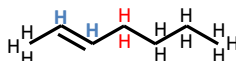
Oxidation of alkenes



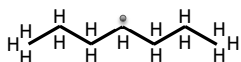
Alkene vs. alkane



6 primary H atoms
10 secondary H atoms



6 primary H atoms
4 secondary H atoms
2 vinyl H atoms (more difficult to remove: high DBE)
2 allyl H atoms (easier to remove)



secondary radical

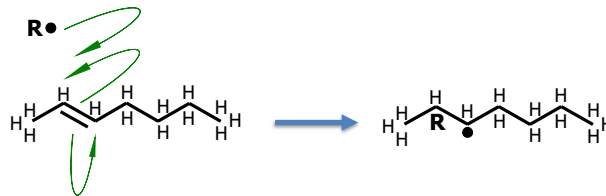


allyl radical (resonantly stabilized)

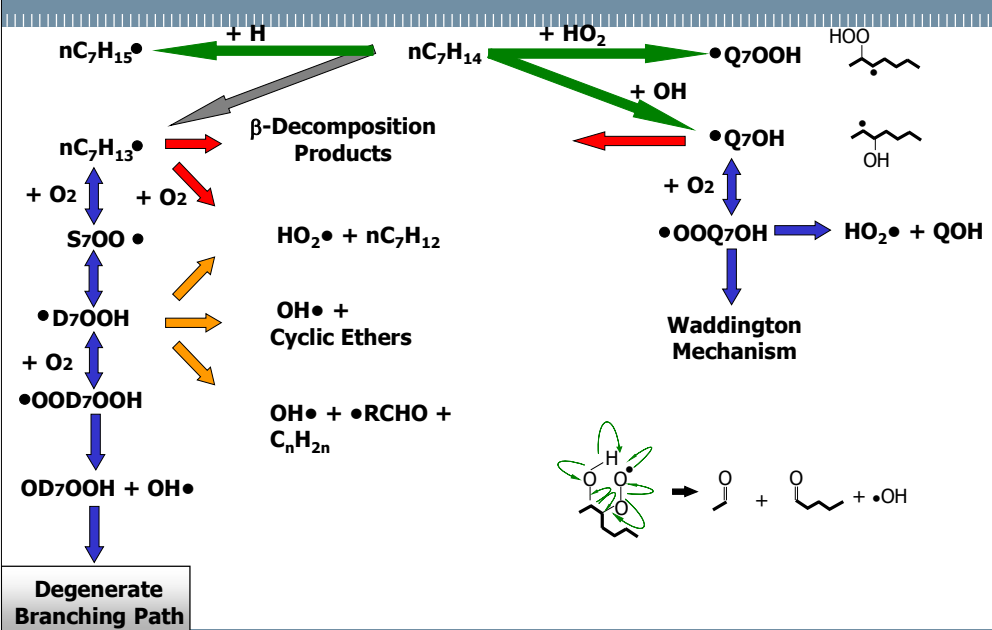
Alkene less reactive than alkane
(double bonds reduce reactivity at low/intermediate temperature)

Addition reactions

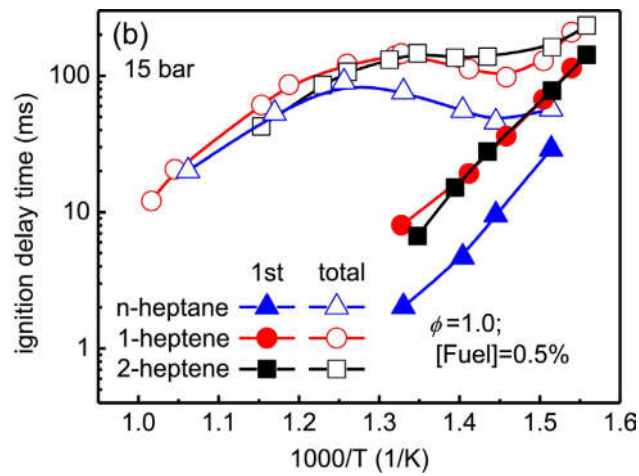
Double bonds allow new reaction classes to occur: addition reactions



Oxidation of alkenes

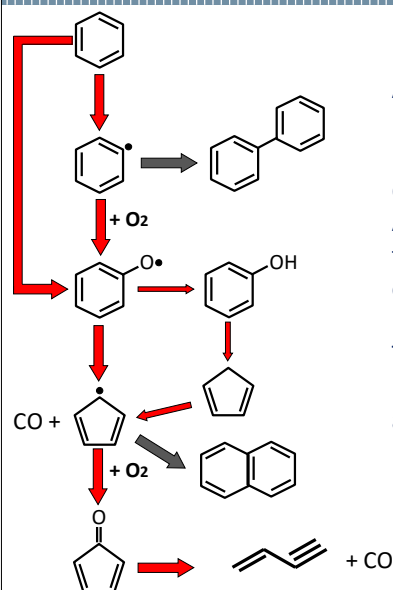


Alkane and alkene ignition delay time



Wu et al., *Combustion and Flame*, 197, 2018, 30-40

Oxidation of aromatics



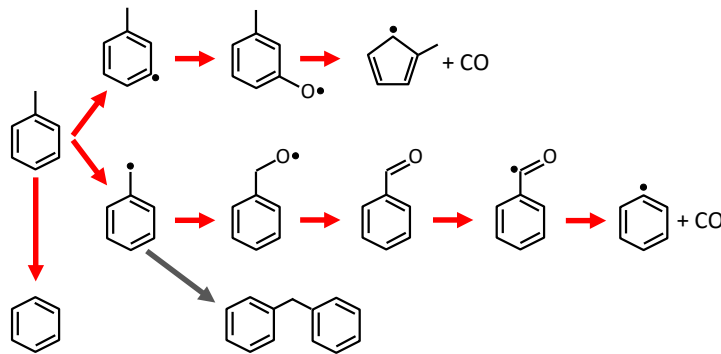
Aromatics only show the high temperature mechanism. High energy is required to initiate the reactions: aromatic rings are very stable and are difficult to be activated.

Aromatics are so stable that oxidation is needed first to allow the successive pyrolysis of the oxygenated species.

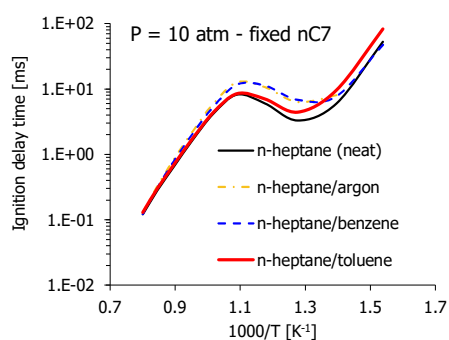
Typically, there is the formation of an aryloxy radical, which in turns open the ring, forming CO and a smaller ring or linear species

Oxidation of alkyl-aromatics

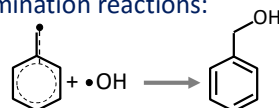
Also toluene shows only the high temperature mechanism. High energy is required to initiate the reactions on the ring. Primary hydrogens of the methyl group are much more available, because of the formation of the long-life resonantly benzyl radical. However, when formed, the benzyl radical is so stable, that it does not easily react further.



Toluene blending effect

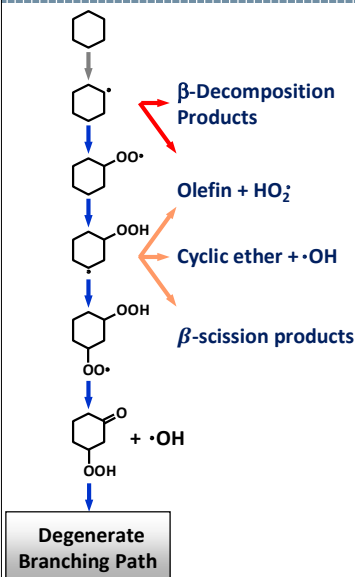


Toluene has an interesting blending effect. At low temperatures, benzyl radical is easily formed, because of its resonant structure. The resonance makes also benzyl a long-lived radical. Thus, benzyl acts as a radical scavenger, removing active radicals (like OH) from the system, through termination reactions:



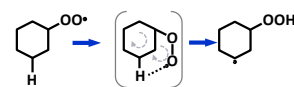
At intermediate T, benzyl radical starts reacting, thus toluene becomes more reactive than an inert or than an aromatic like benzene and the induction time of the mixture is more similar to that of the pure n-heptane, only a bit slowed down.

Oxidation of cyclo-alkanes

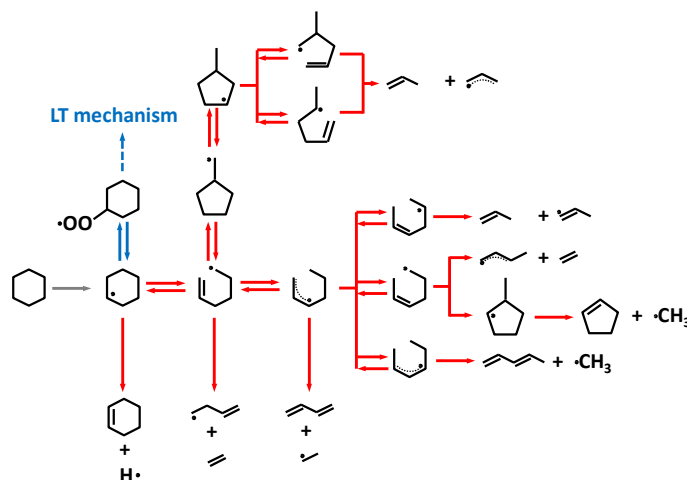


Cyclo-alkanes oxidation pathways are very similar to those of alkanes, with few differences:

- Decomposition involves the ring opening and several isomerizations
- Isomerization of peroxy radicals involves a double ring and consequently some extra strain, compensated by a lower entropy penalty, because the rotors are already blocked

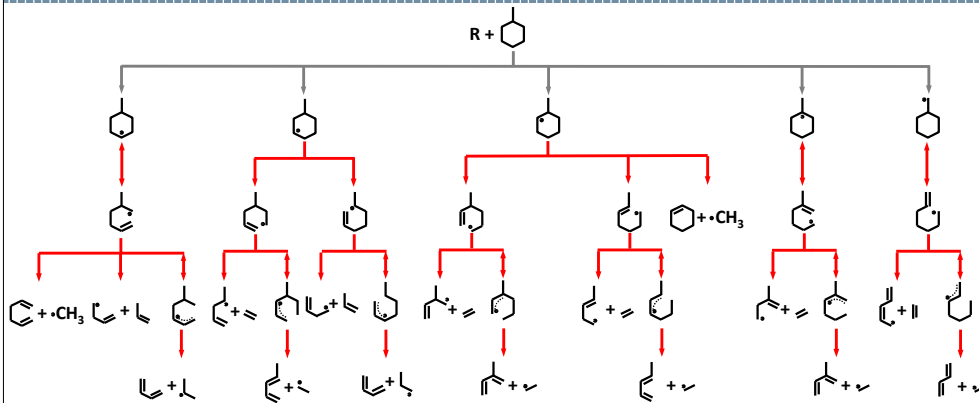


Decomposition of cyclo-alkanes



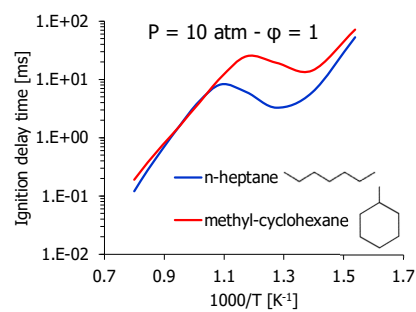
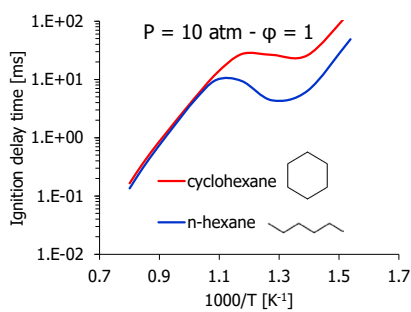
Cyclo-alkanes are isomers of alkenes, thus the isomerization and decomposition reactions of high and intermediate temperatures form a lot of species, whose huge number becomes a problem

Decomposition of alkyl-cyclo-alkanes



Difficulty with the number of species becomes much worse with alkyl-cyclo-alkanes

Alkane and cyclo-alkane ignition delay time



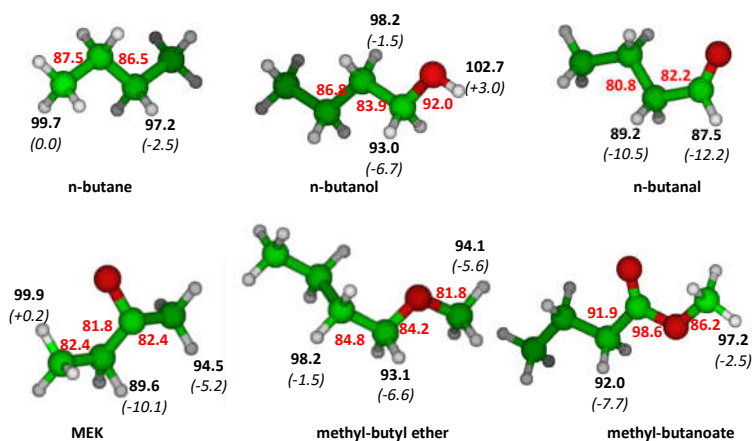
Extra strain of the double ring formation during isomerization reactions of both peroxy (ROO) and peroxy-alkyl-hydroperoxyl (OOQOOH) radicals mainly explains the lower reactivity of cyclo-alkanes when compared to the corresponding alkanes

Biofuels

- **Alcohols** (methanol, ethanol, propanol, butanol)
- **Ketones** (acetone, EMK, DEK)
- **Ethers** (DME, OME, DEE, EME, MTBE, ETBE)
- **Esters** (methyl and ethyl esters)

Oxygenated molecules

Oxygen atom effect on the closest bonds

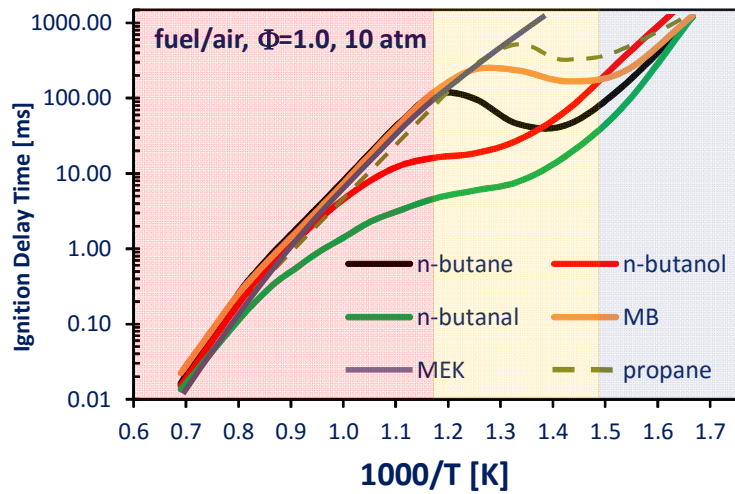


Electronegativity of the oxygen atom reduces the strength of the closest bonds.

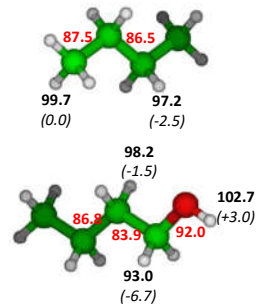
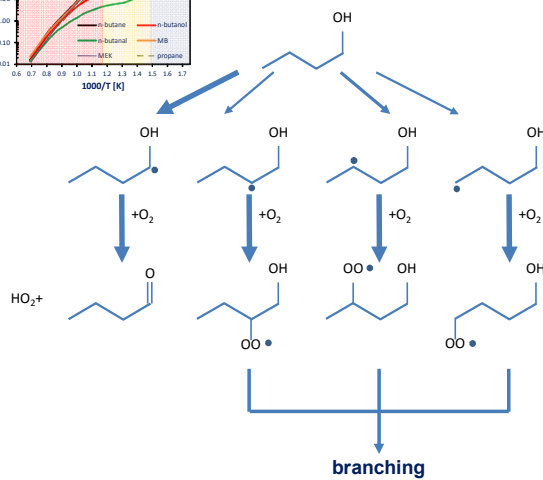
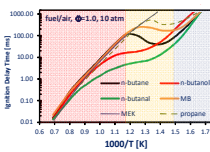
- *n*-butanol, *n*-butanal and MEK show a reduced energy of both the alpha C-C bond and the beta C-H bond.

- Substituted carboxyl group of methyl-butanoate makes the molecule more stable. The mesomeric structures of unshared pair of electrons in the oxygen singly bonded to carbonyl carbon, allow the formation of the ester resonance, which stabilizes the molecule.

Reactivity of oxygenated fuels

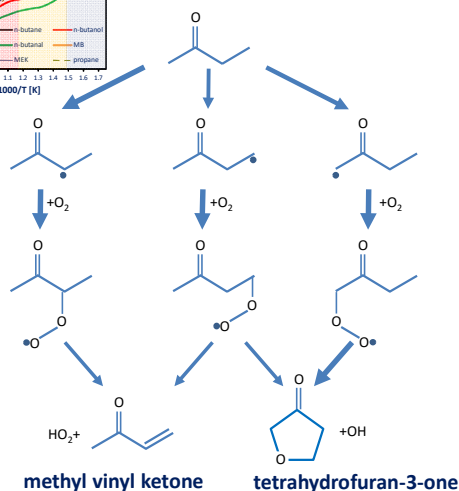
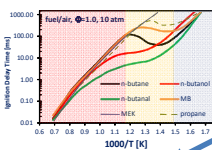


Low T alcohol reactivity

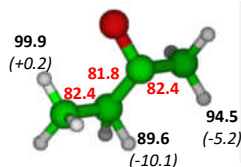
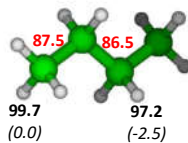


Low reactivity of n-butanol is due to the favored formation (~45% of fuel consumption) of the alpha radical, because of the reduced BDE of the alpha C-H bond induced by the OH group. Once formed, the alpha radical does not undergo the typical low temperature branching mechanism, but it mostly produces n-butanal and HO_2 .

Low T ketone reactivity



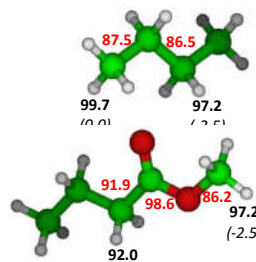
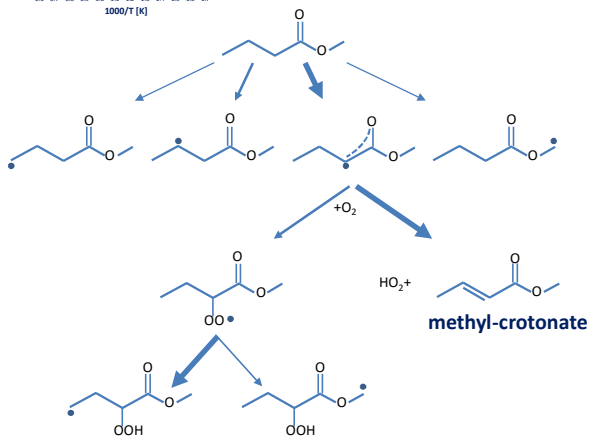
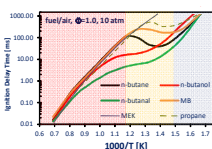
Hoppe et al., *Fuel* 2016
Scheer et al., *PCCP*, 2014



Close hydrogen atom have low BDE, because of the presence of the oxygen atom. Peroxy radicals mainly undergo HO₂ elimination and conjugate alkene formation.

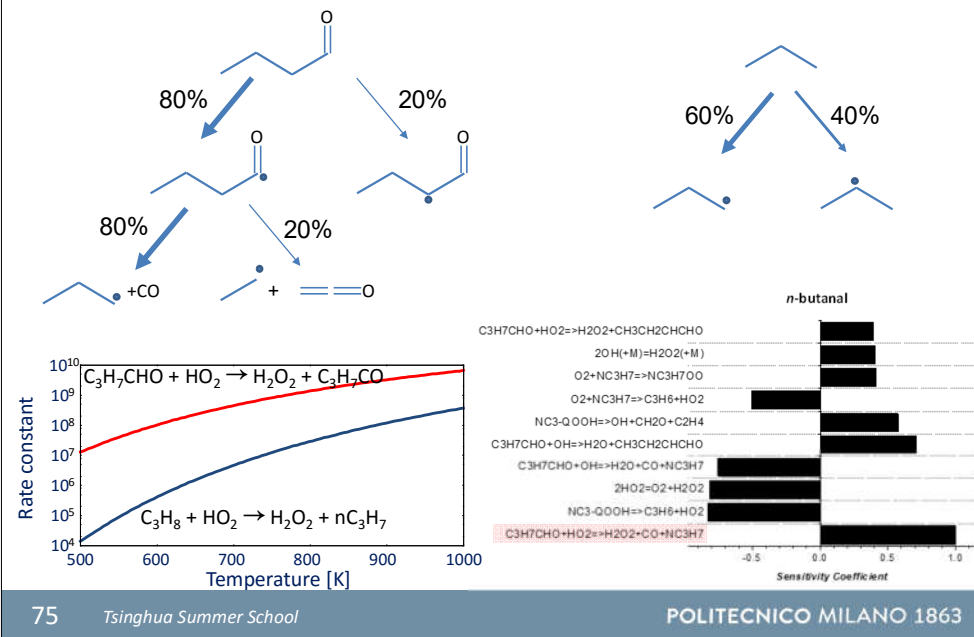
Another competing reaction is the cyclization with the formation of a furan like molecule.

Intermediate T ester reactivity



MB shows the second slowest reactivity. α -C-H bond is weaker, positively contributing to the reaction propagation. The stabilization resonance of the formed radical slows down the oxygen addition. The corresponding α -peroxy-methylbutanoate radical can only isomerize either through 7 or 5 membered ring. Most effective reaction is mainly the formation of HO₂ and the unsaturated methyl-crotonate, which decreases reactivity.

Intermediate T aldehyde reactivity



Oxygen atom: new molecular reaction classes

Alcohol molecular elimination (dehydration)



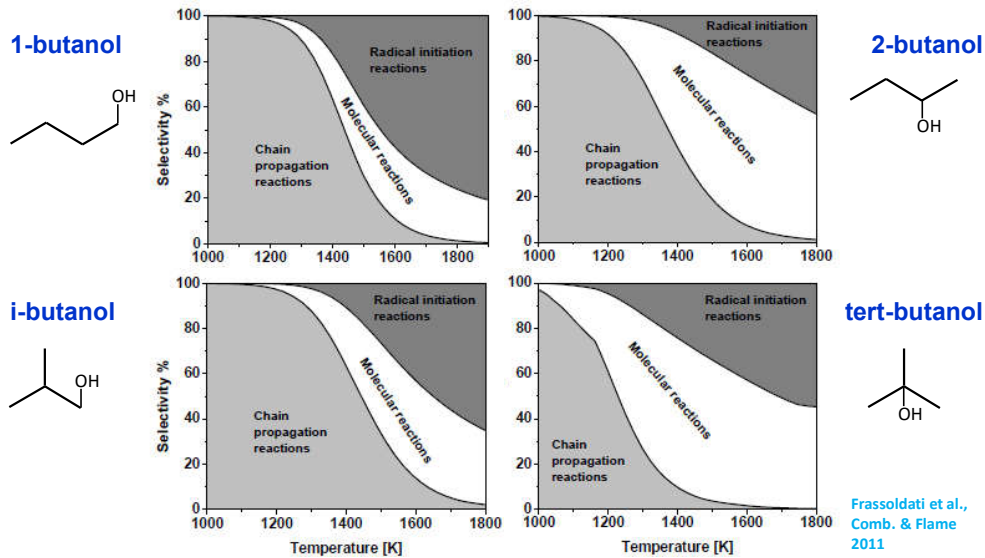
Ether molecular elimination



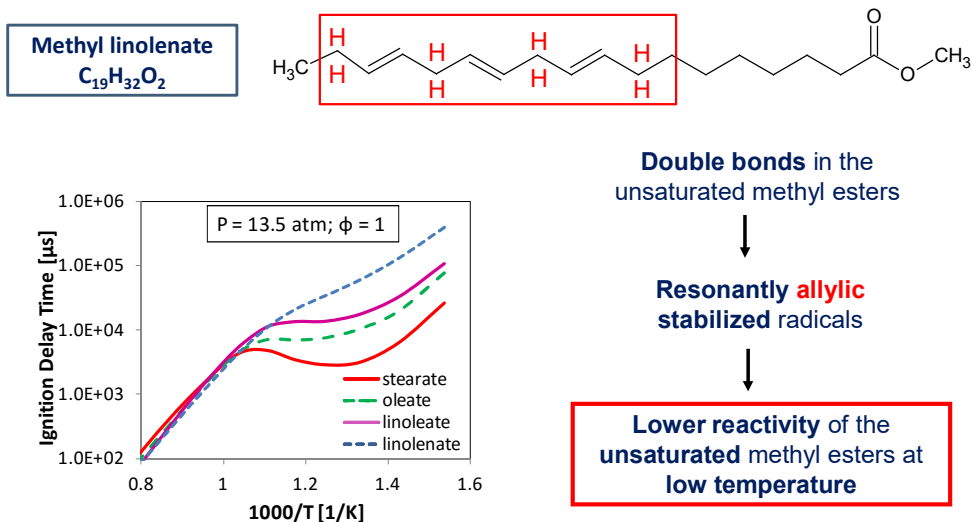
Ester molecular elimination



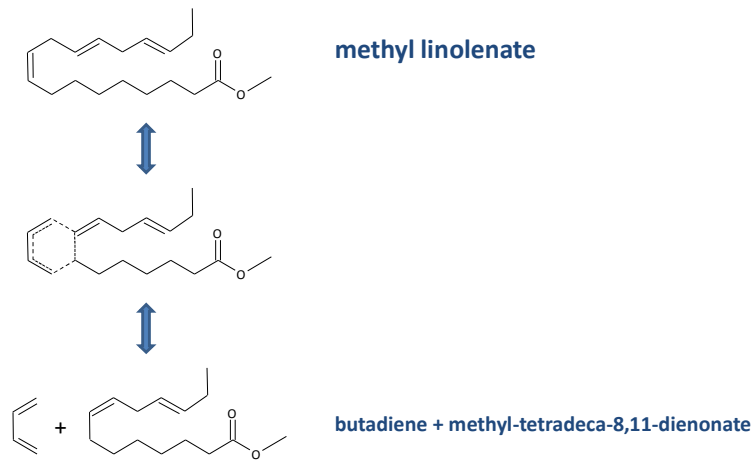
Importance of dehydration molecular reactions



Double bonds reduce reactivity at low T

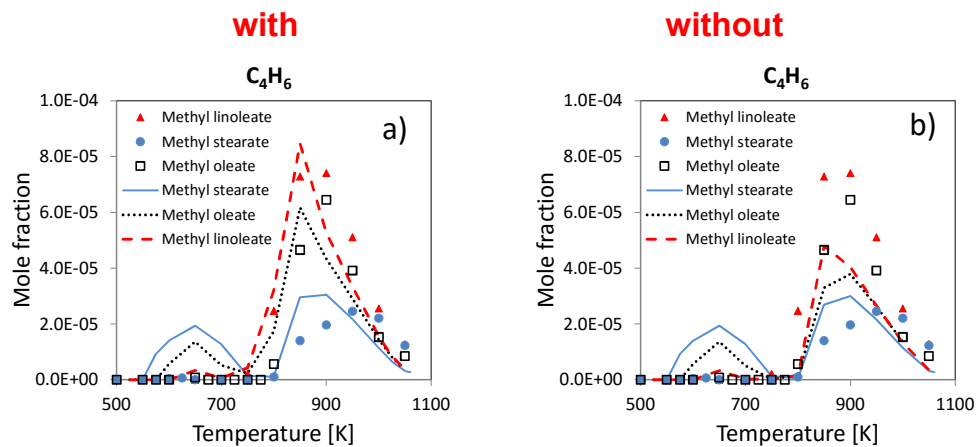


Double bonds allow molecular decomposition



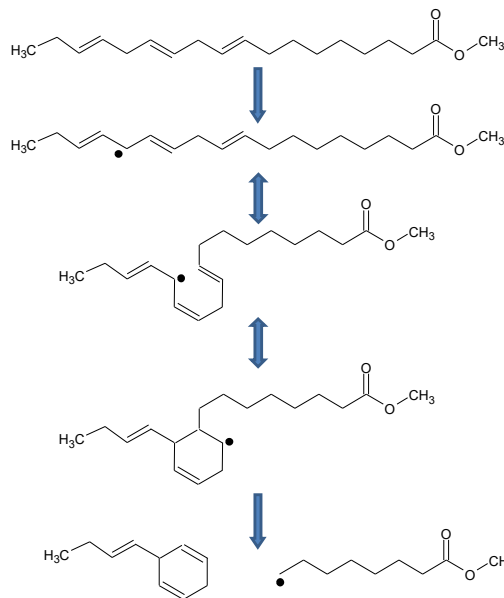
Effect of molecular decompositions

Methyl esters/benzene oxidation in JSR ($P = 106.7$ kPa, $\tau = 2$ s)



Rodriguez, A. et al., Comb & Flame, 2016

Double bonds allow internal cyclo-addition



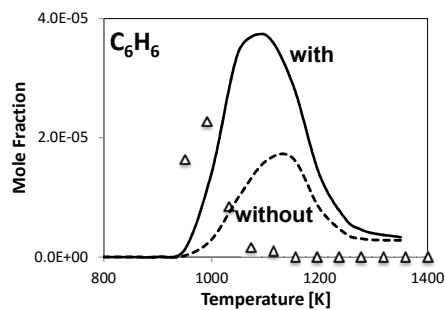
methyl linolenate

H abstraction reactions on the favored allylic position

Formation of **cyclic unsaturated molecules** (aromatic precursors)

Effect of internal cyclo-additions

Stoichiometric oxidation of rapeseed methyl ester in JSR ($P = 1 \text{ atm}$, $\tau = 0.07 \text{ s}$)

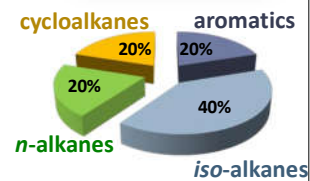
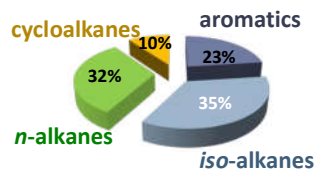
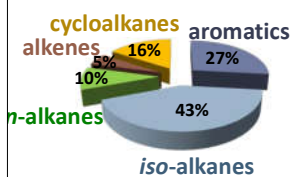


Exp data: P. Dagaut, personal communication

Real fuels: complex mixtures

General requirements for molecular structure of transportation fuels

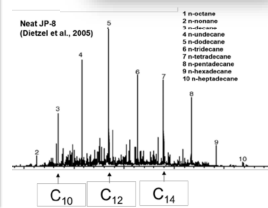
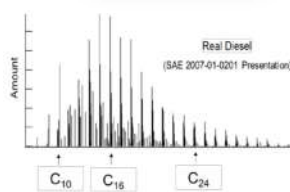
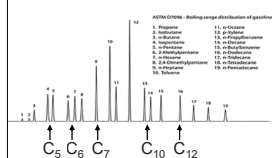
- Gasoline: short ($< C_8$) branched chains, aromatics, high octane number
- Diesel: long ($> C_{12}$), straight chains, substituted naphthenes, aromatics
- Jet Fuel: long ($> C_9$), straight chains, *iso*-alkanes, aromatics



Real fuels: complex mixtures

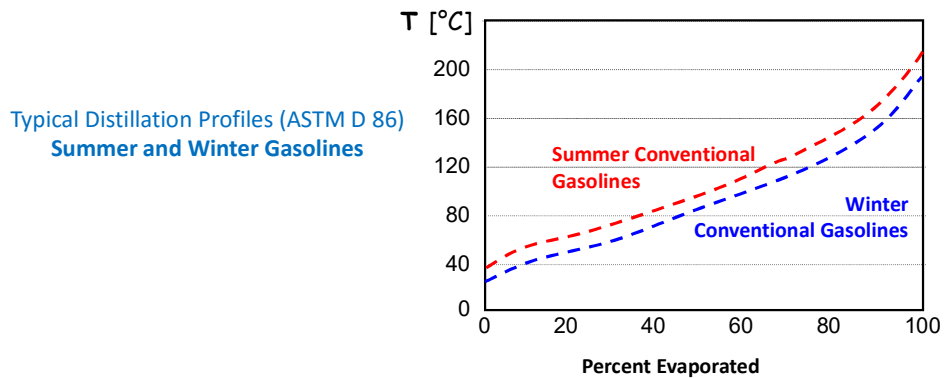
General requirements for molecular structure of transportation fuels

- Gasoline: short ($< C_8$) branched chains, aromatics, high octane number
- Diesel: long ($> C_{12}$), straight chains, substituted naphthenes, aromatics
- Jet Fuel: long ($> C_9$), straight chains, *iso*-alkanes, aromatics



Real fuels: complex mixtures

Real Fuels contain thousands of compounds greatly varying with feedstock origins, with seasons and with economic factors



Surrogate model fuels is the solution to simplify and the problem and make it manageable.

Surrogate fuels are also useful to handle the fuel variability

Real fuels: surrogate mixtures

Fuel surrogates are defined as physical or chemical surrogate depending on whether the surrogate mixture has the similar physical or chemical properties as the fuel to be studied.

Fuel composition (chemical classes, hydrocarbons concentrations, H/C ratio), derived cetane number (DCN), availability of valid chemical kinetic oxidation sub-models can be used to select the components of the model fuels.

Surrogates provide a cleaner basis for developing and testing models of the fuel properties in practical combustors.

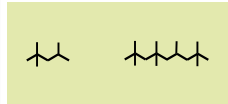
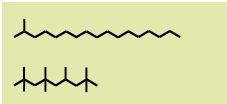
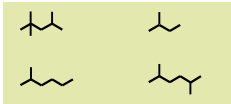
As an example, gasoline surrogates include Primary Reference Fuels (n-heptane and iso-octane), but also aromatic species (toluene).

Detailed reaction mechanisms for surrogates of gasoline, jet, and diesel fuels typically contain large numbers of species and reactions.

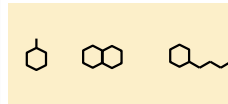
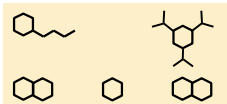
Real fuels: surrogate palettes



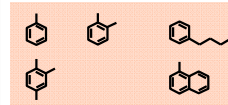
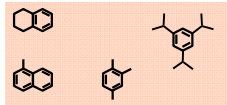
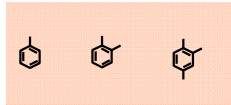
n-alkane



iso-alkane



cyclo-alkane and alkene



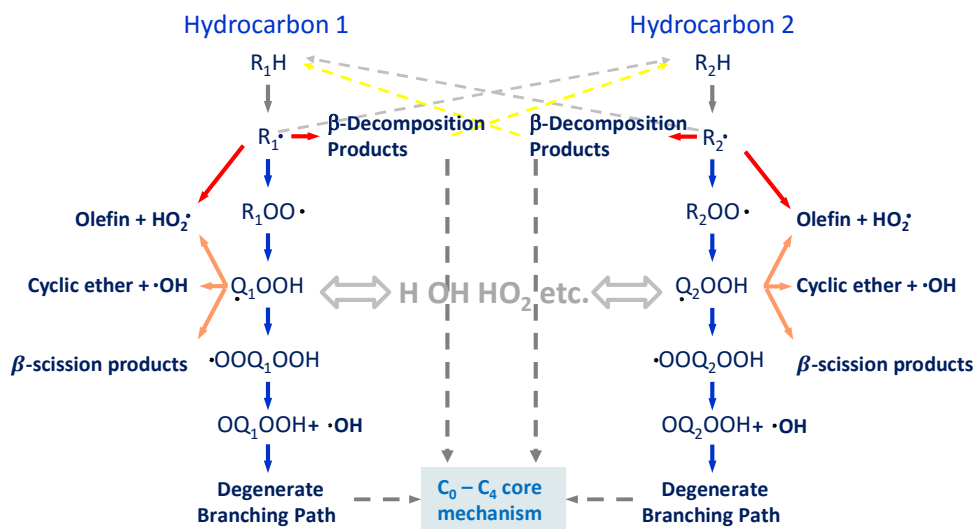
aromatics

Courtesy of Prof. Mani Sarathi, KAUST

Adapted from: Mueller et al., *Energy Fuels* 2016, 30, 1445–1461

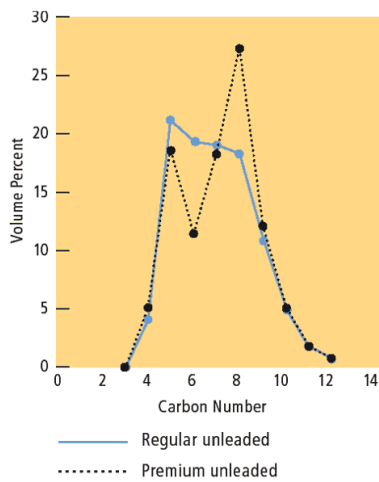
Adapted from: Dooley et al., *Combust. Flame*, 2010, 157, 2333-2339

Mixtures: fuel interactions



Adapted from Henry Curran

Primary Reference Fuels a first surrogate



Primary Reference Fuels define the Octane Number

Surrogate mixtures of **n-heptane** (ON=0) and **iso-octane** (ON=100) (2,2,4-trimethyl-octane)

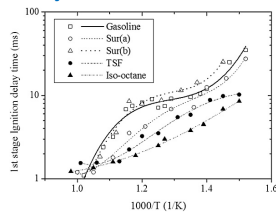
A gasoline with an ON=92 has the same knock as a mixture of 92% isooctane and 8% n-heptane, under the standard test conditions.

Ternary Toluene Reference Fuels (TRFs) can better reproduce H/C ratio and aromatic contents

http://www.chevron.com/products/prodserv/fuels/bulletin/motorgas/3_refining-testing/

Gasoline surrogates

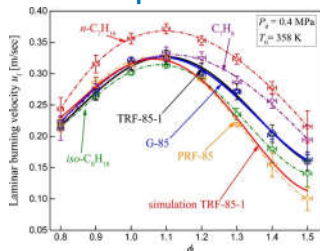
Ignition delay



Chung et al., Energy, 93, 2015, 1505-1514

	Gasoline	Surf(a)	Surf(b)	TSF	Iso-octane
RON	95	95	95	95	100
H/C ratio	1.801	1.801	1.801	1.801	2.25
O/C ratio	0.011	0.011	0.011	0	0
Density at 277 K (g cm ⁻³)	0.749	0.755	0.763	0.730	0.692
QLHV (kJ kg ⁻¹)	42.801	42.712	42.815	42.893	44.310
n-heptane	8.1	5.0	13.7	0	0
Iso-octane	30.9	33.2	42.8	100	0
Cyclohexane	8.4	6.8	0	0	0
Toluene	28.7	23.8	43.3	0	0
Cyclohexene	6.9	8.0	0	0	0
1,3 cyclohexadiene	9.8	16.1	0	0	0
Ethanol	7.2	7.1	0	0	0

Laminar flame speed



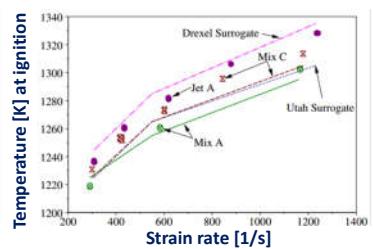
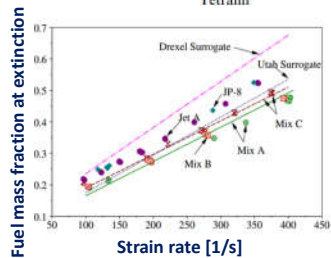
Manna et al., Combust. Flame, 162, 2015, 2311-2321

Fuel index	iso-Octane (vol.%)	n-Heptane (vol.%)	Toluene (vol.%)	RON	S	H/C	ρ (kg/m ³)
TRF-85-1	77.40	17.6	5	85	1.03	2.182	699.9
G-85	Gasoline FACE C			85	2	2.270	675.3

Real fuels and surrogates (jet fuels)

Surrogate mixtures for Jet fuels [5-8]

Surrogate compounds	[5]	[6]	[7]	[8]	A	B	C
Normal alkanes	<i>n</i> -Decane	15			32.6	60	
	<i>n</i> -Dodecane	20	26	30	34.7		60
	<i>n</i> -Tetradecane	15		20			
	<i>n</i> -Hexadecane	10					
Branched alkanes	<i>iso</i> -Octane	5		10			
	<i>iso</i> -Cetane		36				
Cyclo alkanes	Methyl-cyclo-hexane	5	14	20	16.7	20	20
	Cyclooctane	5					
	Decaline		6				
Aromatics	Toluene					20	
	<i>o</i> -Xylene	5		15			20
	Butyl-benzene	5			16		
	Tetra-methyl-benzene	5					
	α -Methyl-naphthalene	5	18				
	TetraIn	5		5			



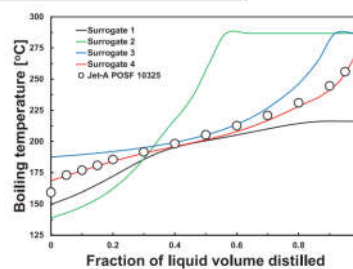
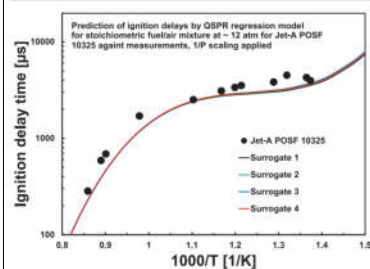
Humer, et al. *Proc. Combustion Institute*, 2007, 31(1), 393-400.

jet fuel surrogate and properties

Details of four surrogate mixtures formulated by CPT matching approach for Jet-A POSF 10,325.

Components	Target jet fuel Jet-A POSF 10,325	Surrogate 1 mole fraction	Surrogate 2 mole fraction	Surrogate 3 mole fraction	Surrogate 4 mole fraction
<i>n</i> -octane					0.023
<i>n</i> -decane					0.050
<i>n</i> -dodecane		0.490		0.312	0.300
<i>n</i> -tetradecane					0.100
<i>n</i> -hexadecane			0.365	0.123	0.014
<i>iso</i> -octane		0.210	0.310		0.034
<i>iso</i> -dodecane				0.243	0.143
1,3,5-trimethylbenzene		0.300	0.325	0.321	0.285
toluene					0.052
CPTs					
DCN	50	50	50.6	50	50
H/C ratio	1.961	1.961	1.947	1.951	1.936
MW [g/mol]	160.8	143.2	156.9	160.8	150.7
TSI	25.5	23.8	25.5	25.5	25.3
Density at 15 °C [kg/m ³]	803	768	777	781	778

While few species are able to match ignition delay times, a larger number of components is required to better emulate boiling curves.



Won et al., *Combust. Flame*, 2017, 183, 39-49.

RECAP

Combustion mechanisms of

- ✓ Hydrogen
 - ✓ Explosion diagram
- ✓ CO
- ✓ Methane
- ✓ Larger alkane
 - ✓ Competition between pyrolysis and oxidation (low and high T mechanism)
 - ✓ Normal and iso-alkane
- ✓ Alkene
- ✓ Cycloalkane
- ✓ Aromatics
- ✓ Oxygenated fuels
- ✓ Real fuels and surrogates

Mechanism use and analysis

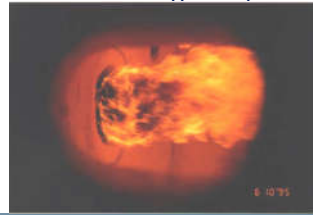
Mechanism development and experimental data

Mechanisms have to be developed on the basis of experimental data. Their validation requires the comparison with experimental data too.

Reaction mechanisms can be conveniently developed and validated looking at experiments in which transport phenomena (mass transfer, i.e. mixing, and heat transfer) are (almost) completely suppressed or well characterized and easily described.

Data performed in complex systems, mainly turbulent, where CFD is required are not suitable for mechanism validation, because:

1. Fluid-dynamic description is not perfect and it is difficult to distinguish between errors (inaccuracies) in the kinetics and errors (inaccuracies) in fluid-dynamics.
2. Computational times are very long, in some cases unmanageable, making the mechanism development too long.



“kinetic reactors”

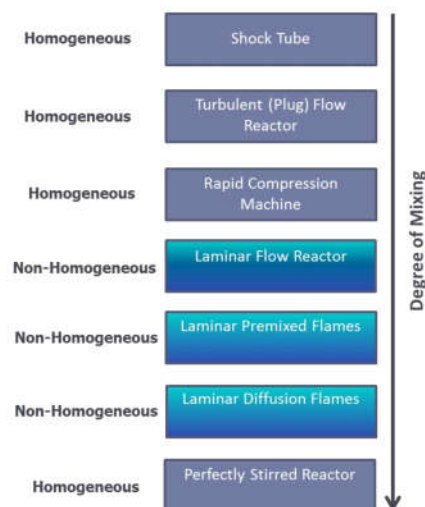
“kinetic reactors” are those which satisfy needs previously discussed

Reactors of this type include:

- shock tubes,
- ideal turbulent flow reactors,
- rapid compression machines.

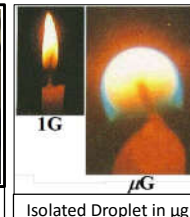
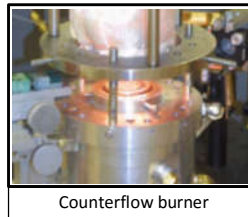
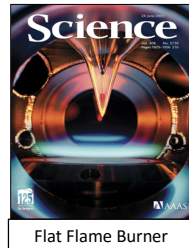
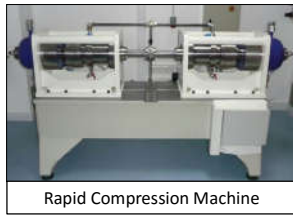
The degree and type of fluid mixing is an important feature in reacting flow simulation.

The mixing can occur among the reactants (diffusion flames) or between reactants and products (premixed flames).



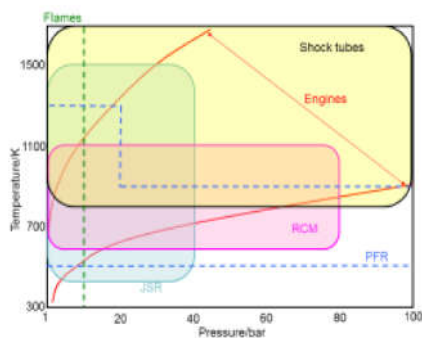
Adapted from H. Wang, Princeton Summer School 2012

Examples of “kinetic reactors”



After H. Curran, COST- Milan Summer School 2013

“kinetic reactors” and operating conditions



Individual reactor experiments have limited operating ranges. By combining them, one can obtain detailed data over the entire range of P/T pertinent to internal combustion engines and gas turbines

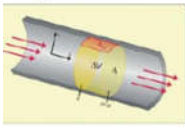
Shock-tubes and Rapid Compression Machine (RCM) are batch reactors which provide both global and detailed combustion data (ignition delay times and speciation).

Measurements of burning velocities and flame structures are limited to ~ 10 bar.

Courtesy of E. Ranzi

Ideal homogeneous chemical reactors

Plug Flow Reactor



$$\begin{cases} \rho v_z \frac{\partial \omega_i}{\partial z} = R_i \\ \omega_i(L=0) = \omega_i^0 \end{cases}$$

ODE system with initial conditions.

In order to better assess chemical kinetics, it is convenient to design experiments where the complexity of physical processes is minimized and data accuracy is maximized.

PSR



$$\begin{cases} \frac{d\omega_i}{dt} = \frac{G_{in}}{\rho V} \omega_{i,in} - \frac{G}{\rho V} \omega_i + \frac{R_i W_i}{\rho} - \frac{\omega_i}{\rho} \frac{d\rho}{dt} \\ \omega_i(t=0) = \omega_i^0 \end{cases}$$

ODE system with initial conditions.
NLS for a steady-state problem

This is the case of **ideal reactors** such as plug-flow reactors, perfectly stirred reactors, and batch.

Batch Reactor



$$\begin{cases} \rho v_z \frac{\partial \omega_i}{\partial z} = R_i \\ \omega_i(t=0) = \omega_i^0 \end{cases}$$

ODE system with initial conditions

Experiments are performed under ideal conditions (e.g., highly diluted and near-isothermal conditions)

Courtesy of Alberto Cuoci

Perfectly stirred reactor (jet stirred reactor)

Reactants are injected into a spherical chamber with a high injection velocity in order to reach an instantaneous mixing and uniform conditions within the reactor.

The reactants steadily burn and the products exit from the reactor chamber, at controlled flow rates, i.e. residence times.

Concentrations of the products, ignition and extinction of the reacting mixture are determined, as a function of Temperature, pressure and residence time.

Further Experimental Devices:

LRGP (ENSIC)-Nancy - Lorraine University (France)
University of Science and Technology, Hefei (China)
CNR-IRC Naples (Italy) ...and many others



Jet Stirred Reactor (CNRS Orléans)

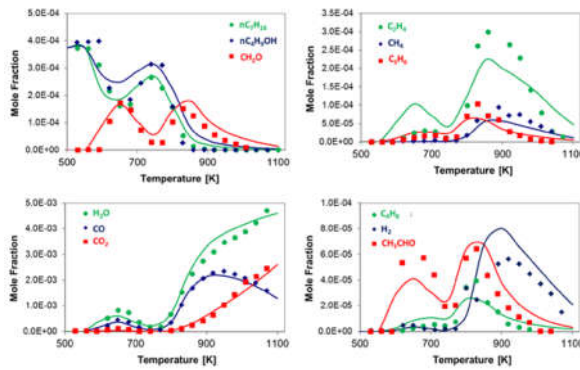
A fused silica jet-stirred reactor (~30 cm³):
4 injectors of 1 mm i.d.
The fuels and O₂ are diluted with N₂.
Controlled Flow rates → res. Time.
On line GC with FID/MS

Dagaut et al., Proc. Comb. Inst. 2013

Mixing times in stirred reactors is far shorter than reaction times:

$$\tau_{Mixing} \ll \tau_{Reaction}$$

jet stirred reactor: result example



Analytical techniques are used after gas sampling performed with **probes** (e.g., low-pressure, cooled, molecular beam) or traps (cold trap, bubblers, absorbers..).

The probes should stop chemical reactions and transfer the sample to the analyzers without changing its composition. Low-pressure probes reduce reactions rates by lowering C and T after gas expansion. Cooled probes reduce reaction rates. Probes can be responsible for disturbances of the reaction system (flow, temperature) which result in additional complications.

Dagaut, P., & Togbé, C. (2009). *Energy & Fuels*, 23(7), 3527-3535.

Turbulent flow reactor

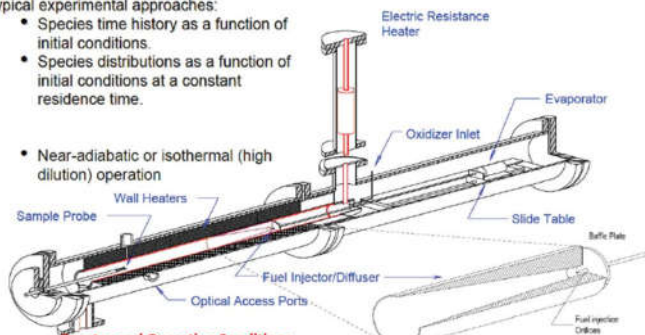
Tubular flow reactors consist of a tube where reactants are injected and heated from outside. The flow inside the tube can be laminar or turbulent.

http://www.princeton.edu/~combust/MURI/papers/Dryer_presentation.pdf

Princeton Variable Pressure Flow Reactor

Typical experimental approaches:

- Species time history as a function of initial conditions.
- Species distributions as a function of initial conditions at a constant residence time.
- Near-adiabatic or isothermal (high dilution) operation



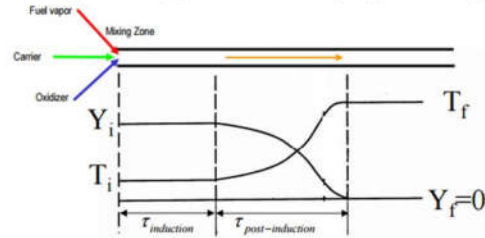
Reactor and Operating Conditions
 Reactor Duct Material: Fused Silica
 Pressure: 0.2 - 20 atm
 Temperature: 300 - 1200 K

Reactor Section Dia. 10 cm
 Mass Flow rate: 10 - 30 grams/sec
 Residence Time: 0.015 - 5 sec

Difficulties in the initial mixing between fuel, oxidizer, and diluent.

Ideal plug flow assumptions

$$-D\rho \frac{d^2(Y)}{dx^2} + \rho u \frac{d(Y)}{dx} + \dot{w} = 0 \quad -\lambda \frac{d^2(T)}{dx^2} + \rho u c_p \frac{dT}{dx} + \dot{w}Q = 0$$



$$T = T_i, Y = Y_i$$

$$\frac{dT}{dx} = \frac{dY}{dx} = 0$$

$$T = T_f, Y = Y_f$$

$$\frac{dT}{dx} = \frac{dY}{dx} = 0$$

- Theoretically, the solution of the governing equations is an initial-value problem
 - Any single matching point of experiment and theory should be equivalent
- Where is "time = 0" for the problem? Many use the "instantaneous" mixing location as a location of $t=0$ for comparison with predictions – this assumption is discussed in depth later



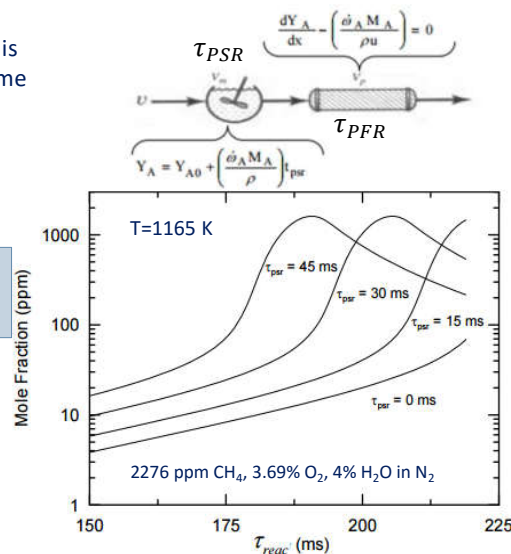
Effect of the Initial Mixing on the reaction time

The overall residence time in the PFR is reduced to account for a residence time inside the mixing zone (PSR):

$$\tau_{tot} = \tau_{PSR} + \tau_{PFR}$$

A simple time shift is sufficient to compare model predictions and experiments, in the absence of reactions in the mixing zone.

At different τ_{PSR} , the CO profiles, can be overlaid identically by time shifting.

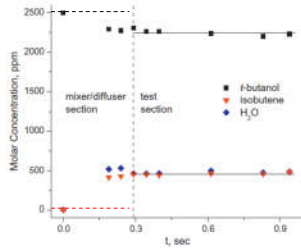


Dryer, F. L., Haas, F. M., Santner, J., Farouk, T. I., & Chaos, M. (2014). *Prog. Energy and Combust. Sci.*, 44, 19-39.

Reactions in the mixing zone

Pyrolysis Experiment t-butanol/N₂=2500/997,500 ppm

Concentrations vs τ in the flow reactor.

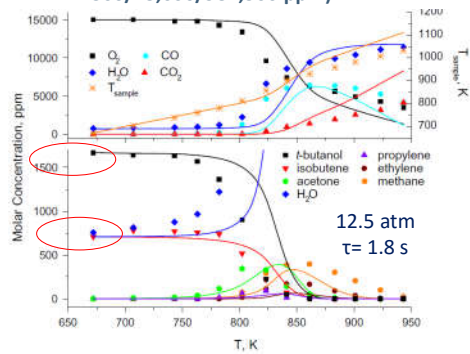


Line represents the end of the mixer region, and horizontal lines shows that there is no conversion after the mixing region.

Similar reactivity, before the complete mixing, is also observed for different oxygenated fuels.

Lefkowitz et al. (2012). *Comb. Flame*, 159, 968-978.

Oxidation of t-butanol (Fuel/O₂/N₂ 2500/15,000/982,500 ppm).



Fuel concentration before mixing and dilution is larger than that in the test, because of the molecular reaction: $t-C_4H_9OH \rightarrow iC_4H_8 + H_2O$

It is necessary to modify the initial conditions.

Grana et al. [2011]

The 4 stroke engine

DESIGN & RESEARCH BY JACOB O'NEAL. VIDEO PROVIDED BY JACOB O'NEAL.

HOW A CAR ENGINE WORKS

[And a note about hybrid gas-electric cars too]

If your only experience with a car engine's inner workings is "How much is that going to cost to fix?" this graphic is for you! Car engines are astoundingly awesome mechanical wonders. It's time you learned more about the magic under the hood!

The 4 Stroke Cycle

Let's take a look inside just one cylinder.

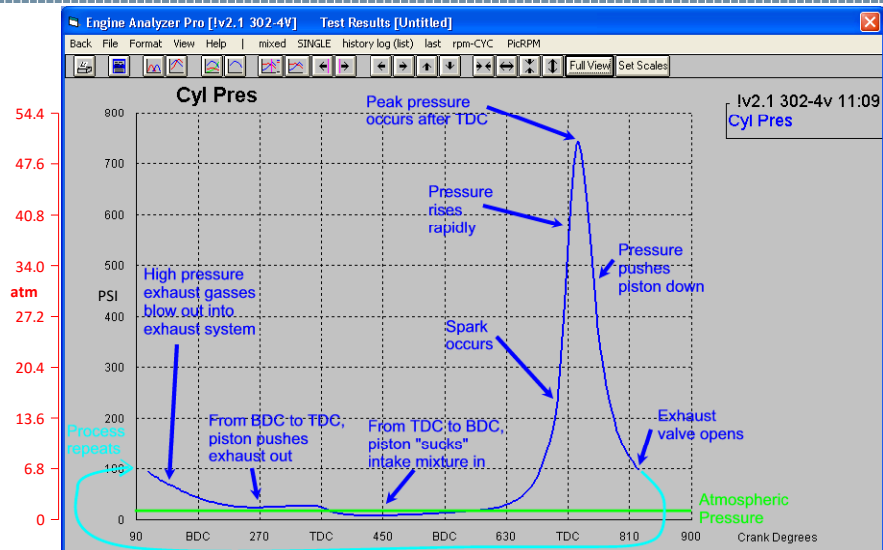
- INTAKE STROKE**
The piston descends, sucking air into the cylinder through open intake valves as fuel is injected.
- COMPRESSION STROKE**
With all valves closed, the piston comes back up, compressing the fuel-air mixture. Compressing the mixture delivers better power and efficiency.
- POWER STROKE**
A spark ignites the compressed fuel-air mixture, and the resulting combustion forces the piston to the bottom of the cylinder again.
- EXHAUST STROKE**
The piston comes back up, pushing the spent mixture out through open exhaust valves.

Select engine parts

©ANIMAPAGES.COM

Source:
<https://giphy.com/gifs/car-works-engine-TMAJKmj3ys2k>

The 4 stroke engine pressure history



Source: <https://www.performancetrends.com/Definitions/Cylinder-Pressure.htm>

Homogeneous reactors miming engines

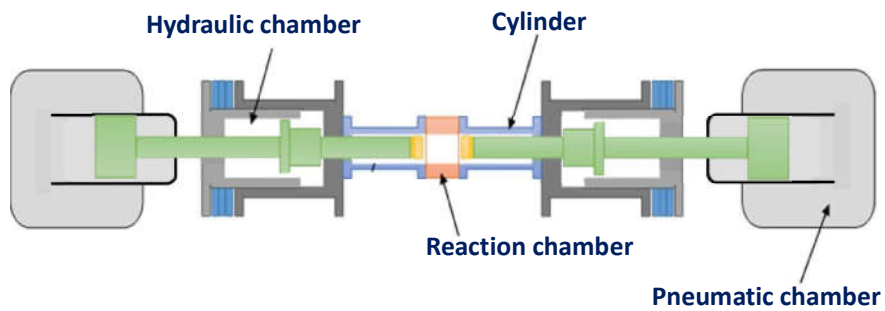


Rapid Compression Machine



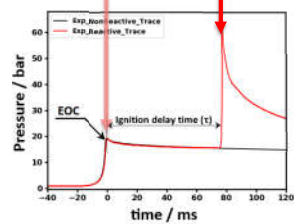
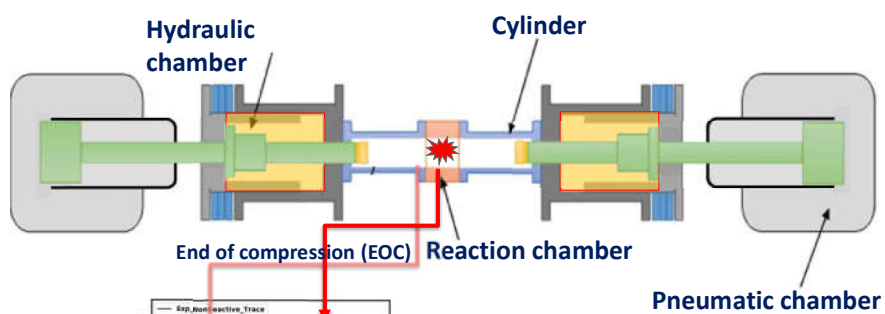
Shock Tube

Rapid compression machine (RCM)



Courtesy of prof. Henry Curran
 Source: Dumitrache C, et al. A study of laser induced ignition of methane-air mixtures inside a Rapid Compression Machine. *Proc Combust Inst* 2017;36:3431–9. doi:10.1016/j.proci.2016.05.033.

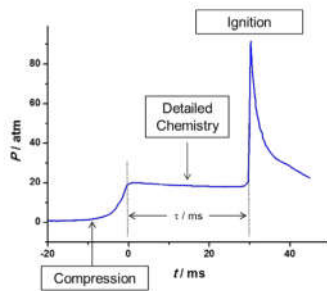
Rapid compression machine (RCM)



Courtesy of prof. Henry Curran
 Source: Dumitrache C, et al. A study of laser induced ignition of methane-air mixtures inside a Rapid Compression Machine. *Proc Combust Inst* 2017;36:3431–9. doi:10.1016/j.proci.2016.05.033.

Data from RCM

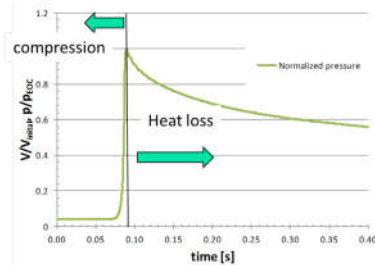
Ideality and 'Facility effects'



The RCM determines the ignition delay times, and can be simulated as a **batch reactor at constant volume**..... but...

Adapted from H. Curran, COST- Milan Summer School 2013

Non-reactive experiments, where N_2 replaces O_2 , characterize the heat loss during compression.

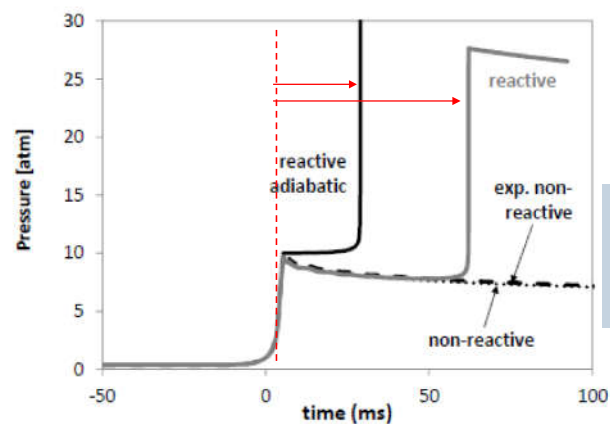


Heat loss effects can be modelled as change in volume.

A **volume profile** is deduced from the pressure profile assuming isentropic behaviour:

$$\frac{p_2}{p_1} = \left(\frac{V_2}{V_1}\right)^{\gamma(T)}$$

RCM variable volume simulation



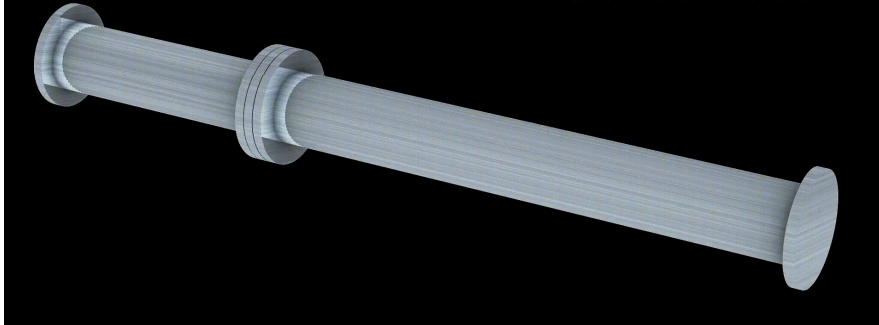
The ignition delay time changes from 20 to 60 ms, accounting for the 'facility effect' $V/V_0=f(t)$

butyl-benzene/air at $\Phi=1$, compressed gas $T=893$ K, $P=10$ atm.
RCM simulation using OpenSMOKE++ and the kinetic mechanism of Nakamura et al. [2014]. Effect of variable volume simulations.

Cuoci, A., Frassoldati, A., Faravelli, T., & Ranzi, E. (2015). *Computer Physics Communications*, 192, 237-264.

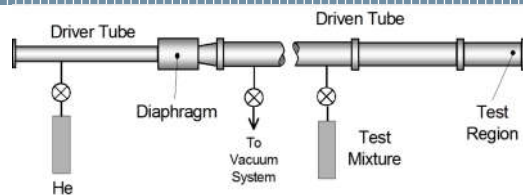
Shock Tube device (ST)

Dynamic Pressure Sensing with a Shock Tube



Source: <https://www.nist.gov/video/dynamic-pressure-sensing-shock-tube>

ST summary



- A diaphragm initially separates a **high** (driver gas) and a **low pressure region** (reacting mixture).
- Bursting the diaphragm, a shock wave is generated and propagates. It acts as a piston.
- **The reactants (test gas) at low T/p are instantly heated and pressurized to high values by incident and reflected shocks.**

The set of equations describing the mass, velocity and temperature profiles downstream of the shock (derived from conservation laws) are similar to the ones of an **adiabatic batch reactor**. Diffusion, and viscous effects are neglected.

Shock tube characteristics

- **Instantaneous** heating/compression from shock waves
- **Accurately known** incident- and reflected-shock conditions
- **Wide range** of post-reflected shock T and p (**~700-3000 K; 0.1-1000 atm**)
- **Typical ignition times** are on the order of **0.1-5. ms**

Shock attenuation and **boundary layer interactions** become important at longer times.

ST experiments

Ignition delay times: important indicator of fuel reactivity

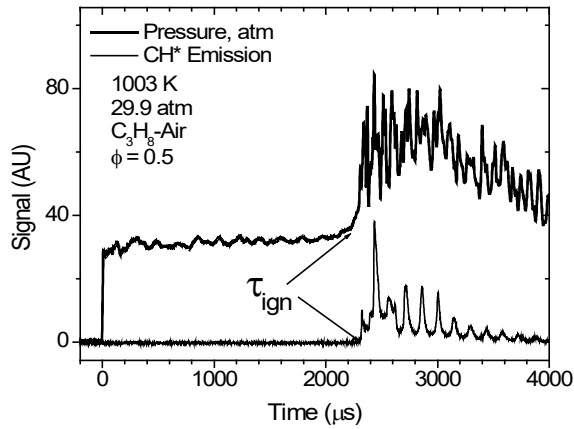
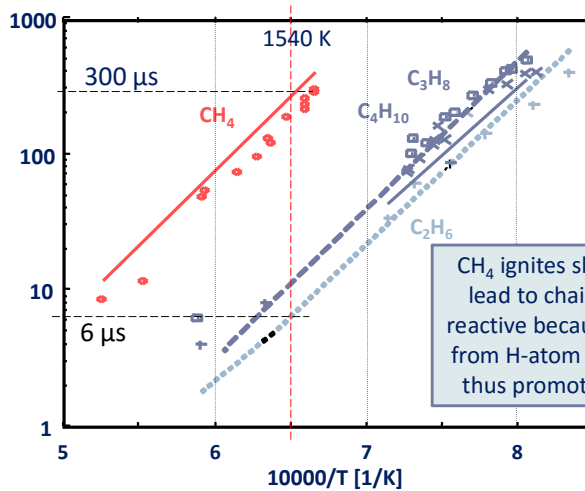


Figure from Prof. E. Petersen

High Temperature Combustion Processes

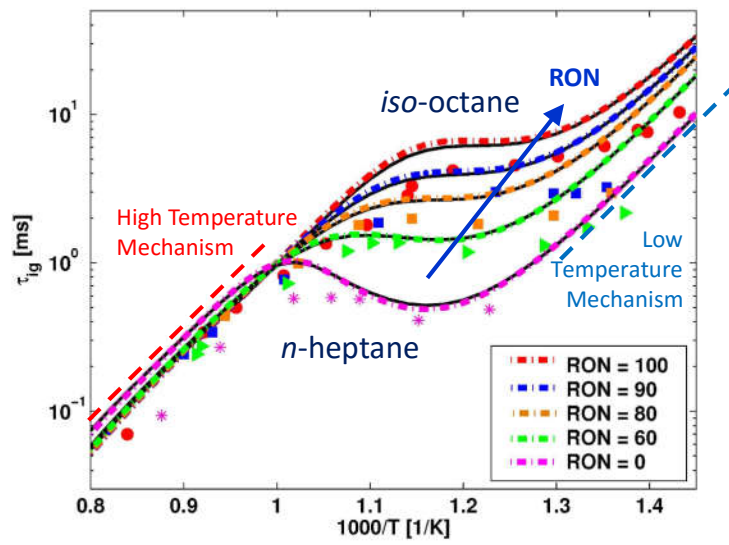
Ignition delay times [μs] vs Temperature [K]



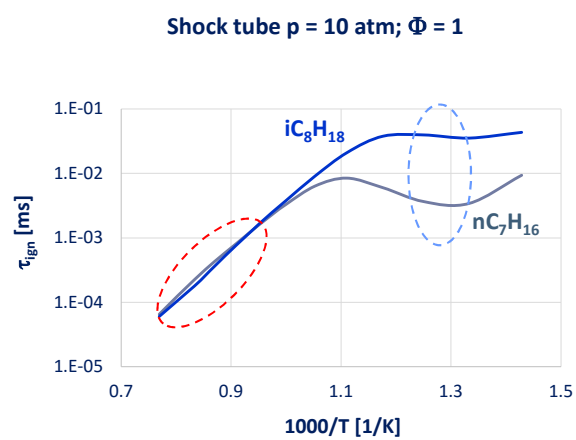
CH₄ ignites slowest because methyl radicals lead to chain termination. Ethane is most reactive because every ethyl radical, resulting from H-atom abstraction, produces H atoms, thus promoting:

$$\text{H} + \text{O}_2 \rightarrow \text{O} + \text{OH}$$

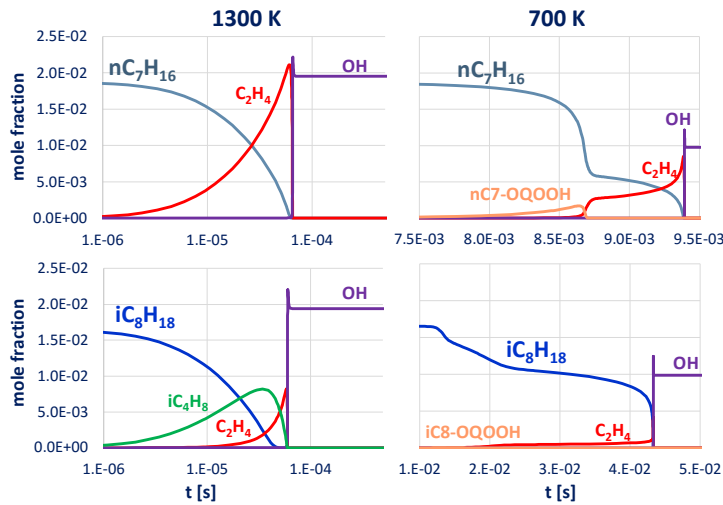
ST ignition delay times



Ignition delay times of nC7 and iC8

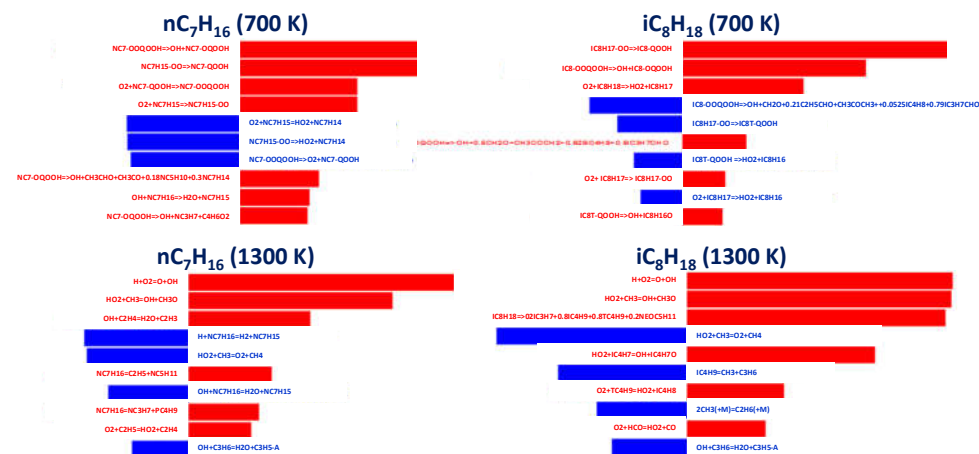


Ignition delay times of nC7 and iC8



In the low T regime, the first controlling ignition (responsible of the temperature increase, which brings to the second ignition) is governed by keto-hydroperoxide. At high T, when ignition occurs, the fuel is completely consumed and pyrolysis products, like C₂H₄, play the main role in conversion.

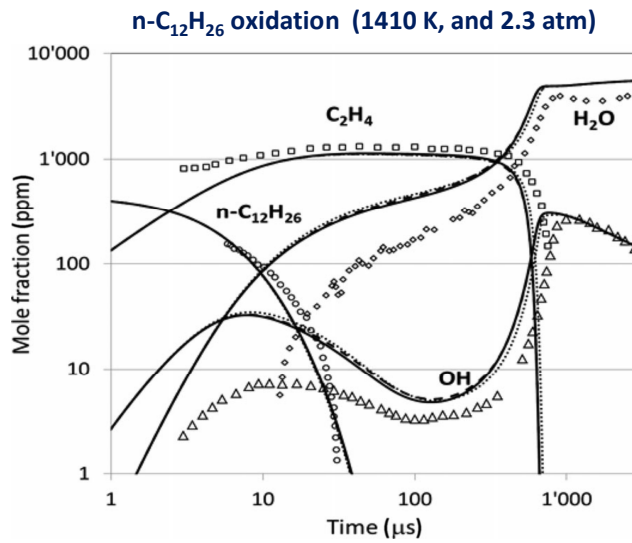
IDT of nC7 and iC8: sensitivity analysis



Sensitivity analysis confirms that most important reactions at low T involve peroxy species of the fuel.

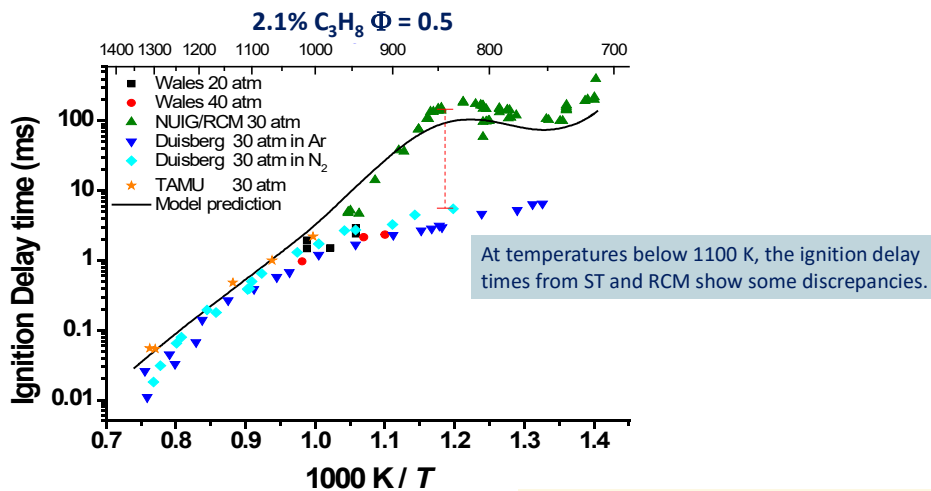
At high T, ignition is controlled by C0-C4 sub-mechanism (pyrolysis products: C₂H₄ for C₇H₁₆ and iC₄H₈ for iC₈H₁₈), with the only exception of fuel decomposition (pyrolysis) reaction.

ST speciation



Davidson, D. F., et al. (2011). *Proc. Comb. Institute*, 33(1), 151-157.

ST vs. RCM ignition delay times

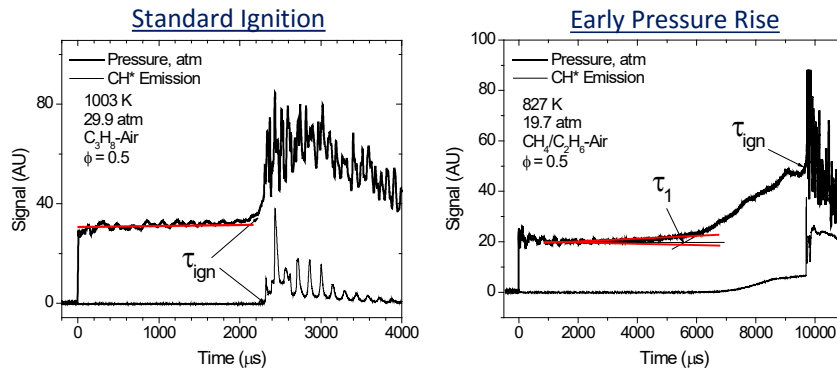


S. M. Gallagher et al. *Combust. Flame*, 153 (2008) 316-333.

ST and RCM are complementary working on different temperature ranges

ST device effect

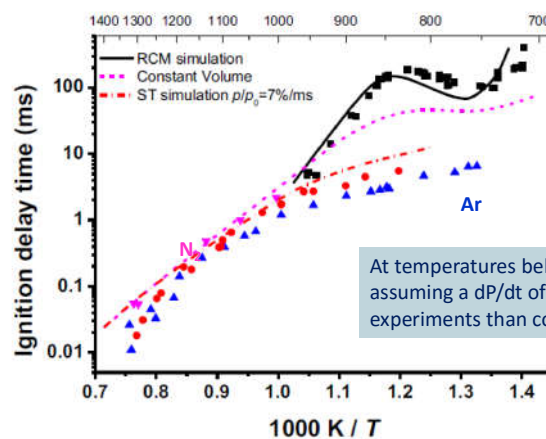
Shock attenuation and **boundary layer interactions** become important at longer times.



ST experiments show a pressure rise before ignition. RCM and ST are not exactly at the same conditions

Figures from Prof. E. Petersen

ST pressure correction



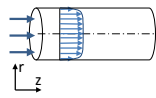
At temperatures below 1100 K, simulations assuming a dP/dt of 7%/ms agree better with the experiments than constant volume simulations.

Propane ignition delay time measurements at low temperatures and high pressures for fuel in 'air' mixtures at $\Phi=0.5$, $p=30$ atm, and comparison with a traditional constant energy and volume (or density) simulation and with a simulation using $dP/dt = 7\%$ [-/ms].

Sung, C. J., & Curran, H. J. (2014), *Progress in Energy and Combustion Science*, 44, 1-18.

Flow reactors

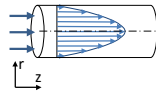
Turbulent flow reactor: flat radial velocity profile. Ideal reactor 0D (no axial and radial diffusion). ODE system of equation with initial conditions



$$\rho v_z \frac{d\omega_i}{dz} = R_i$$

$$\omega_i(z=0) = \omega_i^{in}$$

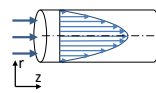
Laminar flow reactor: parabolic radial velocity profile. Axial diffusion. Reactor 1D (no radial diffusion). ODE system of equation with boundary conditions



$$\rho v_z \frac{d\omega_i}{dz} = \frac{d}{dz} \left(\rho \mathcal{D} \frac{d\omega_i}{dz} \right) + R_i$$

$$\begin{cases} \omega_i(z=0) = \omega_i^{in} \\ \frac{d\omega_i}{dz}(z=L) = 0 \end{cases}$$

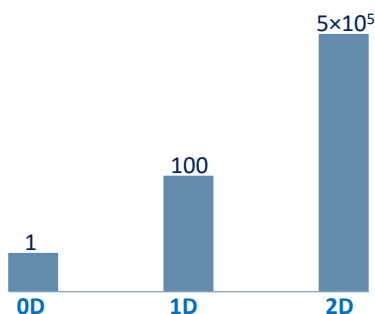
Laminar flow reactor: parabolic radial velocity profile. Axial and radial diffusion. Reactor 2D (cylindrical symmetry). PDE system of equation with boundary conditions



$$\rho v_z \frac{d\omega_i}{dz} + \rho v_r \frac{d\omega_i}{dr} = \frac{d}{dz} \left(\rho \mathcal{D} \frac{d\omega_i}{dz} \right) + \frac{d}{dr} \left(\rho \mathcal{D} \frac{d\omega_i}{dr} \right) + R_i$$

$$\begin{cases} \omega_i(z=0) = \omega_i^{in} \\ \frac{d\omega_i}{dz}(z=L) = 0 \\ \frac{d\omega_i}{dr}(r=0) = 0 \quad (\text{symmetry}) \\ \frac{d\omega_i}{dr}(r=R) = 0 \quad (\text{no flow to the wall}) \end{cases}$$

Computational effort for different flow reactors



The computational effort is strongly dependent on the dimension of the mechanism.

Assuming that 0D reactor can be simulated in the order of one second, 1D requires minutes, whilst 2D up to one week.

This makes the 0D reactor much more useful for the development and validation of mechanisms.

Computational effort for different flow reactors

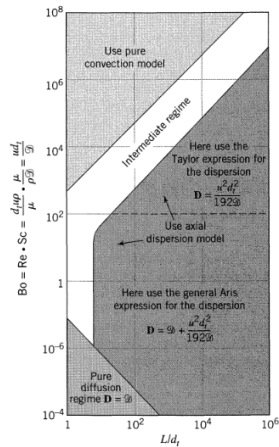


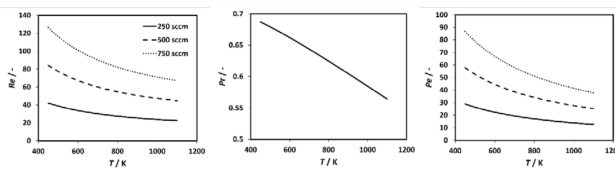
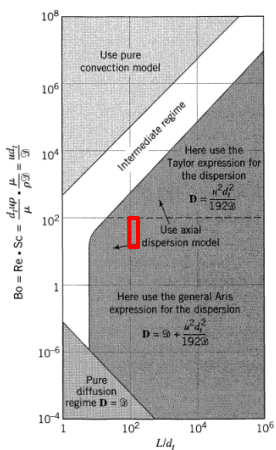
Figure 15.2 Map showing which flow models should be used in any situation.

Octave Levenspiel
 Chemical, Reaction Engineering
 John Wiley & Sons, 1999

In case of laminar flow, it is possible to have an idea of which model can be used for the flow reactor.

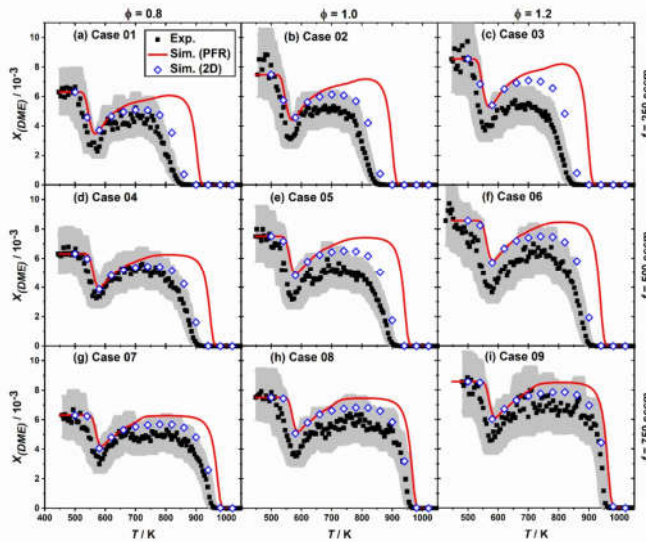
Vessel geometry (L/d_t), flow conditions (Reynolds number) and fluid properties (Schmidt number), can be used to a-priori identify the different regimes through maps.

Bielefeld flow reactor



Laminar flow. Operating conditions fall in the dispersion model region

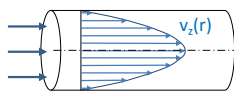
Bielefeld flow reactor



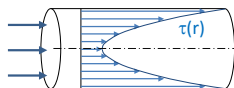
DME oxidation in low-intermediate T conditions

Only 2D simulations allow to match the experimental data in the whole temperature range at the different residence times, whilst 0D simulations strongly underestimate the reactivity in the intermediate temperature range

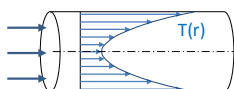
Laminar flow reactor



Laminar flow model assumes no slip conditions between the flow and the wall, i.e. axial velocity (v_z) is equal to zero at the wall and increases toward the axis with a parabolic profile.



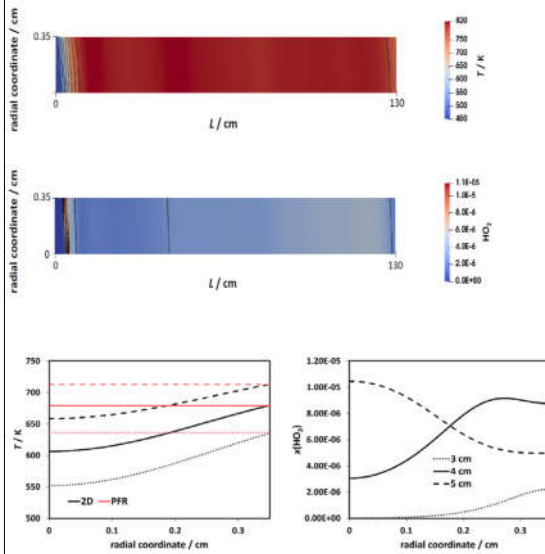
Of course, the residence time (τ) is low on the axis and approaches infinite at the wall



Temperature profile is parabolic too. If the reactor is heated from outside, the temperature is maximum on the wall and minimum on the axis.

Temperature and residence time profiles control the behavior of the laminar flow reactor more or less favoring the formation of important species, like radicals

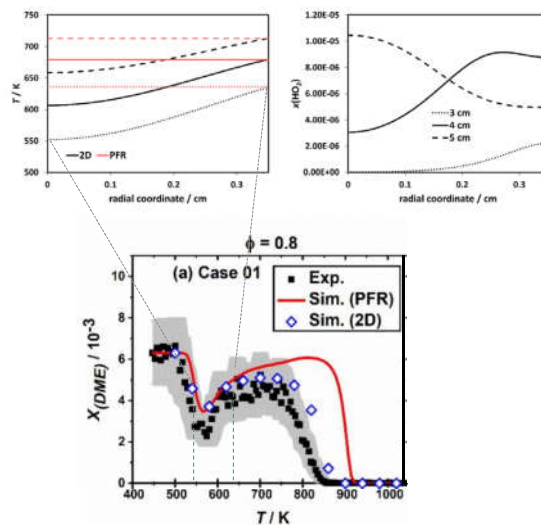
Bielefeld flow reactor



Hydrogen peroxide and temperature maps.

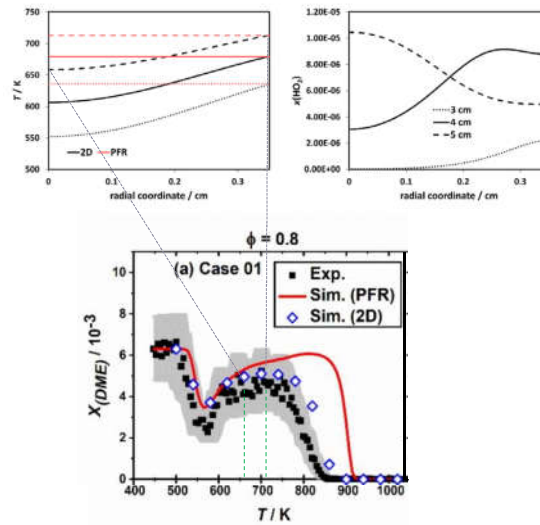
Increasing reactivity @ 3 cm from inlet

At 3 cm from inlet, the wall temperature is ≈ 640 K and decreases to ≈ 550 K on the axis. A temperature of 550 K corresponds to low-temperature conditions where the reactivity has not yet reached its maximum, whilst 640 K is already beyond the maximum of the low-temperature conversion in the NTC region. The DME conversion at these temperatures is very similar, but the longer residence time at the wall allows for HO_2 formation, which is negligible on the axis. The low velocity close to the wall is then the origin of the increased reactivity predicted by the 2D model.



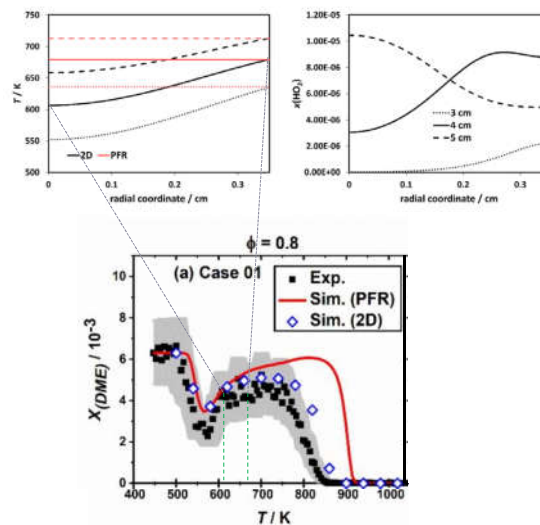
Increasing reactivity @ 5 cm from inlet

At 5 cm, HO_2 is mainly formed in the core of the reactor. In this case, the temperature gradient effect prevails over that of the residence time. The wall temperature of ≈ 710 K is closer to the minimum reactivity of the NTC region, while the lower axial temperature (≈ 660 K) entails a larger reactivity, with a net effect of higher HO_2 concentration on the axis.



Increasing reactivity @ 4 cm from inlet

At 4 cm from the inlet, temperature and residence time compete with each other: the lower temperature favors higher reactivity on the axis, while the residence time increases the reactivity on the wall. This competition results in the presence of a small maximum at about 2.5 mm, with a significant amount of HO_2 in the whole section.



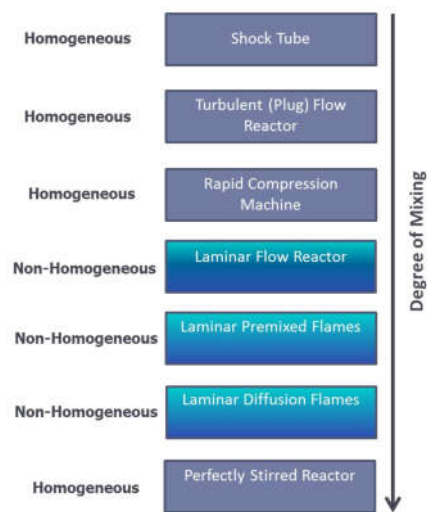
Flames

Flames always involve some mixing and require to account for transport phenomena along with reaction kinetics.

In laminar premixed flames, mixing occurs because of heat and species diffusion at the flame front.

In laminar diffusion flames, sufficient mixing of the fuel and oxidizer by molecular diffusion is a necessity.

Flames can provide valuable data of burning velocities and speciation, although, limiting perturbations by conventional sampling probes remain a major challenge for future work.



Adapted from H. Wang, Princeton Summer School 2012

Examples of Laminar Flames and Devices

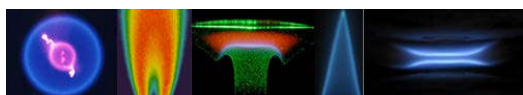
2D, 3D laminar flames => Require computationally expensive simulations are then less useful for mechanism development/validation

1D flames =>

- Premixed flat flames (burner stabilized or freely propagating flames)
- Counterflow (premixed/partially premixed/diffusive/pool flames)
- Isolated fuel droplet in microgravity (1D, but unsteady)

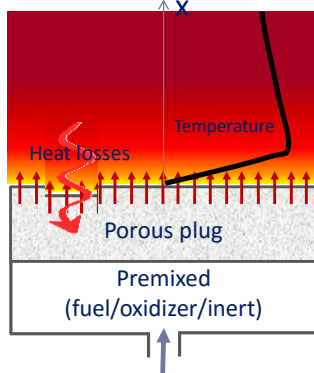
Flames which are modeled using a 1D model are useful for studying High T Kinetics of combustion, in presence of diffusion of heat and mass.

- Flame speed measurements
- Composition profiles (speciation)
- Ignition experiments
- Extinction experiments
- Dynamic response of flames to forced oscillations

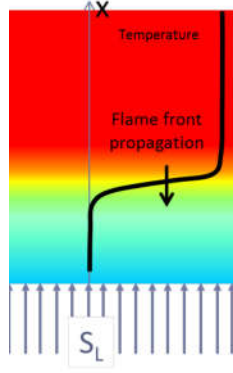


Premixed 1D laminar flames

1. Burner Stabilized Flame



2. Freely Propagating unstretched flame



The propagation speed of the premixed flame with respect to the unburned gases is the laminar flame speed S_L or burning velocity.

Conservation equations are the same, but the boundary conditions are different.

For burner-stabilized flames the cold flow velocity (or mass flow rate) and composition are known, and vanishing gradients are imposed at the hot boundary.

For freely propagating flames LFS is an eigenvalue to be determined.

[Smooke et al., *Comb Sci and Tech* 34:79 (1983)]

Model equations

For these systems, we assume 1-D flow with uniform inlet conditions. The corresponding steady-state governing conservation are:

Continuity equation

Mass flow $\dot{m}^* = \frac{\dot{m}}{A} = \rho v = \text{constant}$

Species

$$\dot{m}^* \frac{d\omega_k}{dx} = - \frac{d(\rho \omega_k V_k)}{dx} + \dot{\Omega}_k \quad k = 1, \dots, N$$

Energy

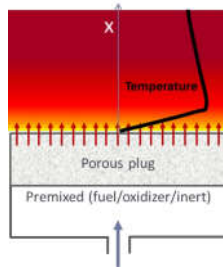
$$\dot{m}^* c_p \frac{dT}{dx} = \frac{d}{dx} \left(\lambda \frac{dT}{dx} \right) - \rho \sum_{k=1}^{N_S} c_{p,k} \omega_k V_k \frac{dT}{dx} - \sum_{k=1}^{N_S} H_k \dot{\Omega}_k$$

Steady-state equations

Formation due to chemical reactions

Diffusion velocity: molecular and thermal diffusion

Specific aspects



The Burner-Stabilized Flames (BSF) are often used for analyzing species profiles in flame experiments.

The mass flow rate through the burner is known and is lower than the flame speed of the mixture. The flame is stabilized over the burner surface, which is heated by the flame.

Because of the **heat losses** (difficult to estimate), the experimental **temperature profile** is used as **input** in numerical simulations of burner-stabilized flames.

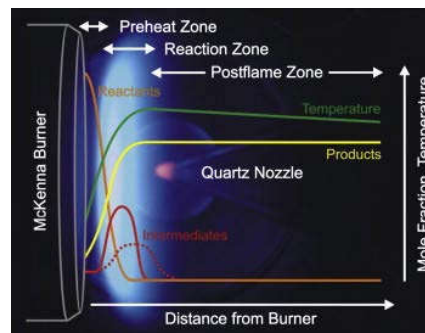
The **energy conservation equation is not included** in the system of equations.

Simulations using assigned and calculated temperature profiles provide indications of heat losses to the burner and to the environment (conductive and radiative).



http://www.danielipineda.com/Daniel_I._Pineda_files/FlatFlame_Syngas_Poster.pdf

Flame structure

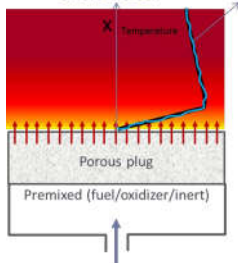


Photograph and schematic structure of a premixed, laminar, low-pressure flat flame. A widespread reaction (luminous) flame zone and the quartz nozzle used for molecular-beam sampling are seen as well

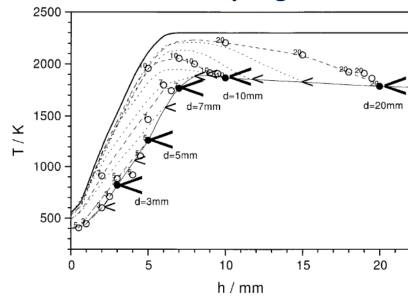
Hansen et al., PECS 35(2) 2009

Measurements uncertainty

Smoothed experimental temperature profiles are used in calculations to avoid artificial gradients and numerical difficulties.



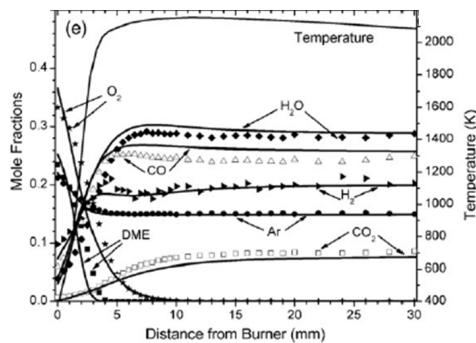
Effects of a Sampling Quartz Nozzle



Solid line: measurements in unperturbed flame [16];
 circles: measurements with nozzle, positions d indicated with bold symbols;
 thin solid line: line connects measurements with $h = 5d$ (solid circles);
 dotted lines: interpolation between measurements at fixed d with h varied (h, d), each dotted line represents a "complete profile" (CP) at given d .

Hartlieb et al., *Combust. Flame*, 2000, 121:610–624

Measurement shift



SHIFT: the "distance from burner" for recorded mole fractions is taken to be 0.9 mm less than the actual separation between the burner and the tip of the sampling cones. This displacement of the data gives good agreement between positions of the maximum mole fraction or key intermediates.

Wang et al., *Phys. Chem. Chem. Phys.*, 2009

A shift is usually required to account that the probe samples gases slightly upstream of the sampling cone orifice and to account for the cooling of the flame by the sampling nozzle.

Experimental mole-fraction profiles are usually shifted by $\sim 1.0 \div 3.0$ mm toward the burner surface for low pressure flames (< 100 mbar).

This shift can be reduced if a disturbed temperature profile is used in simulations

The complex flame disturbances by the sampling cone can be approximated by the use of a disturbed temperature profile, representing the temperature of the sampled gas at each probed position

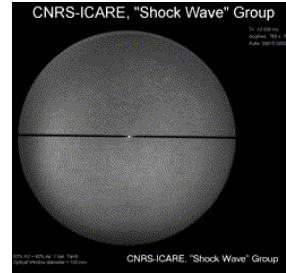
Struckmeier et al., *ZEITSCHRIFT FÜR PHYSIKALISCHE CHEMIE* 223(4-5): 503–537 2009.

Laminar burning velocity

Laminar burning velocity or **laminar flame speed** (s_L) is an intrinsic characteristic of fuels. It measures the velocity at which a planar flame propagates into quiescent unburned mixture at a specified pressure and temperature.

A fuel with a higher laminar burning velocity is expected to show faster combustion in turbulent conditions too (like in an engine).

A quite common way to measure s_L is the so called spherical bomb, which is a spherical vessel with optical access. The fuel is generally ignited by central sparks. The chamber volume should be large enough to minimize wall effects. Possible stretch effects, leading to considerable and systematic errors, must be carefully considered

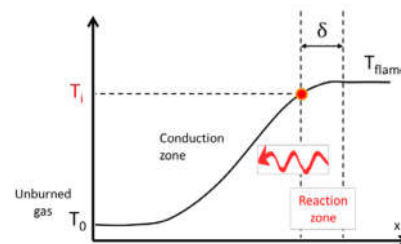


Spherical Bomb at ICARE – CNRS Orleans
<https://icare.cnrs.fr/en/en-research/en-facilities/en-ct-spherical-bombs/en-ct-spherical-bomb-2/>

Simplified approach

Mallard and Le Chatelier in 1883 developed a “**Two zones**” theory of a laminar, premixed flame. The flame is divided into a preheat region (conduction zone) and a burning region (reaction zone) of thickness δ (laminar flame thickness).

In order for the flame to be self-sustaining, the amount of heat conducted from the burning zone must be sufficient to raise the temperature of the unburned fuel/air mixture to its ignition temperature (T_i). Thus, they theorized that in the conduction zone the gases are heated from their initial temperature, T_0 , to T_i , by heat from the combustion reaction. The excess energy released from the combustion further raises the temperature of the gases from T_i to the flame temperature T_f .



They linearized the temperature change in reaction zone and by setting the sensible heat necessary to raise the unburned gases from T_0 to T_i equal to the heat conducted from the flame into the conduction zone. The energy balance then is given by

$$\dot{m}c_p(T_i - T_0) = \lambda \frac{(T_f - T_i)}{\delta} A \quad \lambda \text{ is the thermal conductivity}$$

Pressure effect

the mass flow rate in the preheat region is given by

$$\dot{m} = \rho s_L A$$

The flame thickness is given by the flame speed times some measure of the reaction time.

This reaction time is given by the inverse of the reaction rate

$$\delta = s_L / R^* \quad R^* \text{ is an apparent combustion rate at } T_i$$

$$\rho s_L c_p (T_i - T_0) = \lambda \frac{(T_f - T_i)}{s_L} R^* \Rightarrow s_L = \sqrt{\alpha R^* \frac{(T_f - T_i)}{(T_i - T_0)}} \quad \alpha = \frac{\lambda}{\rho c_p} \text{ is the thermal diffusion}$$

$$R^* = \frac{dx_i}{dt} = k \frac{c_i^n}{c} = k \frac{x_i^n c^n}{c} = k x_i^n c^{n-1} = k^* x_i^n p^{n-1}$$

$$s_L \propto \sqrt{\frac{p^{n-1}}{\rho}}$$

$$s_L \propto \sqrt{p^{n-2}}$$

For 2nd order reactions, laminar flame speed is not affected by pressure

$$s_L = \sqrt{\alpha R^* \frac{(T_f - T_i)}{(T_i - T_0)}} \cong \sqrt{\alpha R^*} \Rightarrow R^* \cong \frac{s_L^2}{\alpha} \Rightarrow \delta = \frac{s_L}{R^*} \cong \frac{\alpha}{s_L} \quad \text{Higher laminar flame speed lower the flame thickness}$$

Premixed 1D flames: laminar flame speed

$$\text{Inlet } x = 0 \quad \begin{cases} T = T_0 \\ \rho v \omega_k + \rho V_k \omega_k = (\rho v \omega_k)_0 \end{cases}$$

vanishing gradients are imposed at the hot boundary

$$\text{Outlet } x = L \quad \begin{cases} \frac{dT}{dx} = 0 \\ \frac{d\omega_k}{dx} = 0 \quad k = 1, \dots, N_S \end{cases}$$

Danckwerts boundary conditions

The length of the computational domain should be sufficient to ensure the physical meaning of these boundary conditions.

For a freely propagating flame the mass flow rate (i.e. S_L) is an eigenvalue of the system and must be determined as a part of the solution [Smooke et al., CST 1983].

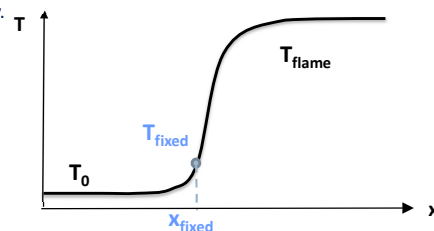
Therefore, an additional constraint is required and it is possible to **fix the temperature at one point**.

This is sufficient to allow for the solution of the flame speed eigenvalue.

It is important to fix this point in such a way that the gradients tend to vanish at the inlet. Otherwise, the calculated S_L will be affected by heat loss at the boundary.

$$\frac{d(\rho v)}{dx} \Big|_{x=0} = 0$$

$$T(x_{\text{fixed}}) = T_{\text{fixed}}$$



Premixed 1D flames: laminar flame speed

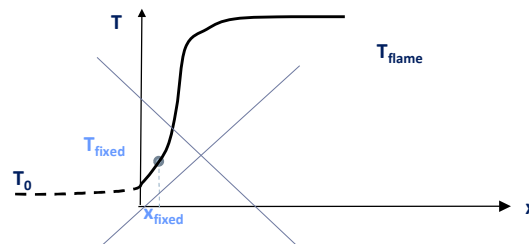
$$\begin{aligned} \text{Inlet } x=0 & \begin{cases} T = T_0 \\ \rho v \omega_k + \rho V_k \omega_k = (\rho v \omega_k)_0 \end{cases} \\ \text{Outlet } x=L & \begin{cases} \frac{dT}{dx} = 0 \\ \frac{d\omega_k}{dx} = 0 \quad k = 1, \dots, N_S \end{cases} \end{aligned}$$

Danckwerts boundary conditions

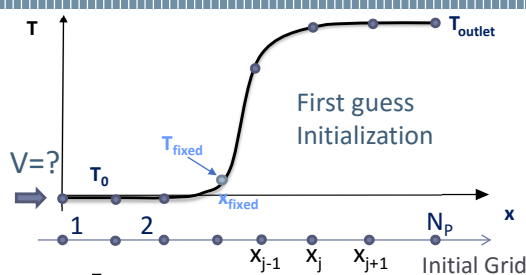
The length of the computational domain should be sufficient to ensure the physical meaning of these boundary conditions.

It is important to fix this point in such a way that the T gradients tend to vanish at the inlet. Otherwise, the calculated S_L will be affected by heat loss at the boundary.

$$\begin{aligned} \frac{d(\rho v)}{dx} \Big|_{x=0} &= 0 \\ T(x_{\text{fixed}}) &= T_{\text{fixed}} \end{aligned}$$



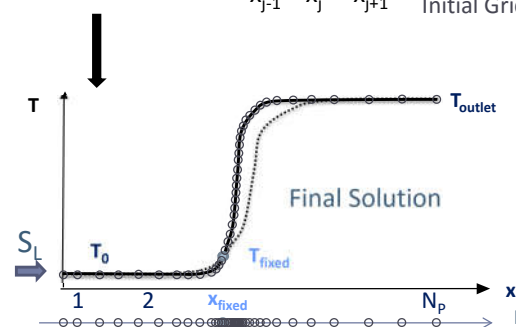
Premixed 1D flames: laminar flame speed



Problem initialization:

the user specifies:

- the fixed temperature (e.g. T_0+20)
- the points of the initial grid (a few grid points: e.g. $N_p \approx 10$).
- a S-shaped temperature profile is given, using an estimated T_{outlet} (e.g. adiabatic flame temperature).



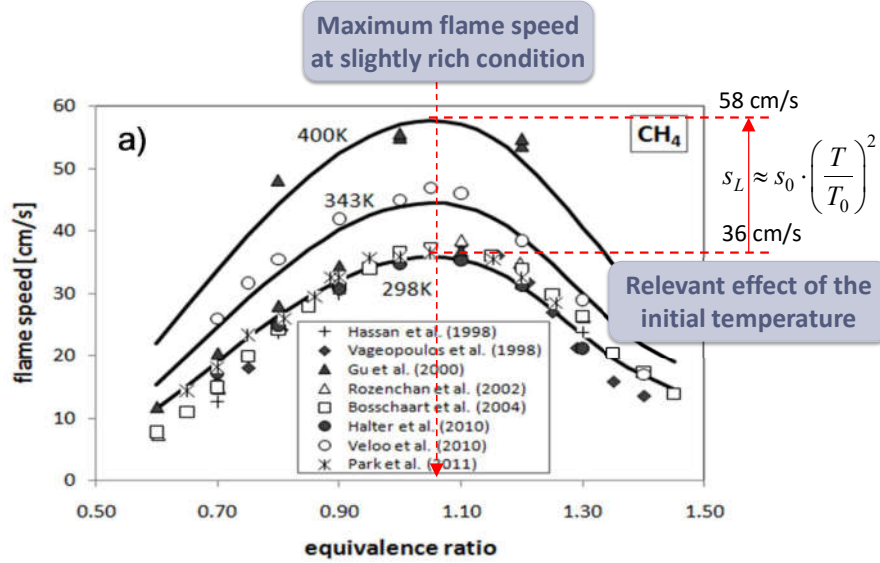
Solution procedure:

-the grid is refined with a careful attention especially to the flame front, where significant gradients are present.

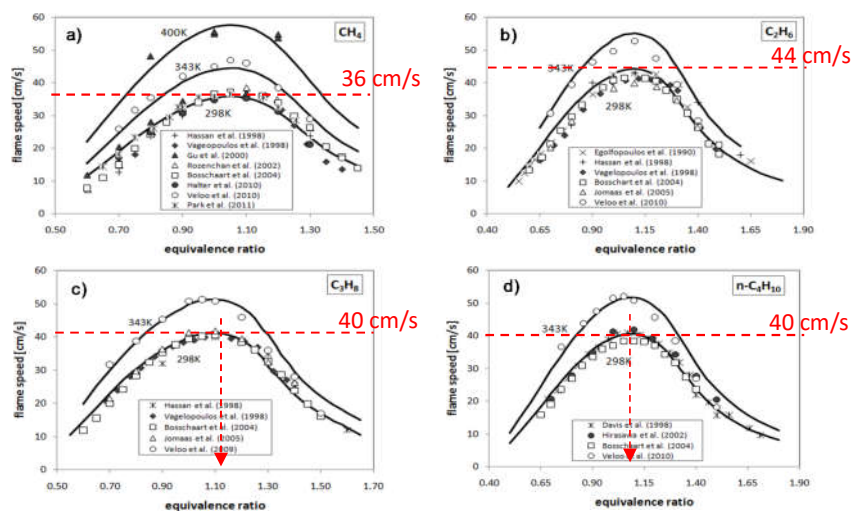
-The value of the fresh charge inlet velocity is the unstretched LFS

Final Grid: $N_p > 100-300$ points

Laminar Flame speed of CH₄



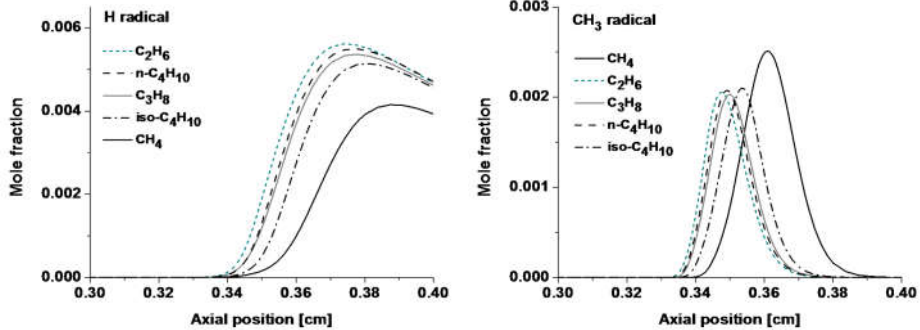
Laminar Flame Speeds of Small Alkanes



Ethane and methane have the highest and lowest flame speeds, respectively.

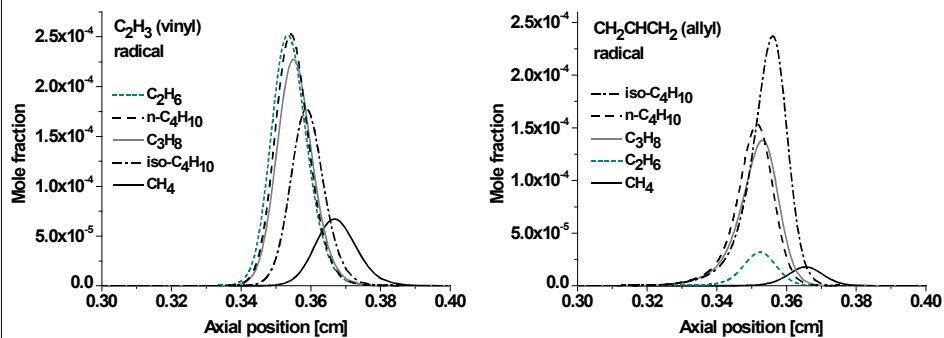
Ranzi et al., 2012 PECS, 38(4), 468-501.

Laminar Flame Speeds of Small Alkanes



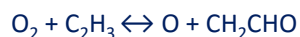
Laminar air-stoichiometric flames of small hydrocarbons ($T_0=298$ K, $P=1$ atm).
1- Predicted profiles of relevant radicals: H, CH_3

Laminar Flame Speeds of Small Alkanes



Laminar air-stoichiometric flames of small hydrocarbons ($T_0=298$ K, $P=1$ atm).
2 - Predicted profiles of relevant radicals: Vinyl, Allyl.

Vinyl and Allyl radicals further contribute in explaining the different combustion rates:

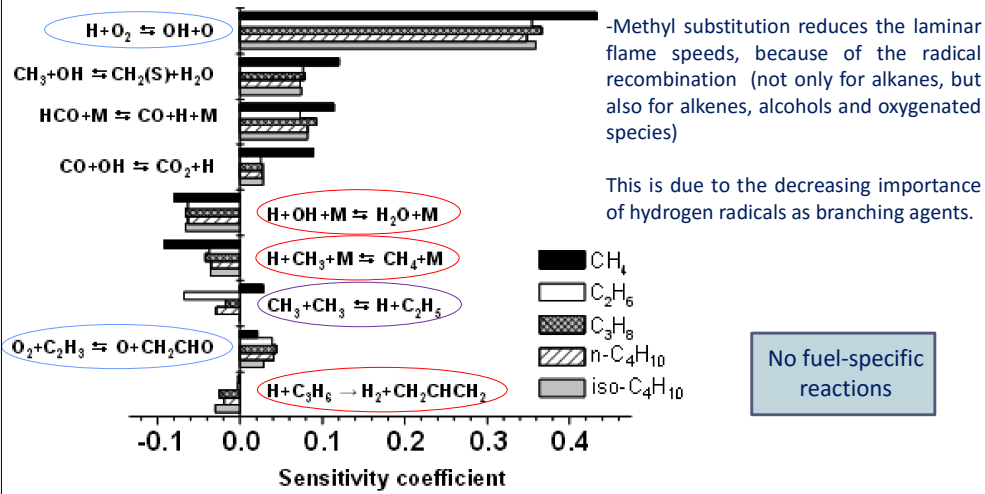


Branching reaction



Recombination reaction

Laminar Flame Speeds of Small Alkanes

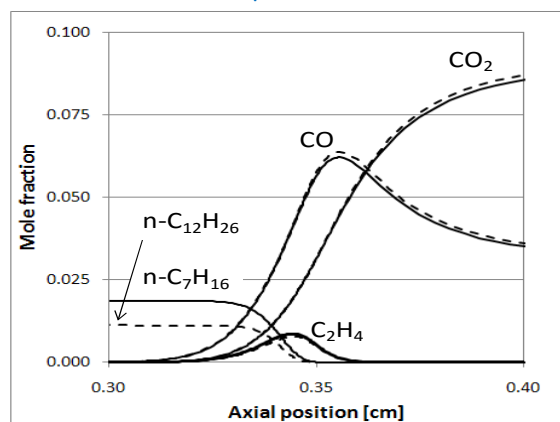


Sensitivity coefficients of laminar flame speed on reaction rate coefficients, for small alkanes/air flames at $\Phi=1$, $T=298$ K and atmospheric pressure.

Ranzi et al., 2012 PECS, 38(4), 468-501.

Laminar Flame Speeds of Large Alkanes

Similarity of structures of air-stoichiometric n-heptane and n-dodecane flames.

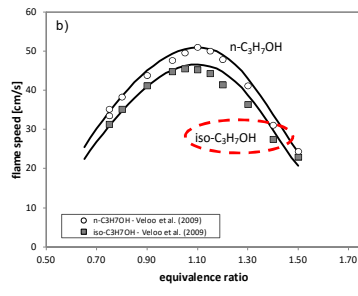
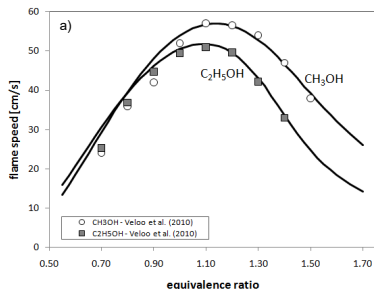


The laminar flame speeds of n-alkanes larger than C_3-C_4 , as well as their flame structures, are very similar and mainly depend on the C_0-C_4 sub mechanism.

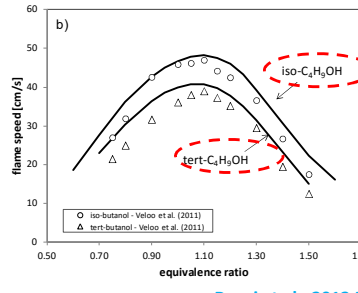
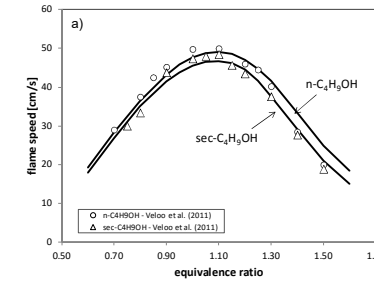
Pyrolysis first

Ranzi et al., 2012 PECS, 38(4), 468-501.

Laminar Flame Speeds of Alcohols



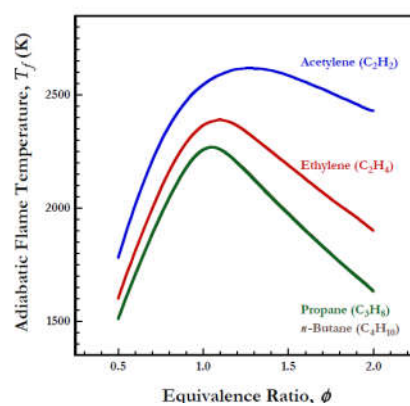
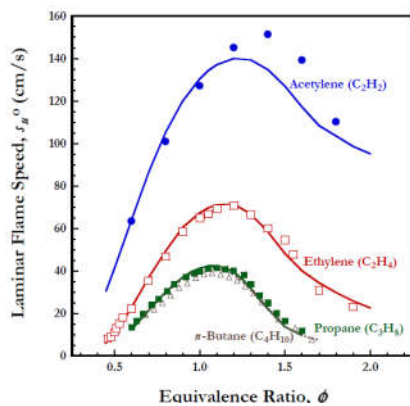
Air
T = 343 K
P = 1 atm



Ranzi et al., 2012 PECS, 38(4), 468-501.

Flame speeds and adiabatic flame temperatures

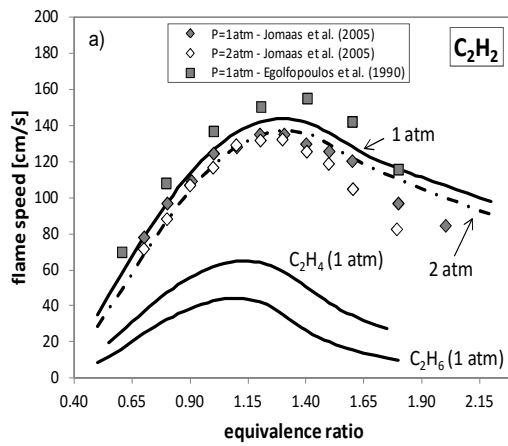
Variation of laminar flame speeds and adiabatic flame temperatures at the atmospheric pressure as a function of the equivalence ratio.



Flame speeds follow a dependence on fuel equivalence ratios in a fashion similar to that between adiabatic flame temperatures and fuel equivalence ratios.

H. Wang (2015)

Flame speeds and adiabatic flame temperatures



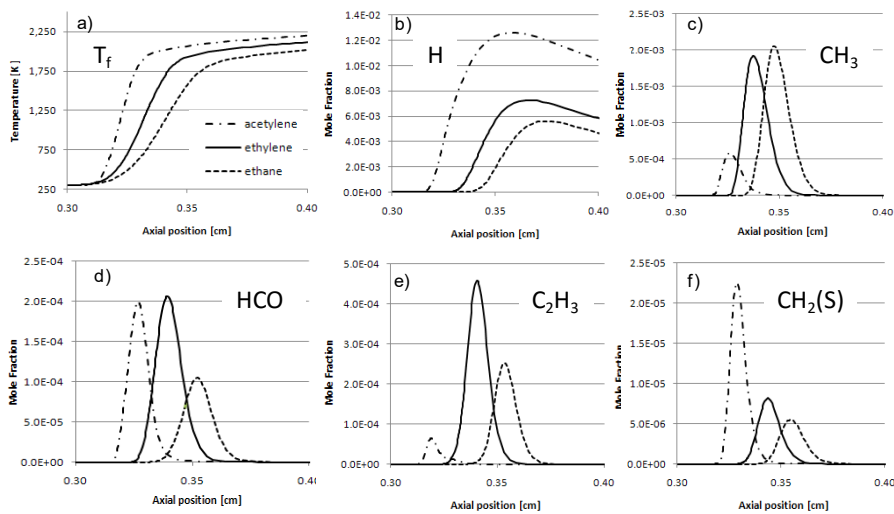
Adiabatic flame temperatures

$C_2H_2 \sim 2550\text{ K}$
 $C_2H_4 \sim 2375\text{ K}$
 $C_2H_6 \sim 2270\text{ K}$

Is it just an effect of the T?

Ranzi et al., 2012 PECS, 38(4), 468-501.

Flame speeds and radicals

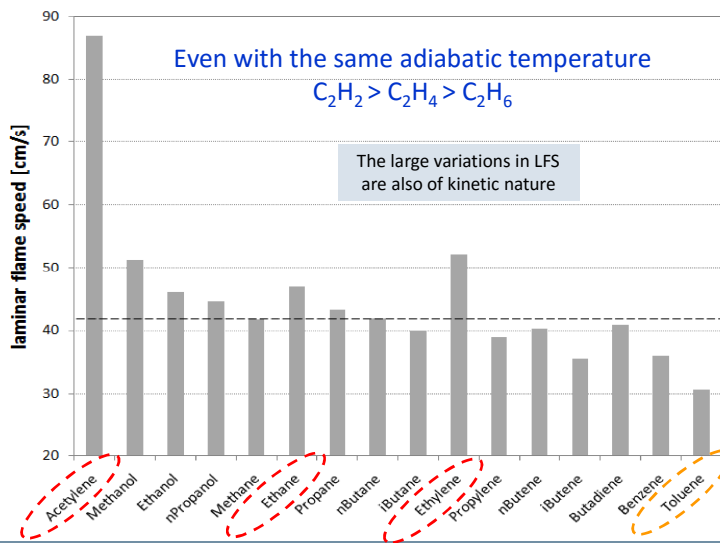


Flame structure and radical profiles at 1 atm and 298 K

Ranzi et al., 2012 PECS, 38(4), 468-501.

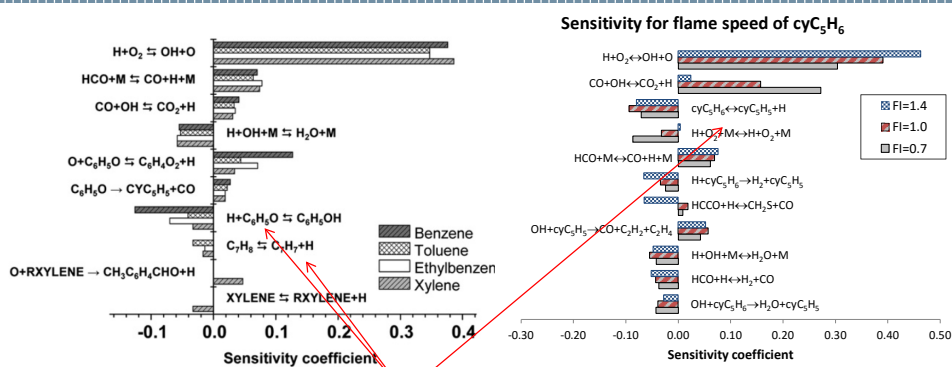
Flame speeds at fixed temperature

Laminar speeds of atmospheric and stoichiometric flames of various fuels at $T_{\text{flame}}=2300\text{ K}$, calculated by modifying heat capacity of N_2



Ranzi et al., 2012 PECS, 38(4), 468-501.

Flame speed: role of Resonantly stabilized radicals



Role of resonantly-stabilized radicals: recombination with H-atoms, which diffuse back from the flame front, greatly affects, reducing, the flame speed.

Fuel-specific reactions are mainly related to the phenoxy as well as the resonantly stabilized radicals. This explains why $S_L(300\text{K}) \approx 40\text{ cm/s}$ for benzene and $S_L(300\text{K}) \approx 35\text{ cm/s}$ for toluene.

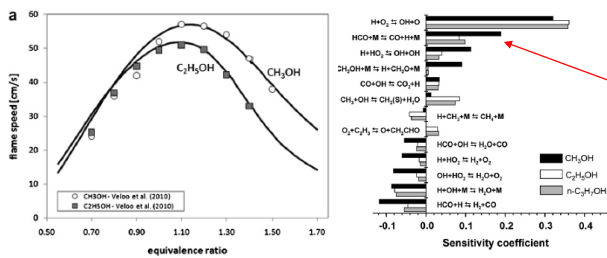
Ranzi et al., 2012 PECS, 38(4), 468-501.

Flame speed kinetics

Detailed chemistry needs to be validated over a wide range of experimental conditions to be predictive. LFS emphasize the role of HT combustion and mainly:

- thermochemistry (exothermicity)
- diffusivity
- some fuel specific reactions

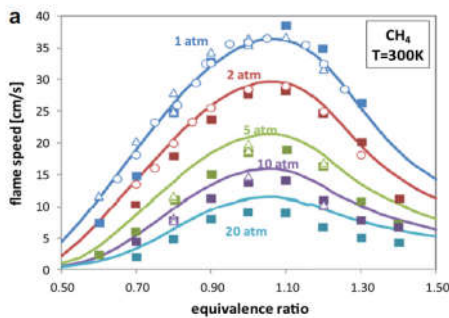
Essentially, the results are mainly dependent on the CO-C4 sub-mechanism, but some fuel specific reactions are important. (Example resonantly stabilized radicals, CH₃OH ecc.)



The difference in the laminar flame speeds of methanol with those of the heavier alcohols is mainly due to kinetics instead of the different adiabatic flame temperatures.

H abstraction reactions on methanol form CH₂O (then HCO) without significant CH₃ radical formation.

Flame speed: pressure effect



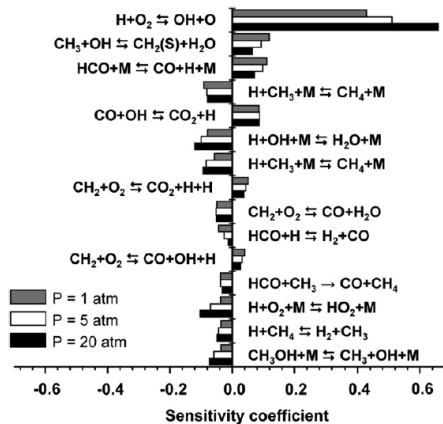
$$S_L = S_{L0} \left(\frac{T}{T_0}\right)^\alpha \left(\frac{p}{p_0}\right)^\beta$$

$$\alpha \approx 1.5 \div 2$$

$$\beta \approx -0.5 \div -0.25$$

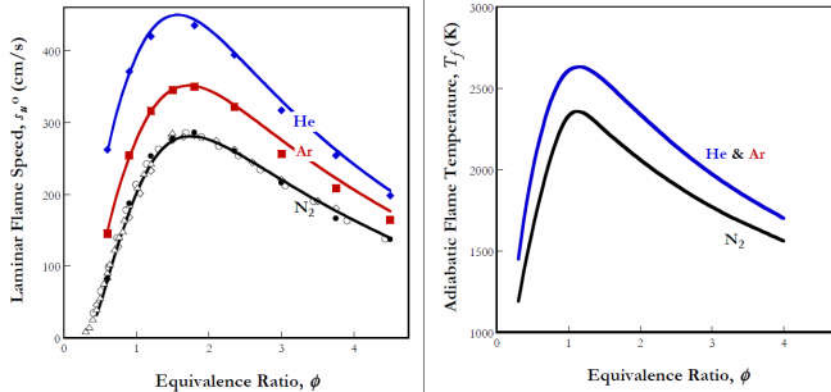
LFS decreases with a pressure power of about -0.5 ÷ -0.3, in relative good agreement with Mallard and Le Chatelier law:

$$S_L \propto \sqrt{p^{n-2}} \implies \beta = \frac{n}{2} - 1$$



Flame speed: thermal diffusivity effect

Hydrogen-Air like mixtures, in which the nitrogen is replaced by helium (He) and argon (Ar). Monoatomic gases (He and Ar) have small specific heats, therefore their adiabatic flame temperature is higher than that of the H_2 -air mixture. Likewise the flame speed of He and Ar substituted mixtures is larger than that of Air mixtures.

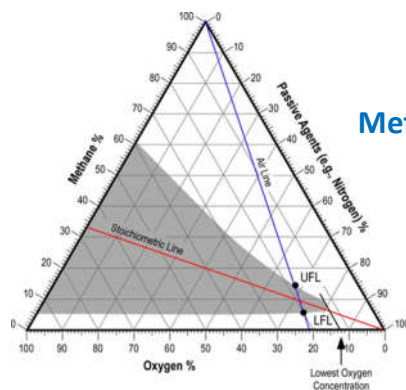


The flame speed of He mixture is larger than that of Ar mixture, despite the same adiabatic flame temp. Differences in flame speeds are caused by the smaller mass density of He and consequently by the larger thermal diffusivity of $H_2/O_2/He$ mixtures.

Flammability Limits

Very rich combustible mixtures with excess of fuel, or a very lean mixtures with excess of oxidizer are nonflammable. The limit compositions defining combustible and noncombustible mixtures are called the Flammability limits.

For a system at given temperature and pressure, these limits are the **lean**, or lower flammability limit (**LFL**) and the **rich**, or upper flammability limit (**UFL**).



Methane Flammability Limits (@ STP)

http://cfbt-us.com/wordpress/wp-content/uploads/2009/04/methane_flammability_diagram_sr.jpg

Flammability Limits for gas

	Lower flammability limit (L) ^a			$\frac{L}{C_u}$	Upper flammability limits (U) ^a		$\frac{U}{C_u}$	S_u^b (m/s)	Minimum ignition energy ^b (mJ)	Minimum quenching distance ^b (mm)
	% Vol	g/m ³	kJ/m ³		% Vol	g/m ³				
Hydrogen	4.0 ^c	3.6	435	0.13	75	67	2.5	3.2	0.01	0.5
Carbon monoxide	12.5	157	1591	0.42	74	932	2.5	0.43	—	—
Methane	5.0	36	1906	0.53	15	126	1.6	0.37	0.26	2.0
Ethane	3.0	41	1952	0.53	12.4	190	2.2	0.44	0.24	1.8
Propane	2.1	42	1951	0.52	9.5	210	2.4	0.42	0.25	1.8
n-Butane	1.8	48	2200	0.58	8.4	240	2.7	0.42	0.26	1.8
n-Pentane	1.4	46	2090	0.55	7.8	270	3.1	0.42	0.22	1.8
n-Hexane	1.2	47	2124	0.56	7.4	310	3.4	0.42	0.23	1.8
n-Heptane	1.05	47	2116	0.56	6.7	320	3.6	0.42	0.24	1.8
n-Octane	0.95	49	2199	0.58	—	—	—	—	—	—
n-Nonane	0.85	49	2194	0.58	—	—	—	—	—	—
n-Decane	0.75	48	2145	0.56	5.6	380	4.2	0.40	—	—
Ethene	2.7	35	1654	0.41	36	700	5.5	>0.69	0.12	1.2
Propene	2.4	46	2110	0.54	11	210	2.5	0.48	0.28	—
Butene-1	1.7	44	1998	0.50	9.7	270	2.9	0.48	—	—
Acetylene	2.5	29	1410	—	(100)	—	—	1.7	0.02	—
Methanol	6.7	103	2141	0.55	36	810	2.9	0.52	0.14	1.5
Ethanol	3.3	70	1948	0.50	19	480	2.9	—	—	—
n-Propanol	2.2	60	1874	0.49	14	420	3.2	0.38	—	—
Acetone	2.6	70	2035	0.52	13	390	2.6	0.50	1.1	—
Methyl ethyl ketone	1.9	62	1974	0.52	10	350	2.7	—	—	—
Diethyl ketone	1.6	63	2121	0.55	—	—	—	—	—	—
Benzene	1.3	47	1910	0.48	7.9	300	2.9	0.45	0.22	1.8

^a Data from Zabetakis (1965). Mass concentration values are approximate and refer to 0°C ($L(g/m^3) \approx 0.45 M_u L$ (vol %)).

^b Data from various sources including Kanury (1975) and Lees (1996). There is uncertainty with some of these data (Harris, 1983; Lees, 1996).

Dydale, D. *An introduction to fire dynamics*. John Wiley & Sons, 2011.

flammability limits: pressure and temperature effect

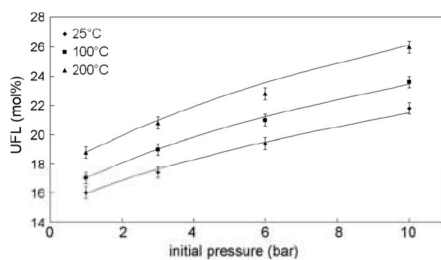


Fig. 7. Comparison of the experimentally determined upper flammability limit (markers) [10] and the pressure dependence estimated based upon the limiting burning velocity approach (solid lines) for methane/air flames.

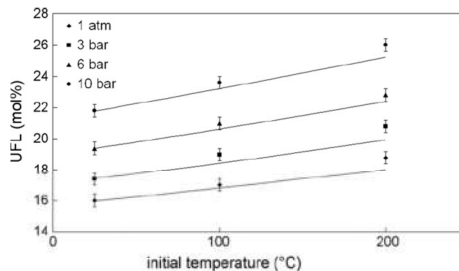
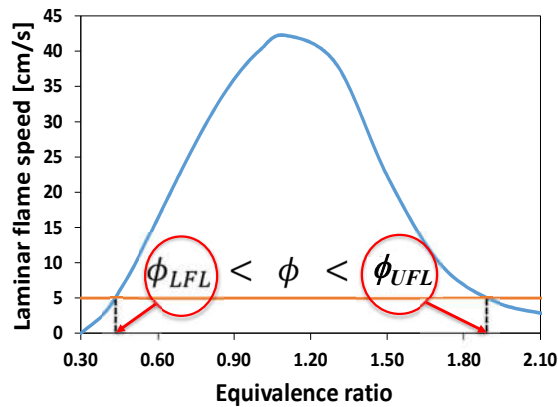


Fig. 8. Comparison of the experimentally determined upper flammability limit (markers) [10] and the temperature dependence estimated based upon the limiting flame temperature approach (solid lines) for methane/air flames.

Van den Schoor et al., *Journal of Hazardous Materials*, 2008, 153, 1301-1307

flammability limits and laminar flame speed



At some point, the laminar flame speed is so low, that combustion cannot be sustained. The equivalence ratios at which this occurs correspond to the lower and upper flammability limits

Radiation correction

Flame speed method has the advantage to model the **quenching** effect of the chamber walls. This is achieved through the insertion of a semi-empirical **radiation term** into the energy transport equation. The latter term rests on the assumption of **optically thin gas** and on the radiative properties of **CO₂, CO, H₂O** and **soot**.

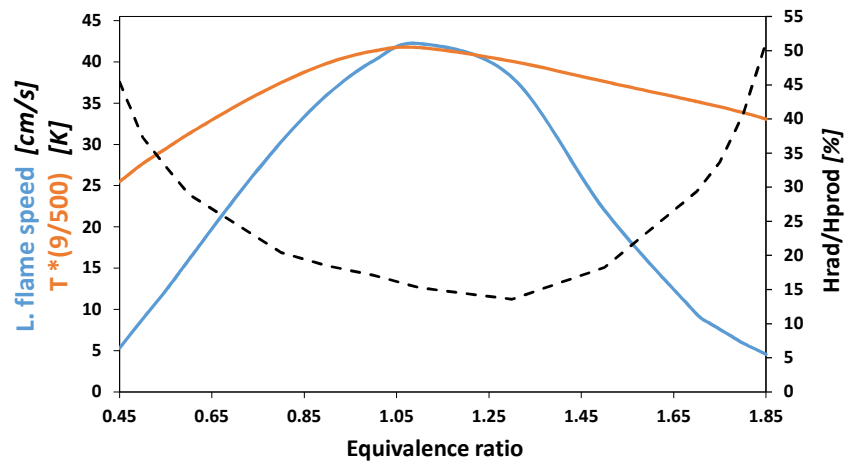
$$Q_{rad} = 4\sigma \left[\sum_{i=1}^n (p_i a_{p,i} + \delta) (T^4 - T_b^4) \right]$$

Widmann Emissivity Model

$\delta = 2370 f_{v,soot} T$ [1/m]

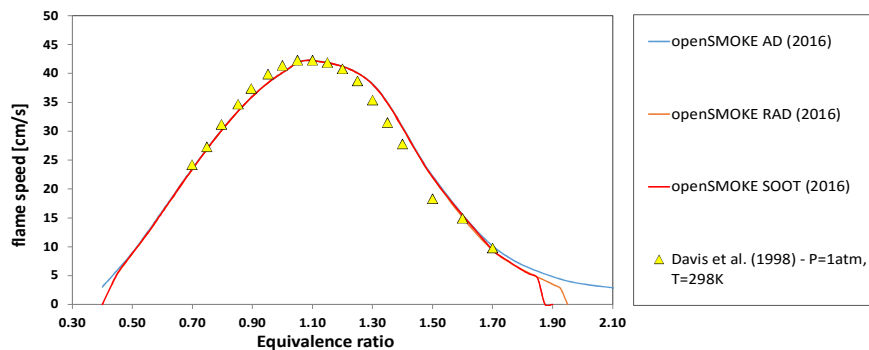
Gas Emissivities:
Calculated as a polynomial function of the Temperature [1/(m · atm)]

Radiation importance

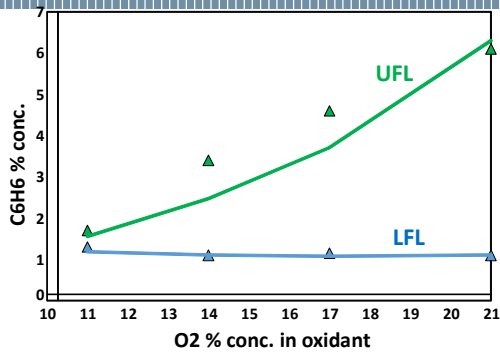


Laminar flame speed extrapolation

Assumption: if the kinetic mechanism is able to reproduce laminar flame speed when $\phi=1$, also reactivity near the limits will be well represented.

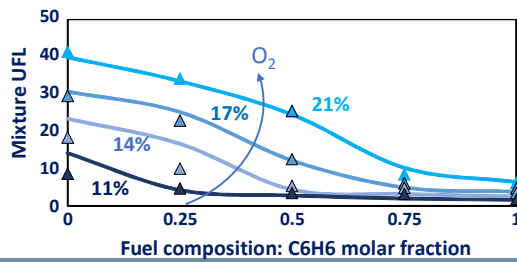


Flammability limit predictions



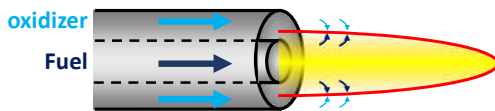
Benzene

Benzene/methanol mixture



Chang et al., Korean Journal of Chemical Engineering volume 22, pages803–812 (2005)

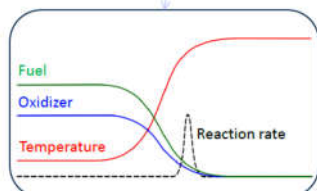
Diffusive flames



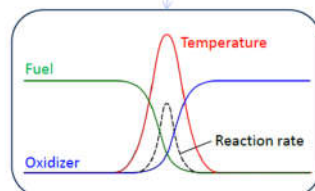
Typical industrial flames are **not premixed**. Fuel and oxidizer are independently fed and diffuse to the flame front



Premixed flames have an assigned equivalence ratio, while in diffusive flames $0 \leq \phi \leq \infty$



Structure of a premixed flame (schematic)



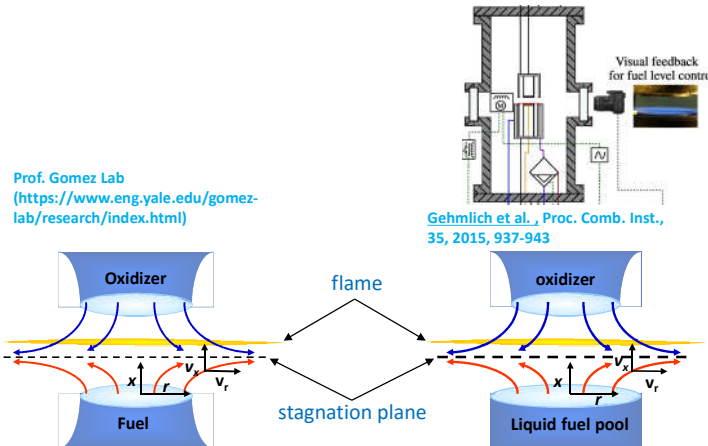
Structure of a diffusion flame (schematic)

Courtesy prof. Pirtsch

Planar counter flow flames

Counterflow diffusion flames represent a 1D diffusion flame structures.

If flow velocities of both streams can be assumed sufficiently large and sufficiently removed from the stagnation plane, the flame is embedded between two potential flows, one coming from the oxidizer and one from the fuel side.



Prof. Gomez Lab
(<https://www.eng.yale.edu/gomez-lab/research/index.html>)

Gehrmlich et al., Proc. Comb. Inst., 35, 2015, 937-943

Model equations

Problem is intrinsically 2D, but 3 assumptions reduce it to 1D

1. Similarity assumption for velocity $v_r = G(x)r$
2. Similarity assumption $p = p_0 - \frac{1}{2}p'r^2 + F(x)$
3. Composition and temperature have no radial dependence close to centerline

$$\rho v_x \frac{d\omega_i}{dx} = -\frac{dj_{i,x}}{dx} + \dot{r}_i$$

$$\frac{d}{dx}(\rho v_x) + 2\rho G = 0$$

$$\rho G^2 + \rho v_x \frac{dG}{dx} = p' + \frac{d}{dx} \left(\mu \frac{dG}{dx} \right)$$

$$\rho v_x c_p \frac{dT}{dx} = \frac{d}{dx} \left(\lambda \frac{dT}{dx} \right) - \sum_{i=1}^n h_i \dot{r}_i - \sum_{i=1}^n c_{p,i} j_{i,x} \frac{dT}{dx}$$

Boundary conditions

Fuel side ($x = 0$)

$$\rho v_x \omega_i + \rho v_{diff} \omega_i = \rho v_x \omega_i \Big|_F$$

$$v_x = v_{x,F}$$

$$G = \frac{dv_r}{dr} \Big|_{F,r=0}$$

$$T = T_F$$

Oxidizer side ($x = L$)

$$\rho v_x \omega_i + \rho v_{diff} \omega_i = \rho v_x \omega_i \Big|_O$$

$$v_x = v_{x,O}$$

$$G = \frac{dv_r}{dr} \Big|_{O,r=0}$$

$$T = T_O$$

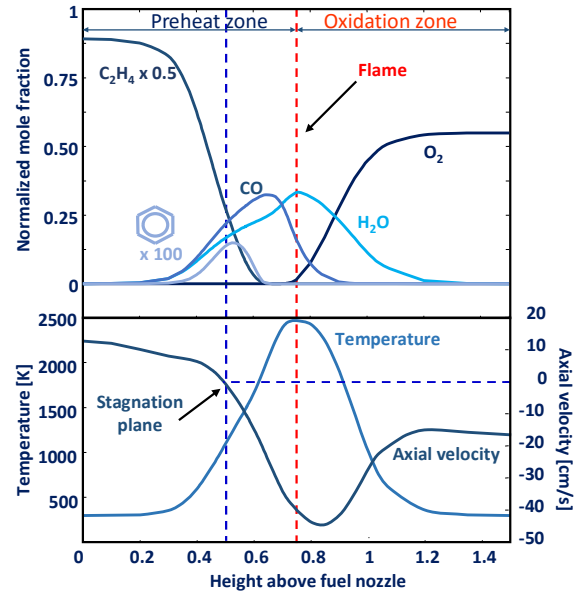
Flame structure

Rich part of the diffusion flame corresponds to the upstream preheat zone of the premixed flame

Pyrolysis products are formed in the rich part of the flame and peak at the stagnation plane

Flame, temperature peak, and main product maxima correspond to the stoichiometric conditions

Lean part corresponds to the downstream oxidation layer of the premixed flame

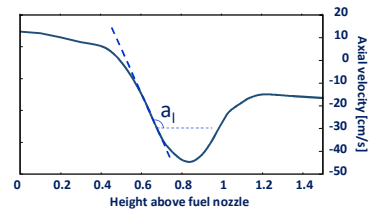


Strain rate

Strain rate is representative of the residence time of reactants in the reaction, or better of the reciprocal of the residence time. In a counter-flow laminar diffusion flame, the aerodynamic strain rate is defined in terms of the gradient of the axial velocity component, $\partial v_x / \partial x$. The convention within literature is to express the local strain rate as:

$$a_l = \left. \frac{dv_x}{dx} \right|_{max} \quad [s^{-1}]$$

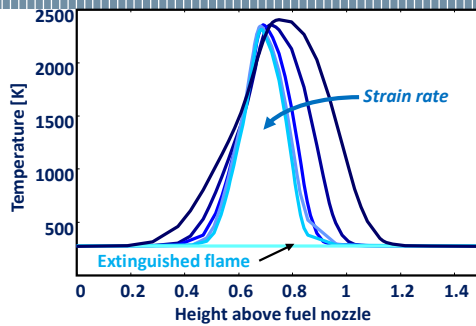
The maximum velocity gradient is just prior to the thermal mixing layer of the flame on either the air or fuel side, depending on the location of the flame with respect to the stagnation plane



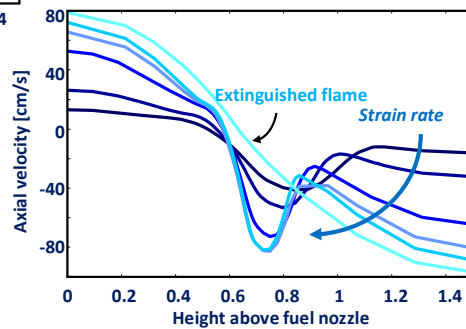
When no measures of the local strain rate are available, it can be approximated by the global strain rate (Seshadri and Williams, 1978):

$$a_g = a = \frac{2v_{x,0}}{L} \left(1 + \frac{v_{x,F}\sqrt{\rho_F}}{v_{x,0}\sqrt{\rho_O}} \right)$$

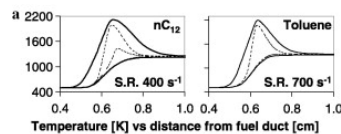
Strain rate effect



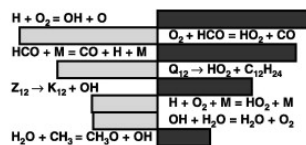
Increasing the strain rate, velocity and temperature profile change up to when the 'residence time' is so low that the flame extinguishes



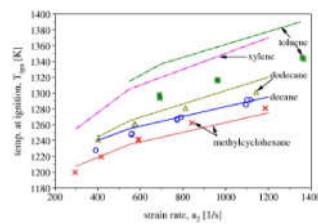
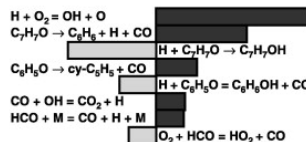
Autoignition and extinction



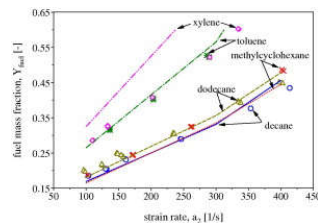
Sensitivity analysis at conditions close to autoignition for **n-dodecane**
 $(T_2 = 1240 \text{ K}, a = 400 \text{ s}^{-1}, Y_{F,1} = 0.3)$



Sensitivity analysis at conditions close to autoignition for **toluene**
 $(T_2 = 1325 \text{ K}, a = 700 \text{ s}^{-1}, Y_{F,1} = 0.3)$

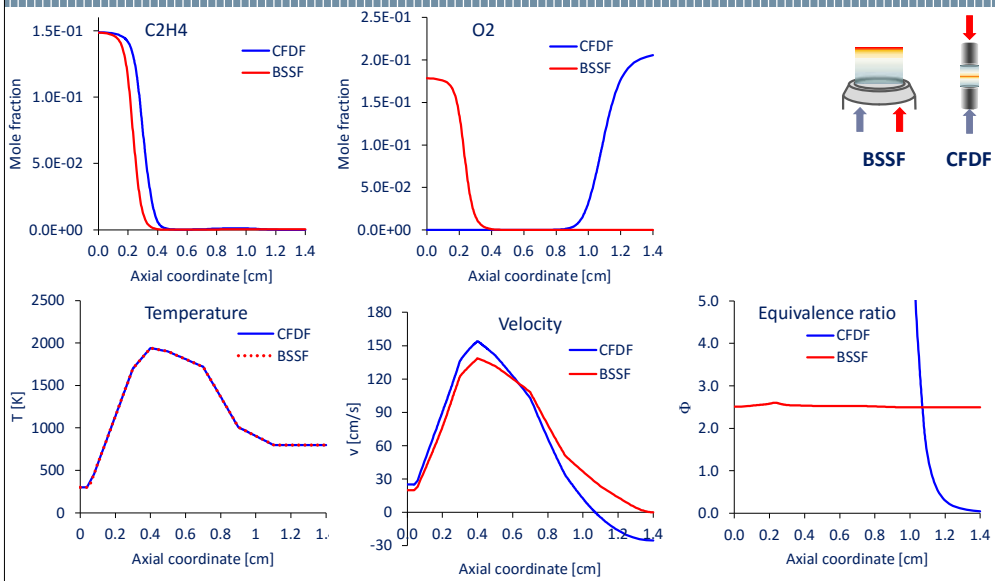


The temperature of the oxidizer stream at autoignition at fixed values of the mass fraction of fuel in the fuel stream $Y_{F,1} = 0.3$.

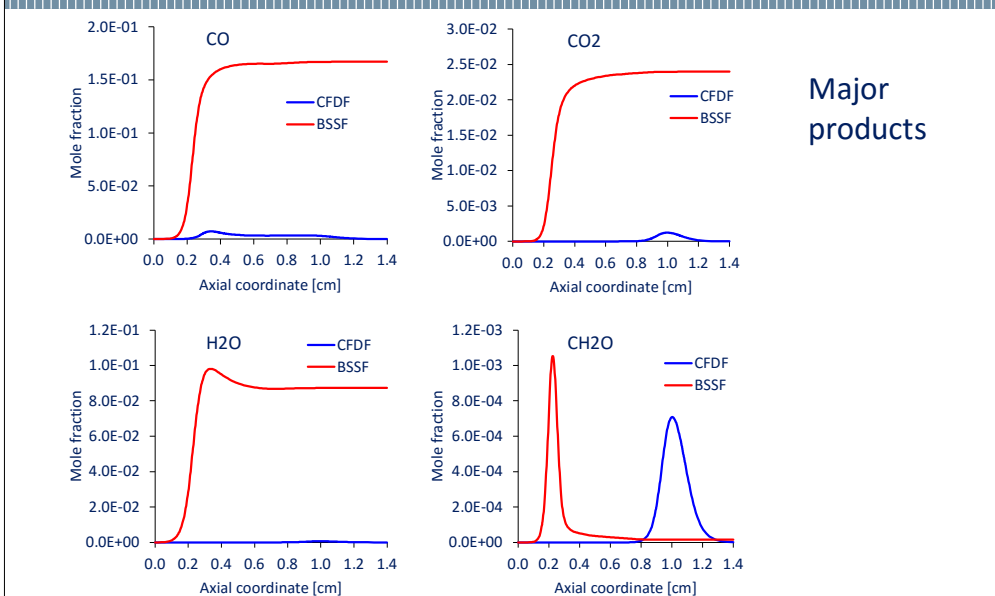


The mass fraction of fuel as a function of the strain rate at extinction.

Ethylene rich premixed and counter flow flames

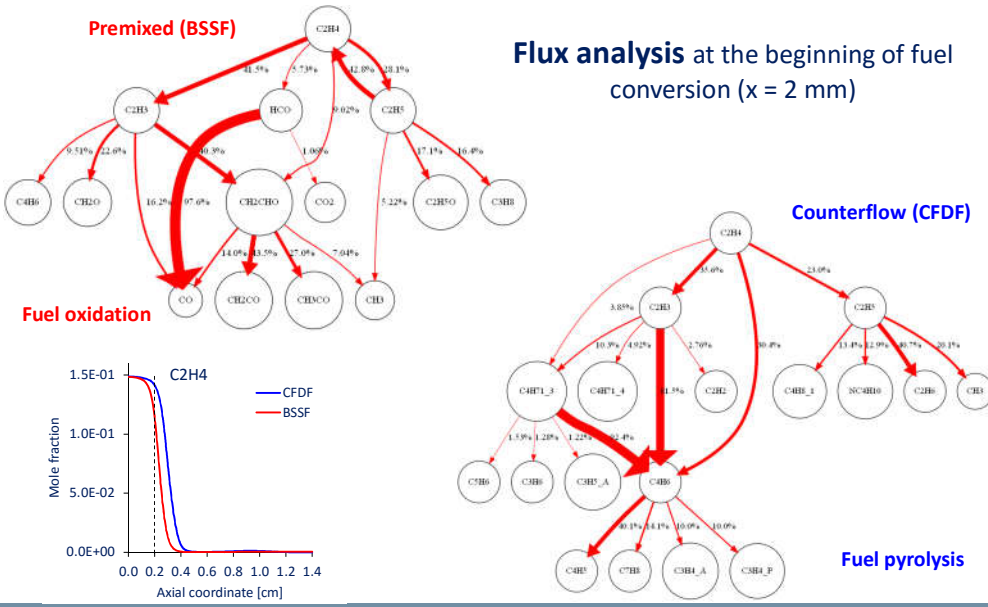


Ethylene rich premixed and counter flow flames

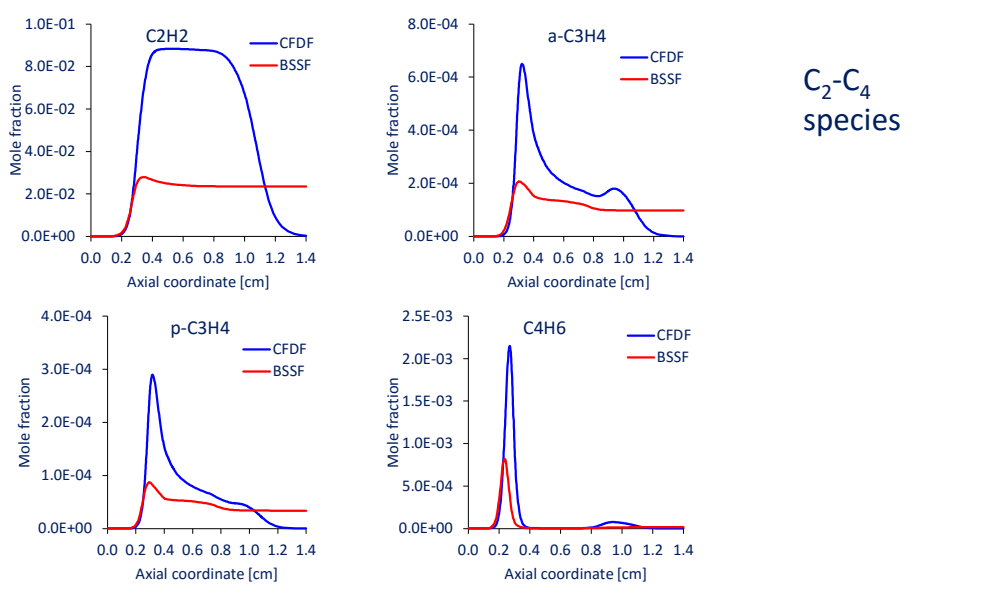


Major products

Ethylene rich premixed and counter flow flames

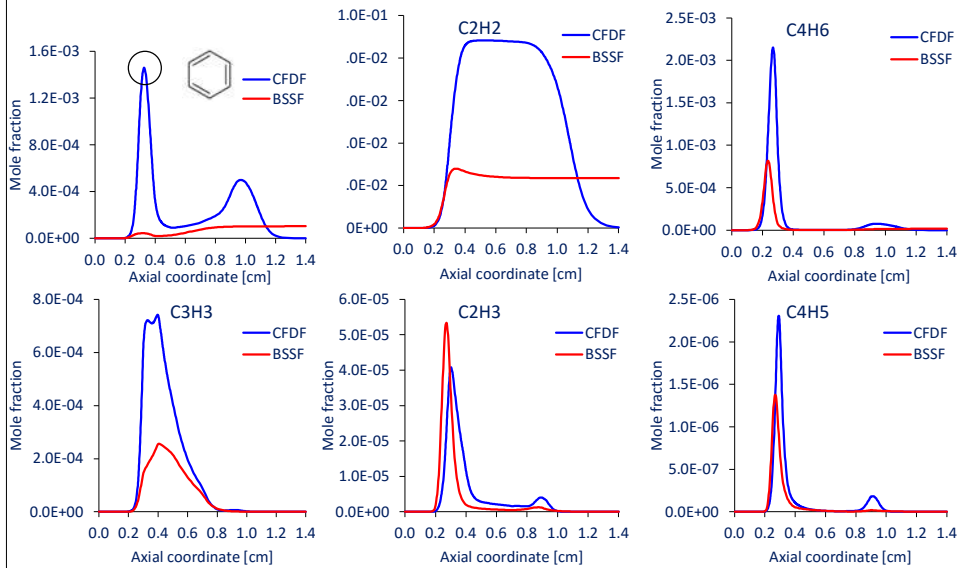


Ethylene rich premixed and counter flow flames



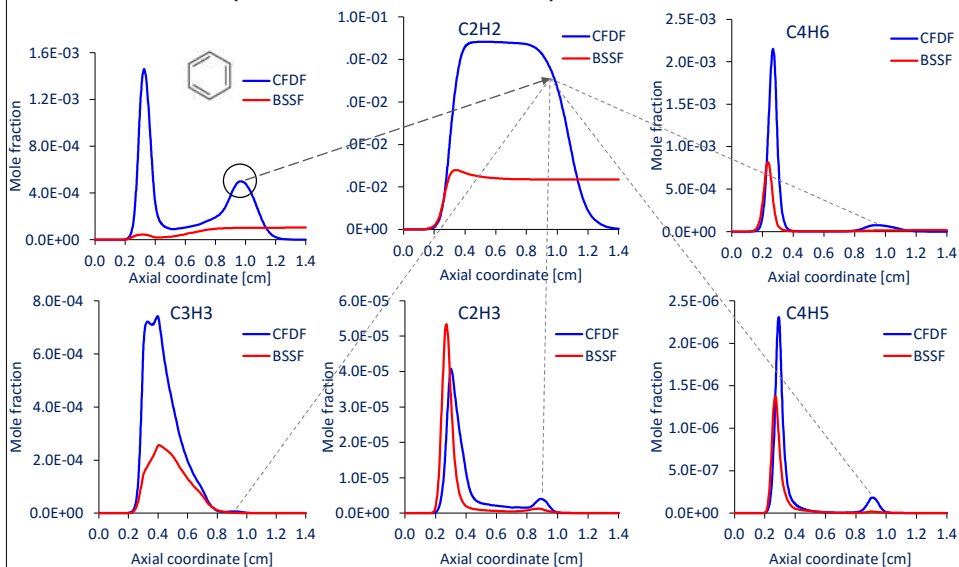
Ethylene rich premixed and counter flow flames

Benzene and its precursors

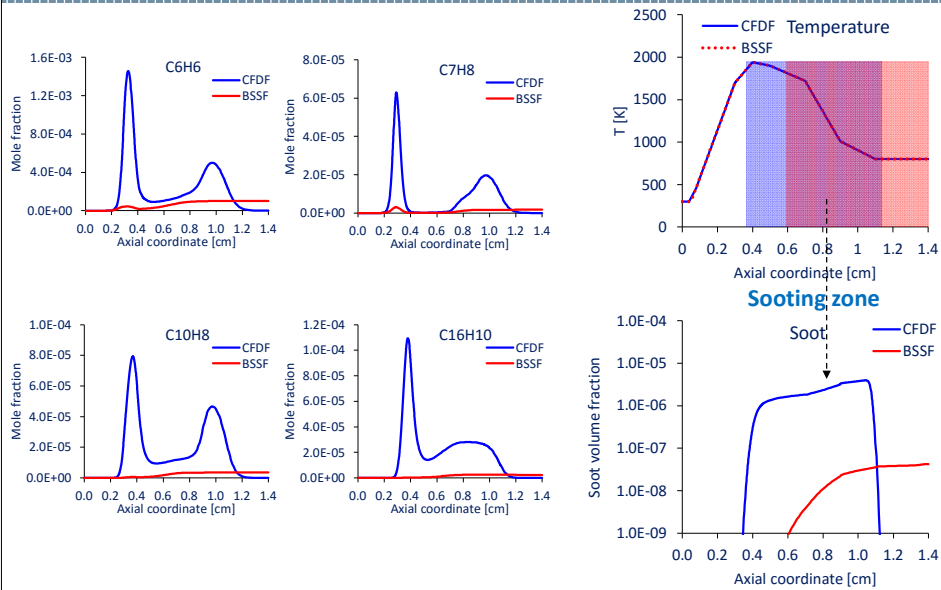


Ethylene rich premixed and counter flow flames

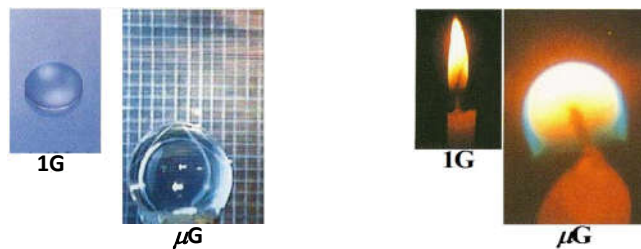
Benzene and its precursors: the second peak



Ethylene rich premixed and counter flow flames



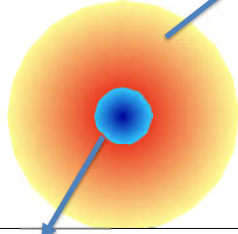
isolated droplet in microgravity conditions



Spherical symmetry
No natural convection

Model equations

- ✓ Spherical symmetry
- ✓ 1D equations
- ✓ Stretched grid



Gas phase

$$\rho_g C_{p,g} \left(\frac{\partial T_g}{\partial t} + v_g \frac{\partial T_g}{\partial r} \right) = \frac{1}{r^2} \frac{\partial}{\partial r} \left(r^2 k_g \frac{\partial T_g}{\partial r} \right) - \rho_g \sum_{i=1}^{nc} (Y_{g,i} V_{g,i} C_{p,g,i}) \frac{\partial T_g}{\partial r} - \sum_{i=1}^{nc} (\omega_{g,i} H_{g,i})$$

$$\frac{\partial \rho_g}{\partial t} + \frac{1}{r^2} \frac{\partial}{\partial r} (r^2 \rho_g v_g) = 0$$

$$\rho_g \left(\frac{\partial Y_{g,i}}{\partial t} + v_g \frac{\partial Y_{g,i}}{\partial r} \right) = -\frac{1}{r^2} \frac{\partial}{\partial r} (r^2 \rho_g Y_{g,i} V_{g,i}) + \omega_{g,i}$$

$$f(V, T_g, P, Y_g) = 0$$

Interface (liquid/gas)

- ✓ Thermodynamic equilibrium
- ✓ Conservation of fluxes

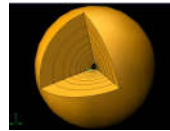
Liquid phase

$$\bar{\rho}_l C_l \frac{\partial T_l}{\partial t} = \frac{1}{r^2} \frac{\partial}{\partial r} \left(r^2 k_l \frac{\partial T_l}{\partial r} \right)$$

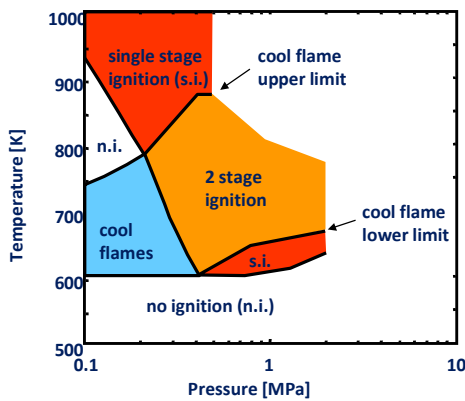
$$\frac{\partial Y_{l,i}}{\partial t} = \frac{1}{r^2} \frac{\partial}{\partial r} \left(r^2 D_{l,i} \frac{\partial Y_{l,i}}{\partial r} \right)$$

$$\bar{\rho}_l \frac{dR_d}{dt} + \frac{R_d}{3} \frac{d\bar{\rho}_l}{dt} = -\rho_g \left(v_g - \frac{dR_d}{dt} \right)$$

Gas radius/liquid radii ~120
 Ideal gas
 Radiative heat transfer
 Soret effect: accounted for

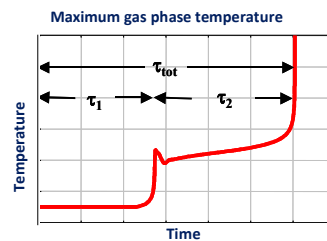
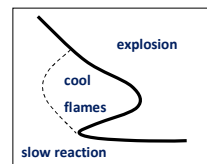


Autoignition map

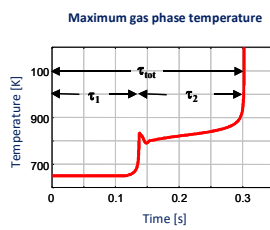
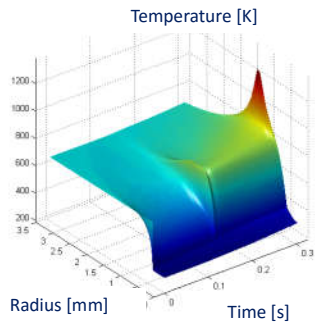


n-heptane, $d = 0.7+0.75$ mm

Experimental data:
 Tanabe M. et al., *Twenty-Six Symposium (International) on Combustion*, The Combustion Institute, Pittsburgh, PA, pp.1637-1643, 1996

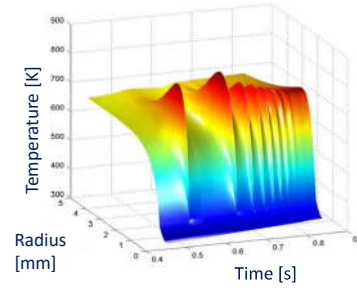


Low T phenomena

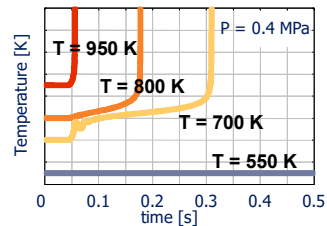
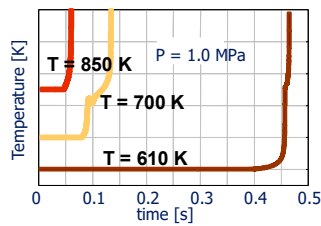
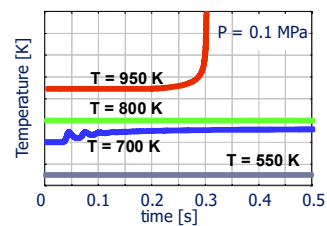
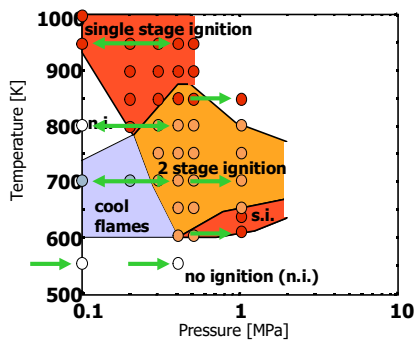


$R_d = 350 \mu\text{m}$
 $T_i^0 = 298 \text{ K}$
 $T_g^0 = 650 \text{ K}$
 $P = 0.5 \text{ MPa}$

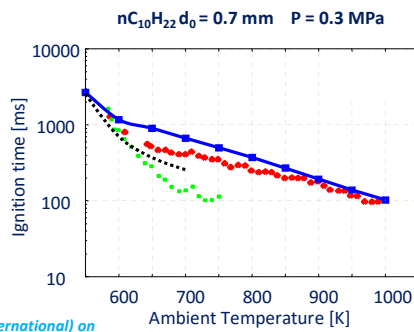
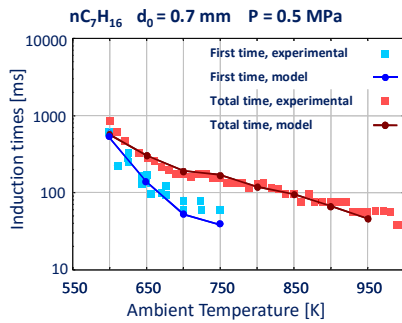
Cool flames



Model predictions ($n\text{C}_{12}\text{H}_{26}d_0 = 0.7 \text{ mm}$)

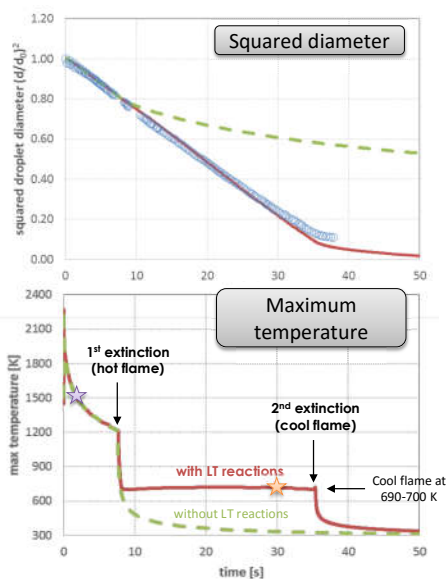


Ignition delay times



Experimental data from: Tanabe M. et al., *Twenty-Six Symposium (International) on Combustion*, The Combustion Institute, Pittsburgh, PA, pp.1637-1643, 1996

Low temperature combustion and extinction



Hot-wire ignition experiments

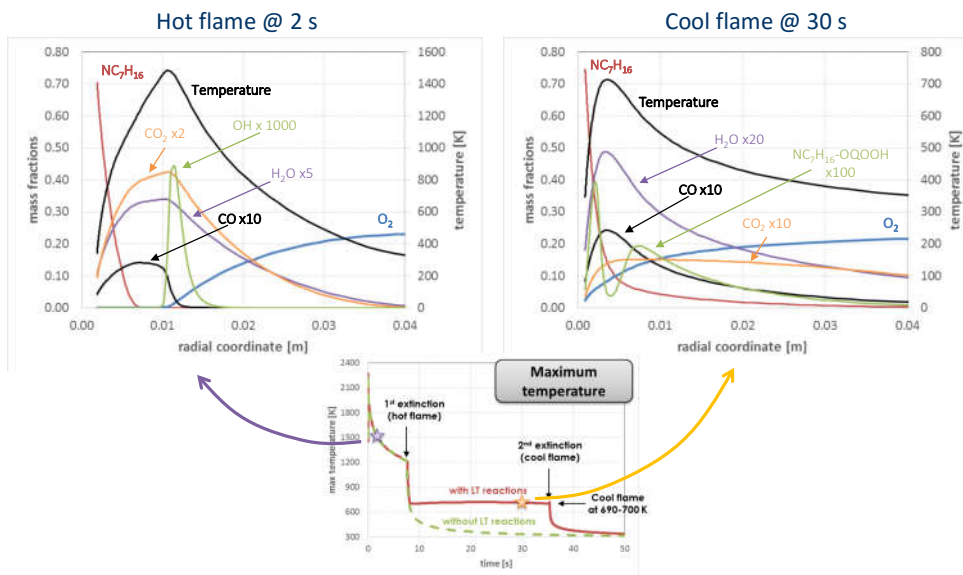
Experiments performed on board the International Space Station (ISS) using the multi-User Droplet Combustion Apparatus (MDCA) installed in the Combustion Integrated Rack (CIR) facility as a part of the Flame Extinguishment Experiments (FLEXs)

Fuel: n-heptane (NC_7H_{16})

Initial diameter: 3.91 mm
 Pressure: 1 atm
 Initial temperature: 300 K
 Gas phase composition: air
 Negligible soot formation
 Droplet tethered by a fine silicon carbide filament

Nayagam V., Dietrich D.L., Ferkul P.V., Hicks M.C., Williams F.A., *Can cool flames support quasi-steady alkane droplet burning?*, *Combustion and flame*, 159, p. 3583-3588 (2012)

Flame structure



RECAP

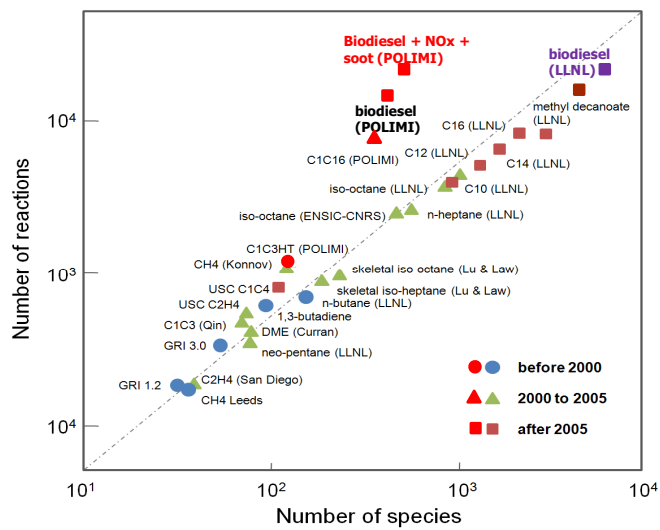
Mechanism development requires experimental data for validation.

Once validated, mechanisms can be used for understanding phenomena

- ✓ Ideal reactors
 - PSR
 - PFR (0D)
 - RCM
 - ST
- ✓ Laminar Flames
 - Premixed
 - Laminar flame speed
 - Flammability limits
 - Diffusive
 - Counterflow
 - Isolated droplet 0G

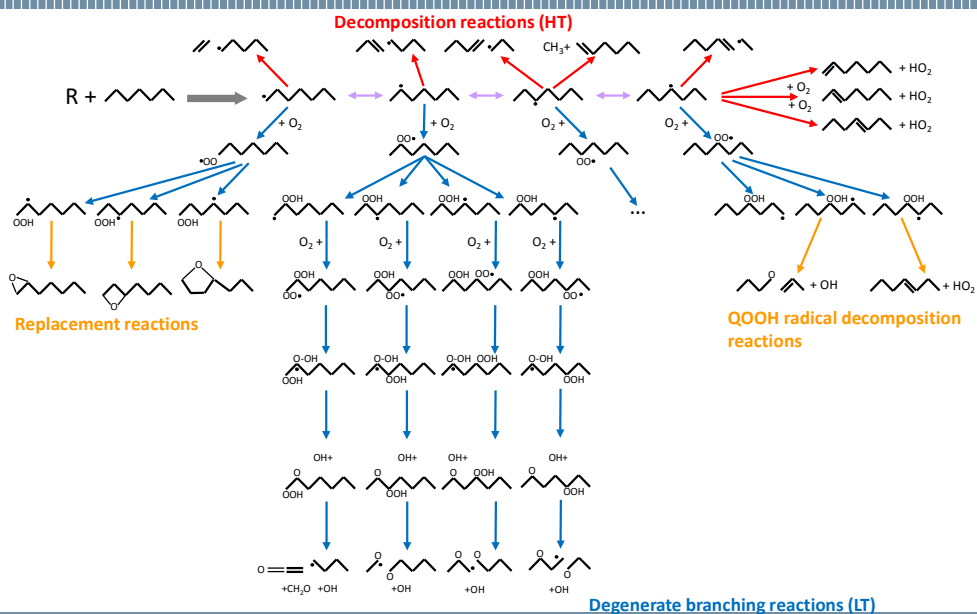
Mechanism lumping

Mechanism dimension

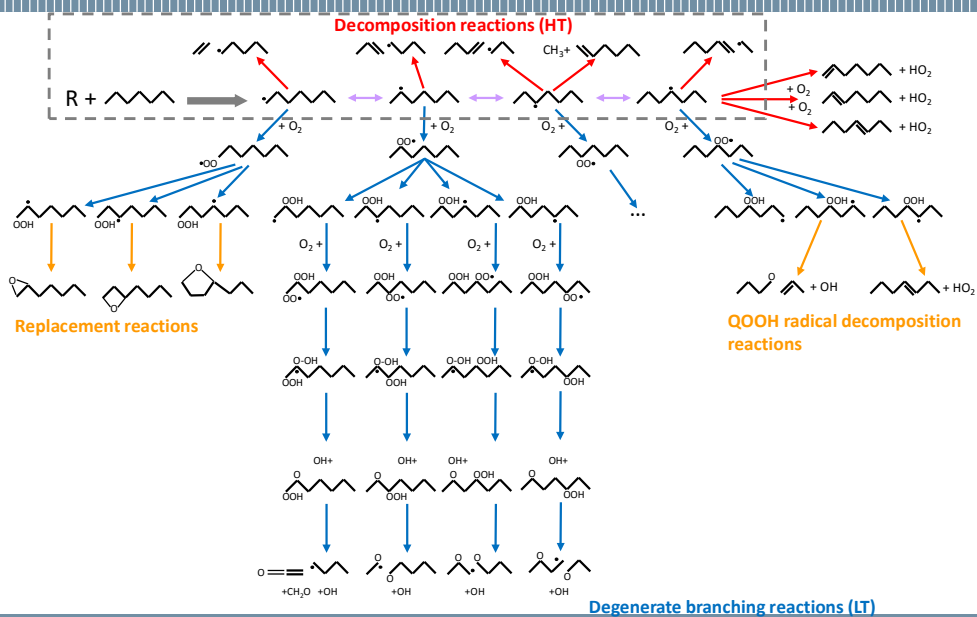


Adapted from: T.F. Lu, C.K. Law, Prog. Energy Comb. Sci., 35 (2009)

Detailed mechanism of n-heptane oxidation

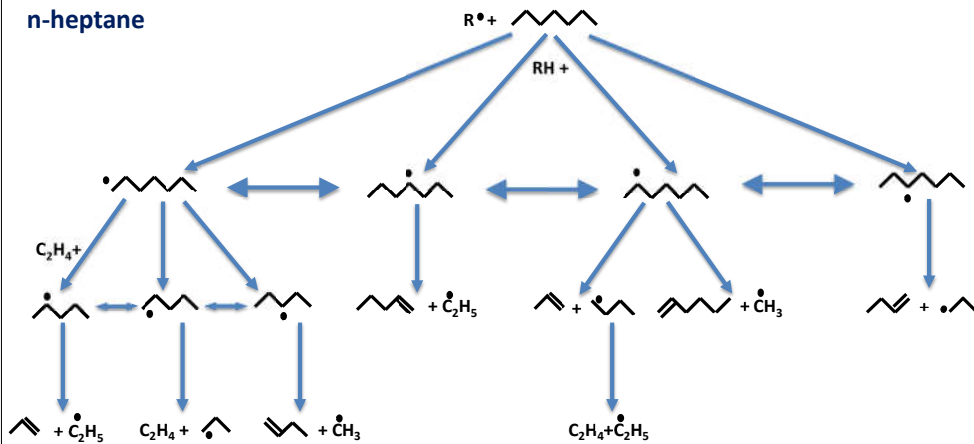


Detailed mechanism of n-heptane oxidation



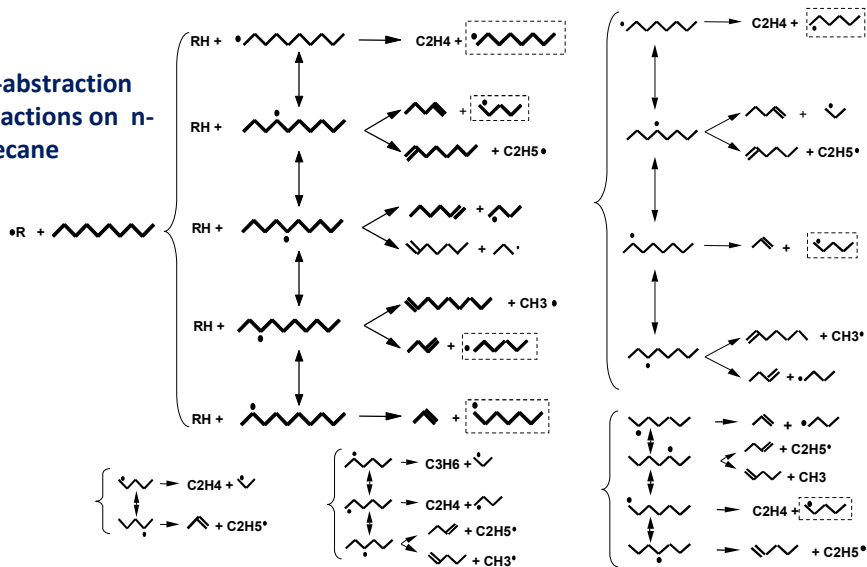
n-heptane high T mechanism

H-abstraction reactions on n-heptane



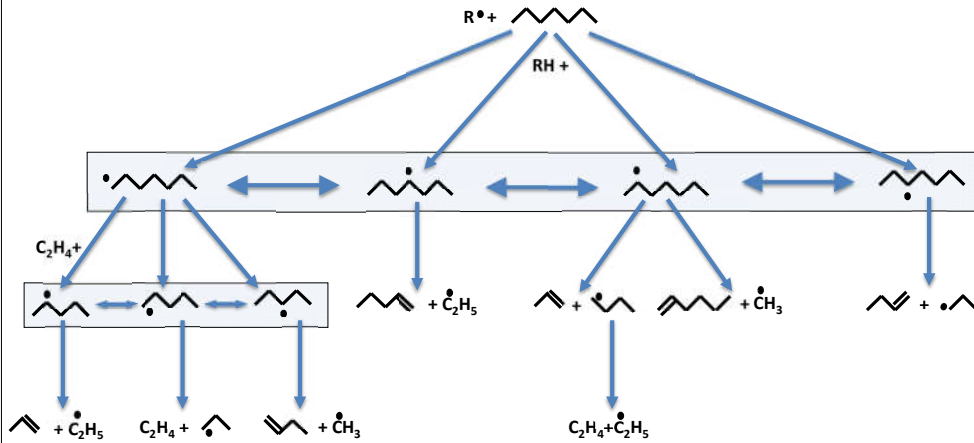
A less simple example: n-decane case

H-abstraction reactions on n-decane



Lumping

Lumping transforms a vector of species to a lower dimensional vector of pseudospecies, thus reducing the system dimension. In proper lumping each species appears in only one lumped pseudospecies

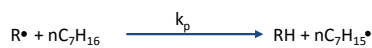
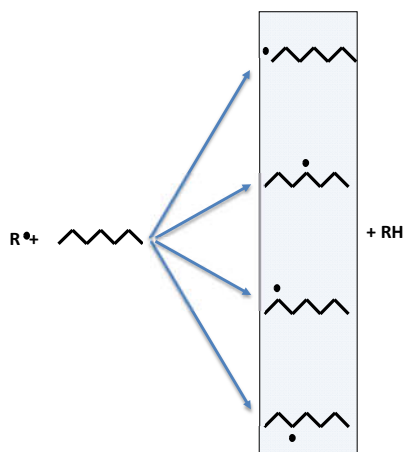


9

Tsinghua Summer School

POLITECNICO MILANO 1863

Lumped pseudospecies properties



Relative detailed i -th species amount in each pseudospecies (α_i):

$$\alpha_i = \frac{k_i}{\sum_{j=1}^n k_j} \quad (i = 1, \dots, n)$$

Enthalpy of formation of pseudospecies is the weighted sum of the enthalpy of formation of each species:

$$\Delta H_{f, \text{pseudospecies}}^0 = \sum_{i=1}^n \alpha_i \Delta H_{f_i}^0$$

$$K_p = \sum_{i=1}^n K_i$$

10

Tsinghua Summer School

POLITECNICO MILANO 1863

Lumping of reactions

Based on the steady-state approximation for the intermediate heptyl radicals, the following linear system for primary decomposition reactions of n-heptane can be easily deduced from continuity equations

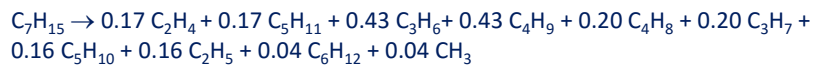
$$r_j(0) + \sum_{i \neq j} k_{i,j} R_i^{(7)} - (\sum_{i \neq j} k_{i,j} + k_{d_j}) R_j^{(7)} = 0 \quad (j = 1 \dots 4)$$

where: $r_j(0)$ is the rate of direct formation of heptyl radical $R_j^{(7)}$ •
 k_{d_j} is the total rate constant for the decomposition reaction of $R_j^{(7)}$ •
 $k_{i,j}$ is the rate constant for the isomerization reaction $R_j^{(7)}$ • \rightarrow $R_i^{(7)}$ •

In this way, it is easy to evaluate the products distribution of an **equivalent or lumped reaction**

Resulting reaction

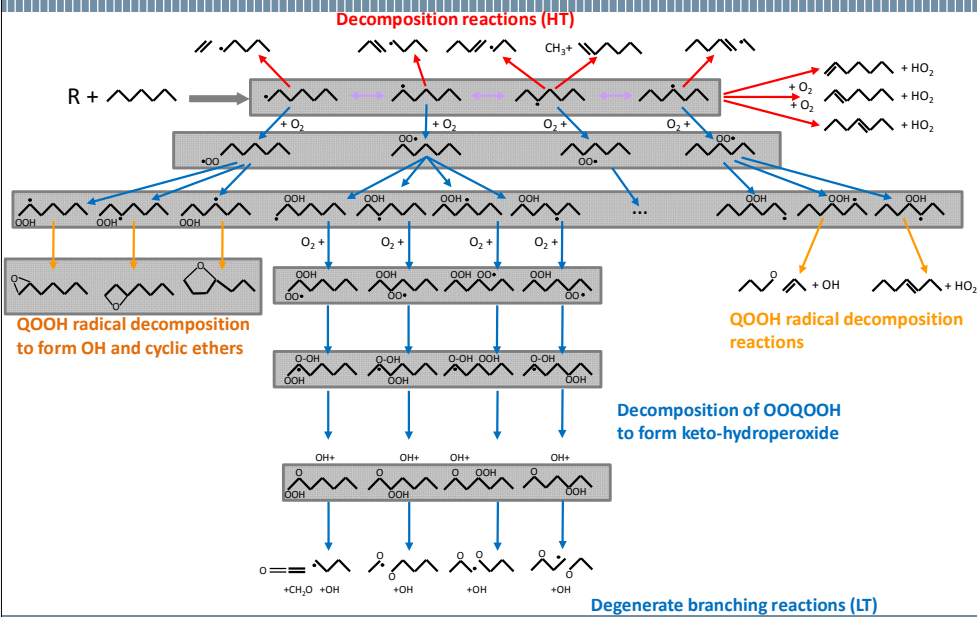
MAMOX++ PROGRAM generates the 'lumped reactions' at assigned Temperature (1000K)



The 'lumped' stoichiometry is only a weak function of T

	800	1000	1200	1500
CH₃	0.03	0.04	0.044	0.045
C₂H₅	0.21	0.16	0.13	0.11
C₃H₇	0.18	0.20	0.21	0.23
C₄H₉	0.43	0.43	0.42	0.41
C₅H₁₁	0.15	0.17	0.196	0.205

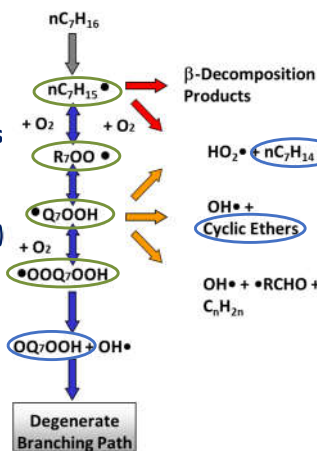
Horizontal lumping of species



Horizontal lumping of species: nC7

Detailed Scheme

- 135** Primary reactions
- 38** Intermediate radicals
- 26** Primary products (retaining nC₇ structure)
- 3** n-heptenes
- 8** cyclic-ethers
- 15** keto-hydroperoxides



Lumped Scheme

- 15** Primary lumped reactions
- 4** Intermediate radicals
- 3** Primary lumped products
- 1** lumped n-heptene
- 1** lumped cyclic-ether
- 1** lumped keto-hydroperoxide

Horizontal lumping of species: nC16

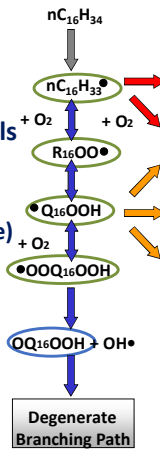
Detailed Scheme

362 Primary reactions

100 Intermediate radicals

80 Primary products
(retaining nC₁₀ structure)

8 n-hexadecene
22 cyclic-ethers
42 keto-hydroperoxides



Lumped Scheme

15 Primary lumped reactions

4 Intermediate radicals

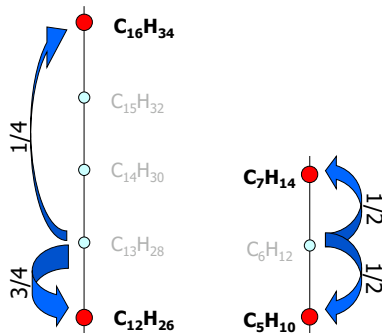
3 Primary lumped products

1 lumped n-hexadecene
1 lumped cyclic-ether
1 lumped keto-hydroperoxide

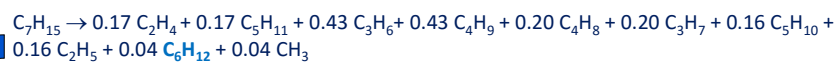
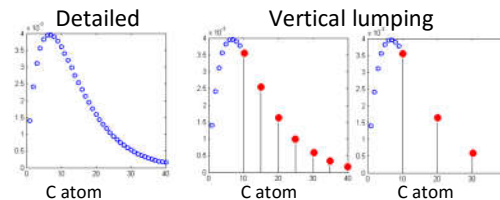
Vertical lumping of species

This lumping technique is equivalent to the discrete section approach:

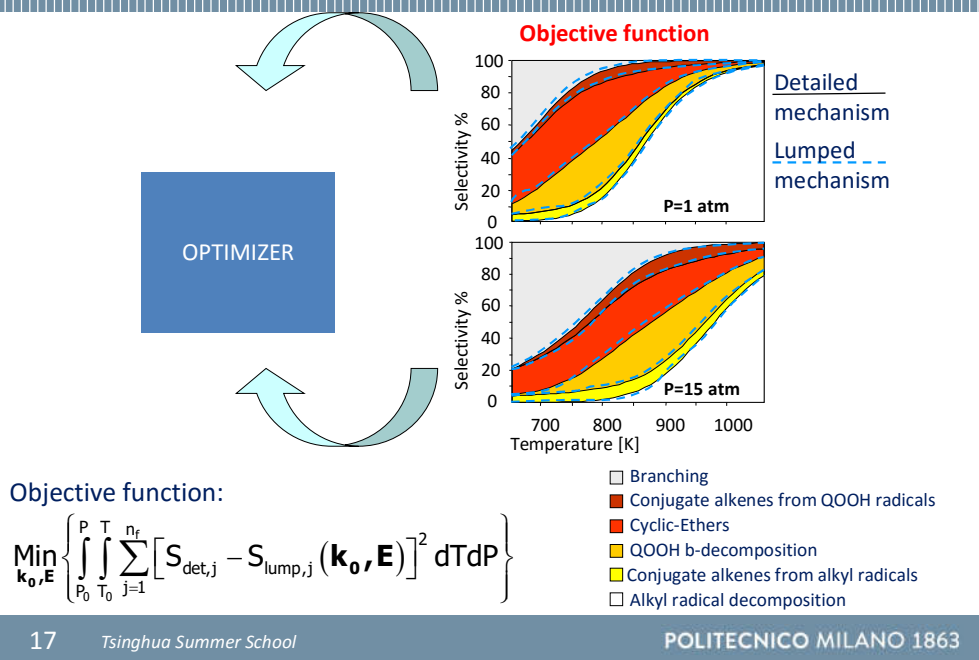
family of species (n-alkanes, iso-alkanes, alkenes, ...) are divided in a finite number of sections or lumped components which represent groups of species.



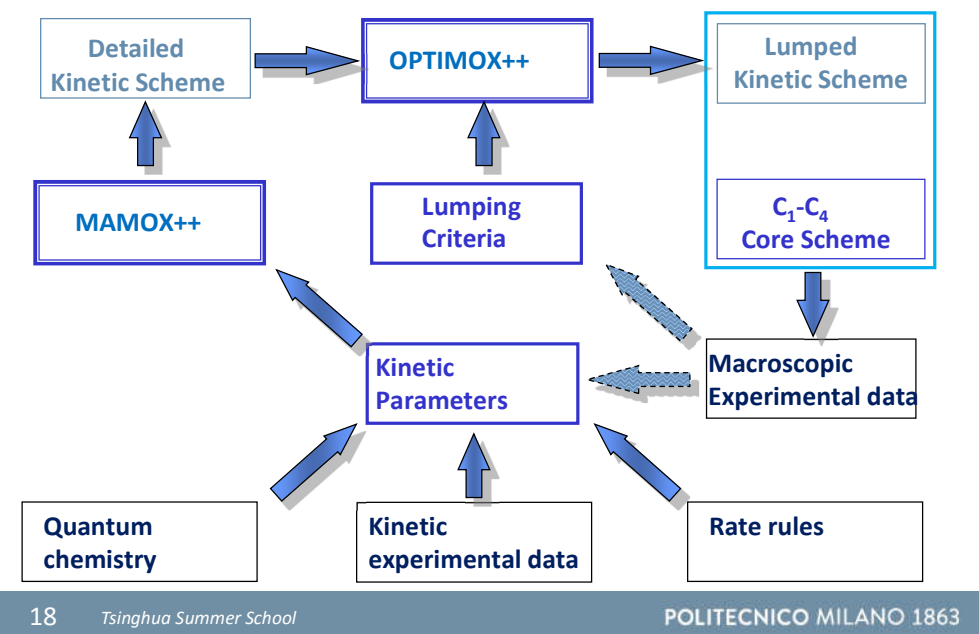
Intermediate species split in the reference pseudocomponents, according to the lever rule



Rate constants of lumped reactions



Lumped mechanism development approach



Methyl-ester mechanism

Methyl butanoate (MB) detailed kinetic scheme

CCCC(=O)OC

Grana et al., Energy (2012)

Methyl decanoate (MD) lumped kinetic scheme

CCCCCCCCC(=O)OC

Grana et al., Combust. Flame (2012)

Biodiesel is a renewable transportation fuel consisting of fatty acid methyl esters (FAME)

Lumped kinetic model of the pyrolysis and oxidation of biodiesel fuels

➤ Laminar flame and **flame speed** computations without further reductions

➤ Ignitions in **internal combustion engines** (HCCI)

➤ More effective reductions for **CFD calculations**

Detailed kinetic schemes			
Scheme	fuel	#species	#reactions
Fisher et al.	M-butanoate	264	2031
Herbinet et al. (2008)	M-decanoate	2878	10021

[Fisher et al., Proc. Comb. Inst. 28, 2000, 1579-1586](#)
[Herbinet et al., Combust. Flame 154, 2008, 507-528](#)

Biodiesel

Biodiesel → Vegetable oils → Fatty acids → **Heavy methyl esters (HME)**

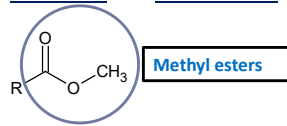
- Rapeseed methyl esters (**RME**) in Western Europe
- Soybean methyl ester (**SME**) in USA

#C : #double bonds	Fatty Acid	Soybean	Cottonseed	Rapeseed	Palm	Lard	Tallow	Coconut
12 : 0	Lauric	0.1	0.1	0.1	0.1	0.1	0.1	53.1
14 : 0	Myristic	0.1	0.7	0.1	1.0	1.5	3.1	21.9
16 : 0	Palmitic	10.3	20.4	4.3	43.1	24.9	25.4	11.2
18 : 0	Stearic	3.7	2.6	1.3	4.5	15.0	21.1	3.4
18 : 1	Oleic	23.0	19.5	59.9	40.8	46.7	46.2	7.9
18 : 2	Linoleic	54.1	56.0	21.1	10.2	11.3	3.2	2.5
18 : 3	Linolenic	8.7	0.6	13.2	0.2	0.4	1.0	0.0

L. Lin, Z. Cunshan, S. Vittayapadung, S. Xiangqian, D. Mingdong, Appl. Energy (2011)

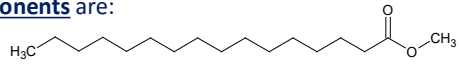
Biodiesel surrogate

Biodiesel is composed by saturated and unsaturated heavy methyl esters.

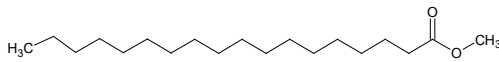


The **five major components** are:

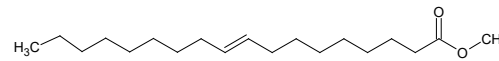
methyl palmitate (MPA) – $\text{CH}_3\text{-C}_{16}\text{H}_{31}\text{O}_2$



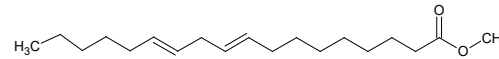
methyl stearate (MSTEA) - $\text{CH}_3\text{-C}_{18}\text{H}_{35}\text{O}_2$



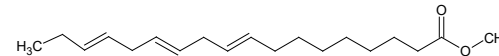
methyl oleate (MEOLE) - $\text{CH}_3\text{-C}_{18}\text{H}_{33}\text{O}_2$



methyl linoleate (MLINO) - $\text{CH}_3\text{-C}_{18}\text{H}_{31}\text{O}_2$



methyl linolenate (MLIN1) - $\text{CH}_3\text{-C}_{18}\text{H}_{29}\text{O}_2$



“Detailed” kinetic scheme

Scheme	#Species	#Reactions
C. K. Westbrook et al. (2011)	~4800	~20000

C.K. Westbrook, C.V. Naik, O. Herbinet, et al., *Combust. Flame* (2011)

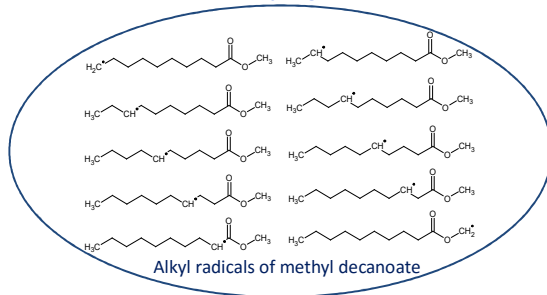
Lumping biodiesel components

Methyl esters structure's **lack of symmetry**

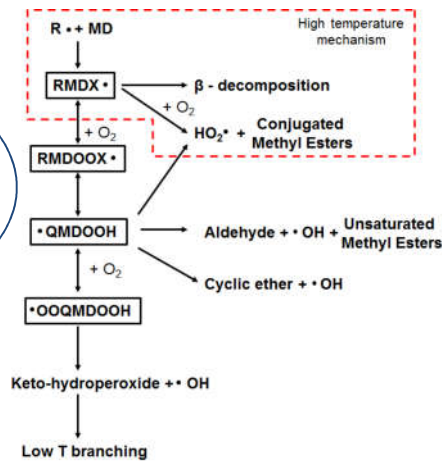
⇒ **huge number of species and radicals** involved in the detailed kinetics

⇒ **Lumped Approach**

Lumping

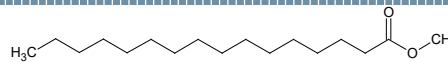


⇓
One single lumped species for different isomers



Methyl palmitate

Methyl palmitate



Detailed Lumped

16

1

16

1

104

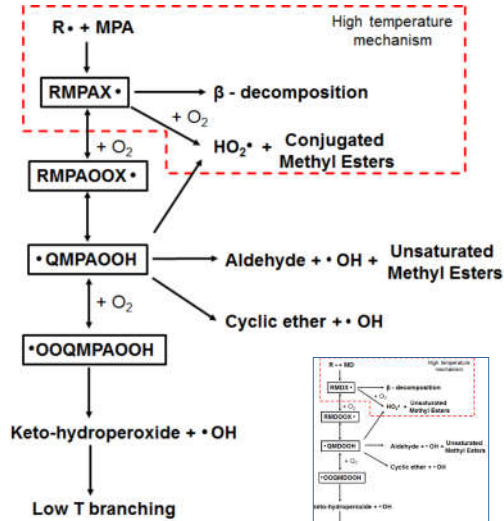
1

104

1

240

4



Vertical lumping biodiesel components

Saturated methyl esters

- Methyl stearate (18)
- Methyl heptanodecanoate (17)
- Methyl palmitate (16)**
- Methyl pentadecanoate (15)
- Methyl myristate (14)
- Methyl tridecanoate (13)
- Methyl laurate (12)
- Methyl undecanoate (11)
- Methyl decanoate (10)**
- Methyl nonanoate (9)
- Methyl octanoate (8)
- Methyl heptanoate (7)**
- Methyl hexanoate (6)
- Methyl pentanoate (5)
- Methyl butanoate (4)**
- Methyl propanoate (3)
- Methyl acetate (2)
- Methyl formate (1)

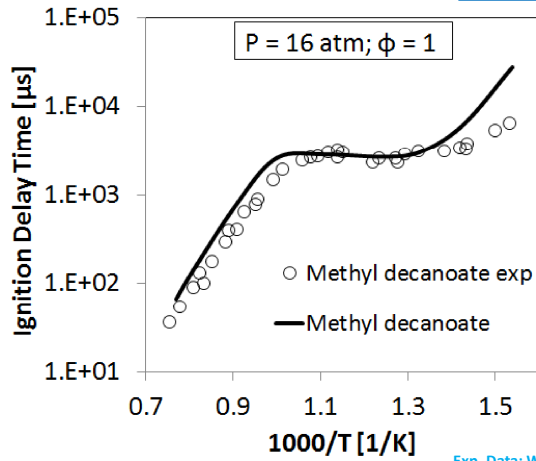
Mono-unsaturated methyl esters

- Methyl oleate (18)**
- Methyl heptanodecenoate (17)
- Methyl palmitoleate (16)**
- Methyl pentadecenoate (15)
- Methyl myristoleate (14)
- Methyl tridecenoate (13)
- Methyl dodecenoate (12)
- Methyl undecenoate (11)
- Methyl decenoate (10)**
- Methyl nonenoate (9)
- Methyl octenoate (8)
- Methyl heptenoate (7)**
- Methyl hexenoate (6)
- Methyl pentenoate (5)
- Methyl crotonate (4)**
- Methyl acrylate (3)**

Relative reactivity of saturated esters

SHOCK TUBE experiments
Methyl decanoate/air

T = 600 – 1400 K
P = 16 atm
 $\Phi = 1$

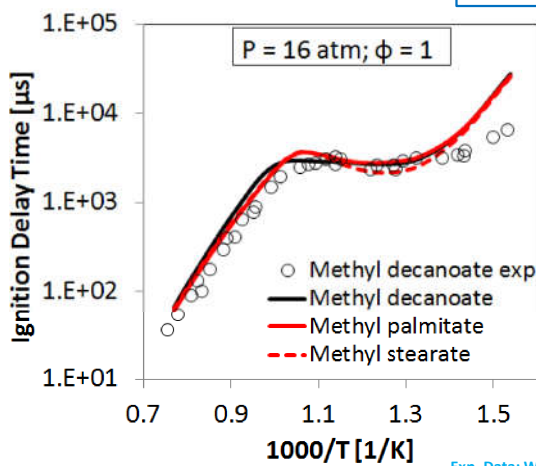


Exp. Data: W. Wang, M.A. Oehlschlaeger, Combust. Flame (2012)

Relative reactivity of saturated esters

SHOCK TUBE experiments
Methyl decanoate/air

T = 600 – 1400 K
P = 16 atm
 $\Phi = 1$

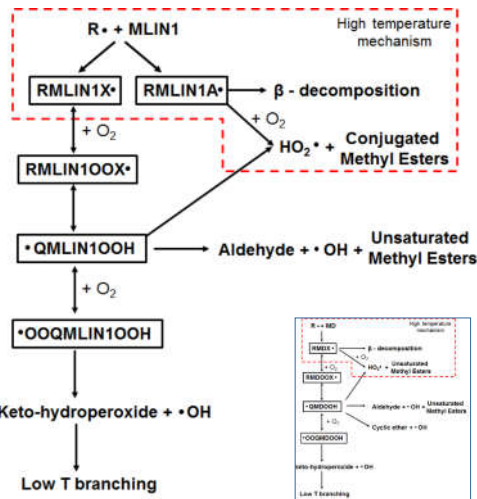
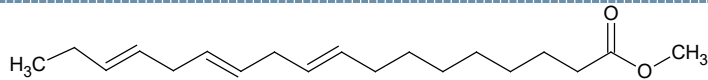


Exp. Data: W. Wang, M.A. Oehlschlaeger, Combust. Flame (2012)

The saturated esters
methyl decanoate, methyl palmitate
and methyl stearate
have **similar** ignition delays.

Unsaturated methyl-esters

Methyl linolenate



Double bonds in the unsaturated methyl esters

Resonantly allylic stabilized radicals

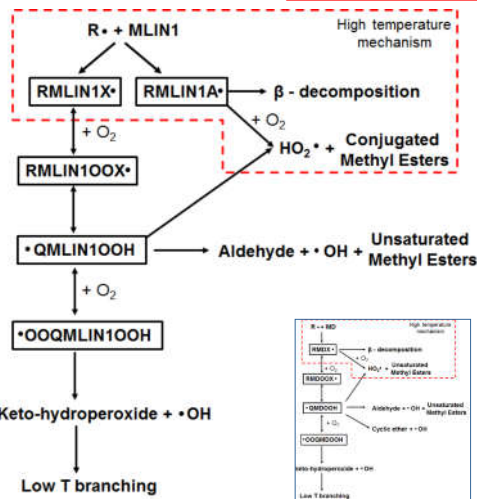
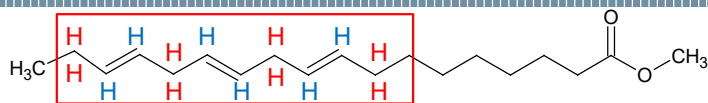
Vinylic H atoms not easily removed

Lower reactivity of the unsaturated methyl esters at low temperature

Westbrook et al., Proc. Combust. Inst. (2012)

Unsaturated methyl-esters

Methyl linolenate



Double bonds in the unsaturated methyl esters

Resonantly allylic stabilized radicals

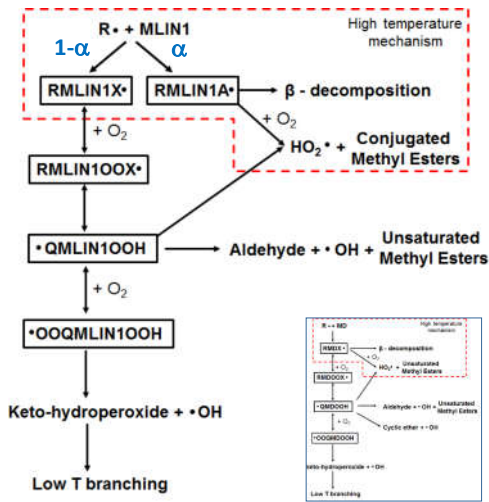
Vinylic H atoms not easily removed

Lower reactivity of the unsaturated methyl esters at low temperature

Westbrook et al., Proc. Combust. Inst. (2012)

Unsaturated methyl-ester lumping

Methyl linolenate



- Two separate lumped radicals:
 - RMLIN1X: primary **propagating** methyl linolenate radical
 - RMLIN1A: primary **allylic** methyl linolenate radical

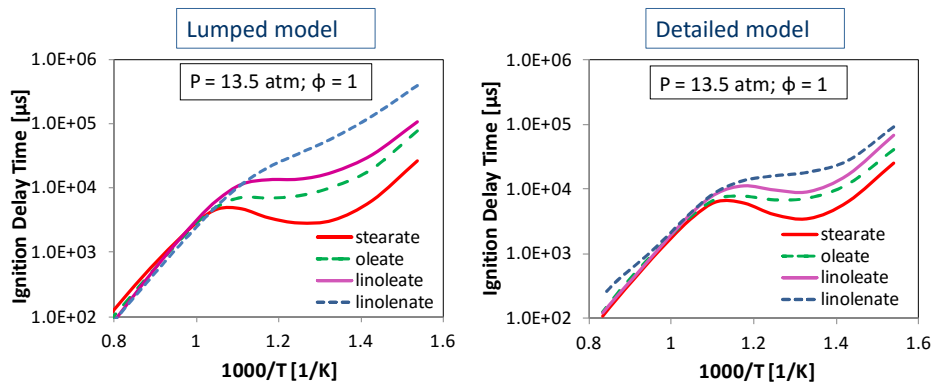


$$\alpha = \frac{\text{RMLIN1A}}{\text{RMLIN1A} + \text{RMLIN1X}}$$

- $\alpha \sim 0.3$ for methyl-oleate
- $\alpha \sim 0.5$ for methyl-linoleate
- $\alpha \sim 0.6$ for methyl-linolenate

Relative reactivity of C18 methyl-esters

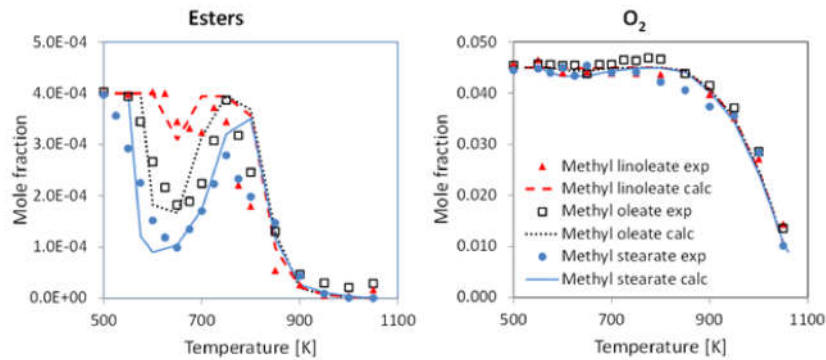
- very few experimental data
- Comparison with detailed model



- Large differences in the LT region – similar reactivity at HT
- Ignition delays in NTC region follow the cetane numbers

Detailed model: Westbrook et al., Combust. Flame (2011)

Oxidation of methyl-esters in a JSR

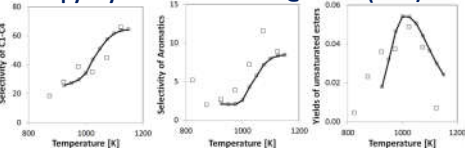


Mole fraction profiles of methyl esters and Oxygen
($P = 1.05 \text{ atm}$, $\tau = 2 \text{ s}$, Esters = 4×10^{-4} , Benzene = 5000, Oxygen 45000 ppm).

Exp. Data: A. Rodriguez et al., *Combust. Flame*, 164, 2016, 346-362

Rapeseed oil validation

RME pyrolysis in flow reactor @ 1 atm (RME/N₂ 1/13)

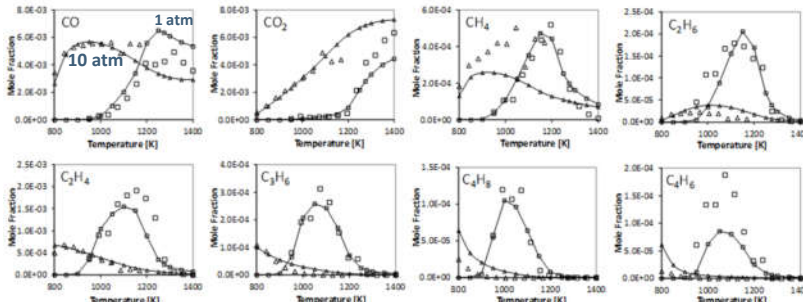


Exp. data: Billaud et al., *J. Am. Oil. Chem. Soc.*, 72 (1995), 1149-1154

Fatty Acid	Rapeseed
Lauric	0.1 (33% MPA – 67% MDE)
Myristic	0.1 (67% MPA – 33% MDE)
Palmitic	4.3
Stearic	1.3
Oleic	59.9
Linoleic	21.1
Linolenic	13.2

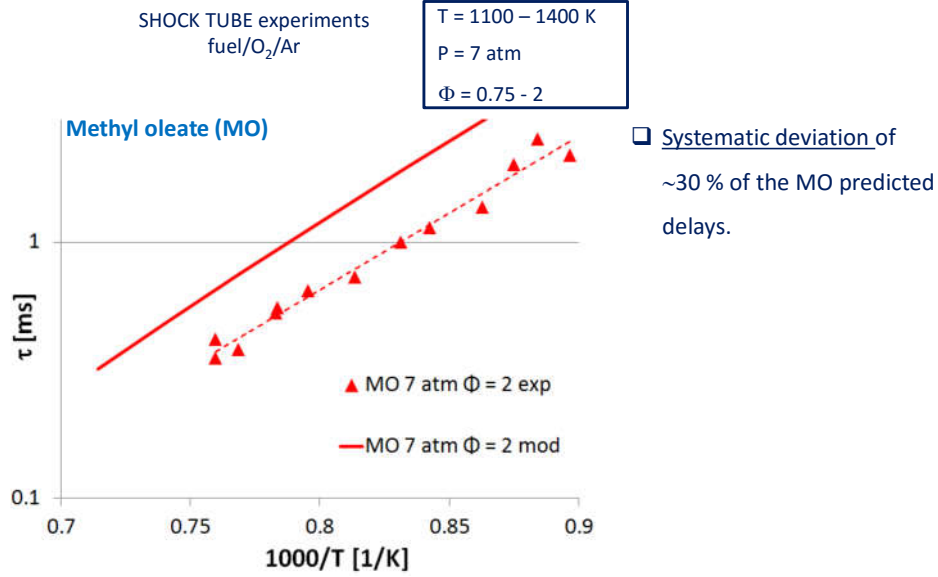
- Methyl stearate (18)
- Methyl heptadecanoate (17)
- Methyl palmitate (16)
- Methyl pentadecanoate (15)
- Methyl myristate (14)
- Methyl tridecanoate (13)
- Methyl laurate (12)
- Methyl undecanoate (11)
- Methyl decanoate (10)
- Methyl nonanoate (9)
- Methyl octanoate (8)
- Methyl heptanoate (7)
- Methyl hexanoate (6)
- Methyl pentanoate (5)
- Methyl butanoate (4)
- Methyl propanoate (3)
- Methyl acetate (2)
- Methyl formate (1)

RME oxidation in JSR



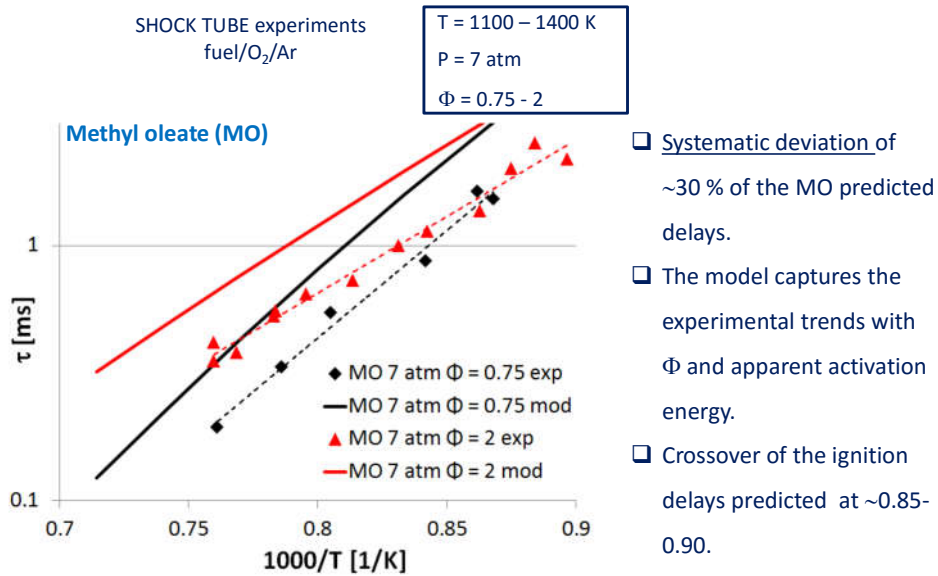
Exp. data: Dagaut et al., *Proc. Comb. Inst.*, 31 (2007), 2955-2961

MO and ML ignition delay times



- ❑ Systematic deviation of ~30 % of the MO predicted delays.

MO and ML ignition delay times

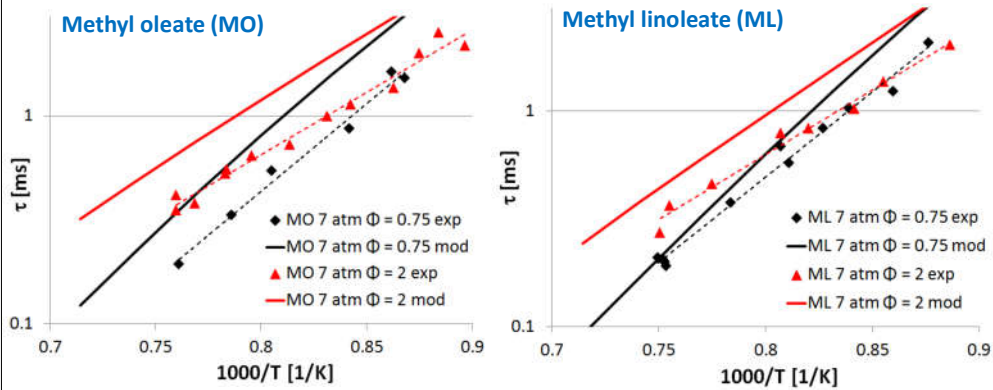


- ❑ Systematic deviation of ~30 % of the MO predicted delays.
- ❑ The model captures the experimental trends with Φ and apparent activation energy.
- ❑ Crossover of the ignition delays predicted at ~0.85-0.90.

MO and ML ignition delay times

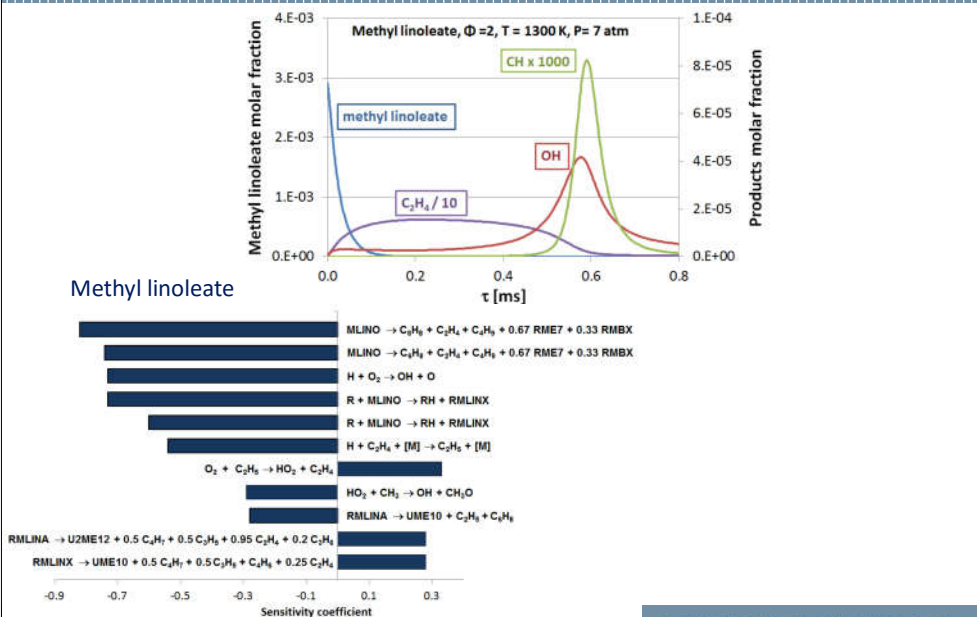
SHOCK TUBE experiments
fuel/O₂/Ar

T = 1100 – 1400 K
P = 7 atm
Φ = 0.75 - 2

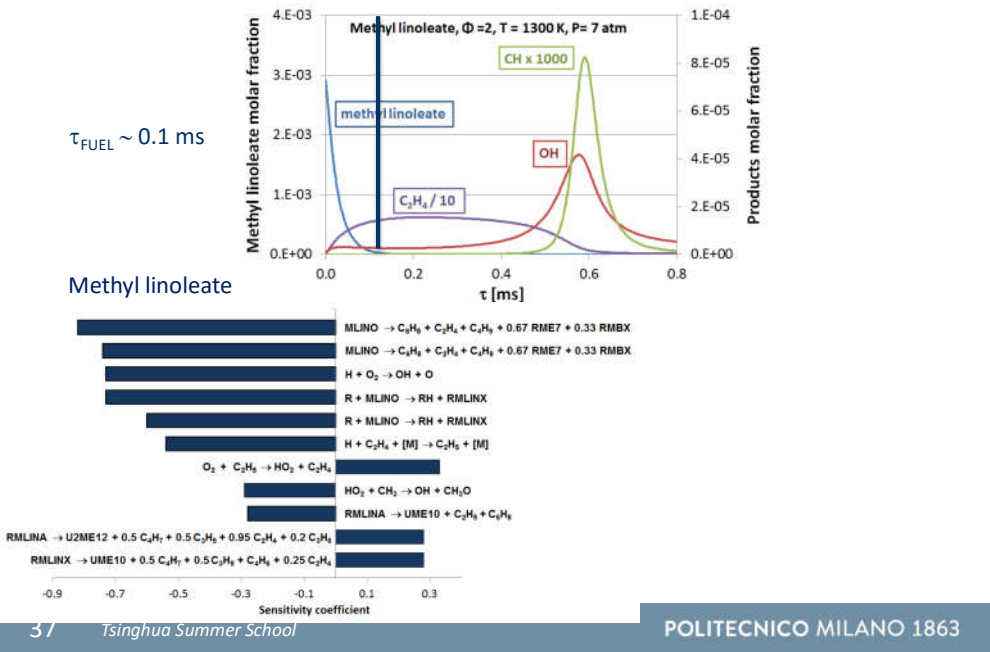


Exp. Data: Campbell et al., Proc. Combust. Inst. (2012)

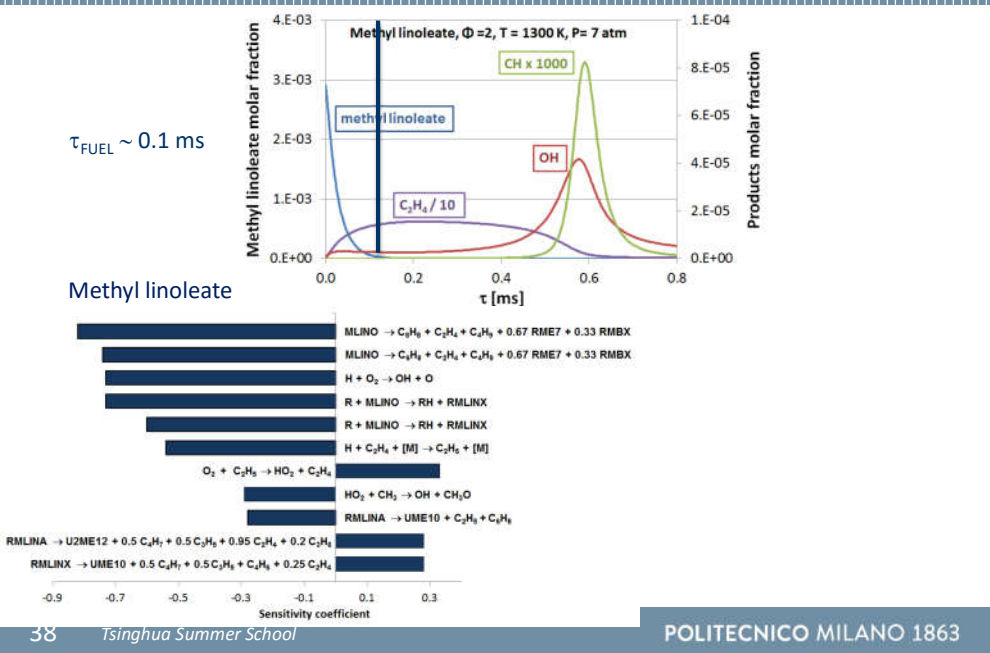
Sensitivity analysis at 1300 K



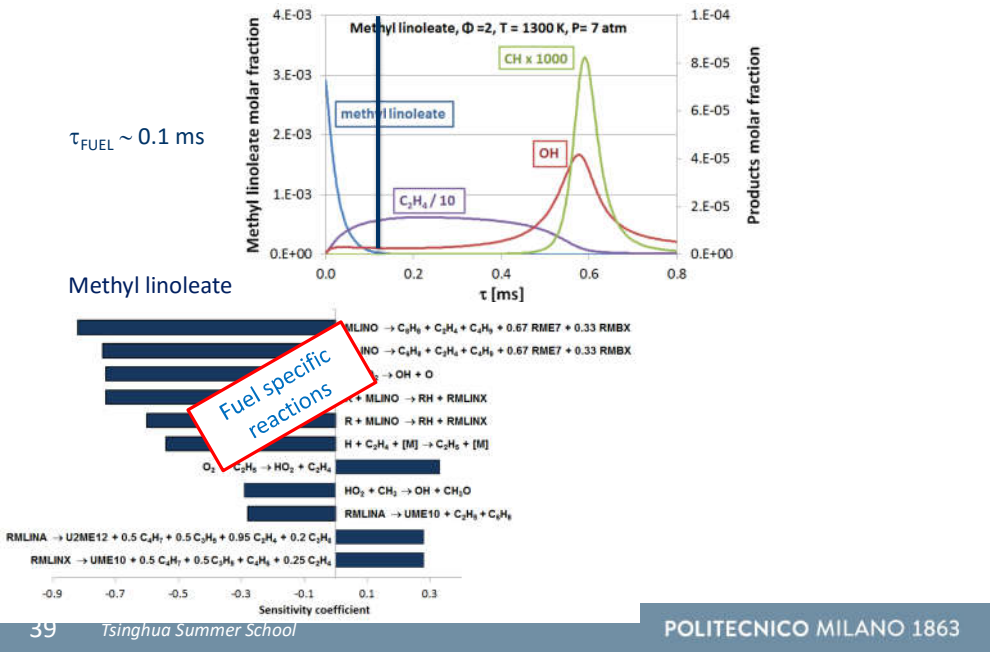
Sensitivity analysis at 1300 K



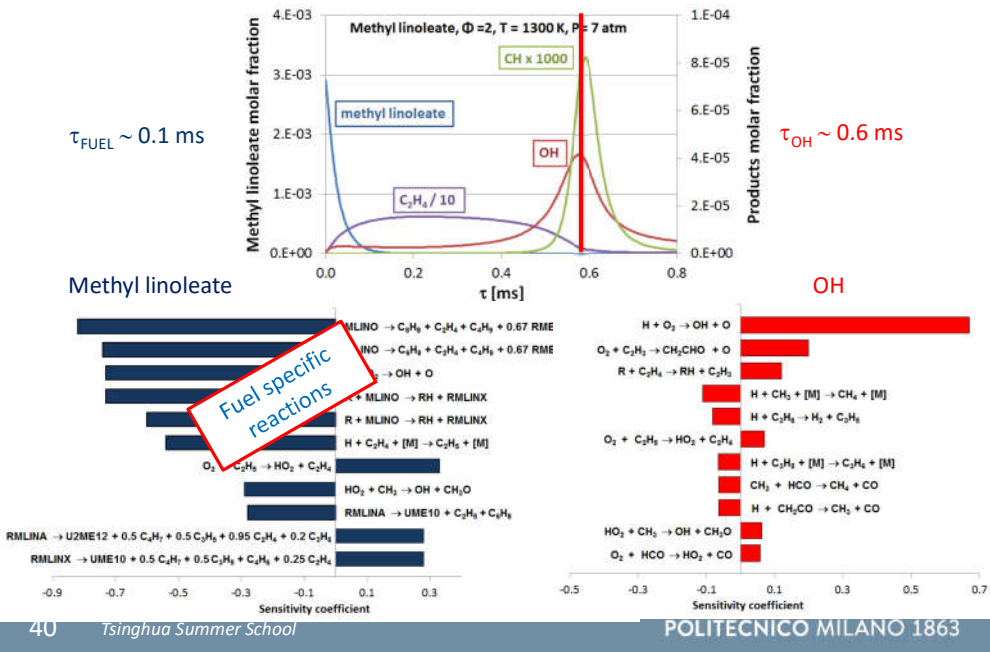
Sensitivity analysis at 1300 K



Sensitivity analysis at 1300 K

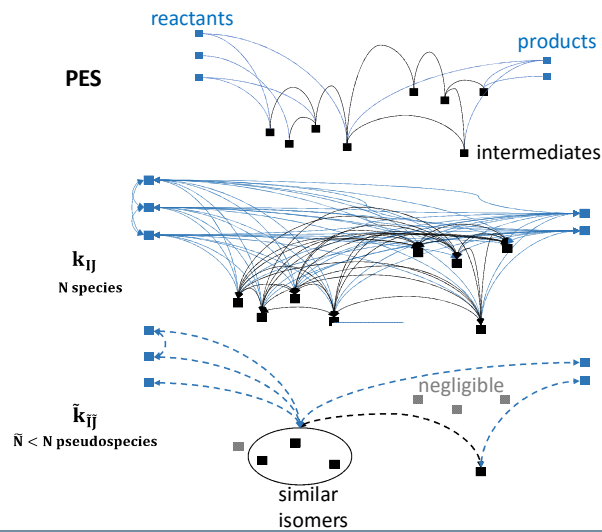


Sensitivity analysis at 1300 K



Master Equation based Lumping approach

Same problem of (very) large number of species can be seen at the fundamental level, for example when evaluating a rate constant through Master Equation



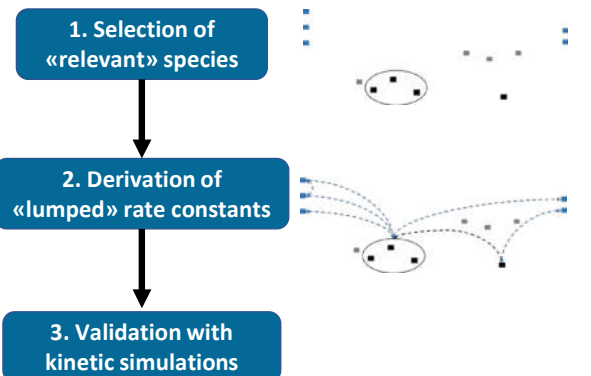
Potential energy surface can include **many** intermediates, which bring to **many** products through **many** transition states

Theory allows to estimate each individual act and the rate of this chemical act: we have all the possible information

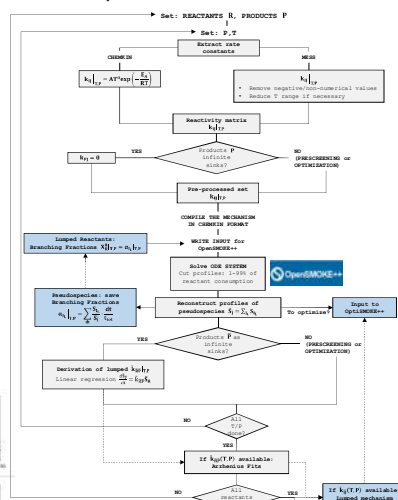
All intermediates with very short characteristic times do not react with the environment and can be neglected. Lumping can be applied as well. Isomers with similar reactivity are lumped together

MEL implementation

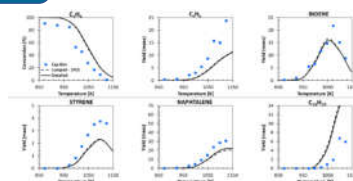
3 main steps



All steps automatized

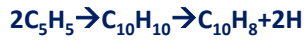


Pratali Maffei et al., Chem. Eng. J., 422, 2021, 129954

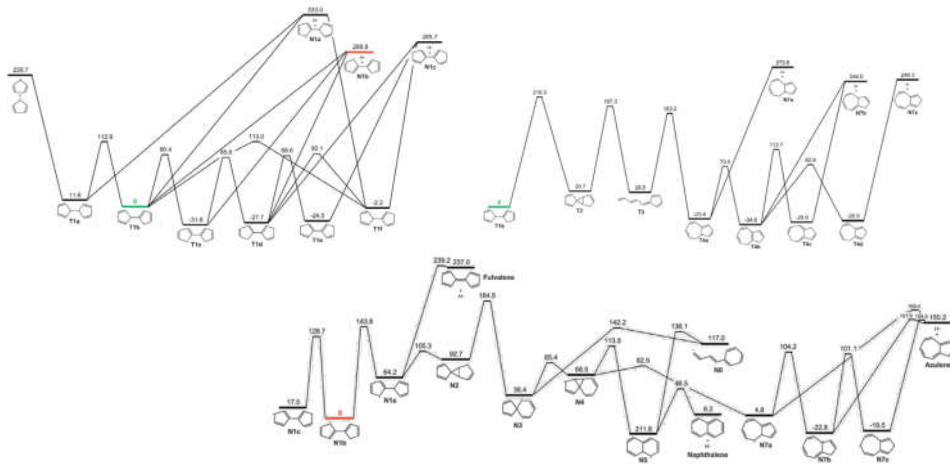


available at: <https://github.com/lpratalimaffei/MEL>

MEL example



31 SPECIES, 328 REACTIONS



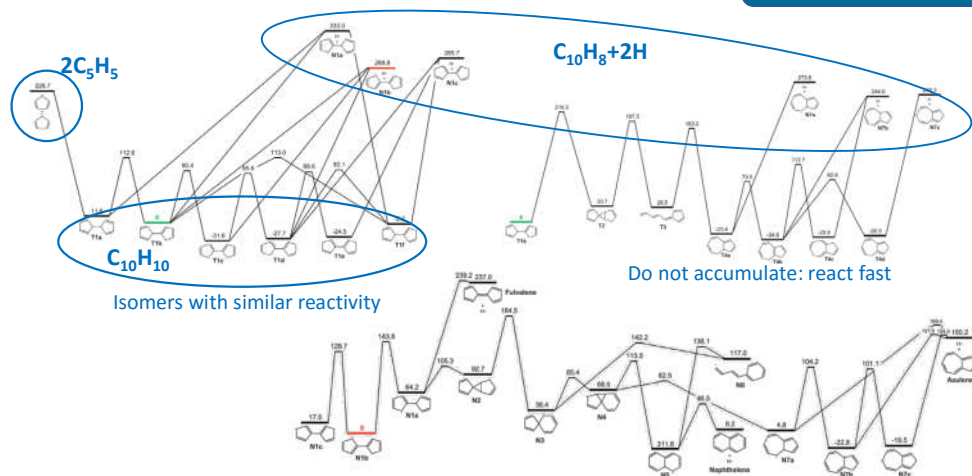
A.E. Long et al., *Combust. Flame.* 187 (2018) 247–256.

MEL example



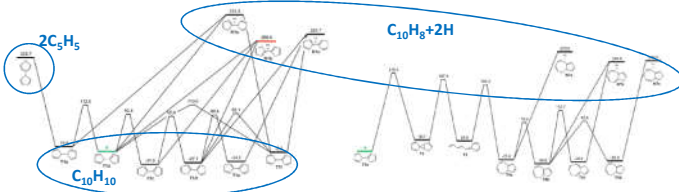
3 equivalent pseudospecies

1. Selection of «relevant» species

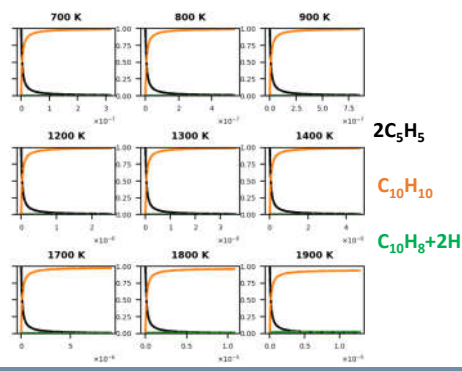


A.E. Long et al., *Combust. Flame.* 187 (2018) 247–256.

MEL example



2. Derivation of «lumped» rate constants



- C₅H₅ is the only reactant
- Reproduce the conditions of kinetic experiments: products do not react back
- Fit the profiles obtained

$$2C_5H_5 \rightarrow C_{10}H_{10} \quad 4.19 \cdot 10^{19} T^{-2.34} \exp\left(\frac{440}{T}\right) \frac{cm^3}{mol \cdot s}$$

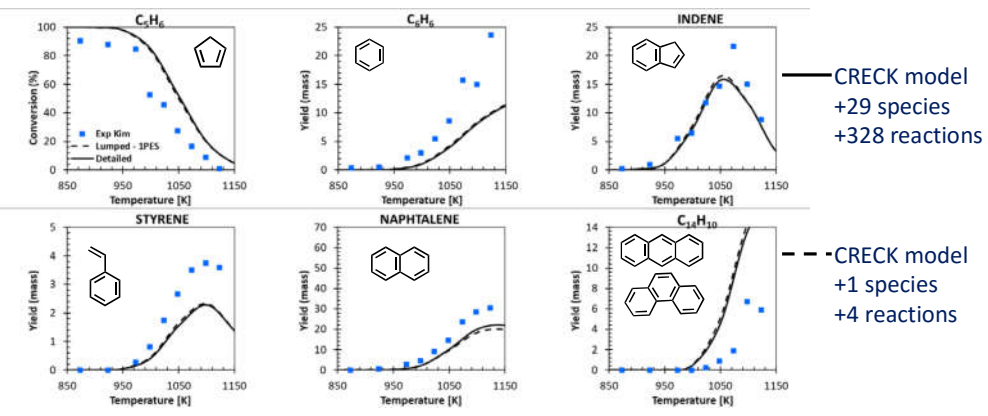
$$2C_5H_5 \rightarrow C_{10}H_8 + 2H \quad 4.55 \cdot 10^{-9} T^{6.11} \exp\left(\frac{-5223}{T}\right) \frac{cm^3}{mol \cdot s}$$

Apply the same procedure for C₁₀H₁₀

MEL example

C₅H₆/Ar PFR 850-1160 K, 1atm

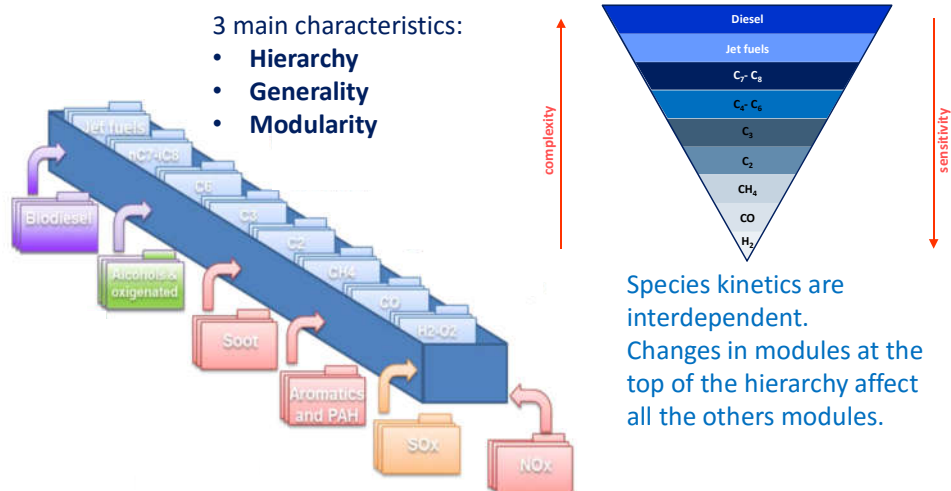
3. Validation with kinetic simulations



Exp. Data: Kim et al., J. Phys. Chem. A, 114 (2010) 12411-12416

Mechanism validation

Detailed mechanism structure

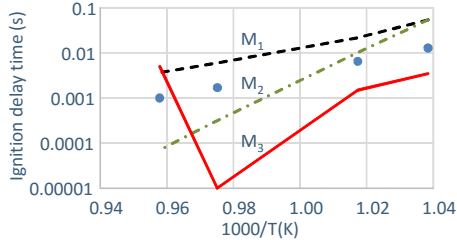


Whenever a modification or a new species is introduced, the whole mechanism must be carefully checked and validated. **Automatic validation** is then very useful (almost indispensable)

Error definition

Which model performs best?

stoichiometric H₂/O₂/Ar/N₂ oxidation in RCM



EFV (M₁) = 213

EFV (M₂) = 203

EFV (M₃) = 168

Model M3 performs best



Error Function Value (EFV)

$$EFV = \frac{1}{N} \sum_{i=1}^N \left[\frac{1}{n_i} \sum_{j=1}^{n_i} \left(\frac{Y_{ij}^{sim} - Y_{ij}^{exp}}{\sigma(Y_{ij}^{exp})} \right)^2 \right]$$

Where:

$$Y_{ij} = \begin{cases} Y_{ij} & \text{if } \sigma(Y_{ij}^{exp}) \cong \text{constant} \\ \ln(Y_{ij}) & \text{if } \sigma(\ln(Y_{ij}^{exp})) \cong \text{constant} \end{cases}$$

N number of datasets
 n_i number of data in each i-th dataset
 Y_{ij}^{exp} j-th experimental observation of the i-th dataset
 Y_{ij}^{exp} corresponding value from numerical simulation
 σ(Y_{ij}^{exp}) standard deviation

Error function value based on the sum of the squared errors does not take into account the shape of the curves

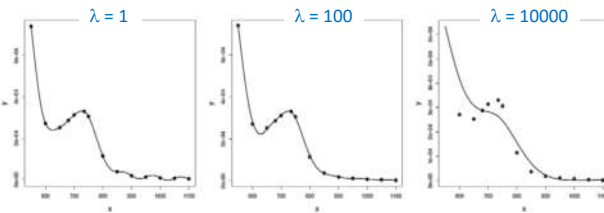


Curve matching

The curve shape requires to compare not only values, but also derivatives. Thus the general idea of the approach (**curve matching**) is to transform the experimental and modeling data in two derivable function f(x) and g(x), respectively. The functional estimation is achieved by spline smoothing (5th order) with a roughness penalty.

$$\hat{f} = \underset{f \in F}{\operatorname{argmin}} \left[\underbrace{\sum_{i=1}^n (y_i - f(x_i))^2}_{\text{SSE}} + \lambda \underbrace{\int (f''(x))^2 dx}_{\text{Smoothing}} \right]$$

Smoothing is necessary to avoid curve overfitting. A large smoothing parameter (λ) results in a smooth curve (a straight line in the limit) and a smaller λ leads to a more rough curve. The optimal λ can be chosen by cross-validation



$$\lambda_{opt} = \underset{\lambda \in R^+}{\operatorname{argmin}} GCV_1(\lambda)$$

$$GCV_1 = \frac{n \sum_{i=1}^{n-1} (y'_i - \hat{f}'(x_i))^2}{(n - NoP)^2}$$

y'_i experimental data first derivative computed with centered differences
 f'(x_i) first derivative of the spline
 NoP Number of Spline parameters

GCV₁ (Generalized Cross-Validation) evaluates the goodness of the spline split. Numerator accounts for derivative agreement. Denominator penalizes the "model complexity" avoiding the overparameterization of the spline.

Similarity indexes

Definition of the norm of the function $f(x)$

$$\|f\| = \sqrt{\int_a^b f(x)^2 dx}$$

a, b minimum and maximum of the abscissa of the experimental data, respectively

Distance

$$d_{L_2}^0(f, g) = \frac{1}{1 + \frac{\|f - g\|}{|D|}} \in (0, 1)$$

Generalization to the continuous case of the Sum of Squared Errors. Particularly, the integration of the norm allows to compute a difference in terms of areas instead of a sum of punctual differences

$$d_{L_2}^1(f, g) = \frac{1}{1 + \frac{\|f' - g'\|}{|D|}} \in (0, 1)$$

Same as previous, applied to derivatives. It considers as perfectly similar two functions that differ only by a vertical translation: $d_{L_2}^1(f, f + a) = 0$

D is the intersection between the domains of the two functions f and g

Similarity

$$d_p^0(f, g) = 1 - \frac{1}{2} \left\| \frac{f}{\|f\|} - \frac{g}{\|g\|} \right\| \in (0, 1)$$

considers as perfectly similar two functions that differ only by a vertical dilation: $d_p^0(f, f \times a) = 0$

$$d_p^1(f, g) = 1 - \frac{1}{2} \left\| \frac{f'}{\|f'\|} - \frac{g'}{\|g'\|} \right\| \in (0, 1)$$

considers as perfectly similar two functions that differ only by a vertical affine transformation (translation and dilation): $d_p^1(f, f \times a + b) = 0$

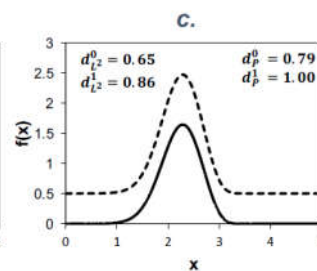
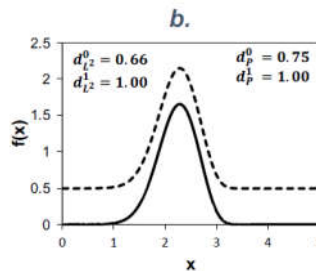
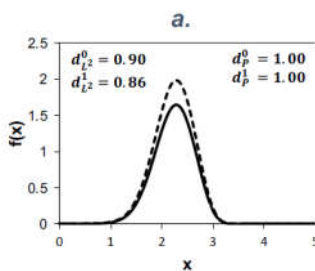
If $f \rightarrow g$ all indices tends to 1: **0** = bad (f and g very different) **1** = good (f and g very similar)

A few examples

- a. $g(x) = a \times f(x)$
- b. $g(x) = f(x) + b$
- c. $g(x) = a \times f(x) + b$

with

$a = 1.2$ $b = 0.5$

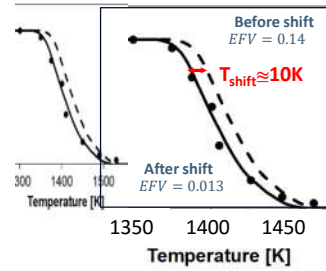


Shift problem

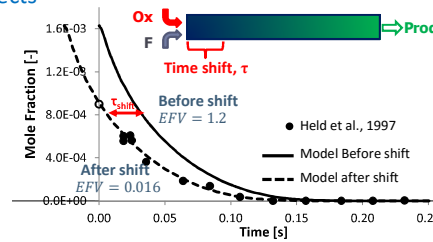
Difference between model and experiments because of x axis uncertainty.

Examples:

Small uncertainty in the measurements of the x variable can produce a large deviation in the y variable



The already discussed flow reactor case: mixing effects at the reactor inlet cause an early reaction. This is typically considered via a 'manual' shift of the time coordinate



Shift index

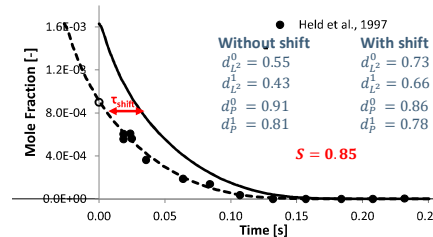
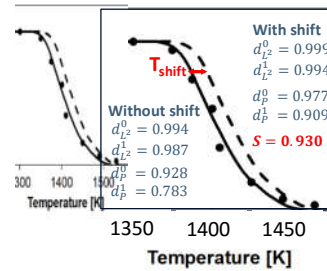
An automatic index for shift evaluation is introduced in the Curve matching approach:

Shift index (S)

$$S = \max\left(1 - \frac{|\delta|}{D}, 0\right) \in (0, 1)$$

Where δ is the domain shift optimizing the alignment, or in other words, maximizing the similarity indexes:

$$\delta = \operatorname{argmax}_{\delta} (d_{L_2}^0 + d_{L_2}^1 + d_P^0 + d_P^1)$$



Global model performance

Model performance can be assumed as a weighted average of all the similarity indexes:

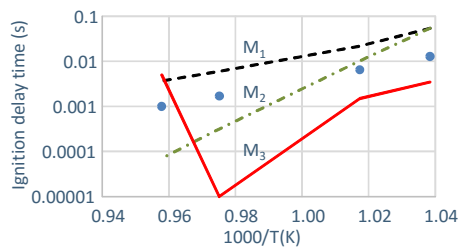
$$CM = \frac{d_{L_2}^0 + d_{L_2}^1 + d_P^0 + d_P^1 + 2S}{6} \in (0, 1)$$

One single value can summarize the model accuracy in respect of a single dataset or of the whole datasets.

It is then possible to not only get the general performance of the model but also to identify where it works better or where (in which conditions) it is less reliable

Anomalous case application

stoichiometric $H_2/O_2/Ar/N_2$ oxidation in RCM



EFV (M_1) = 213

EFV (M_2) = 203

EFV (M_3) = 168

Model M3 performs best



CM (M_1) = 0.801

CM (M_2) = 0.783

CM (M_3) = 0.741

Model M1 performs best



Accounting for experimental error

- Experimental points affected by **uncertainty**
- The higher experimental **uncertainty**, the higher the **variability** of the performance indices
- Need to keep it into account to identify the **confidence interval** of the performance indices

Bootstrap

Random generation of exp datasets with a normal distribution

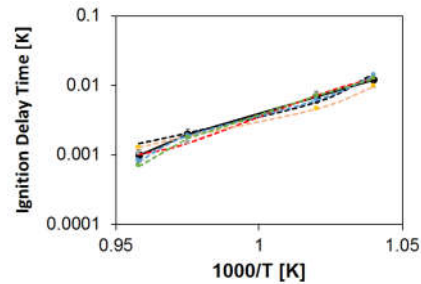
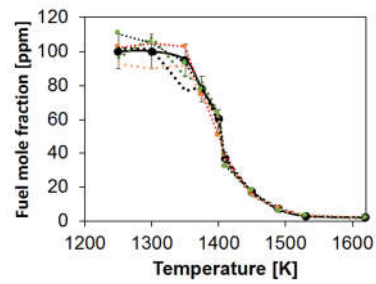
- Data point as the mean value
- Uncertainty as the standard deviation

Curve matching is performed with each generated dataset as reference curve

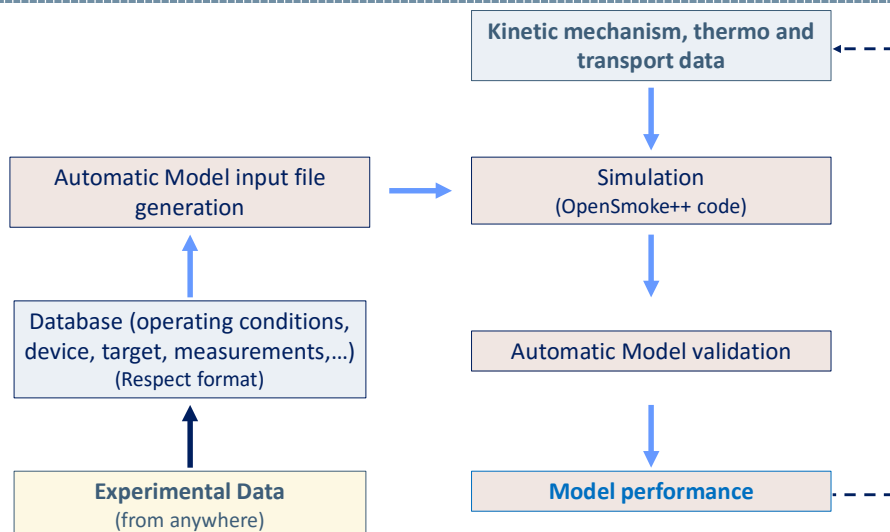
$$M = \frac{\sum_{i=1}^N M_i}{N} \pm s \left(= \sqrt{\frac{\sum_{i=1}^N (M_i - M)^2}{N - 1}} \right)$$

Performance index

Confidence interval



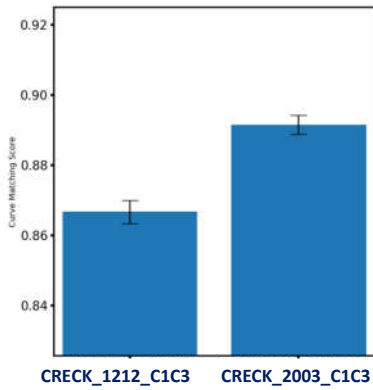
Automatic validation



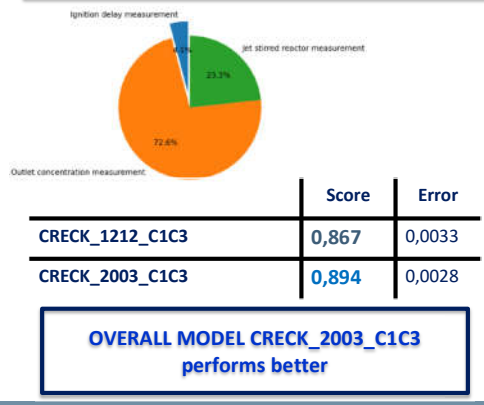
Practical example

Two different models tested

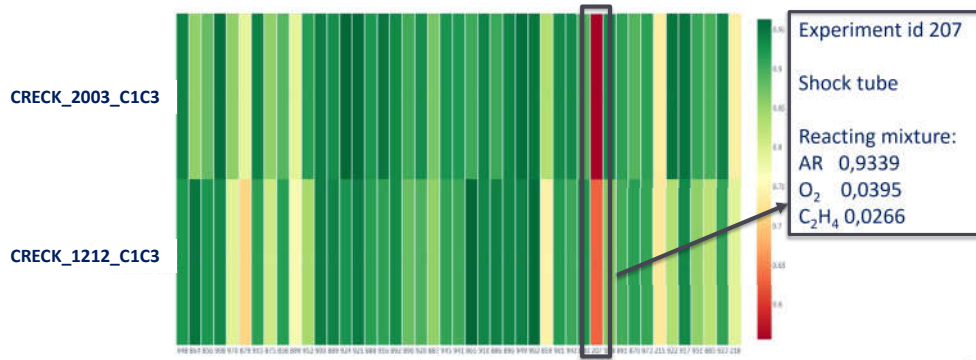
- CRECK_1212_C1C3
- CRECK_2003_C1C3



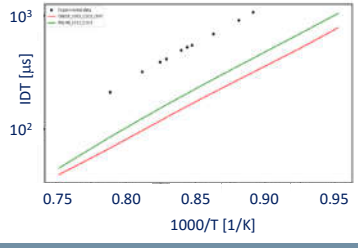
- Ignition Delay Measurement
- Laminar Burning Velocity Measurement
- Outlet Concentration Measurement
- Concentration Time Profile Measurement
- Jet Stirred Reactor Measurement
- Burner Stabilized Speciation Measurement
- Direct Rate Coefficient Measurement



Looking closer



Experiment_ID: 207	Score	Error	d _{L2} ⁰	d _{L2} ¹	d _p ⁰	d _p ¹	Shift
POLIMI_1212_C1C3	0,6300	0,0110	0,7208	0,5014	0,9095	0,8234	0,4125
CRECK_2003_C1C3	0,5554	0,0111	0,7223	0,4981	0,9125	0,8363	0,1815



RECAP

Real fuels oxidation modeling requires large number of species and reactions.

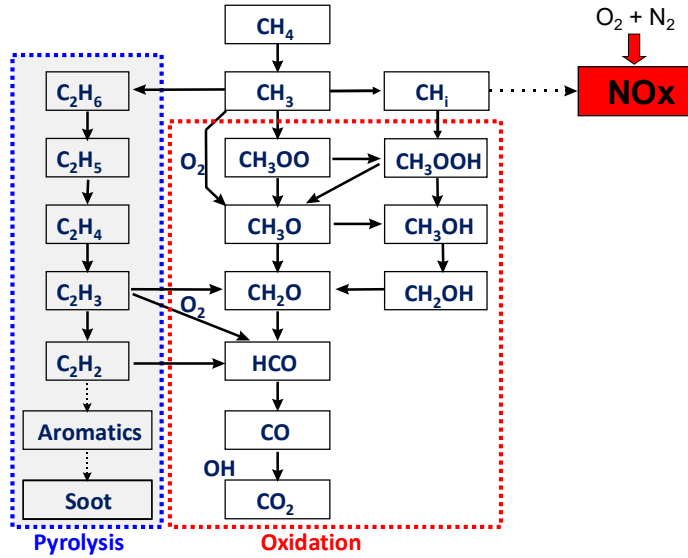
Lumping can be a useful tool to control the mechanism dimension

- ✓ Horizontal lumping groups together isomers of similar reactivity
- ✓ Vertical lumping reduces the number of species of a family
- ✓ Mechanism generation approach can be based on lumping
- ✓ Master Equation based Lumping allows to neglect species with very low characteristic times
- ✓ Automatic validation can be a key tool in the development
 - Curve matching a solution to compare data and predictions, accounting for shapes and not only distances.

Kinetics and time-dependent system

Emissions

Methane Oxidation: complexity increases



NO_x

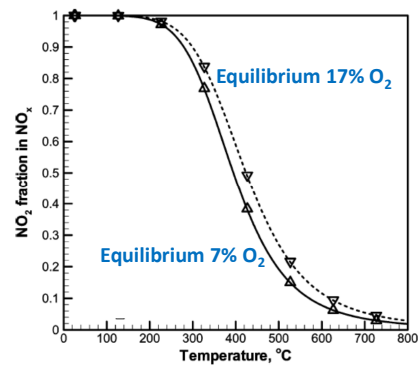
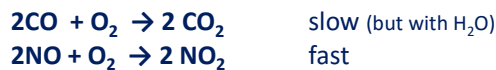
CO/CO₂ equilibrium depends on temperature.
At low T, CO₂ is more stable.
At high T, CO is more stable



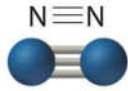
NO/NO₂ equilibrium depends on temperature.
At low T, NO₂ is more stable.
At high T, NO is more stable

In flames NO and CO are especially formed.
In the environment CO₂ and NO₂ are present.

Reaction rates are very different



NOx formation

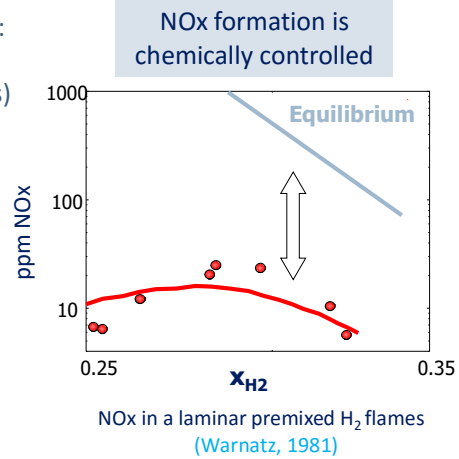
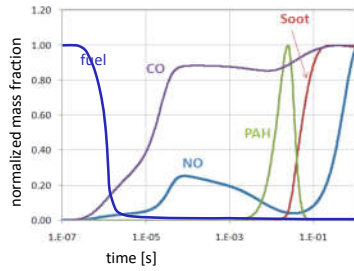


One of the strongest bonds

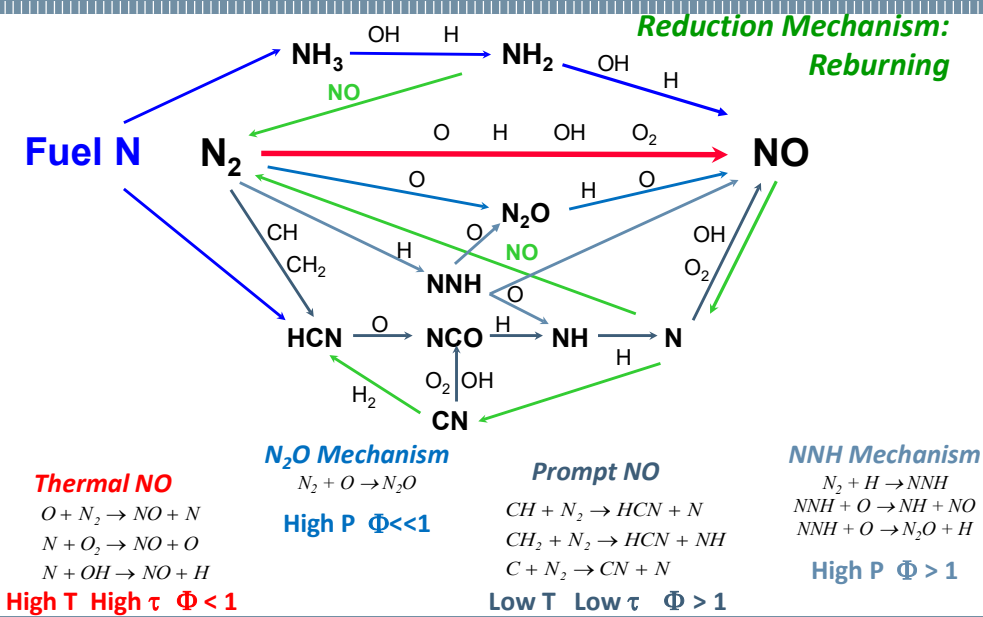
226 kcal/mol

High energy is required to break this bond:

- high temperatures
- very reactive reactants (CH radicals)
- long chemical time



NOx formation mechanism



Thermal NOx (Zel'dovich, 1946)

The **Thermal or Zel'dovich mechanism** consists of three major reactions:



The concentration of O· and OH· radicals are ruled by combustion mechanism.

Rate of NO formation is:

$$\frac{d[\text{NO}]}{dt} = k_1[\text{O}][\text{N}_2] + k_2[\text{N}][\text{O}_2] + k_3[\text{N}][\text{OH}]$$

The **Steady State Approximation for N radicals** gives:

$$\frac{d[\text{N}]}{dt} = k_1[\text{O}][\text{N}_2] - [\text{N}]\{k_2[\text{O}_2] + k_3[\text{OH}]\} \cong 0 \quad [\text{N}] = \frac{k_1[\text{O}][\text{N}_2]}{k_2[\text{O}_2] + k_3[\text{OH}]}$$

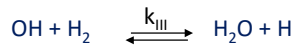
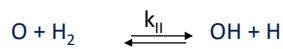
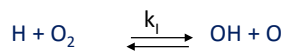
By substituting [N], NO formation rate becomes:

$$\frac{d[\text{NO}]}{dt} = k_1[\text{O}][\text{N}_2] + k_2[\text{N}][\text{O}_2] + k_3[\text{N}][\text{OH}] = 2k_1[\text{O}][\text{N}_2]$$

Thermal NOx is the important contribution at high T

The first reaction is the rate controlling step: it requires the breaking of the tight N₂ bond and is favored at high temperatures. The [O] concentration is obtained by using the partial equilibrium assumption for $\text{O}_2 \leftrightarrow 2 \text{O}$

Partial Equilibrium and Radical concentration



Partial equilibrium (T > 1800 K)

At high temperatures, reactions very fast can be assumed in partial equilibrium

$$k_{I1}[\text{H}][\text{O}_2] = k_{I1r}[\text{OH}][\text{O}]$$

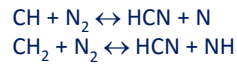
$$k_{II1}[\text{O}][\text{H}_2] = k_{II1r}[\text{OH}][\text{H}]$$

$$k_{III1}[\text{OH}][\text{H}_2] = k_{III1r}[\text{H}_2\text{O}][\text{H}]$$

$$\left\{ \begin{aligned} [\text{H}] &= \sqrt{\frac{k_{I1f}k_{II1f}k_{III1f}^2[\text{O}_2][\text{H}_2]^3}{k_{I1r}k_{II1r}k_{III1r}^2[\text{H}_2\text{O}]^2}} \\ [\text{O}] &= \sqrt{\frac{k_{I1f}k_{III1f}[\text{O}_2][\text{H}_2]}{k_{I1r}k_{III1r}[\text{H}_2\text{O}]}} \\ [\text{OH}] &= \sqrt{\frac{k_{I1f}k_{II1f}[\text{O}_2][\text{H}_2]}{k_{I1r}k_{II1r}}} \end{aligned} \right.$$

Prompt NO_x (Fenimore, 1971)

Under practical conditions, often the amount of NO formed in new burners is higher than Thermal NO_x. Moreover, NO formation is observed in rich conditions, too. The **prompt NO mechanism** involve the initial reaction of N₂ with CH and CH₂, producing NCN, HCN (hydrogen cyanide) and the H and NH radicals:



The HCN and NH formed undergo further reactions forming N (Bowman 1973):



N is then oxidized with the previous thermal NO_x reactions.

N₂O mechanism (Correa, 1992)

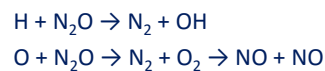
N₂O Mechanism

Important in lean combustion in gas turbines.

At low temperatures and high pressures, a contribution in fuel-lean mixtures is due to:



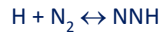
At high Temperatures, N₂O is removed by:



The lifetime of N₂O is less than 10 ms at 1500 K, then the mechanism is active only at realivly low-T.

NNH mechanism (Bozzelli and Dean , 1995)

At high temperatures, especially in rich conditions, H radical can directly add on nitrogen, forming the NNH radical,



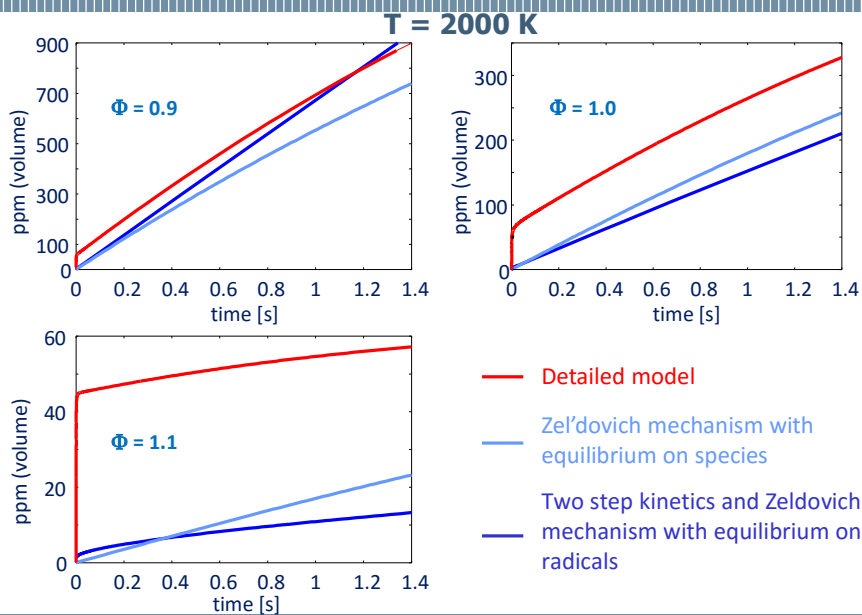
whose typical life time is of a few nanoseconds. This means that NNH attains steady-state conditions. The characteristic time is enough to allow further bimolecular reactions.

In particular, NNH can react with O atom:



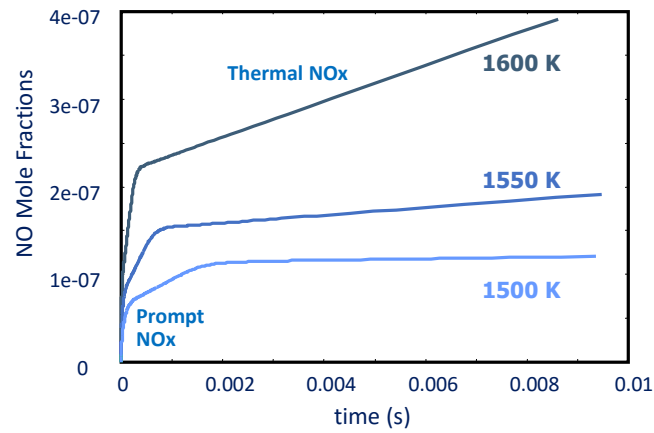
Together with rich conditions (which favor H formation), high pressure facilitates the mechanism, having the H₂ addition reaction a reduction in the number of moles.

Simplified and detailed models



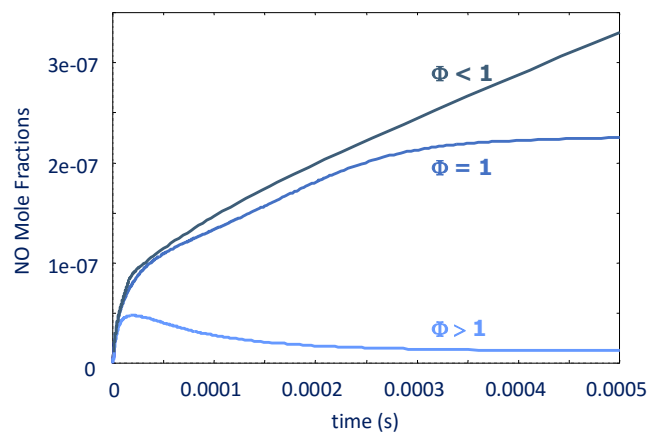
Temperature effect on NO_x formation

Stoichiometric CH₄ Combustion in air
(characteristic time becomes 10⁻² s vs. 10⁻⁵ s for CO conversion)



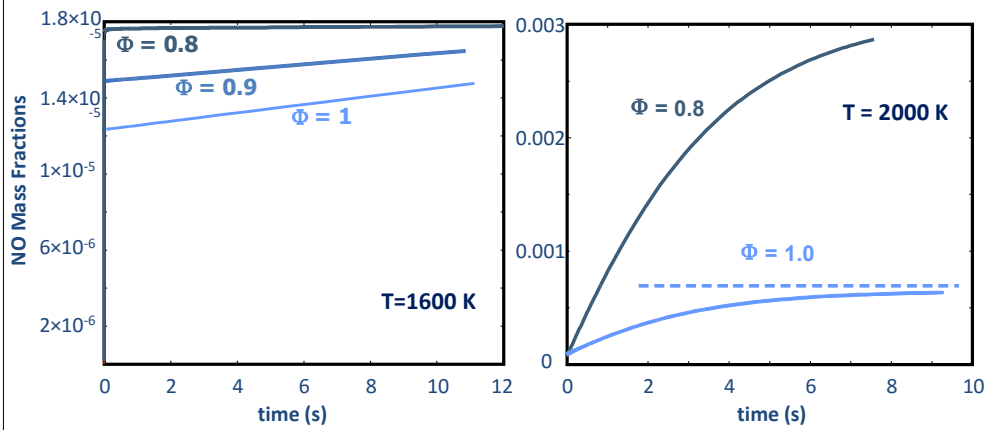
Equivalence ratio (Φ) effect on NO_x formation

CH₄ Combustion in air at 1600 K

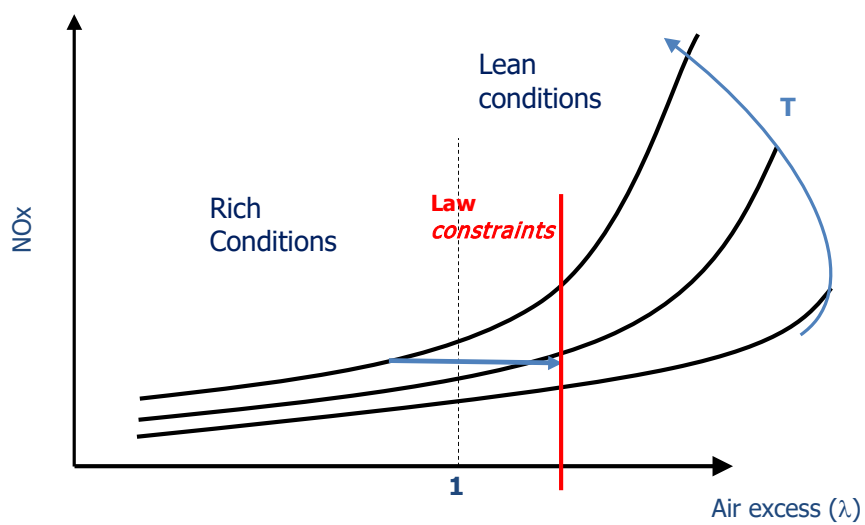


T and Φ effect on NO_x formation

CH₄ Combustion in air

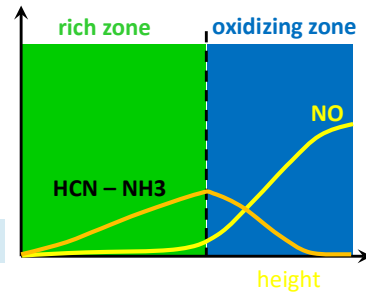
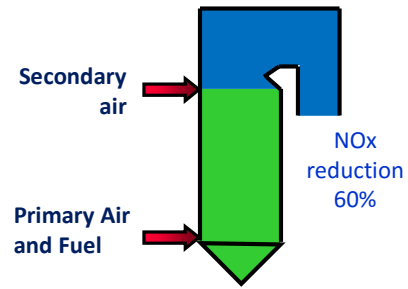
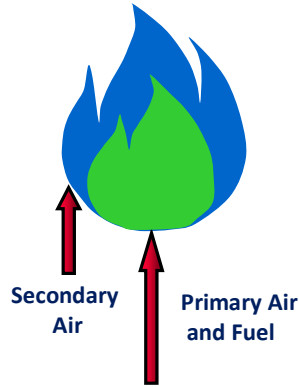


T and Φ effect summary



Air staging technique

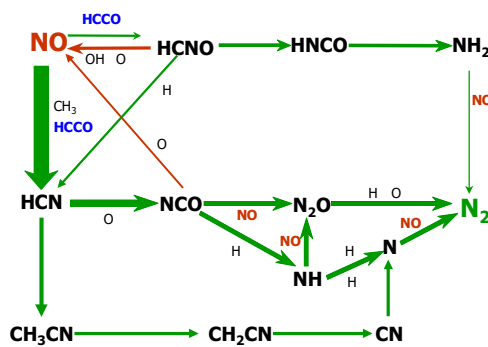
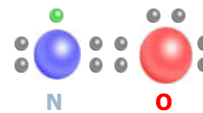
Postcombustion zone (OFA)
 Primary rich combustion zone



Rich, sooting and unstable primary flame

Reburning kinetics

NO has an unpaired electron:
 in between molecule and radical

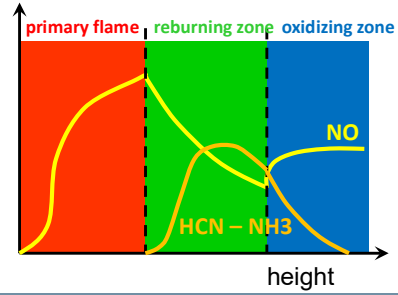
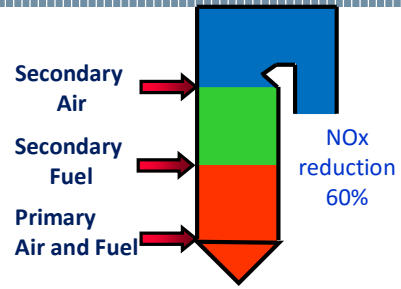
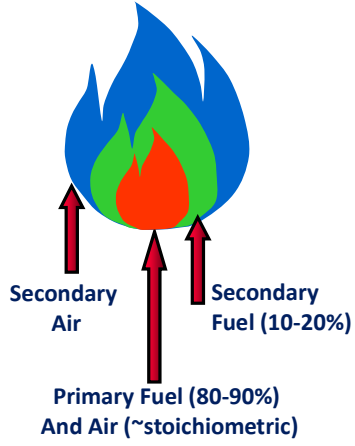


Reburning technique

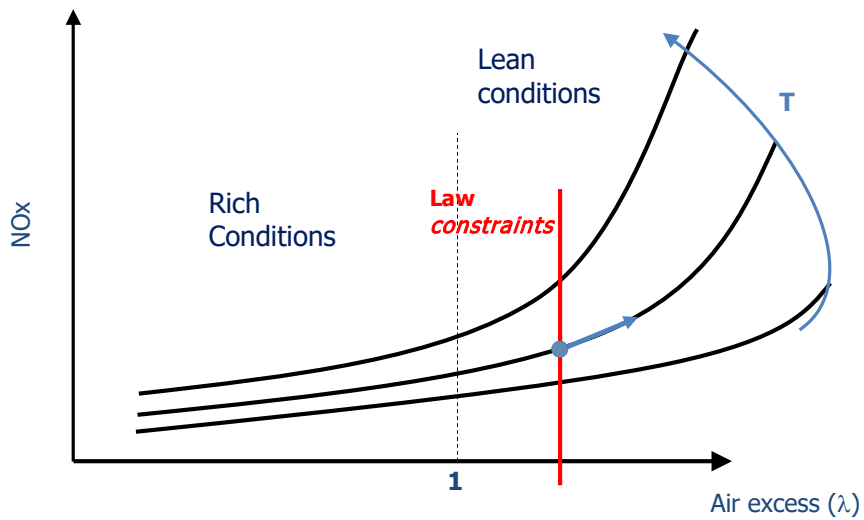
Postcombustion zone (OFA)

Reducing (reburning) zone

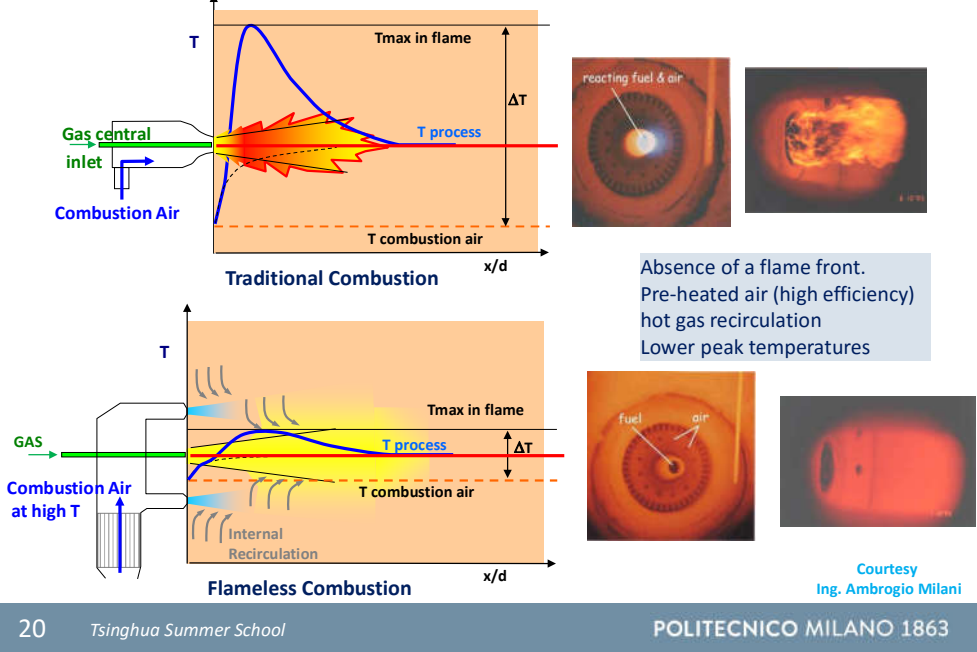
Stoichiometric flame



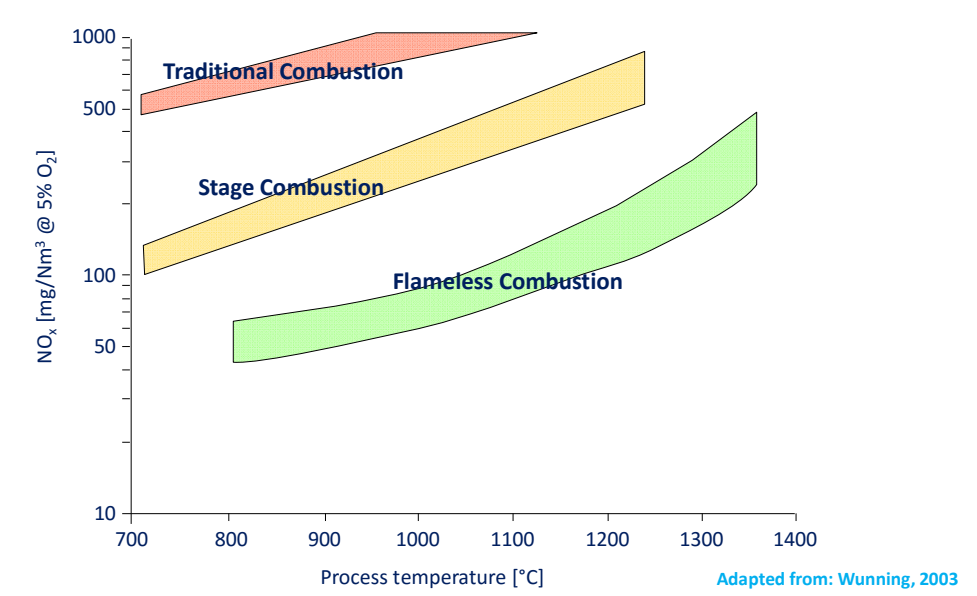
T and Φ effect summary



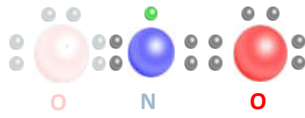
Flameless combustion



NOx emissions



NO electron structure

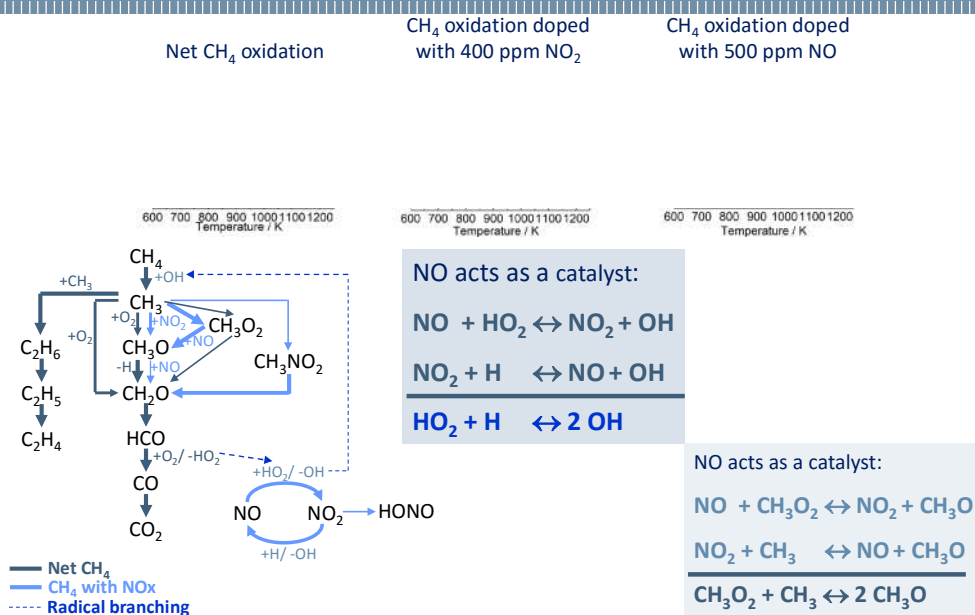


The unpaired electron, even though stabilized, makes NO and (NO₂) very reactive. It acts in some case like a low reactive radical.

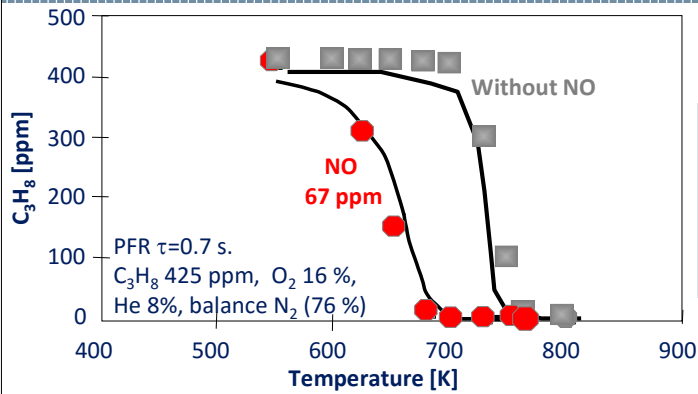
Thus, NO affects combustion process and ignition times

At low temperatures (700-950 K) it can be important in the engines

NOx – CH₄ interactions



NO – C₃H₈ interactions



NO acts as a catalyst:



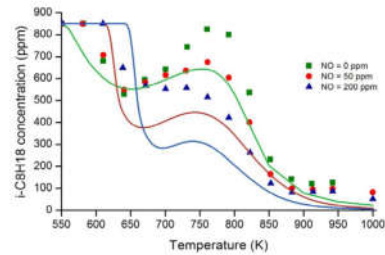
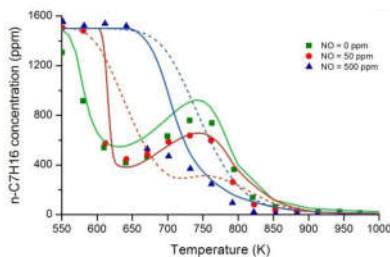
- Small NO doping increases the reactivity of about 100 K.
- Without NO addition, concentration profile is less sharp

NO acts as a catalyst:



(Nelson and Haynes, 1996)

NO – hydrocarbons interactions

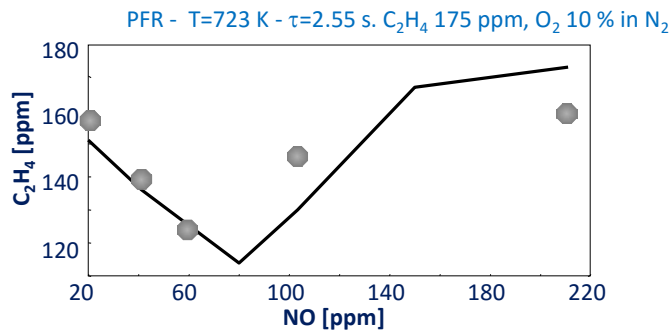


At low temperatures, NO addition inhibits reactivity. The effect vanishes as temperature rises, it persists up to 600 K with 50 ppm NO and 670 K with 500 ppm.

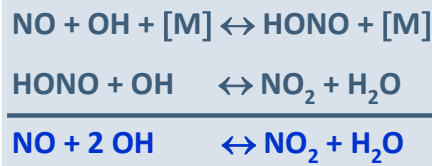
NO inhibits the reaction at 600-650 K (LT mechanism), whereas accelerates it at higher temperatures (NTC region).

An increasing addition of NO
 -shifts the cool flame temperature window towards higher T
 -reduces the NTC
 -makes easier the transition to high T ignition

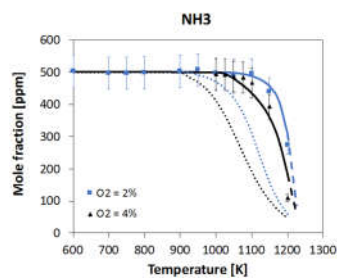
NO – hydrocarbons interactions: inhibiting effect



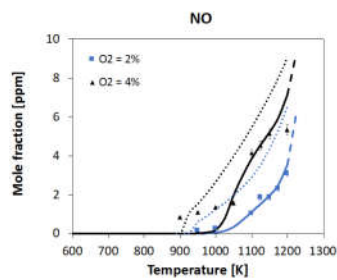
Large amounts of NO inhibit the reactivity, because NO acts as a radical scavenger



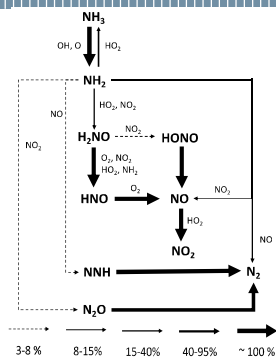
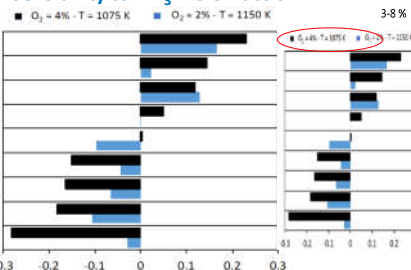
Ammonia oxidation at low T



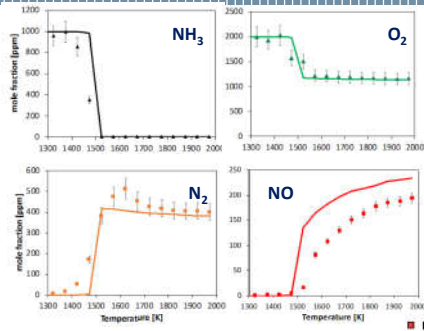
- Jet-Stirred Reactor data obtained in Nancy in diluted conditions
- Literature models predict an **earlier reactivity** (~100 K)
 - Low-temperature reactivity governed by O₂ initiation



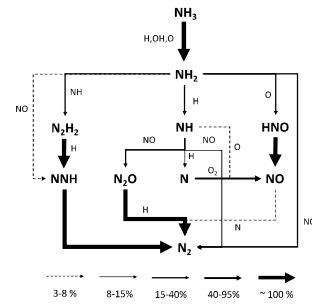
Sensitivity to NH₃ mole fraction



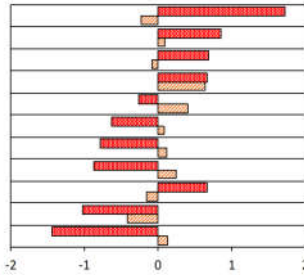
Ammonia oxidation at high T



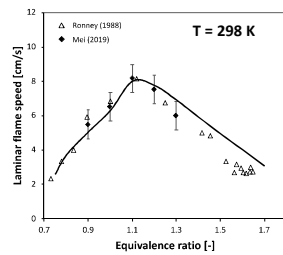
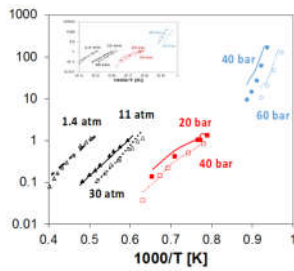
Flow reactor data obtained in Nancy



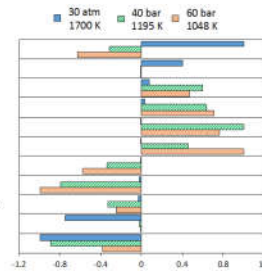
- R23: $\text{NH}_2 + \text{O} \rightarrow \text{H} + \text{HNO}$
- R28: $\text{HNO} \rightarrow \text{H} + \text{NO}$
- R23: $\text{NH}_2 + \text{O} \rightarrow \text{H} + \text{HNO}$
- R6: $\text{NH}_2 + \text{O}_2 \rightarrow \text{HO}_2 + \text{NH}$
- $\text{N}_2\text{O} + \text{H} \rightarrow \text{N}_2 + \text{OH}$
- R16: $\text{NH}_2 + \text{NO} \rightarrow \text{N}_2 + \text{H}_2\text{O}$
- R20: $\text{NH}_2 + \text{H} \rightarrow \text{NH} + \text{H}_2$
- R3: $\text{NH}_2 + \text{OH} \rightarrow \text{NH}_2 + \text{H}_2\text{O}$
- $\text{H}_2 + \text{OH} \rightarrow \text{H} + \text{H}_2\text{O}$
- R2: $\text{NH}_2 + \text{H} \rightarrow \text{NH}_2 + \text{H}_2$
- R27: $\text{NH} + \text{NO} \rightarrow \text{N}_2 + \text{O} + \text{H}$



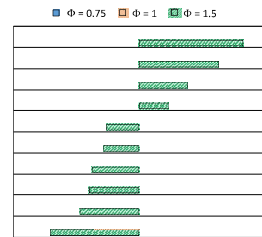
- HNO decomposition drives NO formation
- H-abstractions on NH_3 also affect NO/N_2 ratio



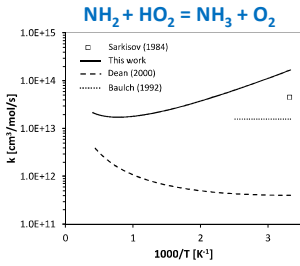
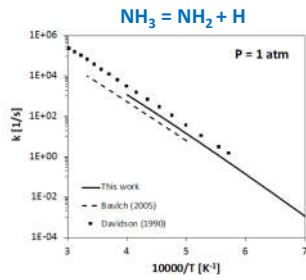
- R6: $\text{NH}_2 + \text{O}_2 \rightarrow \text{NH}_2 + \text{HO}_2$
- R11: $\text{NH}_2 + \text{NH}_2 \rightarrow \text{H}$
- R17: $\text{NH}_2 + \text{NO} \rightarrow \text{NNH} + \text{OH}$
- R36: $\text{H}_2\text{NO} + \text{O}_2 \rightarrow \text{HNO} + \text{HO}_2$
- R15: $\text{NH}_2 + \text{HO}_2 \rightarrow \text{H}_2\text{NO} + \text{OH}$
- R18: $\text{NH}_2 + \text{NO}_2 \rightarrow \text{H}_2\text{NO} + \text{NO}$
- R19: $\text{NH}_2 + \text{NO}_2 \rightarrow \text{N}_2\text{O} + \text{H}_2\text{O}$
- R16: $\text{NH}_2 + \text{NO} \rightarrow \text{N}_2 + \text{H}_2\text{O}$
- R35: $\text{H}_2\text{NO} + \text{NH}_2 \rightarrow \text{NH}_2 + \text{HNO}$
- R2: $\text{NH}_2 + \text{H} \rightarrow \text{NH}_2 + \text{H}_2$
- R3: $\text{NH}_2 + \text{OH} \rightarrow \text{NH}_2 + \text{H}_2\text{O}$



- $\text{NH}_2 + \text{NH} \rightarrow \text{N}_2\text{H}_2 + \text{H}$
- $\text{NH}_2 + \text{NO} \rightarrow \text{NNH} + \text{OH}$
- $\text{H}_2 + \text{O} \rightarrow \text{H} + \text{OH}$
- $\text{HNO} \rightarrow \text{H} + \text{NO}$
- $\text{NH}_2 + \text{NO} \rightarrow \text{N}_2 + \text{H}_2\text{O}$
- $\text{NH} + \text{NO} \rightarrow \text{N}_2\text{O} + \text{H}$
- $\text{NH}_2 = \text{NH}_2 + \text{H}$
- $\text{N}_2\text{H}_2 + \text{H} \rightarrow \text{NNH} + \text{H}_2$
- $\text{NH}_2 + \text{O} \rightarrow \text{HNO} + \text{H}$
- $\text{H} + \text{O}_2 (+\text{M}) \rightarrow \text{HO}_2 (+\text{M})$



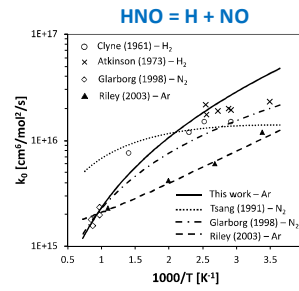
Theoretical rate constant evaluation



High-level quantum chemistry calculation of:

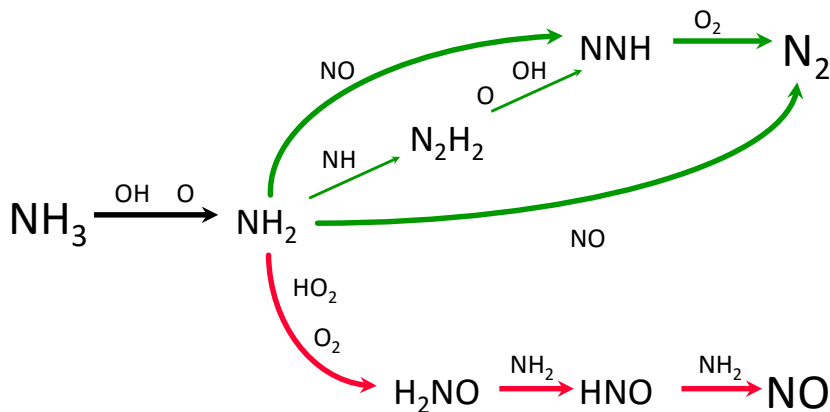
- **Initiation reactions:**
 - $\text{NH}_3 = \text{NH}_2 + \text{H}$
 - $\text{NH}_3 + \text{O}_2 = \text{NH}_2 + \text{HO}_2$
- **H-abstraction reactions:**
 - $\text{NH}_3 + \text{HO}_2/\text{H}/\text{OH}/\text{O} = \text{NH}_2 + \text{H}_2\text{O}_2/\text{H}_2/\text{H}_2\text{O}/\text{OH}$
- **Decomposition reactions:**
 - $\text{HNO} = \text{H} + \text{NO}$

↔ Differences compared to literature ↔



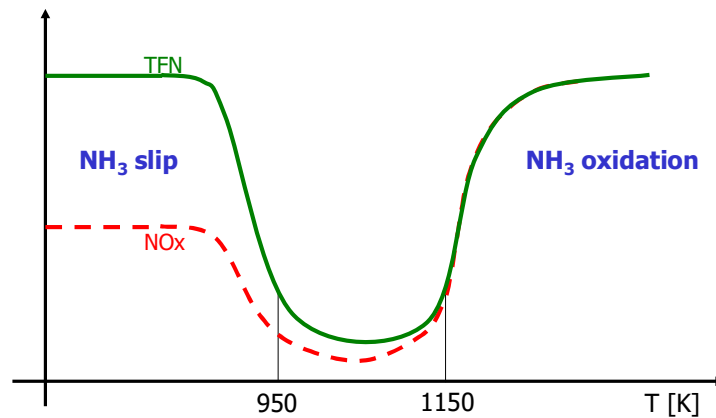
Stagni et al. React Chem Eng 5 (2020)

Ammonia Redox process



There is a competition between the first oxidation to N_2 and the complete oxidation to NO (and NO_2). Temperature controls the competing pathways

SNCR temperature window



Unfortunately there is a quite narrow temperature window, where NH_3 reacts with NO forming N_2

Carbon nanoparticle beauty



S. Mary Magdalen
George de La Tour's (1593-1652)



"You would hardly think that all these substances which fly about London, in the forms of soots and blacks, are the very beauty of the flames..."

Michael Faraday, 1861 'The Chemical History of the Candle'

Carbon nanoparticle ugliness

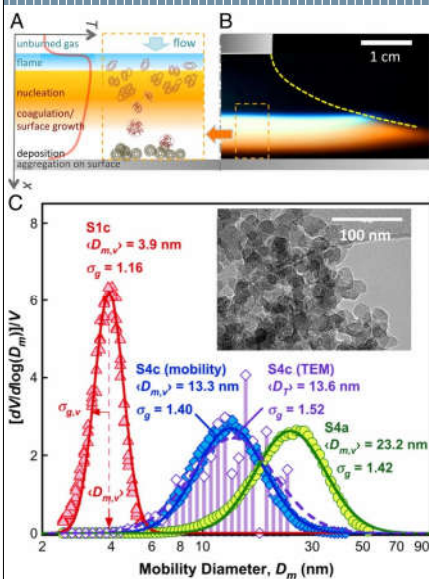


Revealed: every Londoner breathing dangerous levels of toxic air particle
Exclusive: Every area of the capital breaches global standards for PM2.5 pollution particles, with most areas exceeding levels by at least 50%
The Guardian



Smog, Pm10 sopra i limiti: a Milano "l'aria è scadente", divieti in arrivo.
 Superati i 53 giorni di sfornamento dei livelli di inquinanti dall'inizio dell'anno e polveri fuorilegge ininterrottamente da sabato 3: torna l'emergenza.
La Repubblica

Carbon nanoparticle usefulness

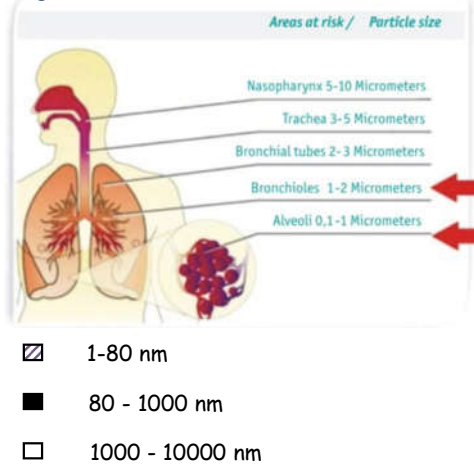
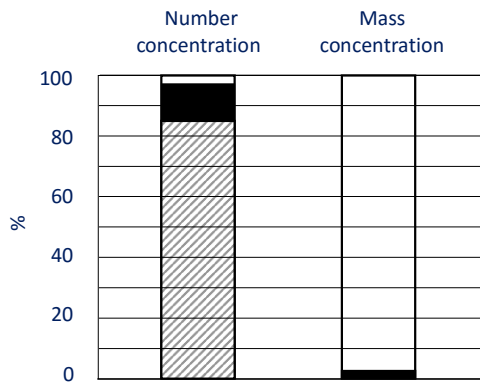


Flame-formed carbon nanoparticles exhibit quantum dot behaviors

C. Liu et al, PNAS, 2019, 116 (26) 12692-12697

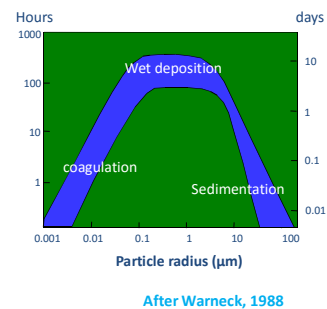
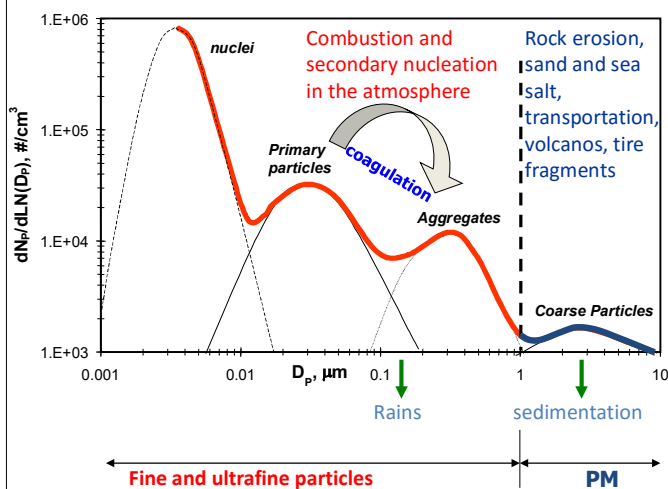
Fine and ultrafine particles and health

Ultrafine Particles are more dangerous than larger ones ^[1].
 Ultrafine Particles are more numerous and with larger surface areas ^[2].



^[1] Oberdorster G. et al., *Inhalation Toxicology*, (2004) 16 (6-7) : 437
^[2] Woo et al., *Aerosol Sci. Technol.*, (2001) 34: 75-87

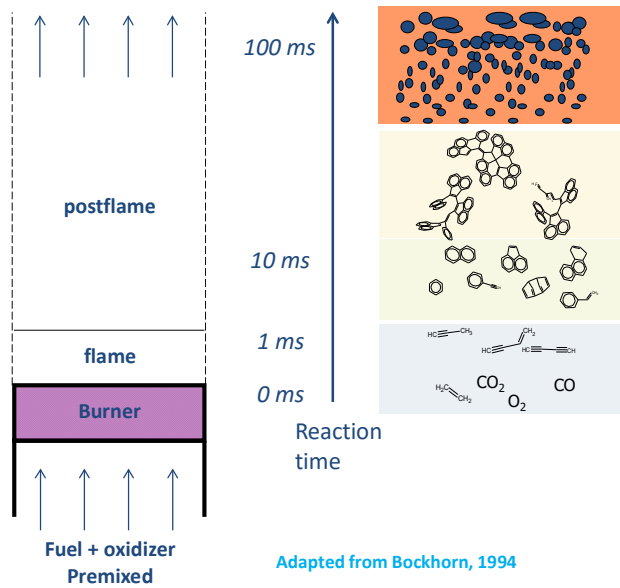
Particles size distribution



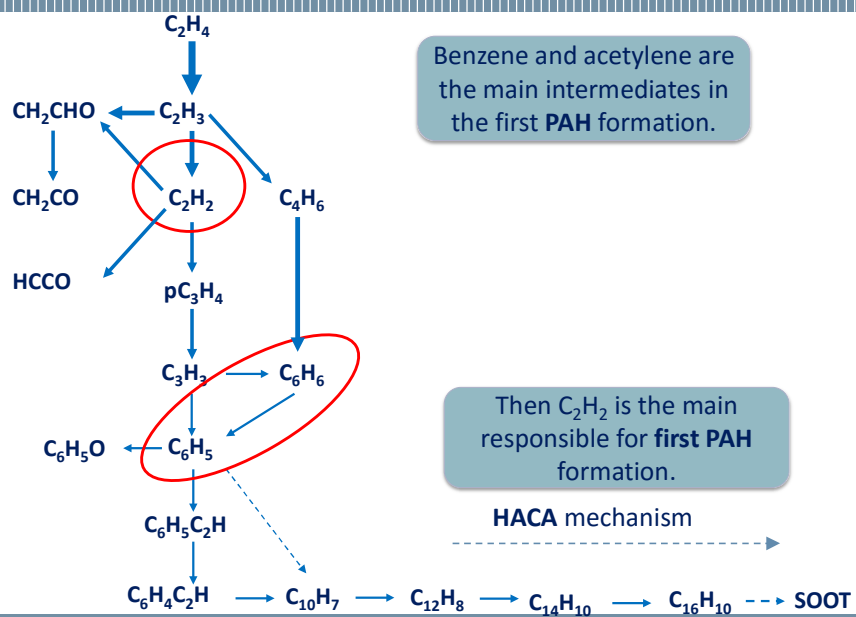
Ultrafine particles (< 0.1 μm) are the main problem

From A. D'Anna (2003)
 Adapted from: Woo et al., (2001)
Aerosol Sci. Technol. 34:75-87

Particles formation



Pyrolysis pathway



First aromatic ring formation

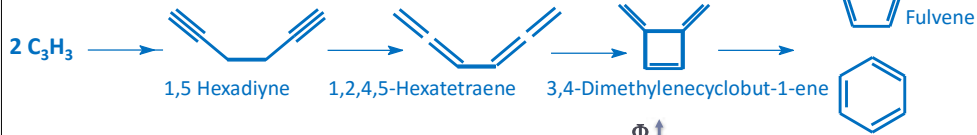
Even mechanism

Frenklach M. and Wang H., (1990). 23rd Symposium (International) on combustion



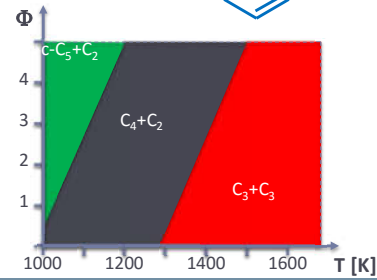
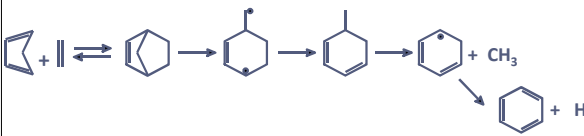
Odd mechanism C₃ + C₃

Huntsman W. D. and Wristers H. J., (1967). J. Amer. Chem. Soc., 89: 342

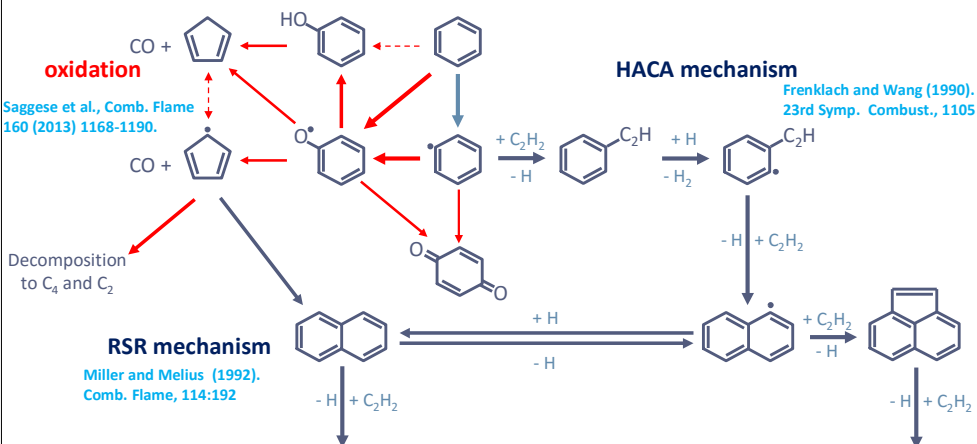


Cy-C₅ + C₂ mechanism

Dente et al., (1979) Comp. & Chem. Eng., 3: 61

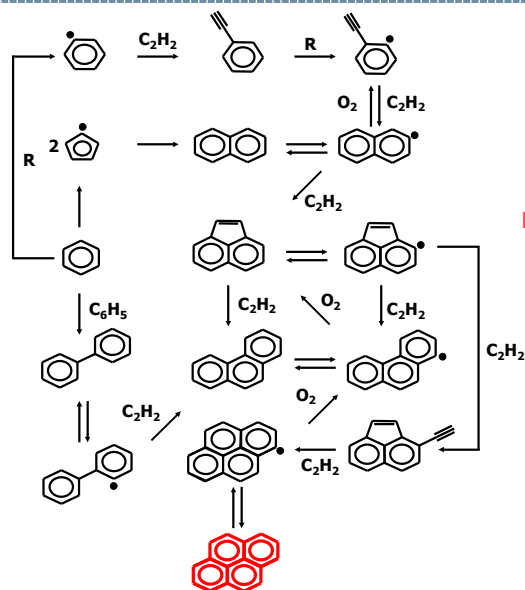


Benzene chemistry



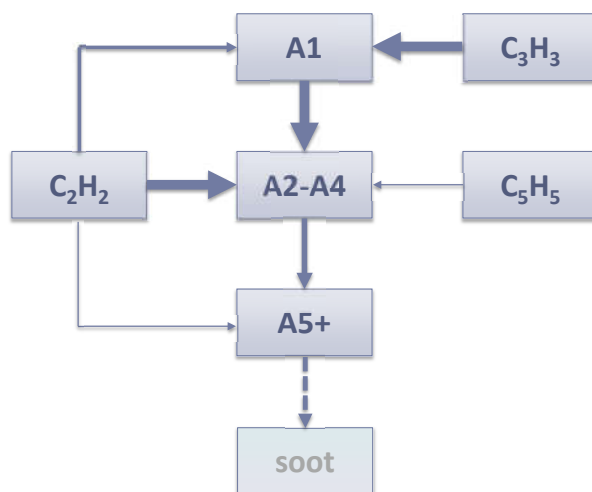
One to four aromatic rings

RSR
Miller and Melius

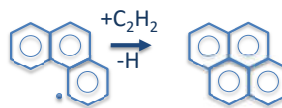
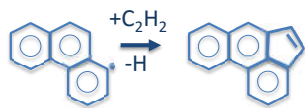


HACA
Frenklach and Wang

Large PAHs



The isomer problem



Some isomers of $C_{16}H_{10}$



Pyrene



Acephenanthrylene



Fluoranthene



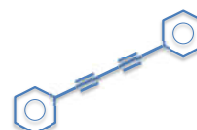
aceanthrylene



1,1'-Biphenyl,2,2'-diethynyl-



indenoindene



Benzene, 1,1'-(1,3-butadiyne-1,4-diyl)bis-

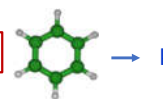
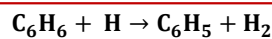
Reaction classes and rate rule based model construction

IDENTIFICATION OF MAIN REACTION CLASSES

Must be possible to assign kinetic parameters through **analogy rules** or **rate rules**
 → all rate constants are similar

THEORETICAL CALCULATIONS OF REFERENCE KINETIC PARAMETERS

EXAMPLE: H-ABSTRACTION BY H FROM THE AROMATIC RING

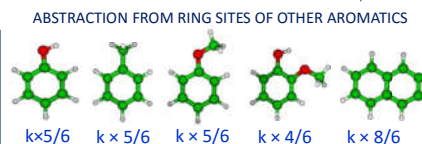


<https://github.com/PACChem/ESTokTP>

Cavallotti et al., *J. Chem. Theory Comput.* 15 (2019) 1122–1145.

EXTENSION OF THOSE PARAMETERS TO THE WHOLE REACTION CLASS

Analogy rules: simple corrections (e.g. number of sites)



MODEL PERFORMANCE ASSESSMENT

Rate rules: corrections of parameters (k_0 , EA..) based on theoretical calculations

- Understand impact of lateral groups or additional rings
- Derive corrections to the reference rates

Hierarchical rate rules for model consistency

THE REACTIVITY OF EACH SPECIES IS DERIVED FROM LOWER LEVELS

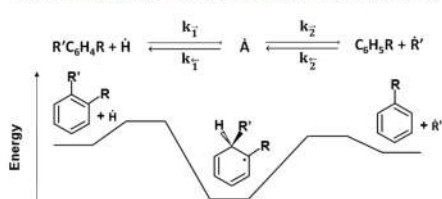
SPECIES	[A1-M][REACTION FAMILY]	[A1,OH-M][REACTION FAMILY]	[A1,OH,OH-M][REACTION FAMILY]
 benzene	[A1-M][BONDFISSION_CH] [A1-M][HABS_R] [A1-M][ADD_O] (IPSO, EL_OH, ISC, ISC_DECO) [A1-M][ADD_O2]		
 phenol	Rate constants: As above *5/6 (number of sites)	[A1,OH-M][BONDFISSION_CO/OH] [A1,OH-M][MOLECULAR_DECO],[EL_H2O] [A1,OH-M][HABS_R] [A1,OH-M][IPSO_H], [IPSO_O]	
 catechol	Rate constants: As above *4/6 (number of sites)	Rate constants: As above *2 (number of sites)	[A1,OH,OH-M] [MOLECULAR_DECO] [A1,OH,OH-M] [EL_H2O]

ADD ONLY PECULIAR REACTIVITY OF OH GROUP

ADD ONLY PECULIAR REACTIVITY OF 2 INTERACTING OH GROUPS

Variations within the same reaction class: rate rules

SYSTEMATIC THEORETICAL INVESTIGATIONS ON EFFECTS OF THE LATERAL GROUPS OF MAHS
 on RATE CONSTANTS FOR H IPSO-SUBSTITUTION REACTIONS



REACTION CLASS(ES):
R' GROUP REPLACEMENT WITH H

SYSTEMATIC INVESTIGATION:
EFFECT OF R LATERAL GROUP – IS THE SAME RATE CONSTANT VALID?

		CLASSES				
R	R'	OH	CH ₃	OCH ₃	CHO	C ₂ H ₅
H						
OH	o					
	m					
	p					
CH ₃	o					
	m					
	p					
OCH ₃	o					
	m					
	p					
CHO	o					
	m					
	p					
C ₂ H ₅	o					
	m					
	p					

■ Ref. rate for each class
■ Effect of lateral group

SET OF
5 + 15 RATE
CONSTANTS



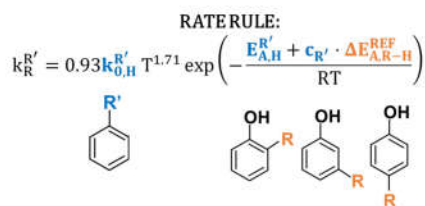
DERIVE A TOTAL
OF 85 RATE
CONSTANTS

How?
Rate rules

Pratali Maffei et al., PCCP, 2020

Variations within the same reaction class: rate rules

SYSTEMATIC THEORETICAL INVESTIGATIONS ON EFFECTS OF THE LATERAL GROUPS OF MAHS
on RATE CONSTANTS FOR H IPSO-SUBSTITUTION REACTIONS



HIGHLIGHTS

- SYSTEMATIC IMPACT OF A LATERAL GROUP R FOR ALL CLASSES
- RATE RULE APPLICABLE FOR DIFFERENT REACTION CLASSES

CLASSES

R \ R'	OH	CH ₃	OCH ₃	CHO	C ₂ H ₅
H					
OH	o				
	m				
	p				
CH ₃	o				
	m				
	p				
OCH ₃	o				
	m				
	p				
CHO	o				
	m				
	p				
C ₂ H ₅	o				
	m				
	p				

■ Ref. rate for each class
■ Effect of lateral group

SET OF
5 + 15 RATE
CONSTANTS



DERIVE A TOTAL
OF 85 RATE
CONSTANTS

How?
Rate rules

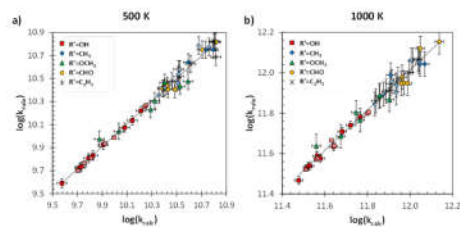
Pratali Maffei et al., PCCP, 2020

Variations within the same reaction class: rate rules

SYSTEMATIC THEORETICAL INVESTIGATIONS ON EFFECTS OF THE LATERAL GROUPS OF MAHS
on RATE CONSTANTS FOR H IPSO-SUBSTITUTION REACTIONS

VERIFY THE RATE RULE WITH A CONTROL SET
OF > 30 CALCULATED RATE CONSTANTS

PARITY PLOTS



CLASSES

R \ R'	OH	CH ₃	OCH ₃	CHO	C ₂ H ₅
H					
OH	o				
	m				
	p				
CH ₃	o				
	m				
	p				
OCH ₃	o				
	m				
	p				
CHO	o				
	m				
	p				
C ₂ H ₅	o				
	m				
	p				

■ Ref. rate for each class
■ Effect of lateral group
■ Set for validation

SET OF
5 + 15 RATE
CONSTANTS



DERIVE A TOTAL
OF 85 RATE
CONSTANTS

How?
Rate rules

Pratali Maffei et al., PCCP, 2020

From 1 to 2 ring : From toluene to α -methyl-naphthalene

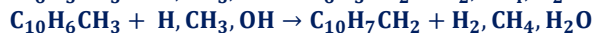
Kinetics of $C_{10}H_7CH_3$ based on the extension of $C_6H_5CH_3$ model



Analogy extension of the model from toluene to AMN:

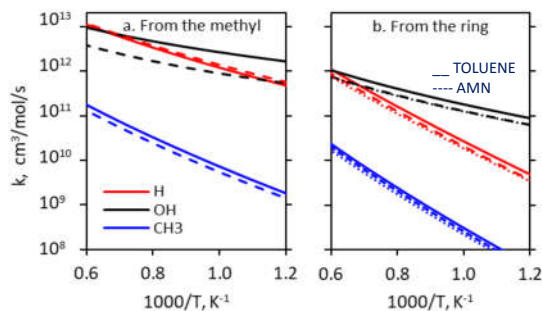
- Symmetry considerations
- Scaling by number of reactive sites

Theoretical validation of analogy rules: H-atom abstraction reactions by H, OH, CH_3 :



Take-home message:

- On average, rate constants for AMN are **lower** than in toluene (factor of 1.2-1.5)
- Different behavior for H-abstraction by **OH**



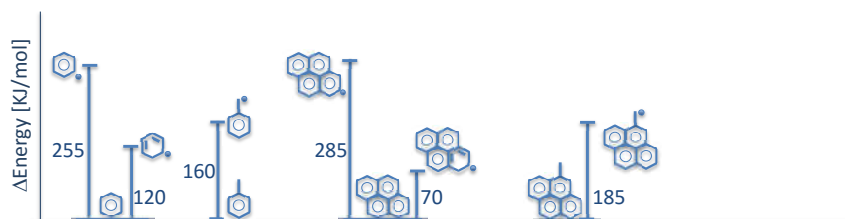
Examples of growth rate rules for PAHs

Growth pathways systematically applied on MAHS/PAHS from 1 up to 4/5 aromatic rings

Reaction class	Applied on	Reference reaction	k_0	α	E_a
MOL+ CH_3	1-3 aromatic rings	$CH_3+C_6H_5C_2H \Rightarrow INDENE+H$	$3.00E+11$	$0.00E+00$	$7.60E+03$
Methyl addition cyclization (MAC)	(XC6H4, C9H8, C13H10)				
RAD+C2H2	2-5 aromatic rings	$C_2H_2+C_{10}H_7=C_{12}H_8+H$	$1.10E+31$	$-4.83E+00$	$2.66E+04$
Hydrogen abstraction carbon addition (HACA)	(C10H7, C12H9, C14H9, C16H9, C18H9)				
RAD+C3H3	1-5 aromatic rings (XC6H4, XC10H6, C12H7, C12H9, C14H9, C16H9, C18H9)	$C_3H_3+C_6H_5 \Rightarrow INDENE$	$5.00E+12$	$0.00E+00$	$3.00E+03$
Radical recombination (RRR)					
RAD+C4H5	1-5 aromatic rings	$C_4H_5+C_6H_5 \Rightarrow C_{10}H_8+2H$	$5.00E+12$	$0.00E+00$	$1.00E+03$
Hydrogen abstraction vinylacetylene addition (HAVA)	(XC6H4, XC10H6, C12H7, C12H9, C14H9, C16H9, C18H9)				
MOL+C6H5 (PAC)	1-4 aromatic rings	$C_6H_5+C_7H_8=C_6H_5CH_2C_6H_5+H$	$1.00E+12$	$0.00E+00$	$8.00E+03$
Phenyl addition dehydrocyclization	(XC6H5, XC10H8, C9H8, C12H8, C6H5XC6H5, C13H10, C14H10, C16H10)				
RSR+C6H5	1-2 aromatic rings	$C_6H_5+C_7H_7=C_6H_5CH_2C_6H_5$	$2.00E+12$	$0.00E+00$	$3.00E+03$
Clustering of hydrocarbons by radical-chain reactions (CHRCR)	(X6H5, XC10H7, C9H7)				

What happens to larger aromatics? Do they still behave in the same way?

PAH Radical stability

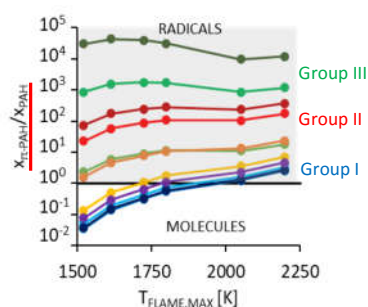
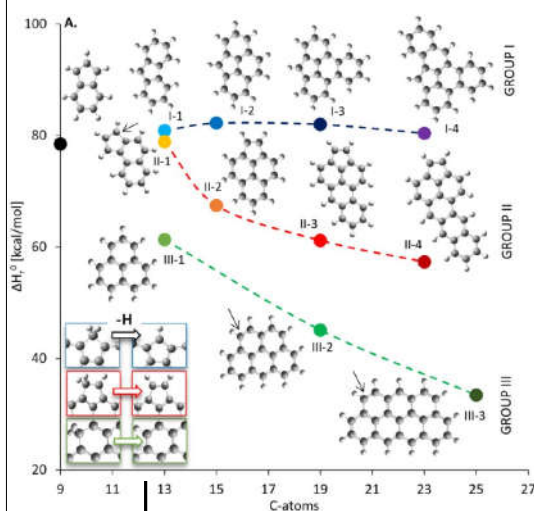


T. Faravelli, ISF meeting 2018

“The experiments show that there is no difference in reactivity between the large open- and closed-shell PAH. The radicals are not of the σ -type with localized reactive sites but π -radicals with no extra reactivity because of delocalization of the unpaired electron. The tendency to form π -radicals increases with the size of the polyaromatic species. Thus, it must be concluded that unpaired electrons in soot particles are also of the π -type and therefore delocalized.”

A. Keller, R. Kovacs and K.-H. Homann, *Phys. Chem. Chem. Phys.*, 2000, 2, 1667-1675

Odd-C-numbered PAHs



Odd-C-PAHs are predominantly π -radicals at flame conditions

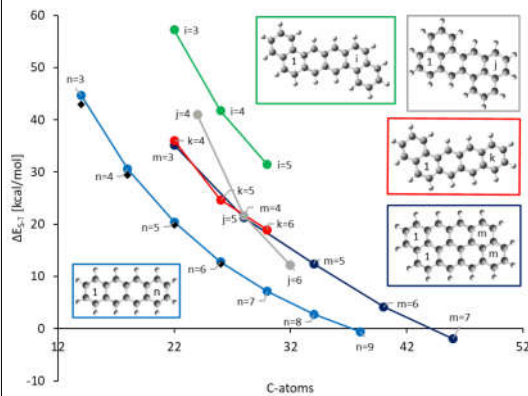
Detailed balance
$$\frac{x_{\pi\text{PAH}\bullet}}{x_{\text{PAH}}} = \exp\left(-\frac{\Delta G_r^0(T)}{RT}\right) \cdot \frac{1}{x_{\text{H}\bullet}} \cdot \frac{P_{\text{rif}}}{P}$$

<https://github.com/PACChem/ESTokTP>

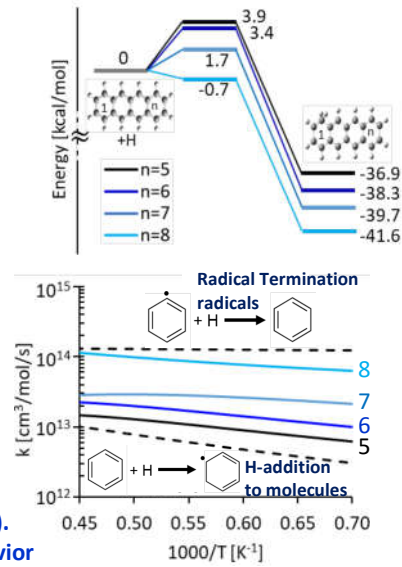
Cavallotti et al. *J. Chem Theory Comput.* 15 (2019) 1122-1145

Even-C-numbered PAHs

Singlet-Triplet energy gap calculations



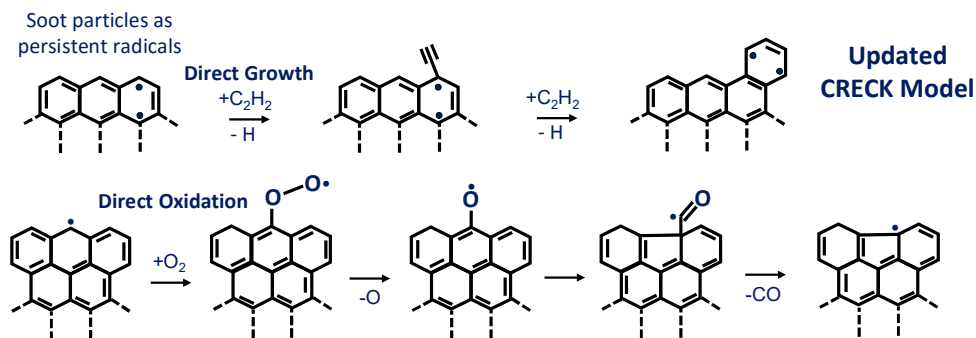
Kinetic analysis



Large acenes have di-radical character (ground state).
Their reactivity is directly related to a radical-like behavior

PAH radical character impact

- Reactivity of closed- and open-shell large PAHs ($n_C > 100$) not distinguished
→ number of lumped-pseudo species (BINS) strongly reduced
- Reference kinetics for soot from gas-phase resonantly stabilized radical (RSR) PAHs
- Discrete Sectional Model



CRECK Soot Discrete Sectional Model

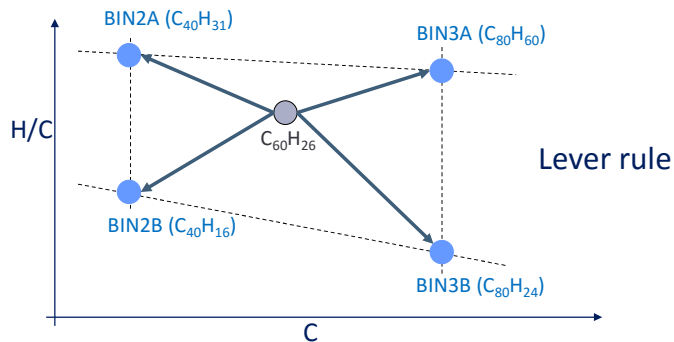
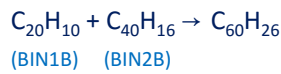
- 25 classes of lumped pseudo-species (BINs) with different H/C
- Spacing factor of 2

Nobili et al., Comb. Flame, 235 (2022) 111692

BIN _i	C atoms	Mass [amu]	D _p [nm]	Main reactions classes	A [$\frac{\text{cm}^3}{\text{mol}\cdot\text{s}}$]	n	E [$\frac{\text{kcal}}{\text{mol}}$]
Heavy PAHs				1. HACA mechanism			
BIN1(•)	20	250	0.81	H• + BIN _i → H ₂ + BIN _i •	5.4·10 ⁸	2	10.5
BIN2(•)	40	500	1.02	C ₂ H ₂ + BIN _i • → products	1.0·10 ¹²	0	10
BIN3(•)	80	1000	1.28	2. Soot inception (i, n < 5)			
BIN4(•)	160	2000	1.60	BIN _i • + BIN _n • → products	1.0·10 ¹²	0	6
				BIN _i + BIN _n → products	1.0·10 ⁹	0.5	0
				BIN _i + BIN _n • → products	1.0·10 ¹²	0	0
Soot Particles				3. Surface growth			
BIN5•	320	4 × 10 ³	2.02	RR + BIN _i • → products	2.0·10 ¹²	0	19
⋮	⋮	⋮	⋮	PAH + BIN _i • → products	5.0·10 ¹⁴	0.5	23
BIN12•	4 × 10 ⁴	4.9 × 10 ⁵	10.11	4. Dehydrogenation			
				BIN _i → H ₂ + BIN _i	1.0·10 ⁸	0	32
				BIN _i • → H• + BIN _i	1.0·10 ¹¹	0	12
				H• + BIN _i → CH ₃ • + products	1.2·10 ¹³	0	5
Soot Aggregates				5. Coalescence and Aggregation (i, n ≥ 13)			
BIN13•	8 × 10 ⁴	9.7 × 10 ⁵	12.73	BIN _i + BIN _n → products	1.6·10 ¹³	0.5	0
⋮	⋮	⋮	⋮				
BIN25•	3.2 × 10 ⁸	3.86 × 10 ⁹	202.12	6. Oxidation			
				OH + BIN _i → products + HCO	1.7·10 ¹⁷	-1	1.6
				O ₂ + BIN _i • → products + CO + H ₂ O	3.5·10 ⁶	1.8	16.5
				O + BIN _i → products + HCCO	2.0·10 ¹³	0	4

Saggese et al., Combustion and Flame 162 (2015) 3356–3369
 Pejpikestakul et al., Fuel 234 (2018) 199–206

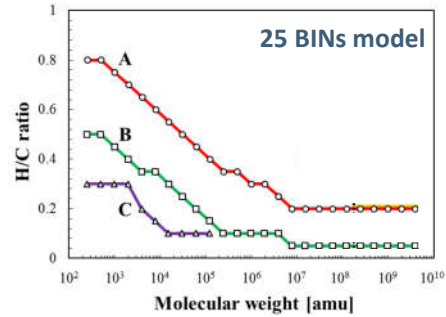
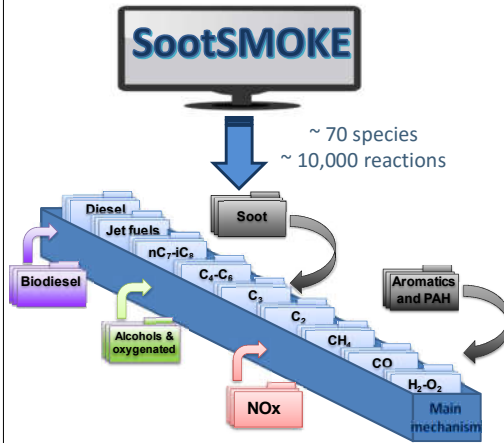
How Discrete Sectional Model works



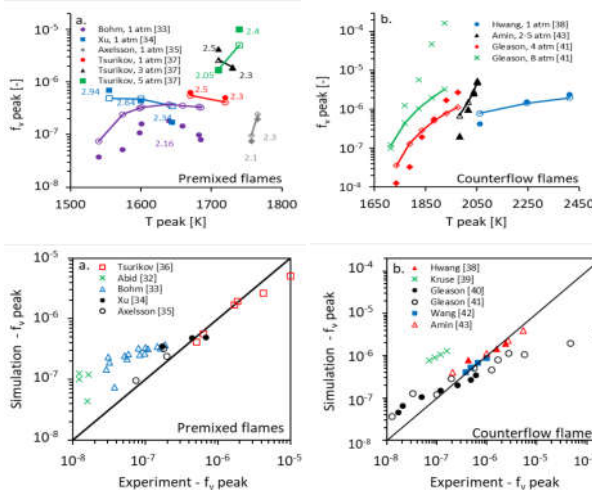
Soot sub-mechanism generator

SootSMOKE is an automated soot sub-mechanism generator

Robust and flexible to study sensitivity to the number of BINs and type of reactions



Mechanism validation



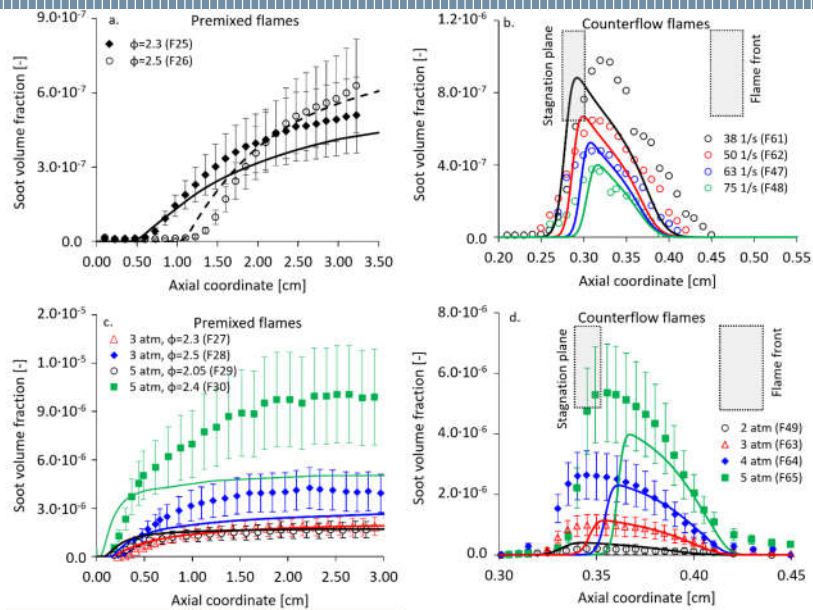
65 premixed and counterflow ethylene flames selected

<https://github.com/acuoci/OpenSMOKE>

Cuoci et al., *Comp. Phys. Comm.* 192(2015)237-264

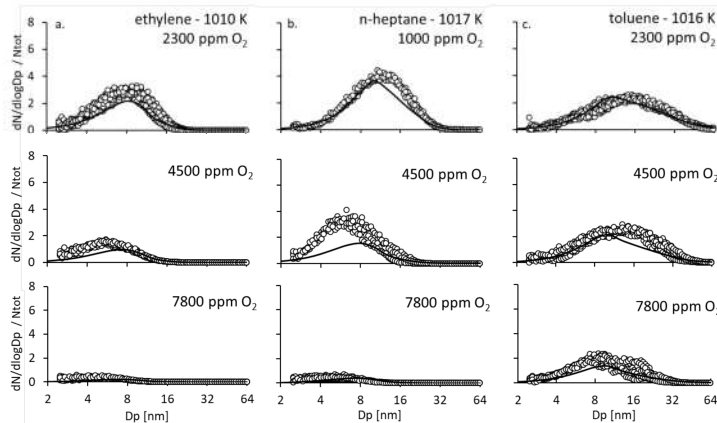
- Overestimation of $f_{v,peak}$ in the range of 0.01-0.1 ppm, while satisfactory agreement in the range of 1-10 ppm
- Discrepancies up to a factor of 8 in the measured $f_{v,peak}$ varying the detection technique

Selected flames

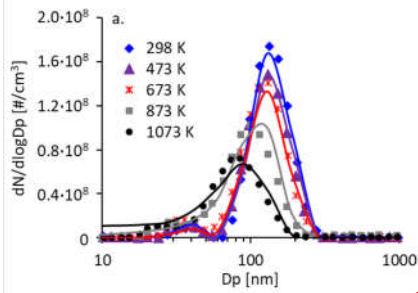


Nascent Soot Oxidation in PFR

- Oxidation of nascent soot particles produced by different fuels, (ethylene, n-heptane, toluene)
- Highly diluted conditions
- Oxidation rates account for particle hydrogenation level (H/C)
- Toluene soot shows the lowest tendency toward oxidation due to its low H/C (~ 0.15)

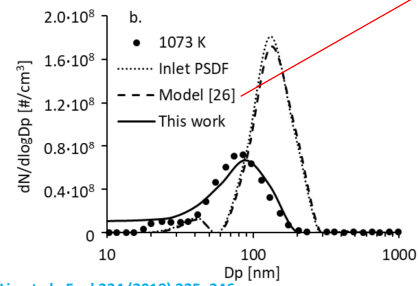


Soot Oxidation

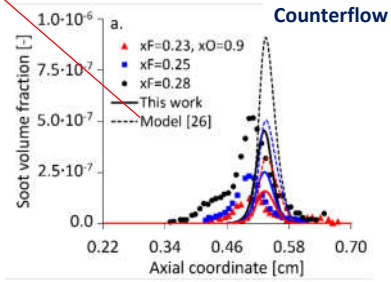


$P = 1 \text{ atm}$, $T = 298 - 1073 \text{ K}$, $\tau = 0.35 \text{ s}$, 10000 ppm O₂ in N₂ (soot formed in a laminar ethylene flame C₂H₄ oxidized in the PFR)

Previous model can not reproduce soot oxidation by O₂ due to the absence of H-abstracting species (high dilution)



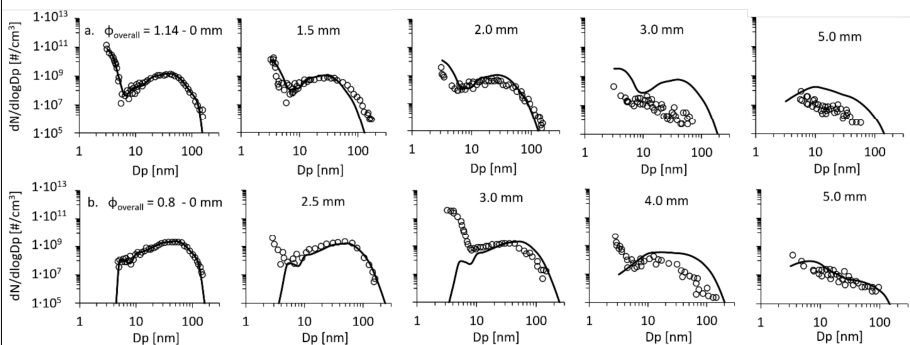
Liu et al., *Fuel* 234 (2018) 335–346



Hwang & Chung, *Combust. Flame* 125 (2001) 752–762

Soot Oxidation

Premixed flame

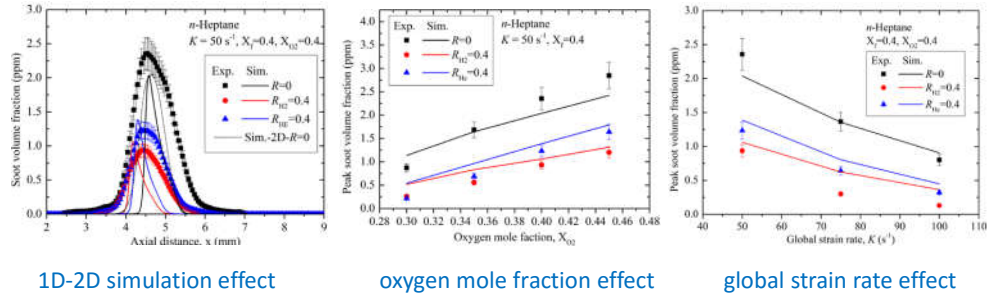


Particle fragmentation not captured

Echavarría et al. *Proc. Comb. Inst.* 33 (2011) 659–666

Soot and hydrogen

NC7 counterflow flames: hydrogen addition and soot



1D-2D simulation effect

oxygen mole fraction effect

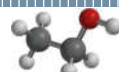
global strain rate effect

$$*R_{H_2(He)} = \frac{x_{H_2(He)}}{x_{fuel} + x_{H_2(He)}}$$

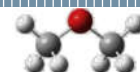
$$K = \frac{2v_F}{L} \left(1 + \frac{v_F \sqrt{\rho_F}}{v_{O_2} \sqrt{\rho_{O_2}}} \right)$$

Oxygenated fuel effect on soot

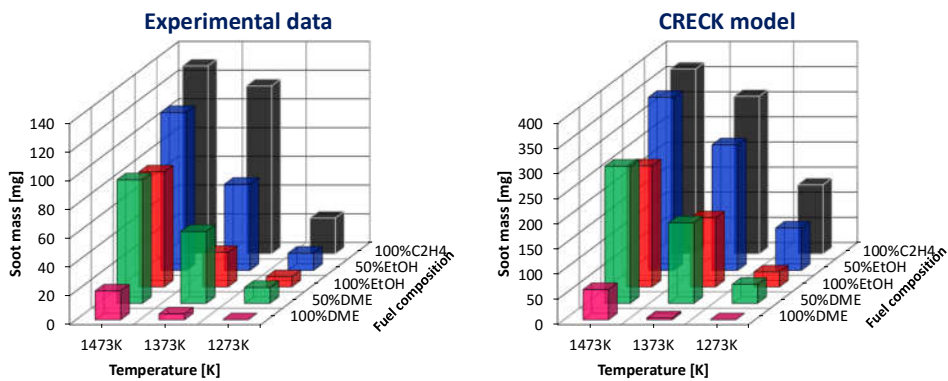
PFR, $P = 1 \text{ atm}$, $\tau = 2 \text{ s}$
 0.02 (mole fraction) pure fuel in AR
 0.01 fuel₁ + 0.01 fuel₂ in AR (50% molar mixture)



Ethanol
 $\text{CH}_3\text{CH}_2\text{OH}$



Dimethyl ether (DME)
 CH_3COCH_3



Zhang et al., *Journal of the Energy Institute*,
 93 (2020) 1288-1304

Ethanol less effective than DME in reducing soot formation

Why ethanol less effective?

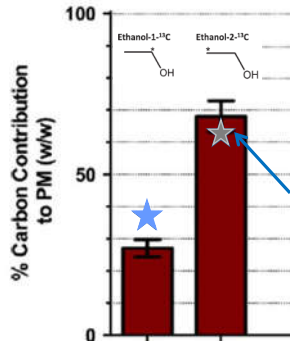
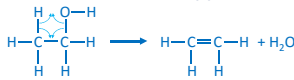
C bond to oxygen does not contribute to soot formation. Assuming the same sooting yield of the C and C atoms forming C2 species, it is possible to calculate the different sooting tendency:

Expected: C = 50 % - C = 50 %

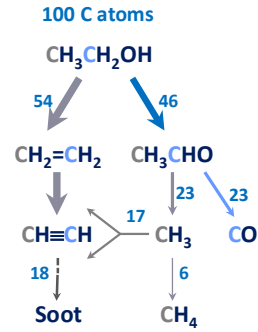
Measured: C = 62 % - C = 38 %

Ethanol reactions to ethylene account for ~54 % of ethanol disappearance

Relevant role of the dehydration reaction, which allows C to be included in the soot.



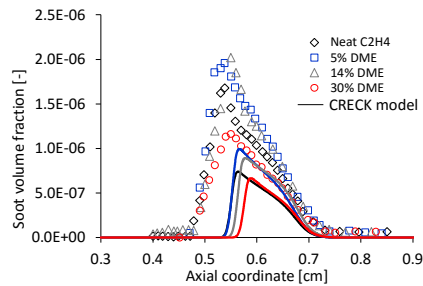
$$\frac{0.5 \times 54 + 17}{54 + 17} = 62\%$$



Not only oxygen presence is important in reducing soot, but also its position

DME effect on soot

Choi et al., J. Mech. Sci. & Tech., 29 (2015) 2259-2267



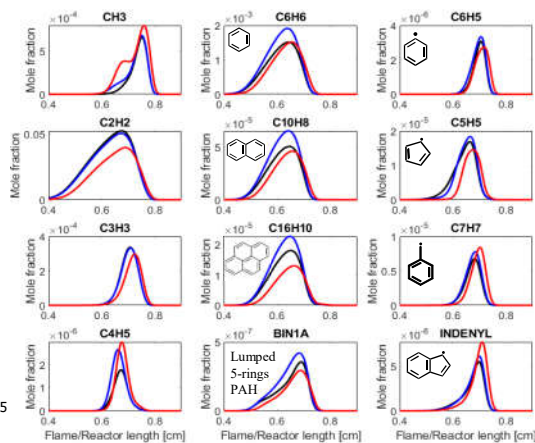
Rate of Production Analysis - Benzene (C₆H₆)



- Neat C₂H₄
- 5% DME
- 30% DME

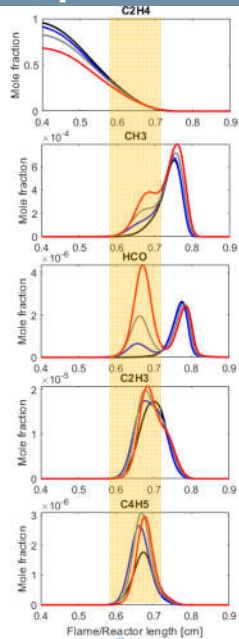
- H+C₇H₈=CH₃+C₆H₆
- C₇H₈=H₂+C₆H₆
- CH₃+C₆H₆=CH₄+C₆H₅
- C₆H₆=H+C₆H₅
- C₂H₄+C₆H₅=C₂H₃+C₆H₆
- 2C₃H₃=C₆H₆
- C₂H₂+C₄H₅=H+C₆H₆
- H+FULVENE=H+C₆H₆
- H+C₆H₆=H₂+C₆H₅

Reaction rate [kmol/m³/s]



From benzene's ROPA it is not easy to understand the non-monotonic behavior of soot

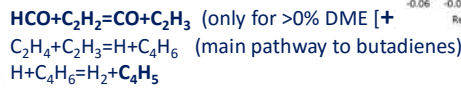
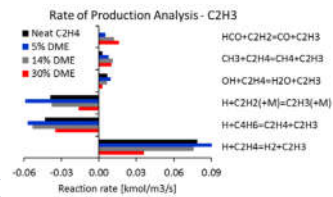
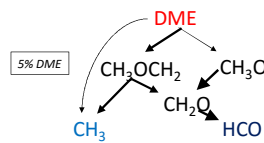
Importance of the even pathway



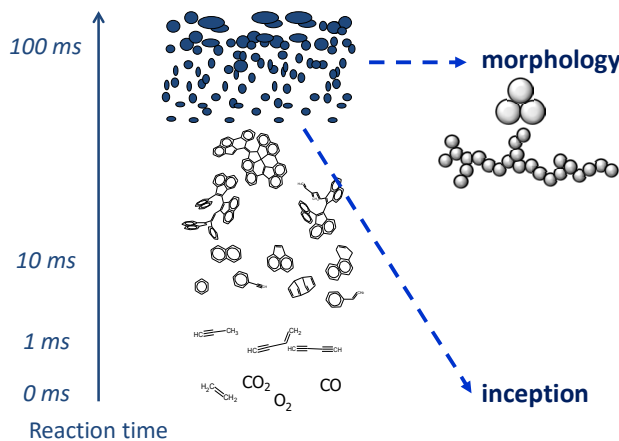
Non monotonic behavior of SVF with DME addition due to competitive effects

(+ vs -). By increasing %DME:

- T_{max} decreases, i.e. from 2245 K (0%) to 2215 K (30%) [+]. (+/- 50K can double/halve SVF)
- Among main precursors of the first ring (benzene):
 - C_2H_2 and C_3H_3 are almost equal for 0% and 5% DME, while strongly decreases for 30% DME [-]
 - C_4H_5 increases \rightarrow from 1- to 5-ring (BIN1) PAHs the relative ratio of soot precursors becomes even more evident [+]
- CH_3 increases \rightarrow branched aromatic molecules and radicals, (C_7H_8 and C_7H_7 [+]) \rightarrow RSR such as benzyl and indenyl (primarily formed from benzyl) dominates soot growth



Some open questions



morphology Same mass, i.e. same bin, but very different surface area: **different reactivity**. It is important to characterize the primary particle distribution and the fractal dimension, without excessively increasing the number of species

inception Chemical and physical interactions of large PAH radicals (π or σ) can be responsible of the first particle formation, but a final quantitative assessment not reached yet.

Adapted from Bockhorn, 1994

RECAP

- ✓ NO_x
 - Thermal mechanism
 - Prompt mechanism
 - N₂O mechanism
 - NNH mechanism
 - Fuel NO_x
 - Reburning
 - SNCR
- ✓ Soot
 - First aromatic ring formation
 - From one to two aromatic rings
 - PAH growth
 - Discrete section approach

RECAP of RECAPS

- ✓ Thermodynamics: enthalpy, entropy and equilibrium constant
- ✓ Chain reaction mechanism: radicals and their stability
- ✓ Reaction rate and rate constant: composition, temperature and pressure effect
- ✓ Rate constant estimation
- ✓ Combustion mechanisms from H₂ to real fuels
- ✓ Validation data and data interpretation
- ✓ Lumping techniques and mechanism generation
- ✓ Automatic validation
- ✓ Pollutant formation: NO_x and soot